Spin-Polarized Donors

as a Building Block for Organic Conductive Magnets

A Thesis Submitted to the University of Tokyo
in Fulfillment of the Requirement
for the Degree of Doctor (Philosophy)

Jotaro Nakazaki

December, 1999

CONTENTS

Chapter 1

General Introduction

Recent progress in the studies on organic conductors and magnets has renewed the traditional image of organic materials, which had been, in general, considered to be insulating and diamagnetic.[1] Nowadays, a lot of organic superconductors[2] or ferromagnets[3] have been reported. Current attention seems to be focused on coexisting system of conductivity and magnetism.

Diamagnetism of general organic materials are derived from their closed shell electronic structures. Free radicals are excepting species and behave paramagnetically. In most cases, free radicals are reactive intermediates and are difficult to be handled, although several stable radicals also exist. When such stable radicals are assembled, unpaired electrons tend to be paired, causing an antiferromagnetic interaction. An idea to align electronic spins intermolecularly was first proposed by McConnell.[4] The validity of this theory was proved by the model studies, such as cyclophane dicarbenes[5] or assembled diphenyl carbene derivatives.[6] Ferromagnetic interactions in the genuine organic ferromagnets reported so far can be rationalized, in most cases, by the application of McConnell theory. However, phase transition temperatures to the ferromagnetic phase are extremely low (typically less than 1 K). Consequently, it is hard to elucidate the accurate mechanism of spin ordering in those organic ferromagnets.

As one of the strategies of introducing larger ferromagnetic interaction among organic radicals, utilization of conduction electrons has been proposed.[7] This proposal is not strange since itinerant electrons are known to play an important role in aligning electron spins in inorganic ferromagnets, such as 3d metals or rare-earth metals.[8] On constructing an organic conducting magnetic system, combination of a conducting moiety and a spin-carrying moiety may be a most plausible approach.
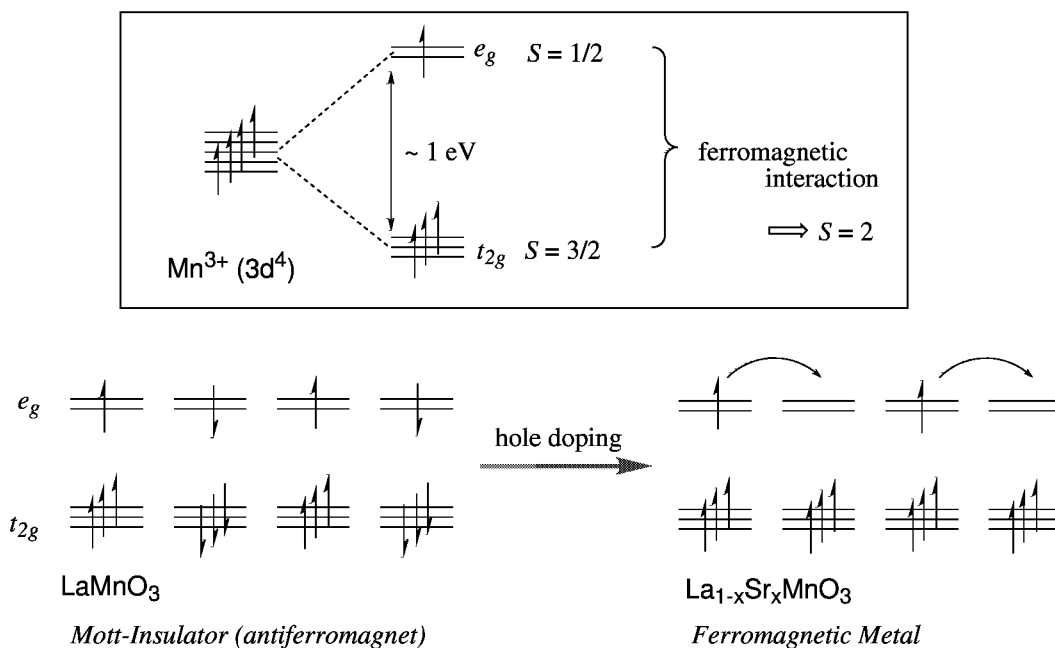
Figure 1-1. Spin alignment in $La_{1-x}Sr_xMnO_3$ based on double exchange mecanism.

In order to consider the spin-alignment in organic conducting materials, a "double exchange" mechanism, operating in metal oxides $La_{1-x}Sr_xMO_3$ (M=Mn, Co), should be referred here.[9] Although $LaMO_3$ (M=Mn, Co) is a Mott insulator and antiferromagnet, it becomes conductive when it is doped with strontium (Figure 1-1). Since the transition metal in $La_{1-x}Sr_xMO_3$ is of a high spin state, localized spins (electrons in t_{2g} orbital) are ferromagnetically coupled with electrons in e_g orbital. When the transition metals are partially doped, the -spin electron in the e_g orbital can migrate along the metal array, aligning the localized spins on Mn or Co to at each metal site. Such a cooperating system of conductivity and magnetism has drawn current attention for their various physical behaviors. If such a conducting magnetic system is realized by organic materials, tunability of organic system may afford a great advantage.

Conduction and magnetic properties of several "organic magnetic conductors", which consist of organic donors or acceptors and magnetic counter ions, have been examined extensively, expecting possible exchange interactions.[10] Preparation of several organic radicals bearing a donor moiety have also been reported.[11] Some of them turned out to afford CT complexes or ion-radical salts. In these donor radicals, however, a radical group is connected with a donor group in a non- -conjugating manner. Therefore, the magnetic interaction between the radical site and the donor site in the singly oxidized state is negligibly small, if any.

2

TMM   Donor-NN
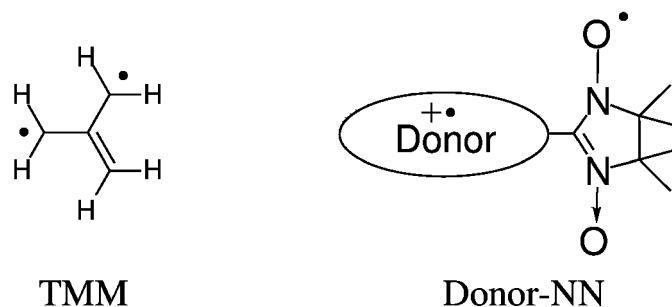
Figure 1-2. Comparison of trimethylenemethane (TMM) and a nitronyl nitroxide (NN) carrying a donor moiety in a singly oxidized state. The donor site is connected with the radical site in a cross-conjugating manner.

In order to realize an organic double exchange system, it is crucial to introduce a ferromagnetic exchange interaction between the radical site and the donor site in the singly oxidized state. For this purpose, careful modification of a non-Kekulé molecule, trimethylenemethane (TMM), was performed, and a group of donor radicals which are called "spin-polarized donors" have been developped (Figure 1-2). A prototypical example of a spin-polarized donor is dimethylamino nitronyl nitroxide (DMANN).[12] The donor site of a spin-polarized donor is connected with the radical site in a cross-conjugating manner, and the ground state spin multiplicity of the oxidized species of a spin-polarized donor is triplet. The electronic structure of DMANN is rationalized based on a perturbational MO method. The characteristics of the electronic structure of a spin-polarized donor is that the triplet state of the oxidized species is based on non-degenerated multi-centered orbitals. -Extended derivatives of DMANN have also been prepared.

On constructing an organic double exchange system, the constituent donor radicals are also requested to have an ability to construct an sufficient conduction path. Although several amine-based organic conductors are known, their conductivity is not enough for the present approach. Design of more conductive materials are needed.

"Macromolecular" approach   "Self-assembling" approach
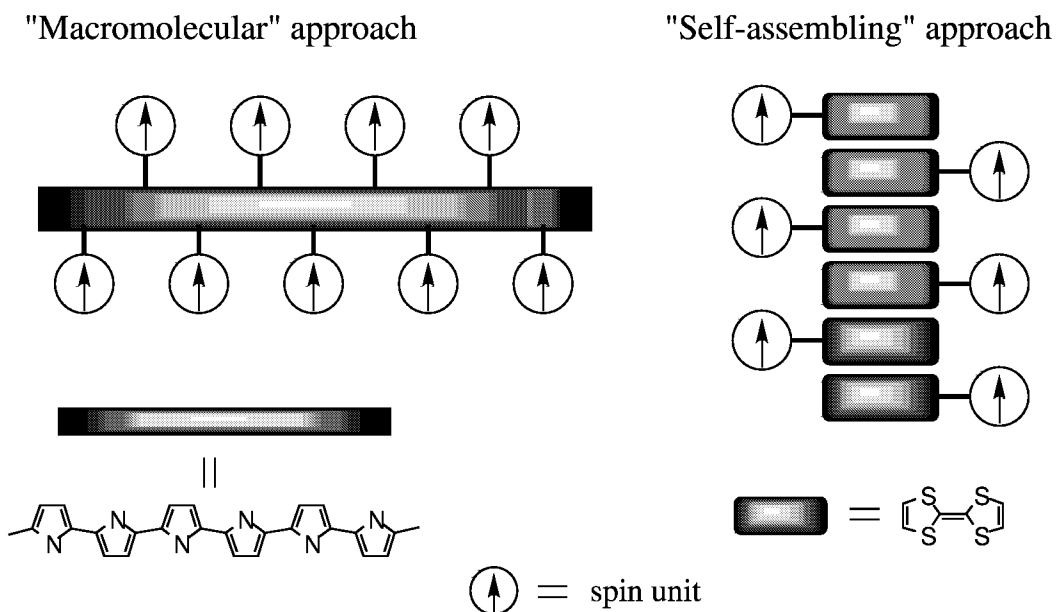
Figure 1-3. Two approaches to construct organic conductive magnets.

In this thesis, the author describes two approaches to construct organic conductive magnets based on spin-polarized donors (Figure 1-3). In a "macromolecular" approach, a -conjugation in a doped polypyrrole is selected as a conduction path. As building blocks for such a system, pyrrole-based spin-polarized donors are designed (Chapter 2). On the other hand, a partially doped columnar stacking of TTF derivatives will work as a conduction path in a "self-assembling" approach. As building blocks for such an assembled material, TTF-based spin-polarized donors are prepared (Chapter 3,4). For pyrrole-based or TTF-based donor-radicals, the connection pattern between a donor part and a radical part turned out to be important to achieve an intramolecular ferromagnetic coupling.

References and Notes

1. a)   , *"   "*,   *No.42*,   , **1983**.

   b) *"   "*,   **1995**, *30*, 157-316.

   c)   , *"   "*,   , **1996**.

   d)   , *"   "*,   *No.35*,   , **1998**.

2. a) Saito G, Kagoshima S, ed., "The physics and chemistry of organic superconductors", Springer-Verlag, **1990**.

   b) Urayama H, Yamochi H, Saito G, Nozawa K, Sugano T, Kinoshita M, Sato S, Oshima K, Kawamoto A, Tanaka J, "A new ambient pressure organic superconductor based on BEDT-TTF with T_C higer than 10 K (T_C = 10.4 K)", *Chem. Lett.* **1988**, 55-58.

   c)   , "   BEDT- TTF   ",   **1991**, 149-162.

   d) Mori T, "Structural genealogy of BEDT-TTF-based organic conductors I. Parallel molecules: β and β" phases", *Bull. Chem. Soc. Jpn.* **1998**, *71*, 2509-2526.

   e) Mori T, Mori H, Tanaka S, "Structural genealogy of BEDT-TTF-based organic conductors II. Inclined molecules: θ, α, and κ phases", *Bull. Chem. Soc. Jpn.* **1999**, *72*, 179-197.

3. a) Kinoshita M, Turek P, Tamura M, Nozawa K, Shiomi D, Nakazawa Y, Ishikawa M, Takahashi M, Awaga K, Inabe T, Maruyama Y, "An organic radical ferromagnet", *Chem. Lett.* **1991**, 1225-1228.

   b) Tamura M, Nakazawa Y, Shiomi D, Nozawa K, Hosokoshi Y, Ishikawa M, Takahashi M, Kinoshita M, "Bulk ferromagnetism in the -phase crystal of the *p*-nitrophenyl nitronyl nitroxide", *Chem. Phys. Lett.* **1991**, *186*, 401-404.

   c) Chiarelli R, Novak MA, Rassat A, Tholence JL, "A ferromagnetic transition at 1.48 K in an organic nitroxide", *Nature* **1993**, *363*, 147-149.

   d) Nogami T, Tomioka K, Ishida T, Yoshikawa H, Yasui M, Iwasaki F, Iwamura H, Takeda N, Ishikawa M, "A new organic ferromagnet: 4-benzylideneamino-2,2,6,6-tatramethyl-piperidin-1-oxyl", *Chem. Lett.* **1994**, 29-32.

   e) Togashi K, Imachi R, Tomioka K, Tsuboi H, Ishida T, Nogami T, Takeda N, Ishikawa M, "Organic radicals exhibiting intermolecular ferromagnetic interaction with high probability: 4-arylmethyleneamino-2,2,6,6-tetramethylpiperidin-1-oxyls and related compounds", *Bull. Chem. Soc. Jpn.* **1996**, *69*, 2821-2830.

   f) Sugawara T, Matsushita MM, Izuoka A, Wada N, Takeda N, Ishikawa M, "An organic ferromagnet: -phase crystal of 2-(2',5'-dihydroxyphenyl)-4,4,5,5-tetramethyl-4,5-dihydro-1*H*-imidazolyl-1-oxy-3-oxide (-HQNN)", *J. Chem. Soc. Chem. Commun.* **1994**, 1723-1724.

   g) Matsushita MM, Izuoka A, Sugawara T, Kobayashi T, Wada N, Takeda N, Ishikawa M, "Hydrogen-bonded organic ferromagnet", *J. Am. Chem. Soc.* **1997**, *119*, 4369-4379.

   h) Cirujeda J, Mas M, Molins E, Panthou FL, Laugier J, Park JG, Paulsen C, Rey P, Rovira C, Veciana J, "Control of the structural dimensionality in hydrogen-bonded self-assemblies of open-shell molecules. Extension of intermolecular ferromagnetic interactions in -phenyl nitronyl nitroxide radicals in three dimensions", *J. Chem. Soc. Chem. Commun.* **1995**, 709-710.

   i) Caneschi A, Ferraro F, Gatteschi D, Lirzin A, Novak MA, Rentschler E, Sessoli R, "Ferromagnetic order in the sulfur-containing nitronyl nitroxide radical, 2-(4-thiomethyl)-phenyl-4,4,5,5-tetramethylimidazoline-1-oxyl-3-oxide, NIT-(SMe)Ph", *Adv. Mater.* **1995**, *7*, 476-478.

   j) Mukai K, Konishi K, Nedachi K, Takeda K, "Bulk ferro- and antiferromagnetic behavior in 1,5-dimethyl verdazyl radical crystals with similar molecular structure", *J. Magn. Magn. Mater.* **1995**, *140-144*, 1449-1450.

4.   McConnell HM, "Ferromagnetism in solid free radicals", *J. Chem. Phys.* **1963**, *39*, 1910.

5. a) Izuoka A, Murata S, Sugawara T, Iwamura H, "Ferro- and antiferromagnetic interaction between two diphenylcarbene units incorporated in the [2.2]paracyclophane skeleton", *J.*

Am. Chem. Soc., **1985**, *107*, 1786-1787.

b) Izuoka A, Murata S, Sugawara T, Iwamura H, "Molecular design and model experiments of ferromagnetic intermolecular interaction in the assembly of high-spin organic molecules. Generation and characterization of the spin states of isomeric bis(phenylmethylenyl) [2,2]paracyclophanes", *J. Am. Chem. Soc.* **1987**, *109*, 2631-2639.

6. a) Sugawara T, Tukada H, Izuoka A, Murata S, Iwamura H, "Magnetic interaction among diphenylmethylene molecules generated in crystals of some diazodiphenylmethanes", *J. Am. Chem. Soc.* **1986**, *108*, 4272-4278.

b) Sugawara T, Murata S, Kimura K, Iwamura H, Sugawara Y, Iwasaki H, "Design of molecular assembly of diphenylcarbenes having ferromagnetic intermolecular interaction", *J. Am. Chem. Soc.* **1985**, *107*, 5293-5294.

7. a)   , "   ",   **1989**, *47*, 306-320.

b) Yamaguchi K, Namimoto H, Fueno T, Nogami T, Shirota Y, "Possibilities of organic ferromagnets and ferrimagnets by the use of charge-transfer (CT) complexes with radical substituents. ab initio MO studies", *Chem. Phys. Lett.* **1990**, *166*, 408-414.

c) Izuoka A, Kumai R, Tachikawa T, Sugawara T, "Approach to organic ferromagnetic metal using novel twin-donors", *Mol. Cryst. Liq. Cryst.* **1992**, *218*, 213-218.

8. a)   , "   ( )   ",   , **1978**, 172-211.

b)   , "   ",   , **1996**.

9. a) Kimura T, Tomioka Y, Kuwahara H, Asamitsu A, Tamura M, Tokura Y, "Interplane tunneling magnetoresistance in a layered manganite crystal", *Science* **1996**, *274*, 1698-1701.

b) Kiryukhin V, Casa D, Hill JP, Keimer B, Vigliante A, Tomioka Y, Tokura Y, "An X-ray-induced insulator-metal transition in a magnetoresistive manganite", *Nature* **1997**, *386*, 813-815.

c)   ,   ,   , "   ",   **1997**, *32*, 258-272.

d) Imada M, Fujimori A, Tokura Y, "Metal-insulator transitions", *Rev. Mod. Phys.* **1998**, *70*, 1039-1263.

10. a) Mallah T, Hollis C, Bott S, Kurmoo M, Day P, Allan M, Friend RH, "Crystal structures and physical properties of bis(ethylenedithio)tetrathiafulvalene charge-transfer salts with FeX_4^- (X = Cl or Br) anions", *J. Chem. Soc. Dalton Trans.* **1990**, 859-865.

b) Kurmoo M, Day P, Guionneau P, Bravic G, Chasseau D, Ducasse L, Allan ML, Marsden ID, Friend RH, "Crystal structure and magnetism of $(BEDT-TTF)_2MCl_4$ (BEDT-TTF = bis(ethylenedithio)tetrathiafulvalene; M = Ga, Fe)", *Inorg. Chem.* **1996**, *35*, 4719-4726.

c) Martin L, Turner SS, Day P, Mabbs FE, McInnes EJL, "New molecular superconductor containing paramagnetic chromium(III) ions", *Chem. Commun.* **1997**, 1367-1368.

d) Day P, Kurmoo M, "Molecular magnetic semiconductors, metals and superconductors: BEDT-TTF salts with magnetic anions", *J. Mater. Chem.* **1997**, *7*, 1291-1295.

e) Yamaura J, Suzuki K, Kaizu Y, Enoki T, Murata K, Saito G, "Magnetic properties of organic conductor $(BEDT-TTF)_3CuBr_4$", *J. Phys. Soc. Jpn.* **1996**, *65*, 2645-2654.

f) Enoki T, Yamaura J, Miyazaki A, "Molecular magnets based on organic charge transfer complexes", *Bull. Chem. Soc. Jpn.* **1997**, *70*, 2005-2013.

g) Kumai R, Asamitsu A, Tokura Y, "A molecular antiferromagnet $TMTSF \cdot FeCl_4$", *Chem. Lett.* **1996**, 753-754.

h) Kobayashi H, Tomita H, Naito T, Kobayashi A, Sakai F, Watanabe T, Cassoux P, "New BETS condutors with magnetic anions (BETS = bis(ethylenedithio)tetraselenafulvalene)", *J. Am. Chem. Soc.* **1996**, *118*, 368-377.

i) Kobayashi H, Sato A, Arai E, Akutsu H, Kobayashi A, Cassoux P, "Superconductor-to-insulator transition in an organic metal incorporating magnetic anions: λ-$(BETS)_2(FeGa_{1-x})Cl_4$ [BETS = bis(ethylenedithio)tetraselenafulvalene; $x \sim 0.55$ and 0.43]", *J. Am. Chem. Soc.* **1997**, *119*, 12392-12393.

j) Akutsu H, Arai E, Kobayashi H, Tanaka H, Kobayashi A, Cassoux P, "Highly correlated organic conductor with magnetic anions exhibiting a -d coupled metal-insulator transition, λ-$(BETS)_2FeBr_xCl_{4-x}$ (BETS = bis(ethylenedithio)tetraselenafulvalene)", *J. Am. Chem.*

Soc. **1997**, *119*, 12681-12682.

k) Akutsu H, Kato K, Ojima E, Kobayashi H, Tanaka H, Kobayashi A, Cassoux P, "Coupling of metal-insulator and antiferromagnetic transitions in the highly correlated organic conductor incorporating magnetic anions, λ-BETS$_2$FeBr$_x$Cl$_{4-x}$ [BETS = bis(ethylenedithio) tetraselenafulvalene]", *Phys. Rev. B* **1998**, *58*, 9294-9302.

l) Brossard L, Clerac R, Coulon C, Tokumoto M, Ziman T, Petrov DK, Laukhin VN, Naughton MJ, Audouard A, Goze F, Kobayashi A, Kobayashi H, Cassoux P, "Interplay between chains of $S = 5/2$ localised spins and two-dimensional sheets of organic donors in the synthetically built magnetic multilayer λ-(BETS)$_2$FeCl$_4$", *Eur. Phys. J. B* **1998**, *1*, 439-452.

m) Ojima E, Fujiwara H, Kato K, Kobayashi H, "Antiferromagnetic organic metal exhibiting superconducting transition, κ-(BETS)$_2$FeBr$_4$ [BETS = bis(ethylenedithio)tetraselena-fulvalene]", *J. Am. Chem. Soc.* **1999**, *121*, 5581-5582.

n) Mori H, Sakurai N, Tanaka S, Moriyama H, "Crystal structures and magnetic properties of d-p organic conductors, (EDT-TTF)$_4$CoCl$_4$(1,1,2-TCE)$_x$ and related materials", *Bull. Chem. Soc. Jpn,* **1999**, *72*, 683-689.

11. a) Sugano T, Fukasawa T, Kinoshita M, "Magnetic interactions among unpaired electrons in charge-transfer complexes of organic donors having a neutral radical", *Synth. Metals* **1991**, *41-43*, 3281-3284.

b) Sugimoto T, Yamaga S, Nakai M, Tsuji M, Nakatsuji H, Hosoito N, "Different magnetic properties of charge-transfer complexes and cation radical salts of tetrathiafulvalene derivatives substituted with imino pyrolidine- and piperidine-1-oxyls", *Chem. Lett.* **1993**, 1817-1820.

c) Ishida T, Tomioka K, Nogami T, Iwamura H, Yamaguchi K, Mori W, Shirota Y, "Intermolecular ferromagnetic interaction of 4-(1-pyrenylmethyleneamino)-2,2,6,6-tetramethylpiperidin-1-oxyl", *Mol. Cryst. Liq. Cryst.* **1993**, *232*, 99-102.

d) Nakatsuji S, Akashi N, Komori Y, Suzuki K, Enoki T, Anzai H, "Preparation and properties of aromatic compounds bearing substituents with unpaired electron", *Mol. Cryst. Liq. Cryst.* **1996**, *279*, 73-76.

e) Nakatsuji S, Takai A, Nishikawa K, Morimoto Y, Yasuoka N, Suzuki K, Enoki T, Anzai H, "Magnetic properties of charge-transfer complexes based on TEMPO radicals", *Chem. Commun.* **1997**, 275-276.

f) Nakatsuji S, Anzai H, "Recent progress in the development of organomagnetic materials based on neutral nitroxide radicals and charge transfer complexes derived from nitroxide radicals", *J. Mater. Chem.* **1997**, *7*, 2161-2174.

g) Nakatsuji S, Takai A, Nishikawa K, Morimoto Y, Yasuoka N, Suzuki K, Enoki T, Anzai H, "CT complexes based on TEMPO radicals", *J. Mater. Chem.* **1999**, *9*, 1747-1754.

h) Fujiwara H, Kobayashi H, "Synthesis and properties of new organic donor containing organic radical part", *Synth. Metals*, in press.

12. a) Sakurai H, Kumai R, Izuoka A, Sugawara T, "Ground state triplet cation diradicals generated from *N,N*-dimethylamino nitronyl nitroxide and its homologues through one-electron oxidation", *Chem. Lett.* **1996**, 879-880.

b) Kumai R, Sakurai H, Izuoka A, Sugawara T, "Ground state triplet cation diradicals having non-degenerated singly occpied molecular orbitals", *Mol. Cryst. Liq. Cryst.* **1996**, *279*, 133-138.

c) Sakurai H, "High-spin cation diradicals derived from open-shell donors", *Thesis, The University of Tokyo*, **1996**.

d) Sakurai H, Izuoka A, Sugawara T, "Design, preparation and electronic structure of high-spin cation diradicals derived from amine-based spin-polarized donors", submitted to *J. Am. Chem. Soc.*

7

Chapter 2

Spin Correlation in Cation Diradicals
Derived from Pyrroles
Carrying Nitronyl Nitroxide

§2-1. Introduction

In order to realize an organic conductive magnet by a "self-assembling" approach, it is crucial to construct a segregated columnar stacking of the donor units with a mixed valency. In "macromolecular" approach, on the other hand, a conduction path should be easily constructed, by doping polypyrroles which are supposed to be formed through oxidation of functionalized pyrrole monomers.

Conducting property of doped polypyrroles is well documented in terms of a polaronic and/or a bipolaronic mechanism.[1] If polypyrroles carrying a stable radical as a pendant group are prepared, both conductive and magnetic properties may be manifested by doping the polymer. Although polymers (or oligomers) bearing stable radicals as a pendant group have been studied,[2] dopable ones have not been reported.

As a functionalized monomer, a pyrrole-based spin-polarized donor should be effective. A simplified framework of a pyrrole-based spin-polarized donor is a pyrrole derivative bearing a nitronyl nitroxide (NN) group. However, validity of the concept of a spin-polarized donor is not ensured for heterocycle-NN systems as seen in TTF-NN.[3] Then, exchange interactions in pyrrole derivatives bearing a NN group of various substitution patterns should be examined.

PyrrolylNN derivatives examined in this chapter are listed in Figure 2-1. A substituent is introduced at 1- (N-) or 3- (β-)position of pyrrole ring not to prohibit the reactivity of polymerization at 2,5-positions. As simplest model

compounds, 1-pyrrolylNN (*N*-**NN**) and 3-pyrrolylNN (β-**NN**), where a NN group is directly introduced to the pyrrole ring, were designed. Since a bulky NN group may affect the reactivity of pyrrole, *p*-phenylene extended derivatives, 4-(1'-pyrrolyl)phenylNN (*N*-**PN**) and 4-(3'-pyrrolyl)phenylNN (β-**PN**) were also examined.

N-**NN**   β-**NN**   *N*-**PN**   β-**PN**
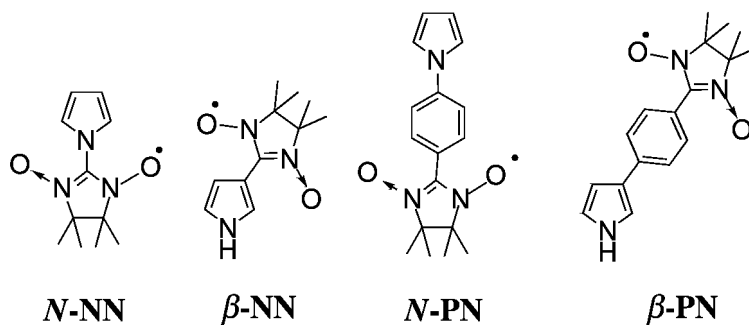
Figure 2-1. Designed pyrrolylNN derivatives.

§2-2. Preparation of PyrrolylNNs

These pyrrolylNN derivatives were prepared by the following reaction schemes (Figures 2-2 to 2-5). Pyrrole was treated with sodium hydride in dimethylformamide, and the resulted anion was reacted with 2-bromonitronyl nitroxide (**2**)[4] to give *N*-**NN**. 3-Formylpyrrole (**3**) was obtained according to the literature method[5] as shown in Figure 2-3, and it was converted to a cyclic hydroxyl amine, which was oxidized by lead dioxide[6] to give β-**NN**. Reaction of 2,5-dimethoxytetrahydrofuran and *p*-bromoaniline in acetic acid gave 1-(4'-bromophenyl)pyrrole (**4**), which was converted to a 4'-formyl derivative **5** by the treatment with *n*-butyllithium followed by dimethylformamide. 3-Bromo derivative **7** was obtained by the literature method[5] as shown in Figure 2-5, and it was lithiated, stannylated, and coupled with *p*-bromobenzaldehyde by Stille coupling.[7] Deprotection of the coupling product **9** afforded 3-(4'-formylphenyl)pyrrole (**10**). These 4'-formylphenyl derivatives **5** and **10** were converted to *N*-**PN** and β-**PN**, respectively, by the same procedure as in the case of β-**NN**.

The molecular structures of *N*-**NN**, β-**NN**, and *N*-**PN** determined by X-ray crystallography are depicted in Figure 2-6. Detailed data are listed in Appendix.
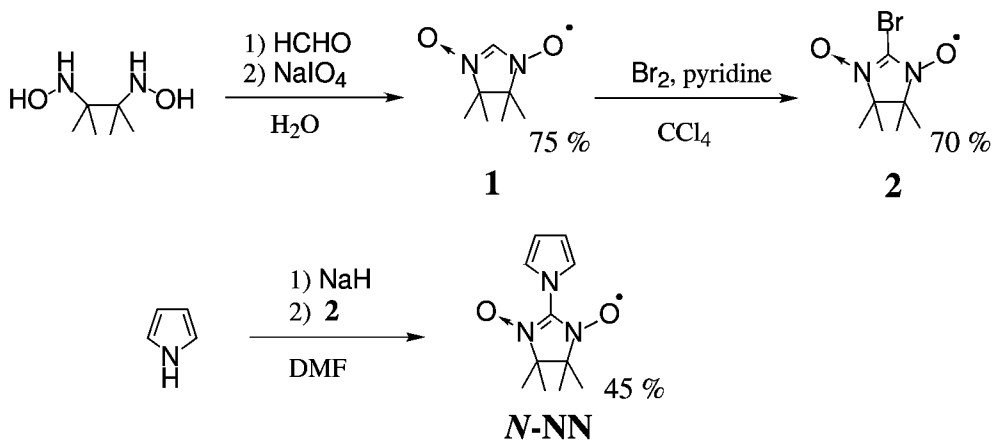
Figure 2-2. Synthetic scheme of *N*-NN.
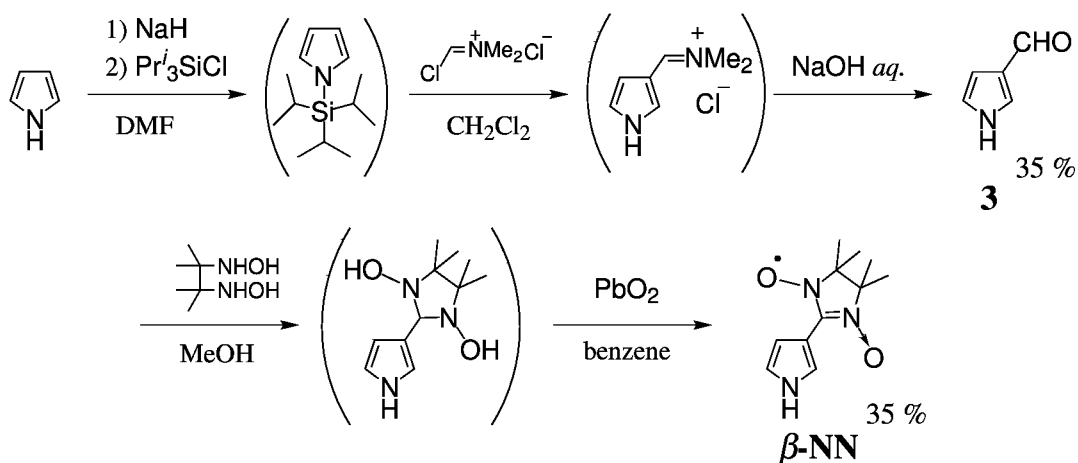
Figure 2-3. Synthetic scheme of β-NN.
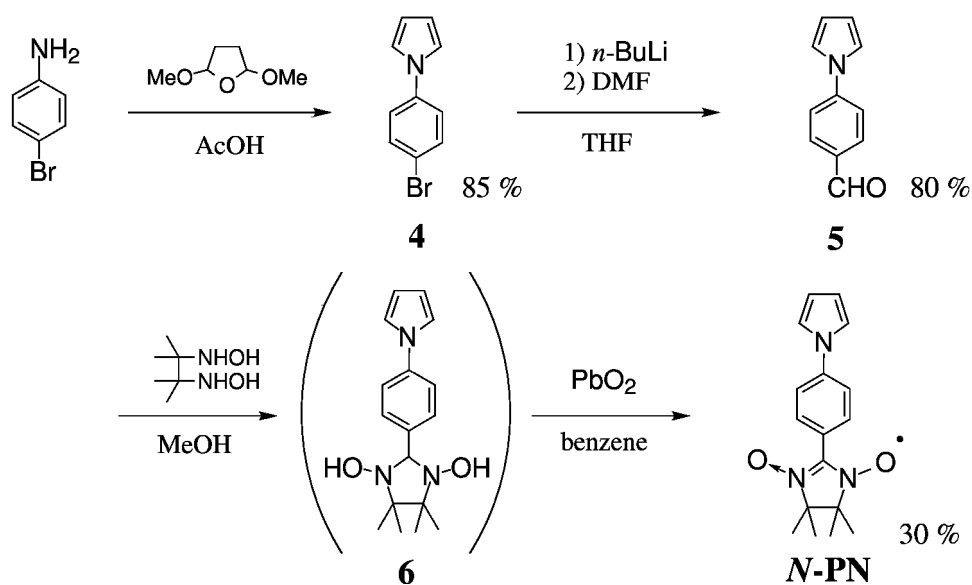
Figure 2-4. Synthetic scheme of *N*-PN.
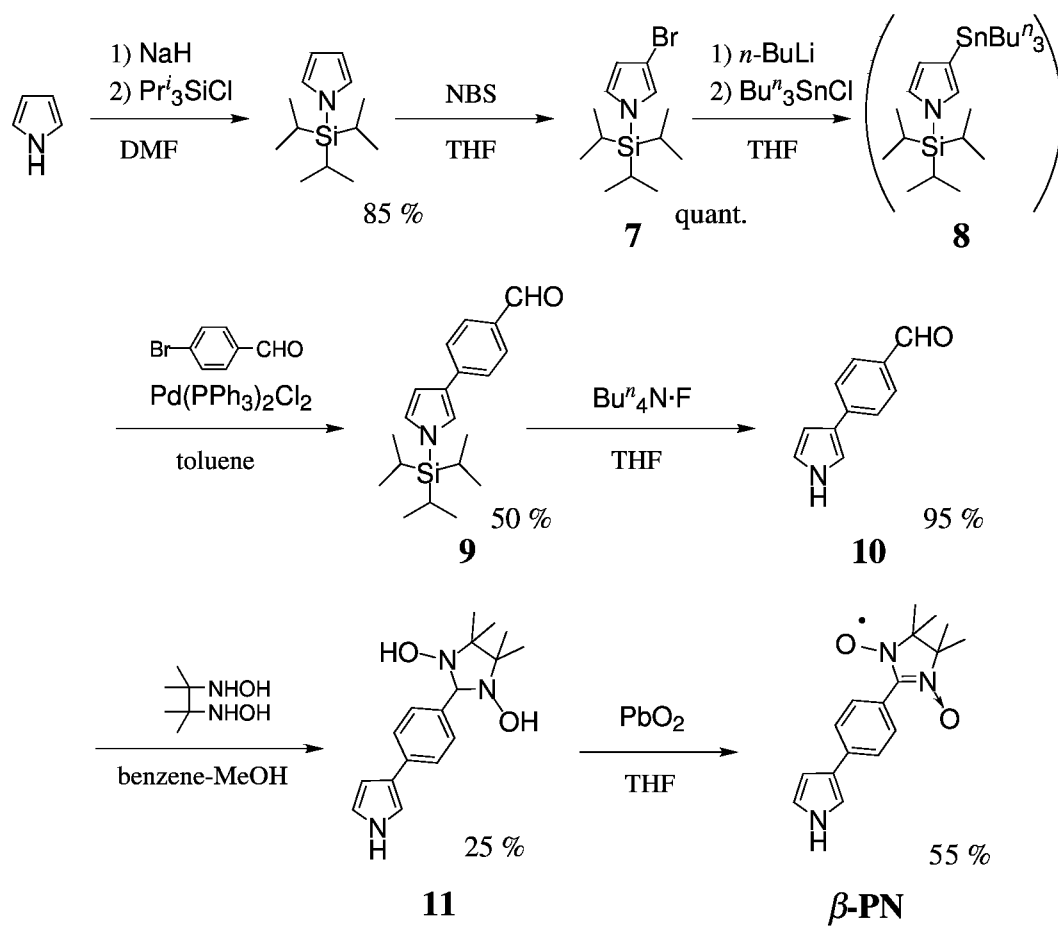
Figure 2-5. Synthetic scheme of β-**PN**.

N-**NN**

β-**NN**

N-**PN**
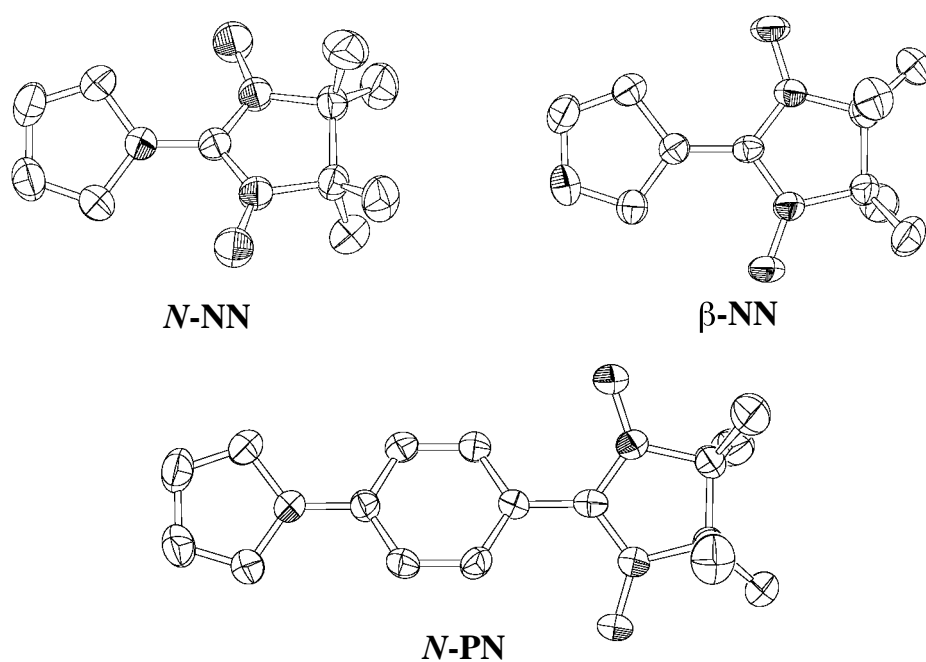
Figure 2-6. ORTEP drawings (50% probability) of molecular structures of pyrrolylNNs

§2-3. Properties of PyrrolylNNs

2-3-1. Cyclic Voltammetry of PyrrolylNNs

Oxidation potentials of these pyrrolylNN derivatives were measured by cyclic voltammetry. If conductive polypyrroles were formed, a redox peak of the polymer should grow up by every scan as shown in Figure 2-7(a). In the case of pyrrolylNN derivatives, such behavior was not observed, indicating that these derivatives are not polymerizable.[8] Since some functionalized pyrrole derivatives are known to need higher potentials to be polymerized, potentials as high as 2.5 V or 3.0 V were applied, but the pyrrolylNNs showed no indication of polymerization. The cyclic voltammogram of *N*-PN is shown in Figure 2-7(b).

The determined oxidation potentials are listed in Table 2-1. The first oxidation potentials are lower than those of pyrrole (0.95 V) and *N*-phenylpyrrole (1.40 V). Except for *N*-NN, the first oxidation occurs at lower potentials than H-NN (**1**) (0.83 V), indicating an effective modulation of the electronic structures by the introduction of the NN group.
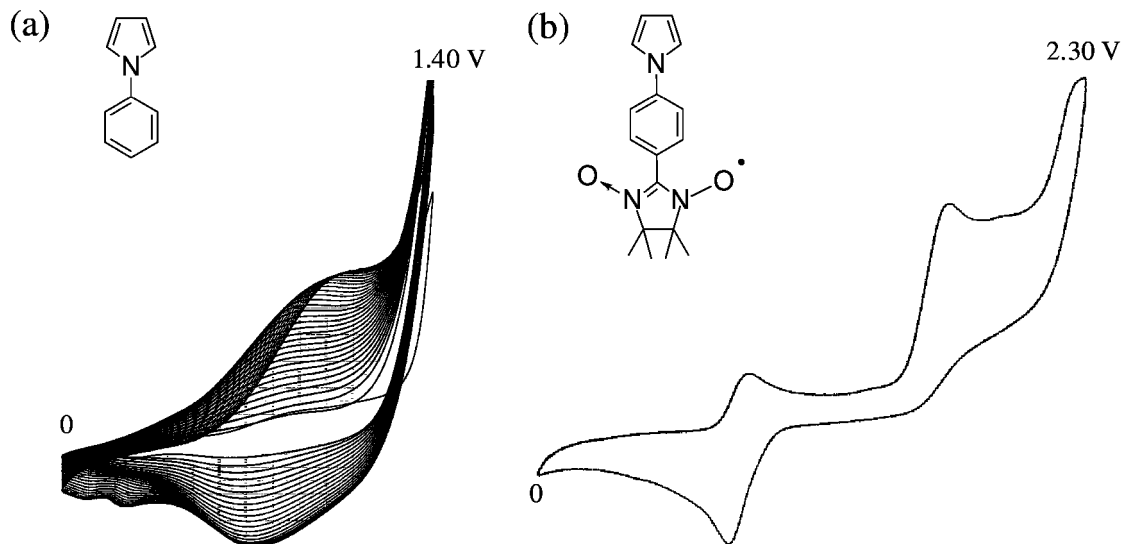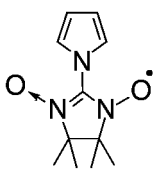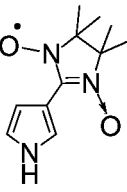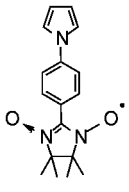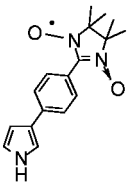
Figure 2-7. Cyclic voltammograms of (a) *N*-phenylpyrrole, and (b) *N*-PN, observed in 0.1 M *n*-Bu$_4$N·ClO$_4$ / CH$_3$CN.

Table 2-1. Oxidation potentials of pyrrolylNNs.

	N-NN	β-NN	N-PN	β-PN
$E_{1/2}{}^1$	0.88 V	0.63 V	0.81 V	0.75 V
$E_p{}^2$	2.15	2.05	1.65	1.52
$E_p{}^3$			2.20	

(measured in 0.1 M n-Bu$_4$N·ClO$_4$ – CH$_3$CN vs. Ag/AgCl)

2-3-2. ESR Spectra of Oxidized Species of PyrrolylNNs

Oxidized species of these pyrrolylNN derivatives were generated by the addition of excess iodine to a tetrahydrofuran solution of these pyrrolylNN derivatives at room temperature.[9] The ESR spectra observed in a frozen matrix are shown in Figure 2-8. Whereas triplet signals were observed for β-**NN**$^{+•}$, N-**PN**$^{+•}$, and β-**PN**$^{+•}$, no signal assignable to a triplet species was detected for N-**NN**$^{+•}$. The zero-field splitting parameters of β-**NN**$^{+•}$ and N-**PN**$^{+•}$ were evaluated to be $|D| = 0.026$ cm^{-1}, $|E| = 0.002$ cm^{-1}, and $|D| = 0.0257$ cm^{-1}, $|E| = 0.0021$ cm^{-1}, respectively. The temperature dependence of the intensity of the triplet signals obeyed Curie law in the temperature range of 7.5-120 K, indicating that the triplet is the ground state of β-**NN**$^{+•}$ and N-**PN**$^{+•}$. A triplet ESR spectrum was also observed for β-**PN**$^{+•}$, although the temperature dependence of the signal intensity could not been measured due to the weak intensity of the signal.
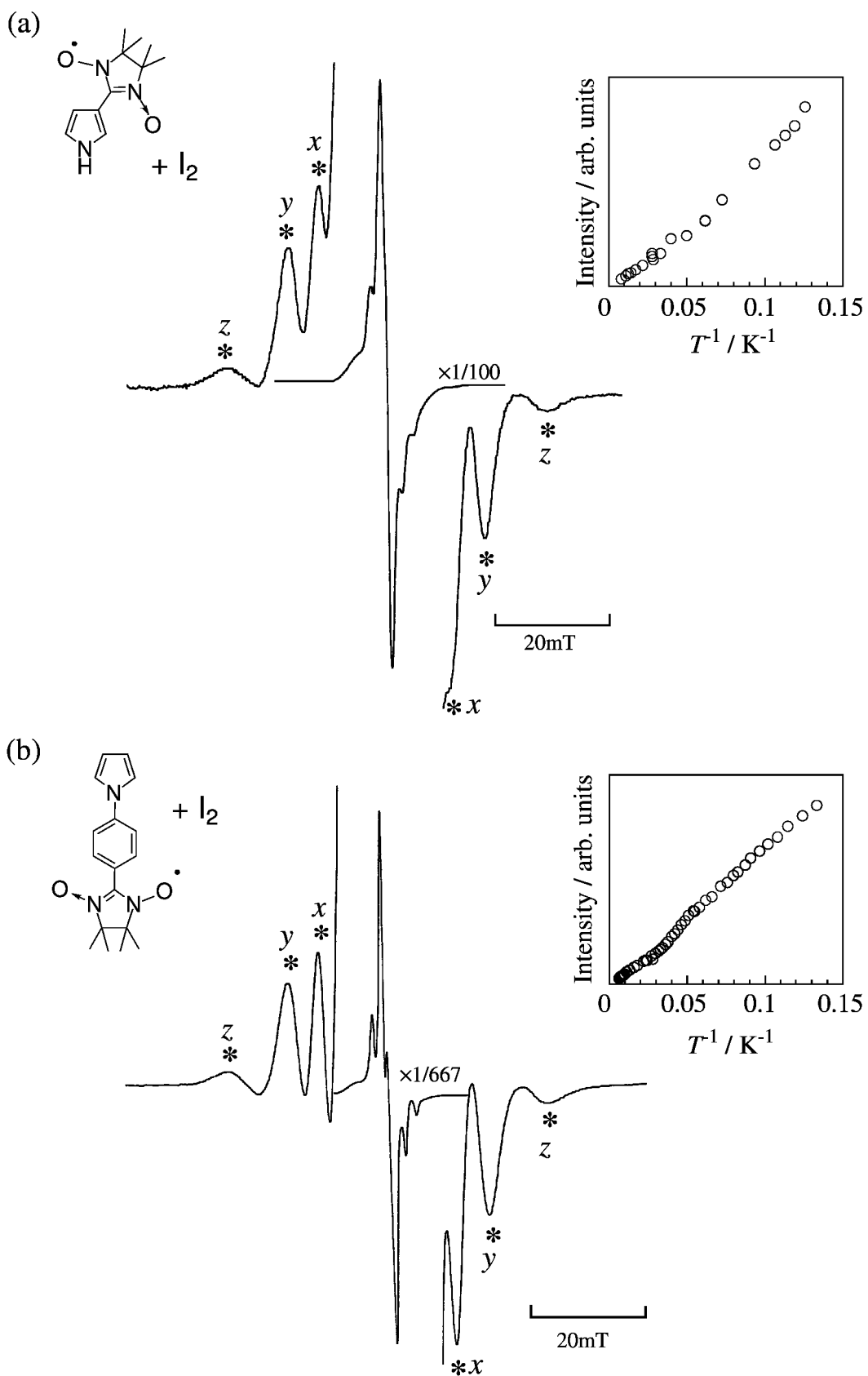
Figure 2-8. ESR spectra and temperature dependence of signal intensity of (a) β-**NN**⁺•, and (b) *N*-**PN**⁺•.

§2-4. Electronic Structure of PyrrolylNNs

2-4-1. Difference in ESR Spectra of Oxidized Species

Whereas triplet ESR spectrum was observed for β-**NN**$^{+\bullet}$, no signal assignable to a triplet species was detected for *N*-**NN**$^{+\bullet}$. There are three possible reasons why *N*-**NN** does not afford a triplet signal:

(i) Ground state of the oxidized species of *N*-**NN** is singlet and its S-T gap is very large.

(ii) The oxidizing ability of iodine is not sufficient enough to generate a cation diradical of *N*-**NN**. Here, the oxidation potential of *N*-**NN** is as high as +0.88 V while that of β-**NN** is +0.63 V.

(iii) The cation diradical of *N*-**NN** is decomposed before being observed because of its kinetic instability. Since the neutral *N*-**NN** is unstable compared to β-**NN**, the oxidized species *N*-**NN**$^{+\bullet}$ might be more unstable than β-**NN**$^{+\bullet}$.

Among these possibilities, (ii) may be excluded because some donor radicals with higher oxidation potentials than *N*-**NN**, such as thianthreneNN (0.97 V),[10] were oxidized by the treatment with iodine. Although the possibility of (iii) can not be excluded strictly, the observation of the reversible redox wave of *N*-**NN** in cyclic voltammetric measurement suggests that *N*-**NN**$^{+\bullet}$ is reasonably stable in solution even at room temperature. Therefore, it is most probable that the ground state of *N*-**NN**$^{+\bullet}$ is singlet. The electronic structures of the ground state singlet *N*-**NN**$^{+\bullet}$ and the ground state triplet β-**NN**$^{+\bullet}$ are discussed in next section. Both *p*-phenylene extended derivatives, *N*-**PN**$^{+\bullet}$ and β-**PN**$^{+\bullet}$, turned out to be ground state triplet. The difference in electronic structure of *N*-**NN** and *N*-**PN** will be discussed in 2-4-5.

2-4-2. Disjoint and Non-Disjoint Classification of PyrrolylNNs

The electronic structure of *N*-**NN**$^{+\bullet}$ and β-**NN**$^{+\bullet}$ are characterized by the "disjoint" and "non-disjoint" classification of diradicals,[11] such as tetramethyleneethane (TME) and trimethylenemethane (TMM).[12] If two radical units are connected at their "inactive" positions (a node of SOMO), the resulted diradical is classified as a "disjoint" one. TME is classified as this type of diradical, where two allyl radicals are connected at their nodal carbons (Figure 2-9(a)), and the ground state of TME is singlet. On the other hand, a "non-disjoint" diradical is formed by connecting two radical units at a "inactive" position and an

15
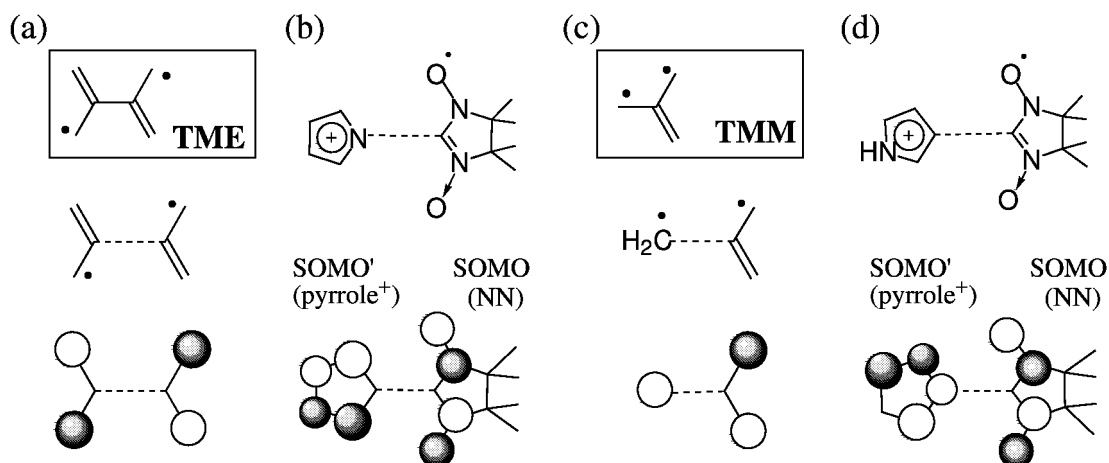
Figure 2-9. Comparison of connection patterns of diradicals.

"active" one, where the coefficient of SOMO is distributed. TMM is classified as this type of diradical, which is composed of an allyl radical and a methyl radical (Figure 2-9(c)). TMM is known to a ground state triplet diradical with the S-T energy gap of *ca.* 13 kcal/mol.[13]

When a pyrrole cation radical and a NN group are connected at the *N*-position of the pyrrole and the -position of the NN, both SOMOs of the pyrrole[+•] and the NN group have nodes at the connecting sites, leading to a disjoint type diradical *N*-**NN**[+•] (Figure 2-9(b)). On the other hand, a NN group is introduced at the 3-position of a pyrrole[+•], the connection should afford a non-disjoint type diradical β-**NN**[+•] (Figure 2-9(d)). The classification of *N*-**NN**[+•] and β-**NN**[+•] is consistent with the experimental results.

2-4-3. Rationalization by Perturbational MO Method

The electronic structures of amine-based spin-polarized donors are found to be rationalized by a perturbational MO method.[14] A similar explanation is effective for the electronic structure of β-**NN**. As shown in Figure 2-10(a), *somo* of the NN group is converted to SOMO of β-**NN** without being perturbed by any MOs of pyrrole. Based on the orbital interaction between *homo* of the pyrrole and *nhomo* of the NN group, the entire-molecular MO (HOMO) is lying at the highest energy level. Such an electronic structure can be maintained due to the large on-site Coulombic repulsion in SOMO. Under this circumstance, an electron should be removed from HOMO upon one-electron oxidation. Since the resulted SOMO' and SOMO are of a space-sharing type, an effective ferromagnetic exchange

16
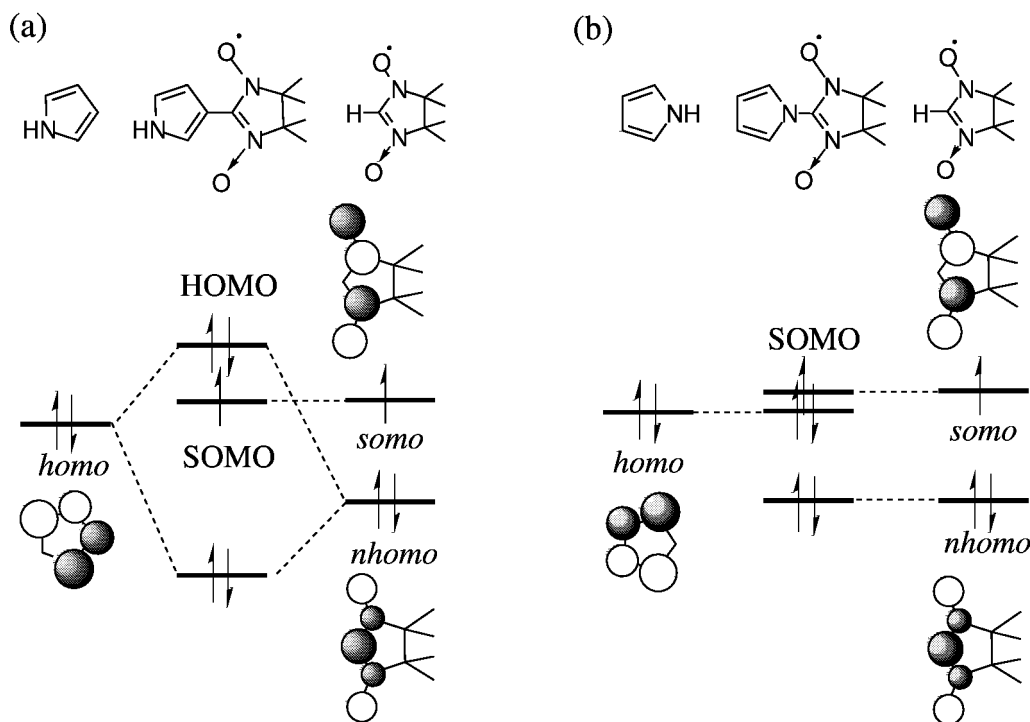
Figure 2-10. Perturbational MO description of (a) β-**NN** and (b) *N*-**NN**.

interaction operates between these two orbitals, giving rise to a ground state triplet cation diradical.

On the contrary, the orbital interaction between *homo* of the pyrrole and *nhomo* of the NN group in *N*-**NN** is considered to be small because the *N*-position of the pyrrole is a node of *homo*. As a result, both orbitals should be left unperturbated as shown in Figure 2-10(b). Since the energy level of *somo* of the NN group is higher than that of *homo* of the pyrrole, SOMO is considered to be the highest orbital of *N*-**NN**. One-electron oxidation of *N*-**NN** should remove the unpaired electron in SOMO, resulting in the generation of a closed-shell cation.

2-4-4. UHF Description of Electronic Structure of PyrrolylNNs

Semi-empirical molecular orbital calculations (UHF/PM3) were performed on these pyrrolylNNs using a MOPAC program. In the case of *N*-**NN**, three MOs are found in the highest energy level region. Two of them are combinations of *homo* of the pyrrole and *somo* of the NN group, and the other is a combination of *nhomo* of the pyrrole and *nhomo* of the NN group. Their energy levels are too close to be discussed quantitatively.

17

(a) *β*-NN   (b) *β*-PN

SOMO

NHOMO(β)

HOMO(α)

HOMO(β)

NHOMO(α)

SOMO
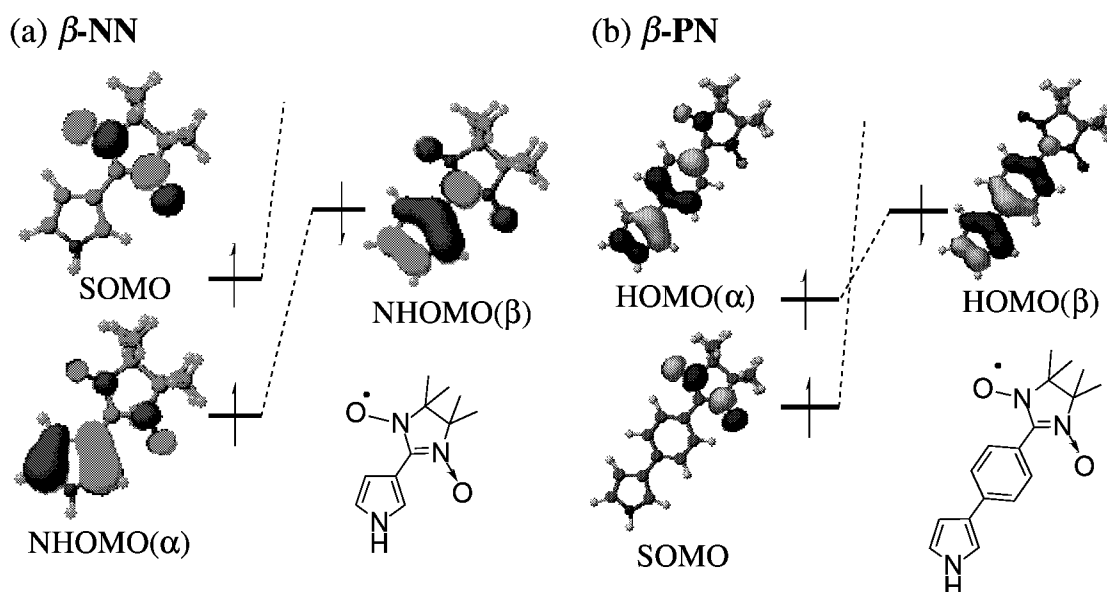
Figure 2-11. Molecular orbitals of β-**NN** and β-**PN** calculated by MOPAC-PM3/UHF. Orbital energy levels are shown qualitatively.

The calculated molecular orbitals of β-**NN** are shown in Figure 2-11(a). The highest energy orbital is NHOMO( ), indicating that an electron to be removed upon one-electron oxidation should be the -spin electron of NHOMO( ). It is to be noted that the orbitals denoted here as NHOMO(,) are attributed to HOMO in PMO description.

The molecular orbitals of β-**PN** are shown in Figure 2-11(b). Showing contrast with those of β-**NN**, HOMO lies at the highest energy level for both - and -spins. When HOMO( ) and HOMO( ) are compared, the -spin orbital is higher in energy level than the -spin one, because of the spin-polarization effect caused by the -spin electron in SOMO.

These electronic structures of β-**NN** and β-**PN** are in accord with the experimental detection of the ground state triplet species by ESR measurements.

A ground state triplet cation diradical was also detected for *N*-**PN**. The UHF calculation for *N*-**PN** revealed that both HOMO( ) and HOMO( ) are higher in energy level than SOMO( ). The molecular orbitals of *N*-**PN** shown in Figure 2-12 indicate that one-electron oxidation of *N*-**PN** should remove the -spin electron in HOMO( ).
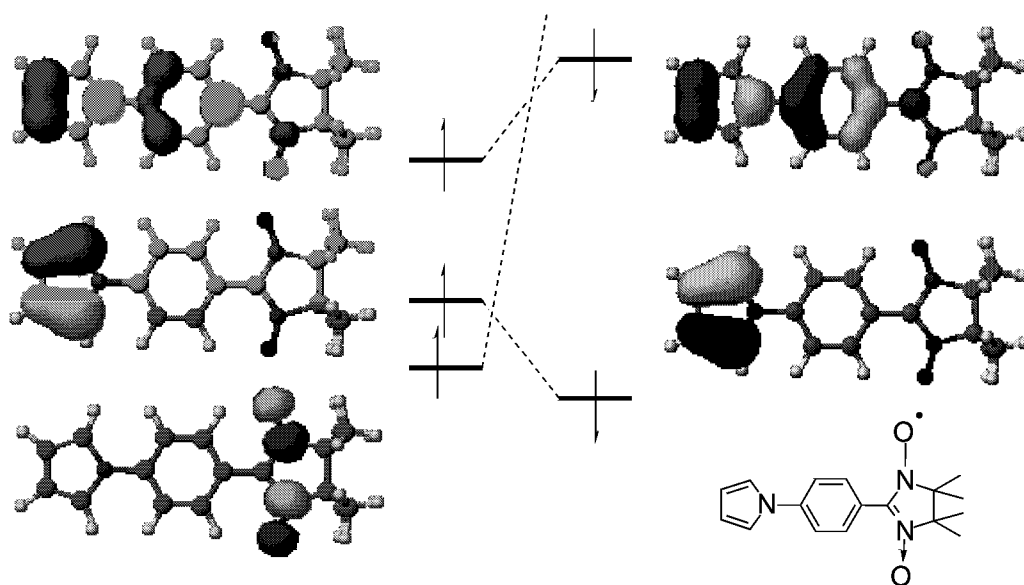
Figure 2-12. Molecular orbitals of **N-PN** calculated by MOPAC/PM3/UHF. Orbital energy levels are shown qualitatively.

2-4-5. Effect of *p*-Phenylene as a Coupler

The difference between the electronic structures of **N-NN** and **N-PN** is also rationalized by using a perturbational molecular orbital method (Figure 2-13). As described above, the connection of pyrrole and NN at the *N*-position does not cause effective interaction between *homo* of pyrrole and *nhomo* of NN. Although *nhomo* of NN interacts with *nhomo* of pyrrole, it may be not enough to afford a ground state triplet species upon one-electron oxidation (Figure 2-13(a)).

On the other hand, *homo* of *N*-phenylpyrrole, which consists of *nhomo* of pyrrole and *homo* of benzene, has coefficients at the *p*-position of benzene ring, where the NN group is connected. Therefore, an effective orbital interaction between *homo* of *N*-phenylpyrrole and *nhomo* of NN affords HOMO of **N-PN**, which spreads over to the entire molecule (Figure 2-13(b)). *homo* of pyrrole and *somo* of NN are left unperturbated in **N-PN**.

The electronic structure of **N-PN** could not be predicted when only a pyrrole cation radical and a NN group are taken into account. Since a *p*-phenylene unit is, in general, an antiferromagnetic coupler of radicals, consideration of the simple connection pattern of a pyrrole cation radical and a NN group with a *p*-phenylene coupler may lead to a wrong answer. Precise examination based on the molecular orbital method is necessary to predict the exact ground state spin multiplicity.

19
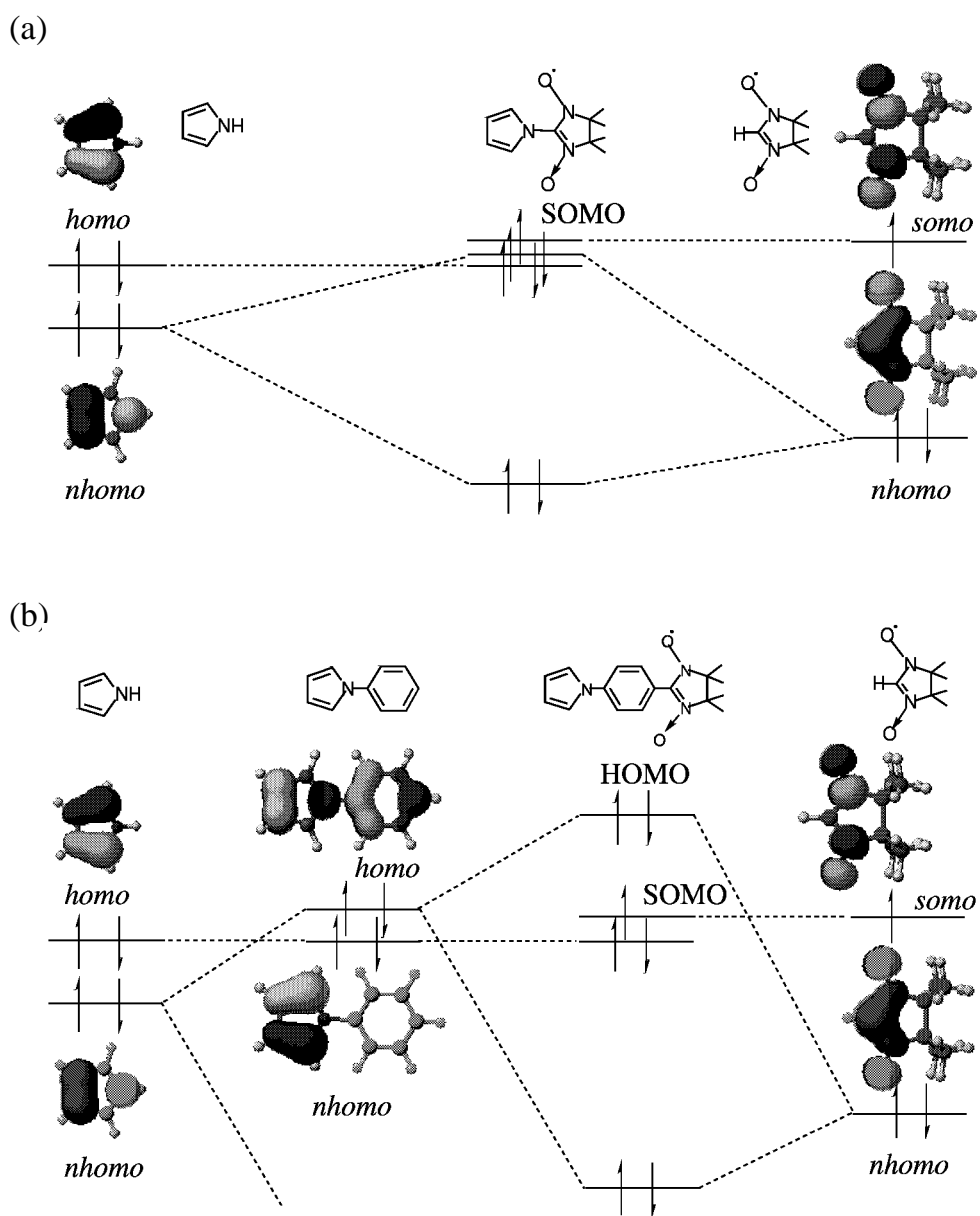
Figure 2-13. Perturbational MO description of (a) *N*-**NN** and (b) *N*-**PN**.

§2-5. Summary

As a basic study of the design of a building block for a conductive magnet, spin correlation in cation diradicals derived from pyrroles carrying nitronyl nitroxide was examined. Since *homo* of pyrrole has a node at the *N*-position, *N*-**NN** did not afford a triplet cation diradical upon one-electron oxidation. On the other hand, β-**NN** and β-**PN** afforded ground state triplet cation diradicals, as expected. A ground state triplet cation diradical was also detected for *N*-**PN**, and the difference between *N*-**NN** and *N*-**PN** was rationalized based on a perturbational MO method. Such results will contribute significantly to the studies on organic high spin molecules.[15]

It turns out that the *p*-phenylene group, which was thought to be a simple spacer of *N*-**PN**, plays, in fact, an important role in the spin correlation in the singly oxidized state of *N*-**PN**. The applicability of *N*-functionalized derivative is advantageous because β-functionalized one has a problem of regioregularity.

Although these pyrrolylNN derivatives are not polymerizable, introduction of pyrrole units as a reaction site at both -positions of the pyrrole ring may enable the polymerization.[16]

§2-6 Experimentals

General Procedures

NMR Spectroscopy. ^{1}H-NMR spectra were recorded on a JEOL JNM-GSX270 spectrometer. The chemical shift references were reported in δ relative to tetramethylsilane (0.00 ppm, for chloroform-d solution) or dimethylsulfoxide-d_5 (2.50 ppm, for dimethyl-sulfoxide-d_6 solution) as an internal standard.

IR Spectroscopy. Infrared spectra were recorded on a Perkin-Elmer 1640 infrared spectrometer using a KBr pellet.

ESR Spectroscopy (in solution). ESR spectra were recorded on a JEOL JES-RE2X spectrometer. The microwave frequency was measured with an Advantest TR5212 counter, and the resonance magnetic field value was measured with the aid of a JEOL ES-FC5 NMR field meter.

Elemental Analysis. Elemental analyses were performed at the Organic Elemental Analysis Center of the Department of Chemistry, Faculty of Science, the University of Tokyo.

Materials

Most of the chemicals were purchased from Wako Pure Chemicals Industries Ltd. (WAKO) and Tokyo Kasei Kogyo Co. Ltd. (TCI). 2-Bromo-4,4,5,5-tetramethyl-imidazoline 3-oxide 1-oxyl (**2**), 3-formylpyrrole (**3**), and 3-bromo-1-(triisopropylsilyl)-pyrrole (**7**) were prepared according literatures.[4,5] 2,3-Bis(hydroxylamino)-2,3-dimethyl-butane was prepared by grinding its sulfate with pottasium hydrogen carbonate, followed by extraction with dichloromethane, and was recrystallized from benzene. There, the sulfate was prepared according literature,[17] while the sulfate used as a catalyst was purchased from Eastman Fine Chemicals (Kodak). Pyrrole (TCI) was distilled from carsium hydride under nitrogen. Dimethylformamide (WAKO) was dried over 4A molecular sieves and distilled under reduced pressure. Tetrahydrofuran (WAKO) was distilled from sodium benzophenone ketyl under nitrogen. Acetonitrile (WAKO) was distilled from carsium hydride under nitrogen. All the other reagents were used as purchased without further purification. Solvents were also purchased from Godo Yozai Co., Ltd. Silica gel was purchased from Fuji Silysia Chemical Co., Ltd. (BW-820MH).

Preparation

2-(Pyrrol-1'-yl)-4,4,5,5-tetramethylimidazoline 3-oxide 1-oxyl (*N*-NN)

Pyrrole (70 µL, 1.0 mmol) was added to a stirred suspension of 45 mg (1.1 mmol) of sodium hydride (WAKO, 60% in mineral oil), which had been washed with hexane, in 10 mL of dimethylformamide at 0 °C under nitrogen atmosphere, and the mixture was stirred for 10 minutes. To the solution, 2-bromo-4,4,5,5-tetramethylimidazoline 3-oxide 1-oxyl (**2**)[4] (230 mg, 1.0 mmol) in 5 mL of dimethylformamide was added, and the mixture was further stirred for 30 minutes. The reaction mixture was extracted with diethylether and water, and the separated organic layer was dried over sodium sulfate,

filtrated, and concentrated in vacuo. The product was purified by column chromatography on silica gel eluted with dichloromethane to afford 97 mg (45%) of **N-NN** as blue solid.

ESR(Benzene): $g = 2.0060$, $a_N = 0.75$ mT (2N).

IR(KBr, cm^{-1}): 1588 (s), 1456 (w), 1405 (s), 1373 (s), 1301 (m), 1260 (m), 1218 (m), 1176 (w), 1143 (m), 1094 (s), 874 (w), 724 (s), 605 (w), 541 (w).

Anal.: calc. C 59.44, H 7.26, N 18.91 %; found C58.89, H 6.98, N 18.39 %.

2-(Pyrrol-3'-yl)-4,4,5,5-tetramethylimidazoline 3-oxide 1-oxyl (β-NN)

To a solution of 302 mg (3.2 mmol) of 3-formylpyrrole (**3**)[5] in 20 mL of benzene, 471 mg (3.2 mmol) of 2,3-bis(hydroxylamino)-2,3-dimethylbutane and catalytic amount of 2,3-bis(hydroxylamino)-2,3-dimethylbutane sulfate were added. The mixture was stirred overnight under nitrogen atomosphere at room temperature. To this suspension, 3.86 g (16.1 mmol) of lead dioxide (WAKO) was added. The mixture was stirred for 30 minutes and filtrated. The filtrate was concentrated and purified by column chromatography on silica gel eluted with ethyl acetate - hexane (3:1 to 1:0) to afford 253 mg (35%) of β-**NN** as blue solid.

ESR(Benzene): $g = 2.0053$, $a_N = 0.76$ mT (2N).

IR(KBr, cm^{-1}): 3183 (m : N-H), 1585 (m), 1496 (m), 1392 (m), 1373 (m), 1341 (s), 1212 (m), 1164 (w), 1134 (w), 1084 (m), 867 (w), 786 (m), 661 (w), 613 (w), 543 (w).

1-(4'-Bromophenyl)pyrrole (4)

To a solution of 15.8 g (92 mmol) of 4-bromoaniline (TCI) in 45 mL of acetic acid, 12.0 mL (92 mmol) of 2,5-dimethoxytetrahydrofuran (TCI) was added, and the mixture was heated under reflux for 1 hour. The solvent was removed under reduced pressure. The residue was dissolved in dichloromethane and passed through a short silica gel plug. Removal of the solvent afforded 18.0 g (85%) of light blown solid.

^{1}H-NMR(CDCl$_3$): $\delta = 7.53$ (d, $J = 8.8$ Hz, 2H), 7.26 (d, $J = 8.8$ Hz, 2H), 7.04 (t, $J = 2.2$ Hz, 2H), 6.35 (t, $J = 2.2$ Hz, 2H).

1-(4'-Formylphenyl)pyrrole (5)

To a solution of 9.0 g (40 mmol) of 1-(4'-bromophenyl)pyrrole (**4**) in 180 mL of tetrahydrofuran, 30 mL (48 mmol) of *n*-butyllithium (WAKO, 1.6 M in hexane) was added dropwise at -70 ˚C under nitrogene atmosphere, and the mixture was stirred for 2 hours. Dimethylformamide (3.6 mL, 47 mmol) was added, and the mixture was further stirred for 4 hours with warming up to room temperature. Small amount of aqueous ammonium chloride was added, and the reaction mixture was extracted with diethylether and water. The separated organic layer was dried over magnesium sulfate, filtrated, concentrated, and purified by column chromatography on silica gel eluted with dichloromethane - hexane (2:1) to afford 5.8 g (80%) of pale blown solid.

^{1}H-NMR(CDCl$_3$): $\delta = 9.99$ (s, 1H), 7.94 (d, $J = 8.8$ Hz, 2H), 7.53 (d, $J = 8.8$ Hz, 2H), 7.18 (t, $J = 2.2$ Hz, 2H), 6.40 (t, $J = 2.2$ Hz, 2H).

2-(4'-(pyrrol-1''-yl)phenyl)-4,4,5,5-tetramethylimidazoline 3-oxide 1-oxyl (N-PN)

To a solution of 230 mg (1.6 mmol) of 2,3-bis(hydroxylamino)-2,3-dimethylbutane in 10 mL of methanol, 200 mg (1.2 mmol) of 1-(4'-formylphenyl)pyrrole (**5**) and catalytic amount of 2,3-bis(hydroxylamino)-2,3-dimethylbutane sulfate were added. The mixture was heated under reflux for 2 hours and stirred overnight at room temperature under

nitrogen atomosphere. After the solvent was removed in vacuo, the residue was suspended in 14 mL of benzene. To this suspension, 2.27 g (9.5 mmol) of lead dioxide (WAKO) was added. The mixture was stirred for 30 minutes and filtrated. The filtrate was concentrated and purified by column chromatography on silica gel eluted with ethyl acetate - hexane (3:1 to 1:0) to afford 103 mg (30%) of **N-PN** as a blue solid.

ESR(benzene): $g = 2.0060$, $a_N = 0.75$ mT.

IR(KBr, cm^{-1}): 1604 (m), 1535 (m), 1495 (m), 1447 (w), 1422 (w), 1396 (s), 1368 (s), 1329 (s), 1303 (w), 1261 (w), 1208 (m), 1165 (w), 1128 (m), 1068 (w), 1019 (w), 920 (w), 842 (m), 736 (m), 618 (w), 542 (w), 502 (w).

Anal.: calc. C 68.44, H 6.76, N 14.08 %; found C 67.97, H 6.61, N 13.95 %.

3-(4'-Formylphenyl)-1-(triisopropylsilyl)pyrrole (9)

To a solution of 5.89 g (19.5 mmol) of 3-bromo-1-(triisopropylsilyl)pyrrole (**7**)[5] 42 in 30 mL of tetrahydrofuran, 15.0 mL (24.0 mmol) of *n*-butyllithium (WAKO, 1.6 M in hexane) was added dropwise at -95 ℃ under nitrogen atomosphere, and the mixture was stirred for 1.5 hours. To this solution, 5.50 mL (20.3 mmol) of tributyltin chloride (TCI) was added dropwise, and the mixture was further stirred for 3.5 hours with gradual increasing of temperature. The reaction mixture was extracted with diethylether and water, and the organic layer was concentrated in vacuo to afford 11.0 g of pale yellow oil. The oil was dissolved in 40 mL of toluene. To the solution, 3.71 g (20.0 mmol) of 4-bromobenzaldehyde (TCI) and 1.40 g (2.00 mmol) of bis(triphenylphosphine)-palladium(II) dichloride (TCI) were added, and the mixture was heated under reflux for 5 hours. The mixture was extracted with water and ethyl acetate. The organic layer was concentrated and purified by column chromatography on silica gel eluted with dichloromethane - hexane (1:1) to afford 3.32 g (50%) of yellow oil.

^{1}H-NMR(CDCl$_3$): δ = 9.95 (s, 1H), 7.83 (dt, J_d = 8.42 Hz, 2H), 7.68 (dt, J_d = 8.43 Hz, 2H), 7.19 (t, 1H), 6.84 (dd, 1H), 6.69 (dd, 1H), 1.50 (seven, 3H), 1.13 (d, 18H).

3-(4'-Formylphenyl)pyrrole (10)

To a solution of 3.32 g (10.1 mmol) of 3-(4'-formylphenyl)-1-(triisopropylsilyl)-pyrrole (**9**) in 30 mL of tetrahydrofuran, 10.0 mL (10.0 mmol) of tetrabutylammonium fluoride (TCI, 1.0 M in tetrahydrofuran) was added dropwise, and the mixture was stirred for 40 minutes. The reaction mixture was extracted with diethylether (*ca.* 160 mL) and water. The organic layer was dried over sodium sulfate, filtrated, concentrated in vacuo, and purified by column chromatography on silica gel eluted with dichloromethane to afford 1.67 g (95%) of ivory powder.

^{1}H-NMR(CDCl$_3$): δ = 9.96 (s, 1H), 7.85 (dt, J_d = 8.80, 2H), 7.68(dt, J_d = 8.06, 2H), 7.24 (m, 1H), 6.88 (m, 1H), 6.62 (m, 1H).

^{1}H-NMR(DMSO-*d6*): δ = 9.90 (s, 1H), 7.78 (dd, J = 9.52 Hz, 8.43 Hz, 4H), 7.45 (dd, J = 2.57 Hz, 1.83 Hz, 1H), 6.85 (dd, J = 2.56 Hz, 1.84 Hz, 1H), 6.57 (dd, J = 2.56 Hz, 1.84 Hz, 1H).

IR (KBr, cm^{-1}) 3276 (s : N-H), 1681 (s : C=O), 1660 (m), 1603 (s), 1570 (m), 1554 (w), 1516 (w), 1483 (w), 1431 (m), 1398 (w), 1347 (w), 1309 (w), 1224 (m), 1172 (s), 1114 (w), 1106 (w), 1080 (w), 916 (w), 840 (s), 796 (s), 752 (w), 718 (m), 686 (w), 597 (m), 511 (w).

1,3-Dihydroxy-2-(4'-(pyrrol-3''-yl)phenyl)-4,4,5,5-tetramethylimidazolidine (11)

3-(4'-Formylphenyl)pyrrole (**10**) (1.42 g, 8.3 mmol) and 2,3-bis(hydroxyamino)-2,3-dimethylbutane (1.22 g, 8.2 mmol) were dissolved in 48 mL of benzene-methanol (5:1). To the solution, a spoon of 2,3-bis(hydroxyamino)-2,3-dimethylbutane sulfate was added and the mixture was stirred for 2 days at room temperature under nitrogen atmosphere. The precipitates were filtrated, washed with benzene, and dried in vacuo to afford 676 mg (25%) of colorless powder.

^{1}H-NMR(DMSO-$d6$): δ = 7.70 (s : 2H), 7.46 (d, J = 8.06 Hz : 2H), 7.38 (d, J = 8.06 Hz : 2H), 7.17 (q, J = 2.56 Hz, 1.83 Hz : 1H), 6.77 (q, J = 2.56 Hz, 2.20 Hz : 1H), 6.41 (q, J = 2.57 Hz, 2.20 Hz, 1.83 Hz : 1H), 4.48 (s : 1H), 1.06 (d, J = 6.96 : 12H).

IR (KBr, cm^{-1}): 3435 (s), 3242 (m), 1614 (m), 1514 (w), 1480 (m), 1428 (m), 1378 (m), 1366 (m), 1155 (m), 1145 (m), 1108 (m), 914 (m), 875 (m), 793 (m), 782 (m), 713 (w), 688 (m).

2-(4'-(pyrrol-3''-yl)phenyl)-4,4,5,5-tetramethylimidazoline 3-oxide 1-oxyl (β-PN)

To a solution of 676 mg (2.2 mmol) of 1,3-dihydroxy-2-(4'-(pyrrol-3''-yl)phenyl)-4,4,5,5-tetramethylimidazolidine (**11**) in 40 mL of tetrahydrofuran, a drop of triethylamine and 2.79 g (11.7 mmol) of lead dioxide (WAKO) were added, and the mixture was stirred for 4 hours. The mixture was filtrated and the filtrate was concentrated in reduced pressure. The residue was purified by column chromatography on silica gel eluted with tetrahydrofuran to afford 378 mg (55%) of β-**PN** as a blue solid.

ESR(benzene): g = 2.0055, a_N = 0.707 mT.

IR(KBr, cm^{-1}): 3347 (br : N-H), 1606 (s), 1497 (w), 1447 (w), 1417 (m), 1392 (s), 1368 (s), 1349 (s), 1306 (m), 1288 (w), 1207 (m), 1169 (m), 1134 (m), 1108 (w), 1083 (w), 1039 (w), 914 (m), 872 (w), 844 (m), 805 (m), 733 (w), 595 (w), 542 (w).

Measurements and Calculations

Cyclic Voltammetry. Cyclic voltammograms were recorded in acetonitrile solution in the presence of 0.1 M tetra-n-butylammonium perchlorate (Nacalai Tesque Inc.) as an supporting electrolyte with a platinum working electrode using a Hokuto Denko HAB 151 potentiostat/galvanostat at room temperature. An Ag/AgCl electrode (BAS Co.) was used for a reference electrode. Scanning rate was 200 mV/s.

ESR Measurement. ESR spectra were measured on a JEOL JES-RE2X spectrometer equipped with an Air Products LTR-3 liquid helium transfer system. The temperature was controlled manually by adjusting helium gas flow rate, and was measured with an Advantest TR2114H digital multi-thermometer with a gold-iron thermocouple. The microwave frequency was measured with an Advantest TR5212 counter, and the resonance magnetic field value was measured with the aid of a JEOL ES-FC5 NMR field meter. Zero-field parameters were calculated by a high-field approximation.

Molecular Orbital Calculation. PM3/UHF molecular orbital calculations were performed using a CAChe MOPAC program provided from SONY Techtronics Inc.

§2-7. References and Notes

1. Conductivity of polymerized materials of pyrrole was discovered early times.[a] such a conductive polypyrrole was found to be obtained by electrochemical polymerization.[b] In earlier studies on the conduction mechanism of conductive polymers, main carriers were characterized as bipolarons.[c-g] Recently, optical and structural studies on oligothiophenes revealed the existence of a -dimer of oligothiophene cation radicals.[h-k] Calculational studies pointed out the important role of polarons in conductive polymers.[l] Further optical study concluded that main carriers in polythiophene are polarons.[m,n] An ESR study on oligopyrrole found a -dimer of cation radicals of oligopyrroles.[o] Argument on the conduction mechanism has not been concluded yet. In the target conductive magnetic polypyrrole, however, charge carriers should be polarons.

a) Armour M, Davies AG, Upadhyay J, Wassermann A, "Colored electrically conducting polymers from furan, pyrrole, and thiophene", *J. Polym. Sci. A-1* **1967**, *5*, 1527-1538.

b) Dall'Olio A, Dascola G, Varacca V, Bocchi V, "Electron paramagnetic resonance and conductivity of an electrolytic oxypyrrole (pyrrole polymer) black", *Compt. Rend. Acad. Sci. Paris Ser. C* **1968**, *267*, 433-435; *Chem. Abstr.* **1968**, *69*, 112026u.

c) Scott JC, Pfluger P, Krounbi MT, Street GB, "Electron-spin-resonance studies of pyrrole polymers: Evidence for bipolarons", *Phys. Rev. B* **1983**, *28*, 2140-2145.

d) Brédas JL, Street GB, "Polarons, bipolarons, and solitons in conducting polymers", *Acc. Chem Res.* **1985**, *18*, 309-315.

e) Genoud F, Guglielmi M, Nechtschein M, Genies E, Salmon M, "ESR study of electrochemical doping in the conducting polymer polypyrrole", *Phys. Rev. Lett.* **1985**, *55*, 118-121.

f) Patil AO, Heeger AJ, Wudl F, "Optical properties of conducting polymers", *Chem. Rev.* **1988**, *88*, 183-200.

g) Heeger AJ, Kivelson S, Schrieffer JR, Su W-P, "Solitons in conducting polymers", *Rev. Mod. Phys.* **1988**, *60*, 781-850.

h) Hill MG, Mann KR, Miller LL, Penneau J-F, "Oligothiophene cation radical dimers. An alternative to bipolarons in oxidized polythiophene", *J. Am. Chem. Soc.* **1992**, *114*, 2728-2730.

i) Bäuerle P, Segelbacher U, Maier A, Mehring M, "Electronic structure of mono- and dimeric cation radicals in end-capped oligothiophenes", *J. Am. Chem. Soc.* **1993**, *115,* 10217-10223.

j) Miller LL, Mann KR, " -Dimers and -stacks in solution and in conducting polymers", *Acc. Chem. Res.* **1996**, *29*, 417-423.

k) Graf DD, Duan RG, Campbell JP, Miller LL, Mann KR, "From monomers to -stacks. A comprehensive study of the structure and properties of monomeric, -dimerized, and -stacked forms of the cation radical of 3',4'-dibutyl-2,5"-diphenyl-2,2':5',2"-terthiophene", *J. Am. Chem. Soc.* **1997**, *119*, 5888-5899.

l) Shimoi Y, Abe S, "Competition between polarons and bipolarons in nondegenerate conjugated polymers", *Phys. Rev. B* **1994**, *50*, 14781-14784.

m) Yokonuma N, Furukawa Y, Tasumi M, Kuroda M, Nakayama J, "Electronic absorption and Raman studies of BF_4^--doped polythiophene based on the spectra of the radical cation and dication of -sexithiophene", *Chem. Phys. Lett.* **1996**, *255*, 431-436.

n) Furukawa Y, "Electronic absorption and vibrational spectroscopies of conjugated conducting polymers", *J. Phys. Chem.* **1996**, *100*, 15644-15653.

o) van Haare JAEH, Groenendaal L, Havinga EE, Janssen RAJ, Meijer EW, " -dimers of end-capped oligopyrrole cation radicals", *Angew. Chem. Int. Ed. Engl.* **1996**, *35*, 638-640.

2.a) Crayston JA, Iraqi A, Walton JC, "Polyradicals: synthesis, spectroscopy, and catalysis", *Chem. Soc. Rev.* **1994**, 147-153.

b) Kakouris C, Crayston JA, Walton JC, "Poly(*N*-hydroxypyrrole) and poly(3-phenyl-*N*-hydroxypyrrole): synthesis, conductivity, spectral properties and oxidation", *Synth. Metals* **1992**, *48*, 65-77.

   c) Yamamoto T, Hayashi H, " -Conjugated soluble and fluorescent poly(thiophene-2,5-diyl)s with phenolic, hindered phenolic and p-$C_6H_4OCH_3$ substituents. Preparation, optical properties, and redox reaction", *J. Polym. Sci. A* **1997**, *35*, 463-474.

   d) Xie C, Lahti PM, "Regiospecific design strategies for 3-arylpolythiophenes with pendant stable radical groups", *J. Polym. Sci. A* **1999**, *37*, 779-788.

   e) Lu HSM, Berson JA, "Catenation of heterocyclic non-Kekulé biradical to tetraradical prototypes of conductive or magnetic polymers", *J. Am. Chem. Soc.* **1997**, *119*, 1428-1438.

   f) Nishide H, Kaneko T, Kuzumaki Y, Yoshioka N, Tsuchida E, "Poly(phenylvinylene) and poly(phenylenevinylene) with nitroxide radicals", *Mol. Cryst. Liq. Cryst.* **1993**, *232*, 143-150.

   g) Kaneko T, Toriu S, Kuzumaki Y, Nishide H, "Poly(phenylenevinylene) bearing built-in *tert*-butylnitroxide. A polyradical ferromagnetically coupled in the intrachain", *Chem. Lett.* **1994**, 2135-2138.

   h) Nishide H, Kaneko T, Toriu S, Kuzumaki Y, Tsuchida E, "Synthesis of and ferromagnetic coupling in poly(phenylenevinylene)s bearing built-in *t*-butyl nitroxides", *Bull. Chem. Soc. Jpn.* **1996**, *69*, 499-508.

   i) Nishide H, Kaneko T, Nii T, Katoh K, Tsuchida E, Yamaguchi K, "Through-bond and long-range ferromagnetic spin alignment in a -conjugated polyradical with a poly(phenylenevinylene) skeleton", *J. Am. Chem. Soc.* **1995**, *117*, 548-549.

   j) Nishide H, Kaneko T, Nii T, Katoh K, Tsuchida E, Lahti PM, "Poly(phenylenevinylene)-attached phenoxyl radicals: Ferromagnetic interaction through planarized and -conjugated skeletons", *J. Am. Chem. Soc.* **1996**, *118*, 9695-9704.

   k) Nishide H, Miyasaka M, Tsuchida E, "High-spin polyphenoxyls attached to star-shaped poly(phenylenevinylene)s", *J. Org. Chem.* **1998**, *63*, 7399-7407.

   l) Nishide H, Miyasaka M, Tsuchida E, "Average octet radical polymer: A stable polyphenoxyl with star-shaped   conjugation", *Angew. Chem. Int. Ed.* **1998**, *37*, 2400-2402.

   m) Nishide H, Maeda T, Oyaizu K, Tsuchida E, "High-spin polyphenoxyl based on poly(1,4-phenyleneethynylene)", *J. Org. Chem.* **1999**, *64*, 7129-7134.

   n) Nishide H, Takahashi M, Takashima J, Pu Y-J, Tsuchida E, "Acyclic and cyclic di- and tri(4-oxyphenyl-1,2-phenyleneethynylene)s: Their synthesis and ferromagnetic spin interaction", *J. Org. Chem.* **1999**, *64*, 7375-7380.

   o) Miura Y, Issiki T, Ushitani Y, Teki Y, Itoh K, "Synthesis and magnetic behavior of polyradical: poly(1,3-phenyleneethynylene) with -toporegulated pendant stable aminoxyl and imine *N*-oxide-aminoxyl radicals", *J. Mater. Chem.* **1996**, *6*, 1745-1750.

   p) Oka H, Tamura T, Miura Y, Teki Y, "Synthesis and magnetic behavior of poly(1,3-phenylene)-based polyradical carrying *N-tert*-butylaminoxyl radicals", *J. Mater. Chem.* **1999**, *9*, 1227-1232.

3.   Kumai R, Matsushita MM, Izuoka A, Sugawara T, "Intramolecular exchange interaction in a novel cross-conjugated spin system composed of -ion radical and nitronyl nitroxide", *J. Am. Chem. Soc.* **1994**, *116*, 4523-4524.

4.   Boocock DGB, Ullman EF, "Studies of stable free radicals. III. A 1,3-dioxy-2-imidazolidone zwitterion and its stable nitronyl nitroxide radical anion", *J. Am. Chem. Soc.* **1968**, *90*, 6873-6874.

5.   Bray BL, Mathies PH, Naef R, Solas DR, Tidwell TT, Artis DR, Muchowski JM, "*N*-(Triisopropylsilyl)pyrrole. A progenitor 'par excellence' of 3-substituted pyrroles", *J. Org. Chem.* **1990**, *55*, 6317-6328.

6.   Ullman EF, Osiecki JH, Boocock DGB, Darcy R, "Studies of stable free radicals. X. Nitronyl nitroxide monoradicals and biradicals as possible small molecule spin labels", *J. Am. Chem. Soc.* **1972**, *94*, 7049-7059.

7.   Stille JK, "The palladium-catalyzed cross-coupling reactions of organotin reagents with organic electrophiles", *Angew. Chem. Int. Ed. Engl.* **1986**, *25*, 508-524.

8.   There are two explanations for the polymerization mechanism of pyrrole. One is based on a coupling reaction of two cation radicals. The other is featured by a radical attack to a neutral molecule. The effect of the NN group on the reactivity of pyrrole is to be

examined.

   a) Zhou M, Heinze J, "Electropolymerization of pyrrole and electrochemical study of polypyrrole. 2. Influence of acidity on the formation of polypyrrole and the multipathway mechanism", *J. Phys. Chem. B* **1999**, *103*, 8443-8450.

   b) Lowen SV, van Dyke JD, "Mechanistic studies of the electrochemical polymerization of pyrrole: deuterium isotope effects and radical trapping studies", *J. Polym. Sci. A* **1990**, *28*, 451-564.

   c) Waltman RJ, Bargon J, "Reactivity/structure correlations for the electropolymerization of pyrrole: An INDO/CNDO study of the reactive sites of oligomeric radical cations", *Tetrahedron* **1984**, *40*, 3963-3970.

9. In general, the lifetime of a cation radical of an -vacant pyrrole derivative is very short. For example, the lifetime of pyrrole$^{+\bullet}$ and tri(isopropylsilyl)pyrrole$^{+\bullet}$ were determined to be 30 μs and 250 μs, respectively. The kinetic stability of the cation diradicals of pyrrolylNNs is considered to be very high compared with these derivatives.

   a) Andrieux CP, Audebert P, Hapiot P, Savéant JM, "Observation of the cation radicals of pyrrole and of some substituted pyrroles in fast-scan cyclic voltammetry. Standard potentials and lifetimes", *J. Am. Chem. Soc.* **1990**, *112*, 2349-2440.

   b) Andrieux CP, Audebert P, Hapiot P, Savéant JM, "Identification of the first steps of the electrochemical polymerization of pyrroles by means of fast potential step techniques", *J. Phys. Chem.* **1991**, *95*, 10158-10164.

10. Borden WT, Davidson ER, "Effect of electron repulsion in conjugated hydrocarbon diradicals", *J. Am. Chem. Soc.* **1977**, *99*, 4587-4594.

11. Izuoka A, Hiraishi M, Abe T, Sugawara T, Sato K, Takui T, "Spin alignment in singly oxidized spin-polarized diradical donor: Thianthrene bis(nitronyl nitroxide)", submitted to *J. Am. Chem. Soc.*

12.a) Cramer CJ, "Paul Dowd and diradicals", *J. Chem. Soc. Perkin Trans. 2* **1998**, 1007-1013.

   b) Dowd P, "Trimethylenemethane", *Acc. Chem. Res.* **1972**, *5*, 242-248.

   c) Dowd P, "Tetramethyleneethane", *J. Am. Chem. Soc.* **1970**, *92*, 1066-1068.

   d) Berson JA, "The chemistry of trimethylenemethanes, a new class of biradical reactive intermediates", *Acc. Chem. Res.* **1978**, *11*, 446-453.

   e) Berson JA, "A new class of non-Kekulé molecules with tunable singlet-triplet energy spacings", *Acc. Chem. Res.* **1997**, *30*, 238-244.

   f) Borden WT, Iwamura H, Berson JA, "Violations of Hund's rule in non-Kekulé hydrocarbons: Theoretical prediction and experimental verification", *Acc. Chem. Res.* **1994**, *27*, 109-116.

   g) Borden WT, Davidson ER, "The importance of including dynamic electron correlation in *ab initio* calculations", *Acc. Chem. Res.* **1996**, *29*, 67-75.

13. Wenthold PG, Hu J, Squires RR, Lineberger WC, "Photoelectron spectroscopy of the trimethylenemethane negative ion. The singlet-triplet splitting of trimethylenemethane", *J. Am. Chem. Soc.* **1996**, *118*, 475-476.

14. Sakurai H, Izuoka A, Sugawara T, "Design, preparation and electronic structure of high-spin cation diradicals derived from amine-based spin-polarized donors", submitted to *J. Am. Chem. Soc.*

15. Development of high spin molecules is an important issue in molecular magnetism.[a] The ground state triplet species reported hitherto can be classified into three categories, *i.e.*, (i) one-centered diradical, (ii) multi-centered diradical with two degenerated MOs, and (iii) multi-centered diradical with two non-degenerated MOs. "Spin-polarized donor" belongs to the third category.

    One-centered diradicals such as carbenes or nitrens have two unpaired electrons in - and -orbitals. Although these orbitals are not degenerated, triplet ground state is realized by larger exchange interaction than the energy difference of the two orbitals. Such a situation resembles to a high-spin state transition metal ion in a weak crystal field.

    Two degenerated MOs are achieved by either high-symmetry or topological effect. High-symmetrical diradicals such as antiaromatics (*ex.* cyclopentadienyl cation)[b] or C$_{60}$

dianion have two degenerated MOs. Even though geometrical symmetry is not high, a topological effect affords degenerated non-bonding MOs in non-Kekulé alternant hydrocarbons, such as *m*-quinodimethane. In these molecules, the unpaired electrons occupy the degenerated molecular orbitals according to Hund's rule at the molecular level, affording the high-spin ground state. Along this line, diradicals connected with a *m*-phenylene, or triradicals connected with a benzene-1,3,5- skeleton have been reported for methyl radical derivatives,[c] aminium radicals,[d] other cation radicals,[e] nitroxide radicals,[f] or nitronyl nitroxide radicals.[g] Such skeleton was combined with carbenic species to afford higher ground state spin multiplicities. The first ground state quintet dicarbene was reported by Itoh and Wasserman.[h]

Such a -topological rule can be extended further. As an extention of the ground state quintet dicarbene, spin multiplicity of a linear tetracarbene was determined to be nonet by Sugawara, in terms of temperature dependence of the magnetic susceptibility and the field dependence of magnetization.[i] The spin quantum number of this molecule exceeds that of transition metal ions, including Fe(III) and Gd(III). Dendrimeric high spin polyradicals,[j] polycarbenes,[k] and poly(aminium)radicals,[l] or macrocyclic polyradicals[m] have been reported to bring up spin quantum number record to $S = 40$. As another extention, polaronic high spin systems was proposed,[n] and several examples have been reported.[o]

The author prepared *m*-phenylene-bispyrrole (**mPBP**) and 1,3,5-tris(pyrrol-2'-yl)benzene (**1,3,5-TPB**), and examined high spin state of doped poly-*m*-phenylene-bipyrrole.[p] The spin-containing unit of polaronic high spin system can also work as a conduction unit.

mPBP **1,3,5-TPB**
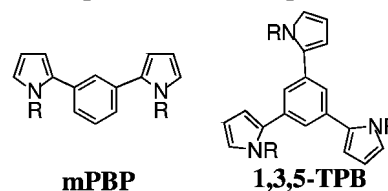
The high spin state based on geometrical symmetry, however, tends to be broken by Jahn-Teller distortion.[q] The high spin state based on -topology sometimes can not be achieved due to a twisting or an effect of hetero-atoms.[r]

a) Lahti PM ed, *"Magnetic Properties of Organic Materials"*, Marcel Dekker, **1999**.

b$_1$) Breslow R, Chang HW, Hill R, Wasserman E, "Stable triplet states of some cyclopentadienyl cations", *J. Am. Chem. Soc.* **1967**, *89*, 1112-1119.

b$_2$) Saunders M, Berger R, Jaffe A, McBride JM, O'Neill J, Breslow R, Hoffman JM Jr, Perchonock C, Wasserman E, Hutton RS, Kuck VJ, "Unsubstituted cyclopentadienyl cation, a ground-state triplet", *J. Am. Chem. Soc.* **1973**, *95*, 3017-3018.

b$_3$) LePege TJ, Breslow R, "Charge-transfer complexes as potential organic ferromagnets", *J. Am. Chem. Soc.* **1987**, *109*, 6412-6421.

b$_4$) Gherghel L, Brand JD, Baumgarten M, Müllen K, "Exceptional triplet and quartet states in highly charged hexabenzocoronenes", J. Am. Chem. Soc. 1999, 121, 8104-8105.

c$_1$) Schlenk W, Brauns M, *Ber. Dtsch. Chem. Ges.* **1915**, *48*, 661.

c$_2$) Leo M, *Ber.* **1937**, *70*, 1691.

c$_3$) Kothe G, Denkel KH, Sümmermann W, "*Schlenk*'s biradical. A molecule in the triplet ground state", *Angew. Chem. Int. Ed.* **1970**, *9*, 906-907.

c$_4$) Kothe G, Ohmes E, Brickmann J, Zimmermann H, "1,3,5-Benzenetriyltris[di(*p*-biphenyl) methyl], a radical having a quartet ground state that dimerizes by entropy bonding", *Angew. Chem. Int. Ed.* **1971**, *10*, 938-940.

d$_1$) Yoshizawa K, Chano A, Ito A, Tanaka K, Yamabe T, Fujita H, Yamauchi J, "Electron spin resonance of the quartet state of 1,3,5-tris(diphenylamino)benzene", *Chem. Lett.* **1992**, 369-372.

d$_2$) Yoshizawa K, Hatanaka M, Tanaka K, Yamabe T, "Molecular orbital study on cationic states of triphenylene and 1,3,5-tris(diphenylamino)benzene as a design of charge-transfer organic ferromagnets", *Synth. Metals* **1995**, *71*, 1829-1830.

d$_3$) Yoshizawa K, Hatanaka M, Ago H, Tanaka K, Yamabe T, "Magnetic properties of 1,3,5-tris[bis(p-methoxyphenyl)amino]benzene cation radicals", *Bull. Chem. Soc. Jpn.* **1996**, *69*, 1417-1422.

29

d$_4$) Sato K, Yano M, Furuich M, Shiomi D, Takui T, Abe K, Itoh K, Higuchi A, Katsuma K, Shirota Y, "Polycationic high-spin states of one- and two-dimensional (diarylamino) benzenes, prototypical model units for purely organic ferromagnetic metals as studied by pulsed ESR / electron spin transient nutation spectroscopy", *J. Am. Chem. Soc.* **1997**, *119*, 6607-6613.

d$_5$) Nakamura Y, Iwamura H, "Magnetic properties of CT complexes between 2,2",5,5"-tetrakis(dimethylamino)terphenyls and TCNQF$_4$", *Bull. Chem. Soc. Jpn.* **1993**, *66*, 3724-3728.

d$_6$) Sasaki S, Iyoda M, "Synthesis and oxidation of di-, tri-, tetra-, and pentaamines", *Mol. Cryst. Liq. Cryst.* **1995**, *272*, 175-182.

d$_7$) Stickley KR, Blackstock SC, "Triplet dication and quartet trication of a triaminobenzene", *J. Am. Chem. Soc.* **1994**, *116*, 11576-11577.

d$_8$) Stickley KR, Selby TD, Blackstock SC, "Isolable polyradical cations of polyphenylene-diamines with populated high-spin states", *J. Org. Chem.* **1997**, *62*, 448-449.

d$_9$) Selby TD, Blackstock SC, "Preparation of a redox-gradient dendrimer. Polyamines designed for one-way electron transfer and charge capture", *J. Am. Chem. Soc.* **1998**, *120*, 12155-12156.

d$_{10}$) Wienk MM, Janssen RAJ, "Stable triplet-state di(cation radicals) of a *N*-phenylaniline oligomer", *Chem. Commun.* **1996**, 267-268.

d$_{11}$) Wienk MM, Janssen RAJ, "Stable triplet-state di(cation radicals) of a *meta-para* aniline oligomer by 'acid doping'", *J. Am. Chem. Soc.* **1996**, *118*, 10626-10628.

d$_{12}$) Wienk MM, Janssen RAJ, "High-spin cation radicals of *meta-para* aniline oligomers", *J. Am. Chem. Soc.* **1997**, *119*, 4492-4501.

e$_1$) Iyoda M, Fukuda M, Yoshida M, Sasaki S, "Multi-tetrathiafulvalene systems. New donors containing two or three tetrathiafulvalene-substituents at 1,3- and 1,3,5-positions of aromatic rings", *Chem. Lett.* **1994**, 2369-2372.

e$_2$) Okada K, Matsumoto K, Oda M, Murai H, Akiyama K, Ikegami Y, "Preparation and spin-spin interactions of 4,4'-(*m*-phenylene)bis(1-methyl-2,6-diphenylpyridinyl) and its analogue", *Tetrahedron Lett.* **1995**, *36*, 6689-6692.

e$_3$) Wienk MM, Janssen RAJ, "High-spin cation radicals of methylenephosphoranes", *J. Am. Chem. Soc.* **1997**, *119*, 5398-5403.

f$_1$) Calder A, Forrester AR, James PG, Luckhurst GR, "Nitroxide radicals. V. *N,N'*-di-*t*-butyl-*m*-phenylenebinitroxide, a stable triplet", *J. Am. Chem. Soc.* **1969**, *91*, 3724-3727.

f$_2$) Mukai K, Nagai H, Ishizu K, "The proof of a triplet ground state in the *N,N'*-di-*t*-butyl-*m*-phenylenebinitroxide biradical", *Bull. Chem. Soc. Jpn.* **1975**, *48*, 2381-2382.

f$_3$) Ishida T, Iwamura H, "Bis[3-*tert*-butyl-5-(*N*-oxy-*tert*-butylamino)phenyl]nitroxide in a quartet ground state: A prototype for persistent high-spin poly[(oxyimino)-1,3-phenylenes]", *J. Am. Chem. Soc.* **1991**, *113*, 4238-4241

g$_1$) Izuoka A, Fukada M, Sugawara T, Sakai M, Bandow S, "Magnetic property of 1,3,5-tris(4',4',5',5'-tetramethylimidazolin-2'-yl)benzene 3',3",3'''-trioxide 1',1",1'''-trioxyl in 1:1 mixed crystals with 1,3,5-trinitrobenzene", *Chem. Lett.* **1992**, 1627-1630.

g$_2$) Izuoka A, Fukada M, Sugawara T, "Stable mono-, di-, and triradicals as constituent molecules for organic ferrimagnets", *Mol. Cryst. Liq. Cryst.* **1993**, *232*, 103-108.

g$_3$) Shiomi D, Tamura M, Sawa H, Kato R, Kinoshita M, "Magnetic properties of an organic biradical, *m*-BNN: *m*-phenylene bis(-nitronyl nitroxide)", *J. Phys. Soc. Jpn.* **1993**, *62*, 289-300.

h$_1$) Itoh K, "Electron spin resonance of an aromatic hydrocarbon in its quintet ground state", *Chem. Phys. Lett.* **1967**, *1*, 235-238.

h$_2$) Wasserman E, Murray RW, Yanger WA, Trozzolo AM, Smolinsky G, "Quintet ground states of *m*-dicarbene and *m*-dinitrene compounds", *J. Am. Chem. Soc.* **1967**, *89*, 5076-5077.

i$_1$) Sugawara T, Bandow S, Kimura K, Iwamura H, Itoh K, "Magnetic behavior of nonet tetracarbene, *m*-phenylenebis((diphenylmethylen-3-yl)methylene)", *J. Am. Chem. Soc.* **1984**, *106*, 6449-6450.

i_2) Sugawara T, Bandow S, Kimura K, Iwamura H, Itoh K, "Magnetic behavior of nonet tetracarbene as a model for one-dimensional organic ferromagnets", *J. Am. Chem. Soc.* **1986**, *108*, 368-371.

j_1) Rajca A, Utamapanya S, Xu J, "Control of magnetic interactions in polyarylmethyl triplet diradicals using steric hindrance", *J. Am. Chem. Soc.* **1991**, *113*, 9235-9241.

j_2) Rajca A, Utamapanya S, "Toward organic synthesis of a magnetic particle: dendritic polyradicals with 15 and 31 centers for unpaired electrons", *J. Am. Chem. Soc.* **1993**, *115*, 10688-10694.

k_1) Nakamura N, Inoue K, Iwamura H, Fujioka T, Sawaki Y, "Synthesis and characterization of a branched-chain hexacarbene in a tridecet ground state. An approach to superparamagnetic polycarbenes", *J. Am. Chem. Soc.* **1992**, *114*, 1484-1485.

k_2) Nakamura N, Inoue K, Iwamura H, "A branched-chain nonacarbene with a nonadecet ground state: A step nearer to superparamagnetic polycarbenes", *Angew. Chem. Int. Ed. Engl.* **1993**, *32*, 872-874.

k_3) Matsuda K, Nakamura N, Takahashi K, Inoue K, Koga N, Iwamura H, "Design, synthesis, and characterization of three kinds of -cross-conjugated hexacarbenes with high-spin (S = 6) ground states", *J. Am. Chem. Soc.* **1995**, *117*, 5550-5560.

k_4) Matsuda K, Nakamura N, Inoue K, Koga N, Iwamura H, "Design and synthesis of a 'starburst'-type nonadiazo compound and magnetic characterization of its photoproduct", *Chem. Eur. J.* **1996**, *2*, 259-264.

k_5) Matsuda K, Nakamura N, Inoue K, Koga N, Iwamura H, "Toward dendritic two-dimensional polycarbenes: Synthesis of 'starburst'-type nona- and dodecadiazo compounds and magnetic study of their photoproducts", *Bull. Chem. Soc. Jpn.* **1996**, *69*, 1483-1494.

l_1) Yoshizawa K, Tanaka K, Yamabe T, Yamauchi J, "Ferromagnetic interaction in poly(*m*-aniline): Electron spin resonance and magnetic susceptibility", *J. Chem. Phys.* **1992**, *96*, 5516-5522.

l_2) Ito A, Saito T, Tanaka K, Yamabe T, "Synthesis of oligo(*m*-aniline)", *Tetrahedron Lett.* **1995**, *36*, 8809-8812.

l_3) Bushby RJ, Ng KM, "High-spin organic polymers", *Chem. Commun.* **1996**, 659-660.

l_4) Bushby RJ, McGill DR, Ng KM, Taylor N, "Coulombic effects in radical-cation-based high-spin polymers", *Chem. Commun.* **1996**, 2641-2642.

l_5) Bushby RJ, McGill DR, Ng KM, Taylor N, "Disjoint and coextensive diradical diions", *J. Chem. Soc. Perkin Trans. 2* **1997**, 1405-1414.

l_6) Bushby RJ, McGill DR, Ng KM, Taylor N, "p-Doped high spin polymers", *J. Mater. Chem.* **1997**, *7*, 2343-2354.

l_7) Bushby RJ, Gooding D, "Higher-spin pi multiradical sites in doped polyarylamine polymers", *J. Chem. Soc. Perkin Trans. 2* **1998**, 1069-1075.

m_1) Rajca A, Lu K, Rajca S, "High-spin polyarylmethyl polyradical: fragment of a macrocyclic 2-strand based upon calix[4]arene rings", *J. Am. Chem. Soc.* **1997**, *119*, 10335-10345.

m_2) Rajca A, Wongsriratanakul J, Rajca S, "Organic spin clusters: ferromagnetic spin coupling through a biphenyl unit in polyarylmethyl tri-, penta-, hepta-, and hexadecaradicals", *J. Am. Chem. Soc.* **1997**, *119*, 11674-11686.

m_3) Rajca A, Wongsriratanakul J, Rajca S, Cerny R, "A dendritic macrocyclic organic polyradical with a very high spin of S = 10", *Angew. Chem. Int. Ed.* **1998**, *37*, 1229-1232.

m_4) Rajca A, Rajca S, Wongsriratanakul, "Very high-spin organic polymer: -conjugated hydrocarbon network with average spin of S 40", *J. Am. Chem. Soc.* **1999**, *121*, 6308-6309.

n) Fukutome H, Takahashi A, Ozaki M, "Design of conjugated polymers with polaronic ferromagnetism", *Chem. Phys. Lett.* **1987**, *133*, 34-38.

o_1) Kaisaki DA, Chang W, Dougherty DA, "Novel magnetic properties of a doped organic polymer. A possible prototype for a polaronic ferromagnet", *J. Am. Chem. Soc.* **1991**, *113*, 2764-2766.

o_2) Murray MM, Kaszynski P, Kaisaki DA, Chang W, Dougherty DA, "Prototypes for the polaronic ferromagnet. Synthesis and characterization of high-spin organic polymers", *J.*

Am. Chem. Soc. **1994**, *116*, 8152-8161.

o₃) Sato T, Hori K, Tanaka K, "Confinement of a polaronic state in poly(*m*-phenylene-oligothienylene)", *J. Mater. Chem.* **1998**, *8*, 589-593.

p₁) Nakazaki J, Matsushita MM, Izuoka A, Sugawara T, "Ground state spin multiplicity of cation diradicals derived from pyrroles carrying nitronyl nitroxide", *Mol. Cryst. Liq. Cryst.* **1997**, *306*, 81-88.

p₂)   ,   ,   , "   ", *27*
              , **1997**,   1P03.

q) Miller JS, Dixon DA, Calabrese JC, Vazquez C, Krusic PJ, Ward MD, Wasserman E, Harlow RL, "Hexaazaoctadecahydrocoronene. Structural and physical properties of [HOC]^n ($n = 0$, 1+, 2+, 3+, 4+)", *J. Am. Chem. Soc.* **1990**, *112*, 381-398.

r₁) Dvolaitzky M, Chiarelli R, Rassat A, "Stable *N,N'*-di-*tert*-butyl-*meta*-phenylene-bisnitroxides – Unexpected ground-state singlets", *Angew. Chem. Int. Ed. Engl.* **1992**, *31*, 180-181.

r₂) Kanno F, Inoue K, Koga N, Iwamura H, "4,6-Dimethoxy-1,3-phenylenebis(*N-tert*-butyl nitroxide) with singlet ground state. Formal violation of a rule that *m*-phenylene serves as a robust ferromagnetic coupling unit", *J. Am. Chem. Soc.* **1993**, *115*, 847-850.

r₃) Kanno F, Inoue K, Koga N, Iwamura H, "Persistent 1,3,5-benzenetriyltris(N-tert-butyl nitroxide) and its analogs with quartet ground states. Intramolecular triangular exchange coupling among three nitroxide radical centers", *J. Phys. Chem.* **1993**, *97*, 13267-13272.

r₄) Fang S, Lee MS, Hrovat DA, Borden WT, "*Ab initio* calculations show why *m*-phenylene is not always a ferromagnetic coupler", *J. Am. Chem. Soc.* **1995**, *117*, 6727-6731.

r₅) Okada K, Imakura T, Oda M, Murai H, "10,10'-(*m*- and *p*-Phenylene)diphenothiazine dications: Violation of a topology rule in heterocyclic high-spin -systems", *J. Am. Chem. Soc.* **1996**, *118*, 3047-3048.

r₆) Okada K, Imakura T, Oda M, Kajiwara A, Kamachi M, Sato K, Shiomi D, Takui T, Itoh K, Gherghel L, Baumgarten M, "10,10',10"-(Benzene-1,3,5-triyl)triphenothiazine trication", *J. Chem. Soc. Perkin Trans. 2* **1997**, 1059-1060.

r₇) Okada K, Imakura T, Oda M, Kajiwara A, Kamachi M, Yamaguchi K, "Remarkable heteroatom dependence of the spin multiplicity in the ground state of 9,9'-(*m*-phenylene)dixanthyl and -dithioxanthyl diradicals", *J. Am. Chem. Soc.* **1997**, *119*, 5740-5741.

16. Watanabe (Ibaraki Univ.) are preparing P₂-*N*-PN. In order to make handling easier, a bis(thiophene)-substituted derivative, T₂-*N*-PN, was prepared by Chung (Univ. of Tokyo), and it turned out to afford a ground state triplet cation diradical by the treatment with iodine. Watanabe also prepared formyl precursors of (*N*-PN)₂ and (*N*-PN)₃. The properties of these derivatives will be reported near future.

N-PN   P₂-*N*-PN   T₂-*N*-PN   (*N*-PN)₂   (*N*-PN)₃
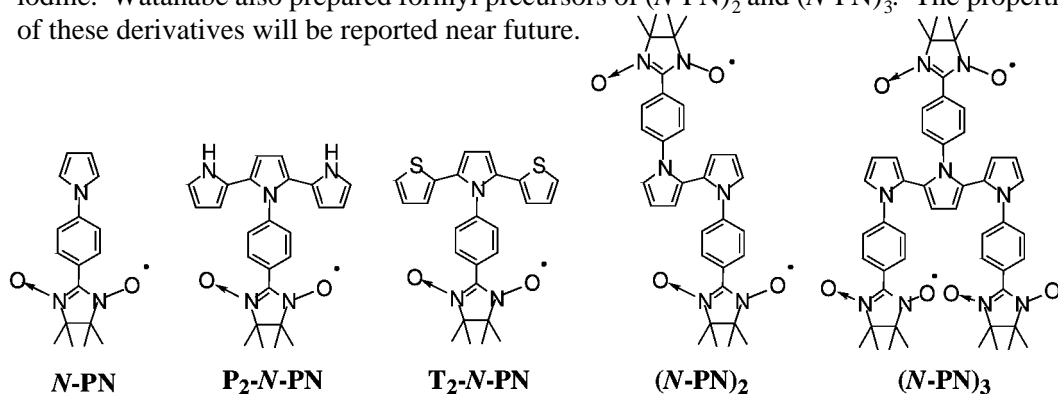
a)   ,   , **2000**.
b)   ,   , **2000**.

17. Lamchen M, Mttag TW, "Nitrones. part IV. Synthesis and properties of a monocyclic -dinitrone", *J. Chem. Soc. C* **1966**, 2300-2303.

Chapter 3

Design of TTF-Based Spin-Polarized Donors Affording Ground State Triplet Cation Diradicals

§3-1. Introduction

In order to realize an organic conducting magnet, the constituent donor radicals are requested to have an ability to construct a sufficient conduction path. Since TTF derivatives are well known as representative building blocks for organic conductors, utilization of a TTF derivative as a donor unit of a spin-polarized donor is considered to be suitable for the present request. A prototype of such a donor radical, **TTF-NN** was already reported.[1] Although a triplet ESR spectrum was observed in the iodine-doped sample of **TTF-NN**, the triplet signal was found to be a thermally populated one. In order to construct an organic double exchange system, a donor radical is required to show ferromagnetic intramolecular interaction when the donor radical is singly oxidized. Therefore, design of another TTF-based spin-polarized donor which affords a ground state triplet cation diradical upon one-electron oxidation should be requested.

As described in Chapter 2, the ground state spin multiplicity of the oxidized species of a pyrrolylNN derivative (*N*-**NN**) was converted to triplet by the insertion of a *p*-phenylene moiety (*N*-**PN**). A similar methodology was applied to **TTF-NN**, *i.e.*, TTF-phenylNN (**TTF-PN**) was designed. In order to enhance the inter-molecular interaction and the kinetic stability of the oxidized species, sulfur extended derivatives, ethylenedithio-methylthio-TTF-phenylNN (**EMPN**) and ethylenedithio-methylthio-TTF-thio-phenylNN (**EMTN**), were also examined. The electronic structures of these TTF-based donor radicals will be discussed in

Section 4 based on the results in Section 3. Application of these donor radicals to the preparation of CT complexes is documented in Section 5.
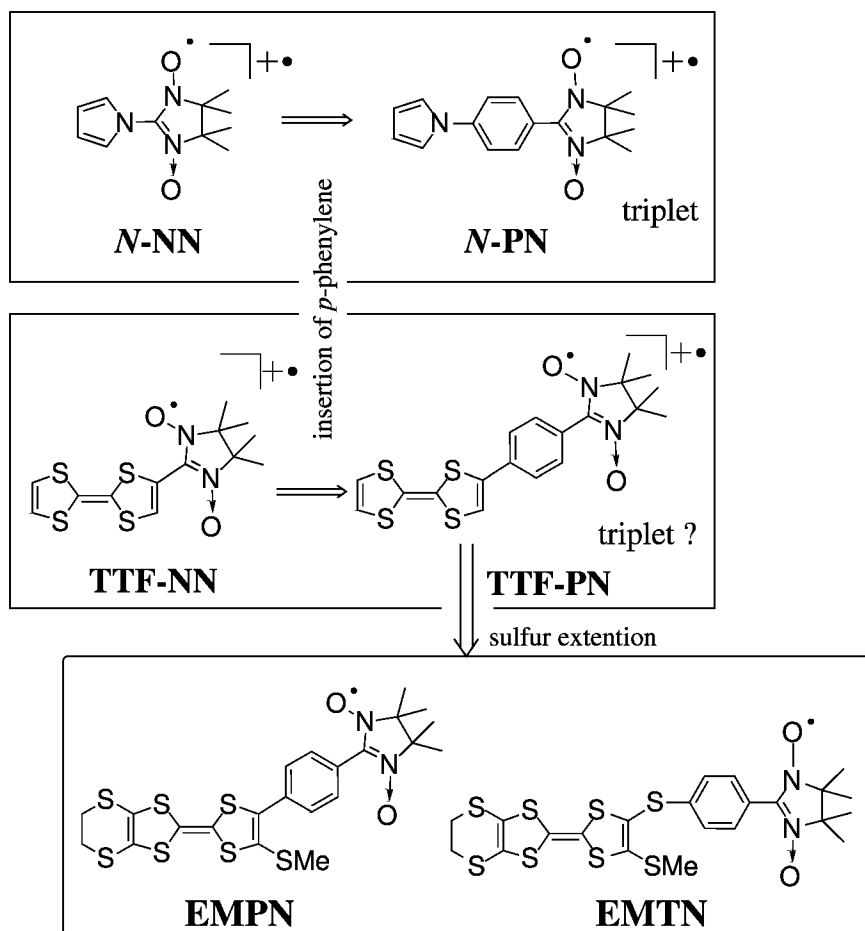
Figure 3-1. Design of TTF-based spin-polarized donors.

§3-2. Preparation of TTF-Based Donor Radicals

The synthetic schemes of the donor radicals, **TTF-PN**, **EMPN**, and **EMTN** are shown in Figures 3-2, 3-3, and 3-4, respectively. All these nitronyl nitroxide derivatives were prepared from their aldehyde precursors, **13**, **20**, and **26**, respectively, by the ordinary method.[2]

The aldehyde precursor (**13**) of **TTF-PN** was synthesized as follows (Figure 3-2). TTF was lithiated with lithiumdiisopropylamide (LDA), and treated with trimethyltin chloride to afford a stannyl derivative **12**, which was converted to *p*-formylphenyl-TTF (**13**) by cross-coupling with *p*-bromobenzaldehyde using a palladium catalyst.[3]
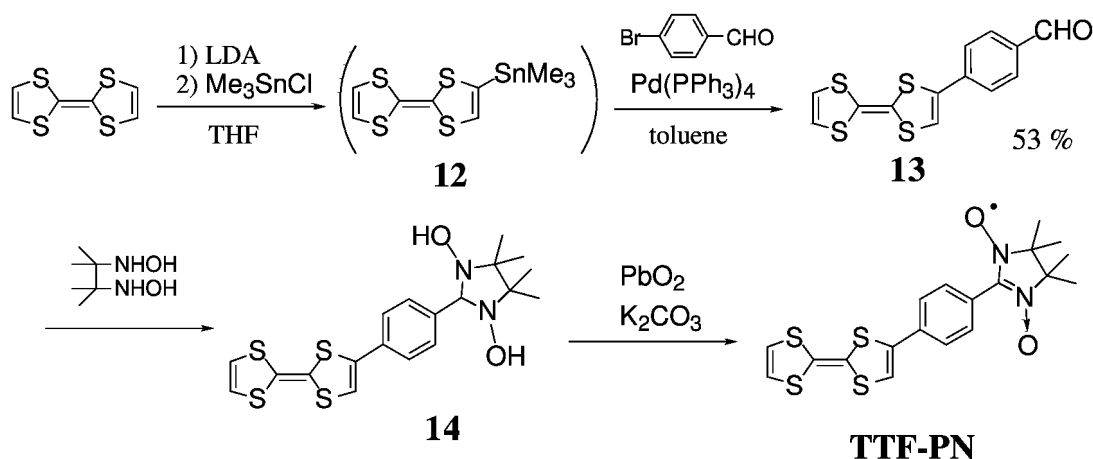
Figure 3-2. Synthetic scheme of **TTF-PN**.

As a coupling unit of **EMPN** and **EMTN**, 4-methylthio-1,3-dithiol-2-thione (**17**) was prepared by route A or B (Figure 3-3(c)). Route B is preferable because the product from route A is a mixture of bis-, mono-, and non-(methylthio) derivatives. Another coupling unit, ketone **15**, was prepared by a reported procedure (Figure 3-3(a)).[4]

The aldehyde precursor (**20**) of **EMPN** was synthesized as follows (Figure 3-3(d)). The thione **17** was coupled with ketone **15** to afford a TTF derivative **18**, which was lithiated, stannylated, and coupled with *p*-iodobenzaldehyde (**16**) using a palladium catalyst. In order to obtain the target *p*-formylphenyl derivative **20**, addition of aqueous base into the reaction mixture was required.[5]

As a synton for **EMTN**, disulfide **23** was prepared from *p*-methylthiobenzaldehyde, making use of Pummerer rearrangement (Figure 3-4(a)).[6] The aldehyde precursor (**26**) of **EMTN** was synthesized by two routes (Figure 3-4(b)). TTF derivative **18**, which was prepared by above method, was lithiated and treated with disulfide **23**, and the product **25** was hydrolyzed to give the aldehyde **26**. Lithiation of thione **17**, followed by the treatment of disulfide **23**, afforded thione-acetal **24**, which was also converted to **25**. The latter route gave a better yield.

(a) Preparation of ketone **15**.

CS_2 $\xrightarrow[\text{2) } ZnCl_2, NH_3aq., Et_4NBr]{\text{1) } Na, DMF}$ $(Et_4N)_2\left[S=\underset{S}{\overset{S}{\diagup}}\underset{S}{\overset{S}{\diagdown}}Zn\underset{S}{\overset{S}{\diagup}}\underset{S}{\overset{S}{\diagdown}}=S\right]$

$\xrightarrow{PhCOCl}$ [thione with SCOPh groups] $\xrightarrow[\text{2) } Br\frown Br]{\text{1) } NaOMe}$ [structure] $\xrightarrow{Hg(OAc)_2}$ **15**
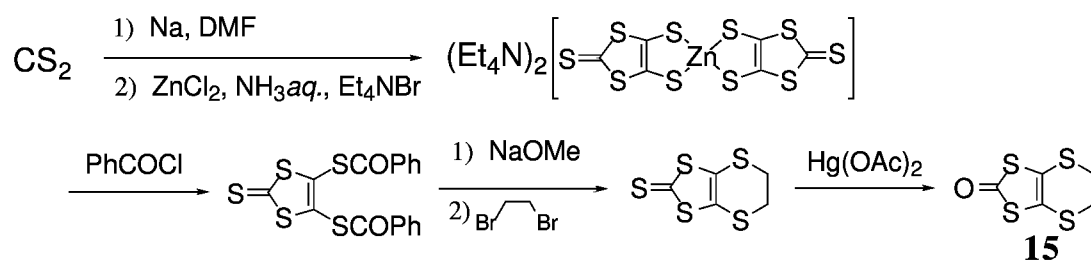
(b) Preparation of p-iodobenzaldehyde

I—⟨C$_6$H$_4$⟩—I $\xrightarrow[\text{2) DMF}]{\text{1) } n\text{-BuLi}}$ I—⟨C$_6$H$_4$⟩—CHO
16
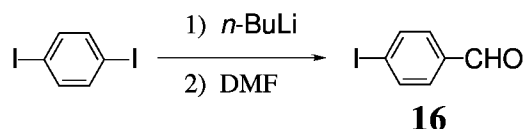
(c) Preparation of thione **17**.

Route A

[structure] $\xrightarrow[\text{THF} \qquad 47\%]{\text{1) LDA} \quad \text{2) S} \quad \text{3) MeI}}$ [structure with SMe]
17

Route B

[SNa/OEt structure] $\xrightarrow[\text{MeOH}]{Cl\frown COOMe}$ [COOMe/OEt structure] $\xrightarrow[\text{1) } CS_2, Bu^tONa}{\text{DMF}}$ [COOMe/SMe structure] $\xrightarrow[\text{pyridine}\atop 73\%]{LiBr\cdot H_2O}$ [SMe structure]
2) MeI
17

(d) Preparation of **EMPN**.

[structure **17** with SMe] $\xrightarrow[P(OEt)_3]{\textbf{15}}$ **18** 52% $\xrightarrow[\text{THF}]{\text{1) LDA} \atop \text{2) } Me_3SnCl}$ ([structure with SnMe$_3$ and SMe]) **19**

16
$\xrightarrow[\substack{\text{toluene -} \\ \text{1M } Na_2CO_3 \ aq.}]{Pd(PPh_3)_4}$ [structure **20** with CHO and SMe] 52% $\xrightarrow[\text{benzene-MeOH}]{\substack{\text{—NHOH} \\ \text{—NHOH}}}$ **21** 60%

$\xrightarrow[\text{THF}]{PbO_2, K_2CO_3}$ **EMPN** 52%
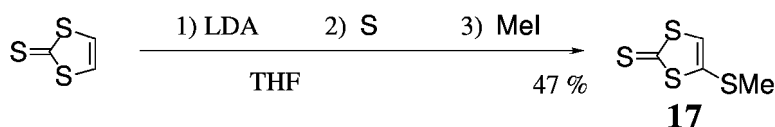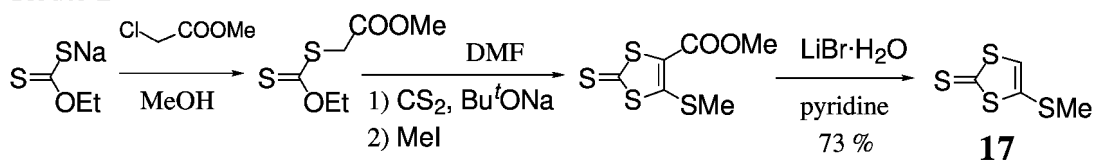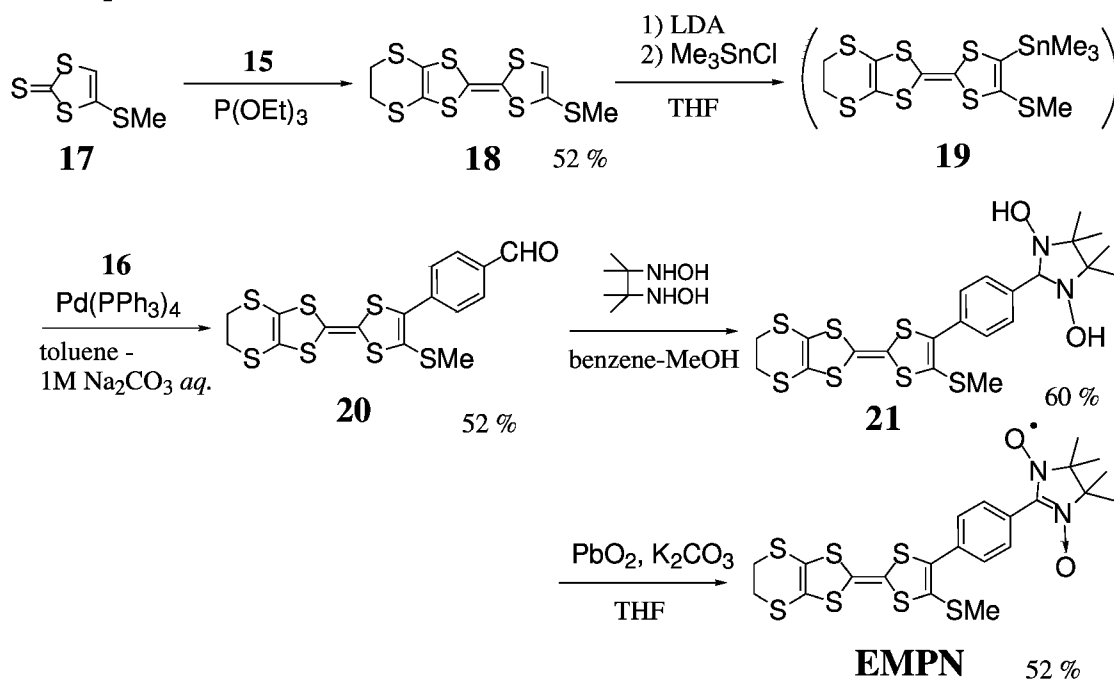
Figure 3-3. Synthetic schemes of **EMPN**.

(a) Preparation of disulfide **23**.
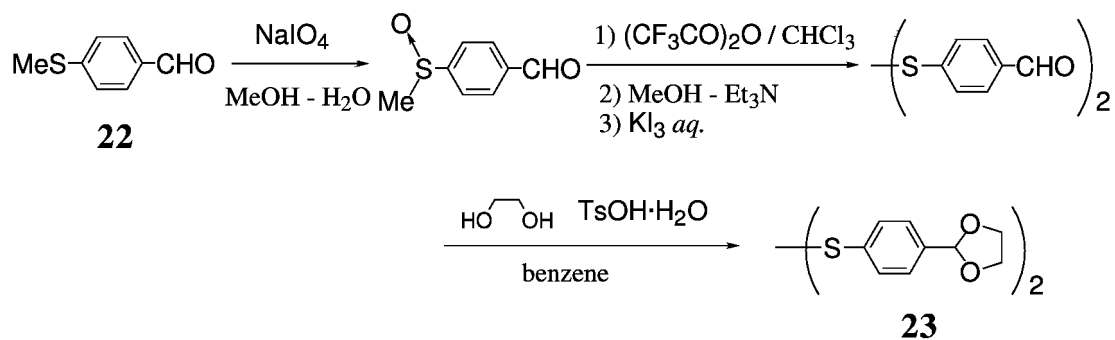
(b) Preparation of **EMTN**.
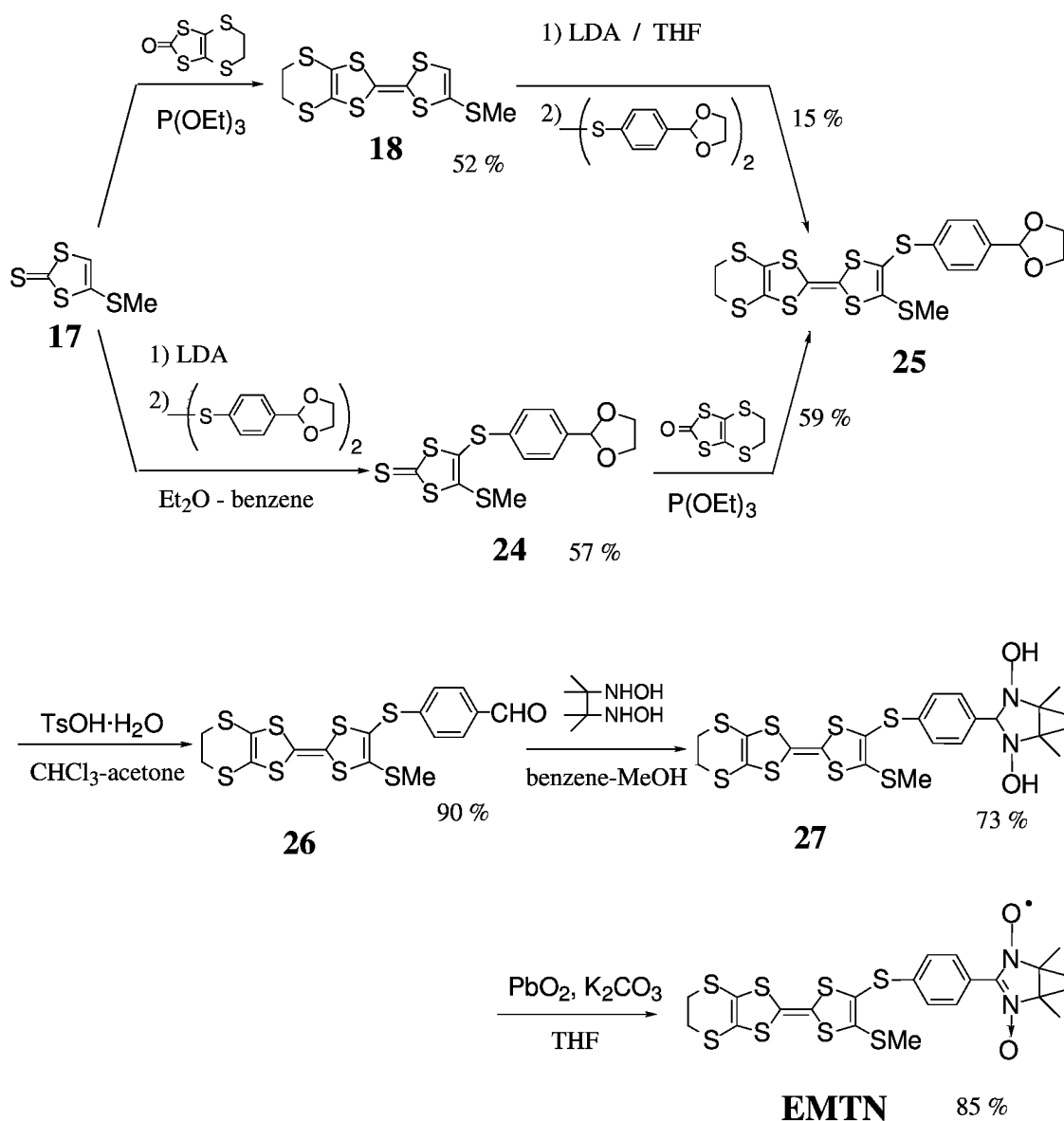
Figure 3-4. Synthetic scheme of **EMTN**.

§3-3. Properties of TTF-Based Donor Radicals

3-3-1. Cyclic Voltammetry of TTF-Based Donor Radicals

Oxidation potentials of the donor radicals are determined by cyclic voltammetry. Observed voltammograms showed two reversible waves, and the second wave is considered to be derived from a two electron process. The voltammogram of **EMTN** is shown in Figure 3-5, and the determined oxidation potentials of the donor radicals are summarized in Table 3-1, together with those of reference compounds.

The first oxidation potential of **TTF-PN** is 0.44 V, which is slightly higher than that of TTF (0.34 V). The first oxidation potentials of **EMPN** and **EMTN** are 0.56 V and 0.60 V, respectively, which are the same or slightly higher than that of BEDT-TTF (0.56 V). The data indicate that the donor abilities of these donor radicals are practically same as those of the parent donors.

The second and the third oxidation of the donor radicals were observed at 0.79-0.89 V, which are similar to the oxidation potential of phenylNN (0.80 V) and the second oxidation potentials of TTF (0.71 V) or BEDT-TTF (0.86 V). One of those potentials may be assigned to the oxidation of the NN radical, and the other is attributed to the oxidation of cation radical of the donor.

Therefore, the first oxidation process of these donor radicals should generate open-shell diradical species. This assignment is not conflict with the results obtained by ESR spectroscopy on the singly oxidized donor radicals (*vide infra*).
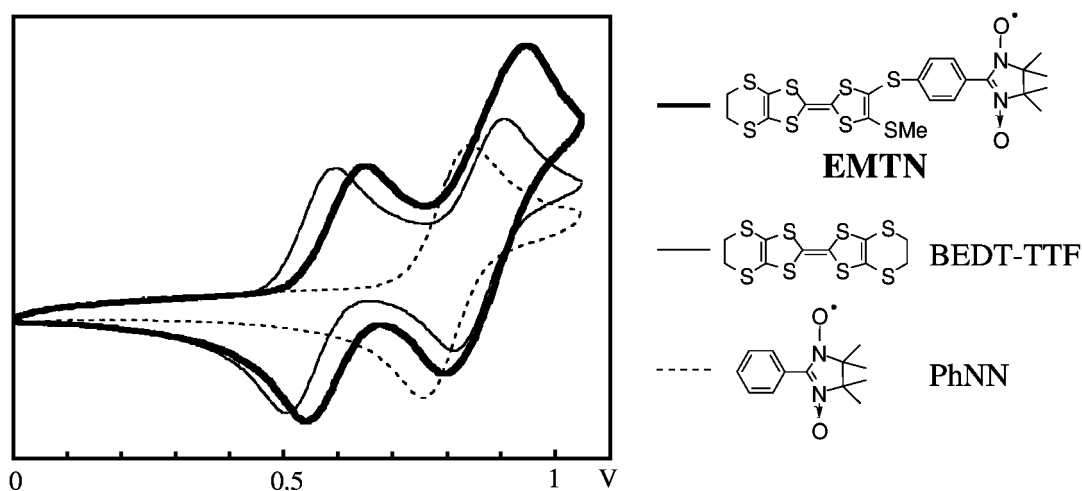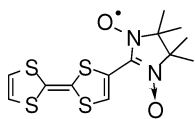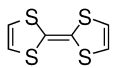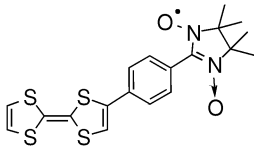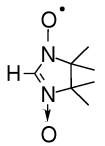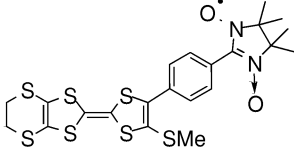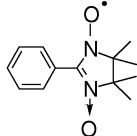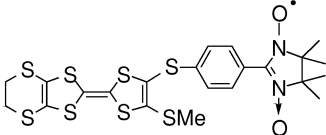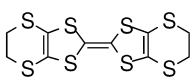
Figure 3-5. Cyclic voltammograms of **EMTN** and related compounds measured in 0.1 M *n*-Bu$_4$N·ClO$_4$ - PhCN solution by 200 mV·s^{-1}.

Table 3-1. Oxidation potentials of donor radicals and related compounds.

Donor radical	$E_{1/2}$ / V	Donor or Radical	$E_{1/2}$ / V
TTF-NN[¶]	0.32 0.77 (irr.) 1.00 (irr.)	TTF[¶]	0.34 0.71 (irr.)
TTF-PN[¶]	0.44 0.79	H-NN[#]	0.82
EMPN	0.56 0.86 0.89	PhNN	0.80
EMTN	0.60 0.85 0.89	BEDT-TTF	0.56 0.86

measured in 0.1 M n-Bu$_4$N·ClO$_4$ - PhCN solution.   (¶ : in CH$_2$Cl$_2$, # : in MeCN)

3-3-2. Electronic Spectra of TTF-Based Donor Radicals

The UV absorption spectra of donor radicals and reference compounds measured in a dichloromethane solution are shown in Figure 3-6. The spectrum of **EMPN** showed absorption maxima at 306 and 376 nm, and shoulders around 280, 315, 340, 465 nm. The spectrum of **EMTN** showed maxima at 309 and 375 nm, and a shoulder around 350 nm.

As seen in Figure 3-6(a), the spectrum of **EMPN** is not a superposition of those of phenylNN and BEDT-TTF, suggesting a significant electronic interaction between BEDT-TTF and phenylNN moieties. On the other hand, the spectrum of **EMTN** can be interpreted as a superposition of those of p-methylthiophenylNN and BEDT-TTF. The fact indicates that the mutual electronic perturbation between the donor part and the radical part is not so large, at least in the neutral state. The result may imply that the introduction of TTF to the *para*-position of phenylNN causes an electronic effect similar with the introduction of a methylthio group. Such a tendency is presumably derived from the twisting of TTF unit from the rest of the molecule.

The absorption of donor radicals are extended to longer wave lengths than the parent compounds as a result of the extension of the conjugation length.

(a)

(b)
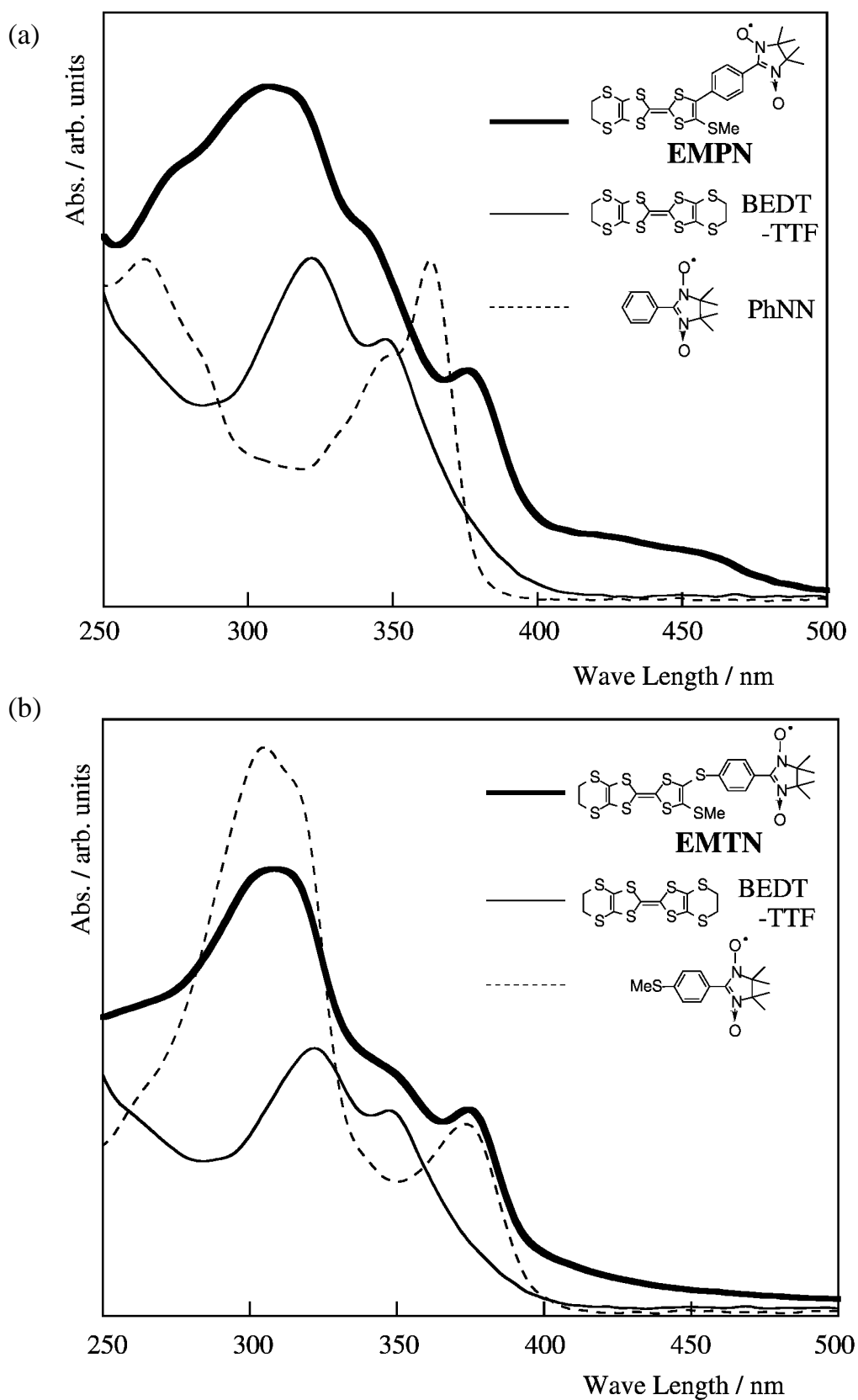
Figure 3-6. Absorption spectra of donors and radicals in CH_2Cl_2.

3-3-3. ESR Spectra of Oxidized Species of TTF-Based Donor Radicals

Oxidized species of the donor radicals, **TTF-PN**, **EMPN**, and **EMTN**, were generated by the addition of excess iodine to a tetrahydrofuran solution of the donor radical at room temperature. The ESR spectra observed in a frozen matrix are shown in Figures 3-7 to 3-9. In each case, the triplet signal appeared as marked *x*, *y*, *z*, and the observed spectra were in accord with the simulated ones. Zero-field splitting parameters and anisotropic *g* values are listed in Table 3-2. The triplet species are attributable to the cation diradicals of the donor radicals. The temperature dependence of the intensity of the triplet signals obeyed Curie law, indicating that the triplet is the ground state of these cation diradicals. These results are in contrast to the case of the iodine-doped **TTF-NN**.
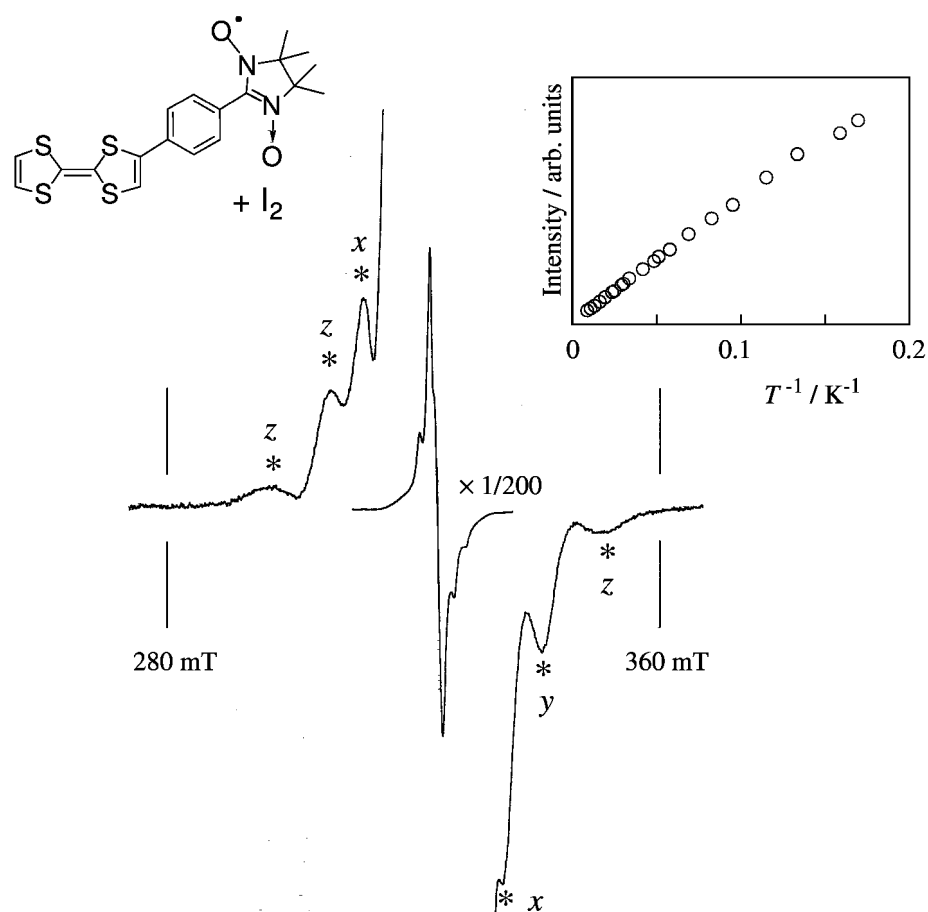
Figure 3-7. ESR spectrum of **TTF-PN$^{+\bullet}$** observed in DMSO glass at 5 K and temperature dependence of signal intensity.

41
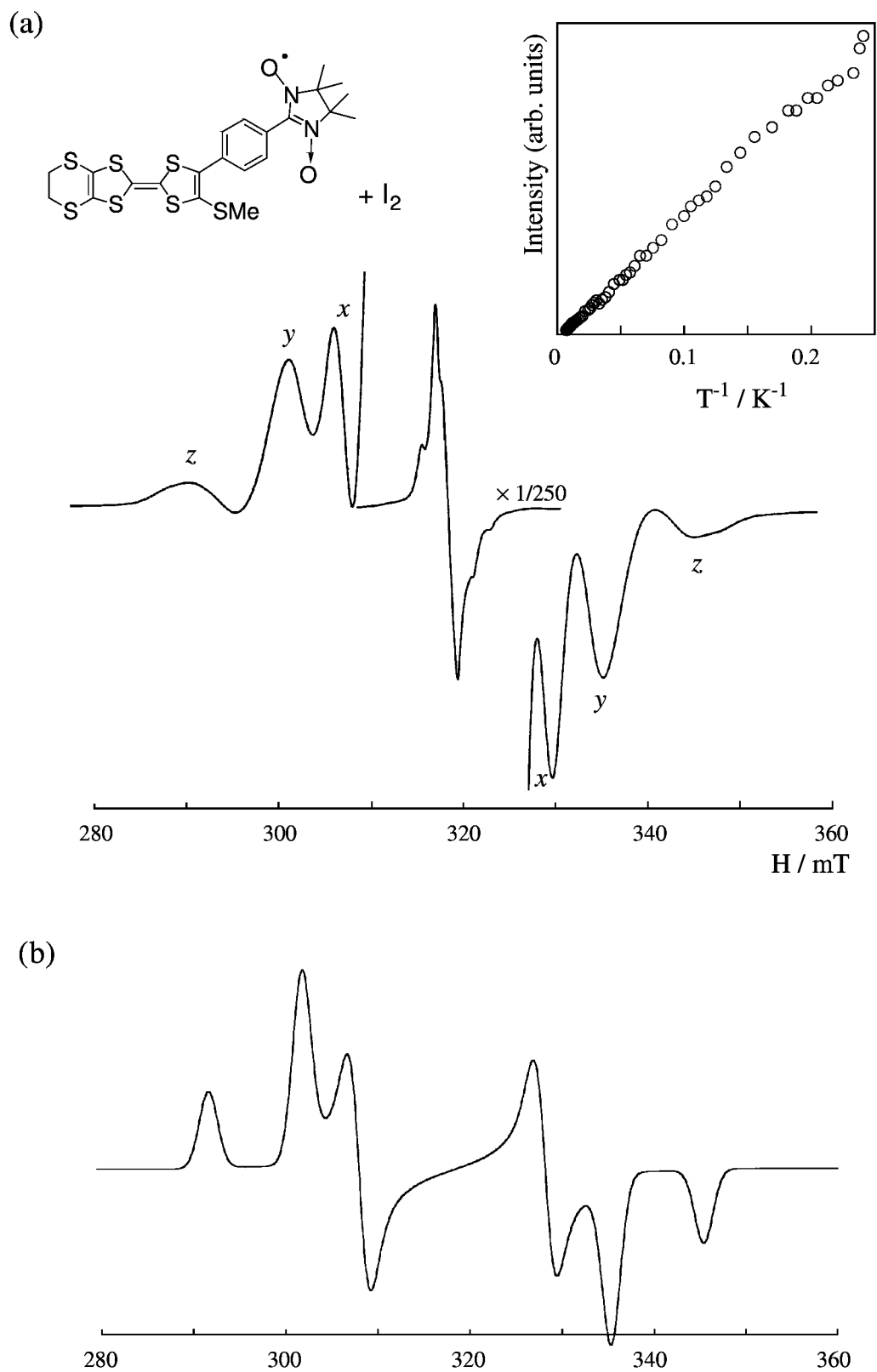
Figure 3-8. ESR spectrum of **EMPN$^{+\bullet}$**: (a) Observed spectrum in THF glass at 4.2 K and temperature dependence of signal intensity, (b) simulated spectrum.

(a)

(b)
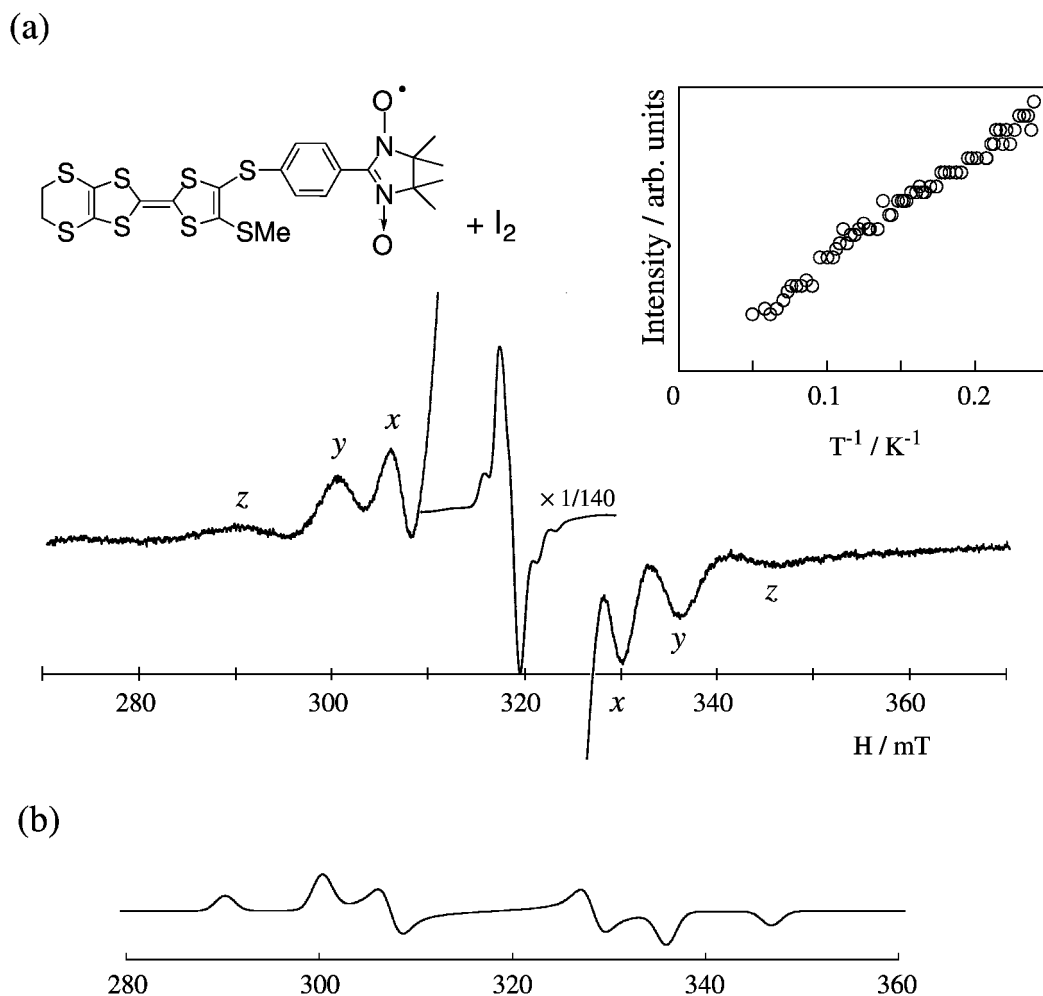
Figure 3-9. ESR spectrum of **EMTN⁺•**: (a) Observed spectrum in THF glass at 9.3 K and temperature dependence of signal intensity, (b) simulated spectrum.

Table 3-2. Zero-field splitting parameters and anisotropic g value.

	$|D|$ / cm^{-1}	$|E|$ / cm^{-1}	g_x	g_y	g_z	g_{av}
TTF-NN⁺•	0.0214	0.0022	2.0111	2.0094	2.0031	2.0079
TTF-PN⁺•	0.0255	0.0023	2.0111	2.0084	2.0046	2.0080
EMPN⁺•	0.0252	0.0021	2.0077	2.0053	2.0070	2.0067
EMTN⁺•	0.0265	0.0023	2.0090	2.0080	2.0070	2.0080

43

§3-4. Electronic Structure of TTF-Based Donor Radicals

3-4-1. Revision of TTF-NN

The prototypical donor radical, **TTF-NN**, afforded ground state singlet cation diradical upon one-electron oxidation. Before considering the electronic structure of novel donor radicals, the origin of the antiferromagnetic interaction in **TTF-NN**$^{+\bullet}$ should be revealed.

The molecular orbitals of **TTF-NN** calculated by a PM3/UHF method are shown in Figure 3-10. The orbital energy of SOMO is lower than that of the entire-molecular HOMO by *ca.* 1 eV, indicating that one-electron oxidation should occur from HOMO. However, the energy levels of HOMO( ) and HOMO( ) are practically same, and the spin configuration in the oxidized species cannot be predicted. Although HOMO and SOMO are sharing same atomic orbitals on NN site, the difference of spin-dependent Coulombic repulsion is negligibly small because of small overlap or large energy difference between these orbitals.

HOMO(α) : -7.99 eV   HOMO(β) : -7.99 eV

SOMO(α) : -9.03 eV
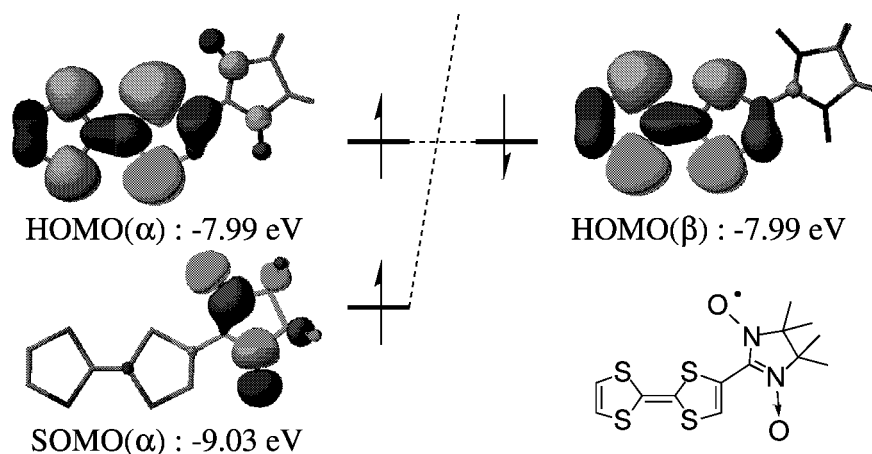
Figure 3-10. Molecular orbitals of **TTF-NN** calculated by MOPAC/PM3/UHF.

The similar calculations were performed on the cation diradical, **TTF-NN**$^{+\bullet}$, assuming a planar conformation (Figure 3-11). Calculated heat of formation for the triplet configuration is 248.87 kcal/mol, and that for the singlet configuration is 249.40 kcal/mol. The result means that triplet state is more stable than singlet state by *ca.* 0.6 kcal/mol. However, this is not the case for the experimental results.

(a) triplet　　　　　　　　　　　(b) singlet

SOMO　　　　SOMO'　　　　　　SOMO　　　　SOMO'
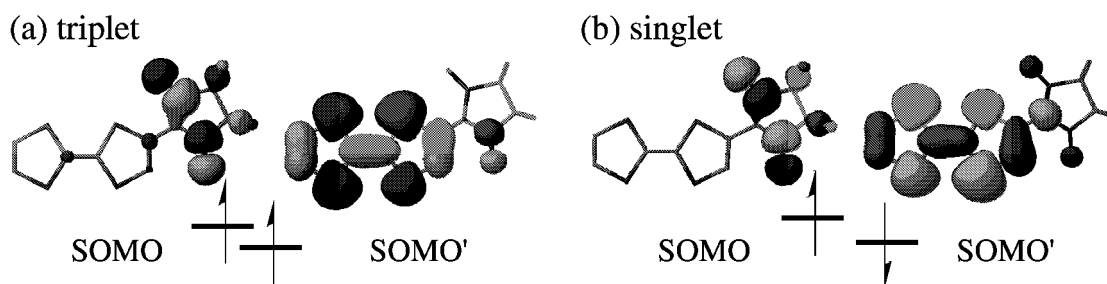
Figure 3-11. Molecular orbitals of **TTF-NN$^{+\bullet}$** for (a) triplet configuration and (b) singlet configuration.

In order to rationalize the experimental data, a suppression of the delocalization of SOMO' to the NN site caused by twisting of the NN group from the TTF plane should be taken into account. Such a twist is plausible because the contact between a NO group of the NN site and a sulfur atom of the TTF site is considered to be serious in a planar conformation. Localization of SOMO' to the TTF site significantly decreases the exchange interaction between unpaired electrons residing in SOMO and SOMO'.

However, this effect rationalizes only the decrease of ferromagnetic interaction, not explaining the antiferromagnetic interaction in **TTF-NN$^{+\bullet}$**. The twist of the NN group makes the C-S -orbital of the TTF unit nearly parallel to the -orbitals of the NN group, enabling the hyper-conjugation between these orbitals. Such a through-bond interaction may cause an antiferromagnetic coupling between two spins on the NN site and the sulfur atom in the TTF site by a spin-polarization effect (Figure 3-12). In order to diminish such a twist, relaxation of steric repulsion by the insertion of a spacer unit is considered to be effective.
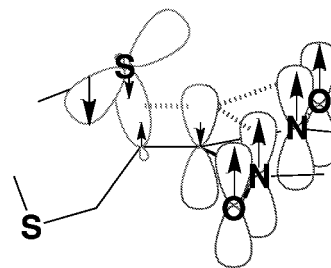
Figure 3-12. Through-bond spin-polarization.

Because of the chemical unstability of **TTF-NN**, further examination or application of **TTF-NN** has been limited. The improved donor, **TTF-PN**, turned out to be also unstable. Their unstability may be caused by the existence of reactive olefinic carbons. On the other hand, sulfur extended derivatives, **EMPN** and **EMTN** are reasonably stable. Their stability guarantees the possibility of further applications.

45

3-4-2. Exchange Interactions in TTF-Based Donor Radicals

Molecular orbitals of **TTF-PN** calculated by PM3/UHF method are shown in Figure 3-13. The coefficients of HOMO on the NN site is only detectable when the threshold value is lowered. Furthermore, the orbital energy of HOMO( ) is lower than that of HOMO( ). Such a situation seems to be unfavorable to generate a ground state triplet cation diradical, but the experimental data showed triplet ground state of **TTF-PN**[+•].
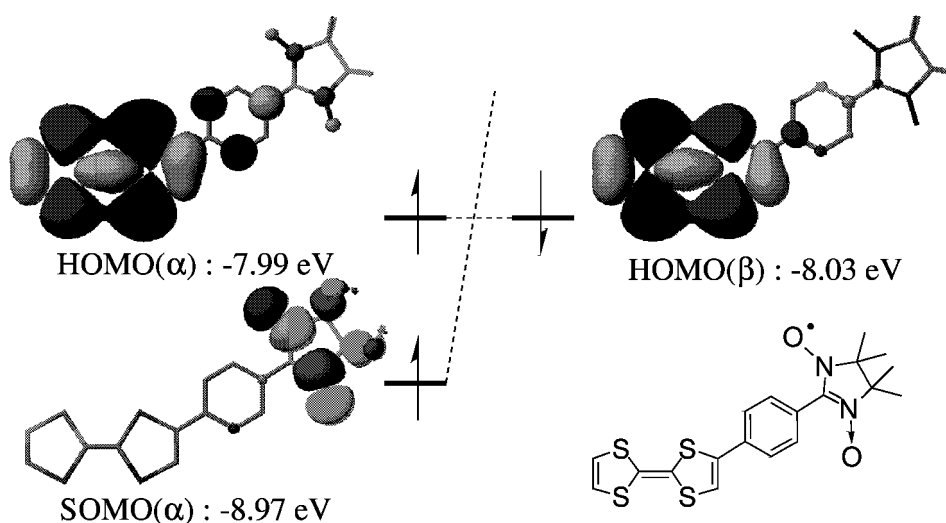
Figure 3-13. Molecular orbitals of **TTF-PN** calculated by MOPAC/PM3/UHF.

PM3/UHF calculation was also performed on **TTF-PN**[+•] of singlet and triplet configurations. The result showed that triplet is more stable than singlet by 8.23 kcal/mol. As shown in Figure 3-14, the coefficients of SOMO' spreads over entire molecule, especially to the NN site. As a result, exchange interaction between SOMO and SOMO' is considered to be large.[7]
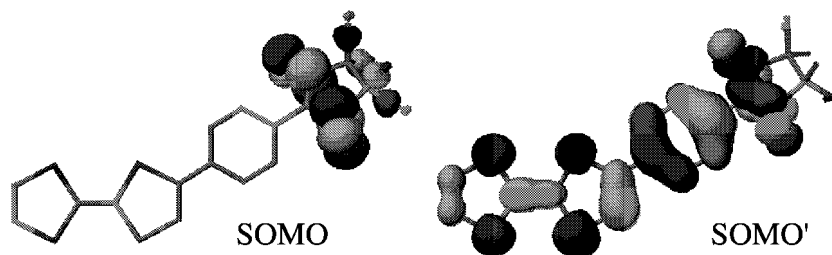
Figure 3-14. Molecular orbitals of **TTF-PN**[+•] in triplet configuration.

(a)

HOMO(α) : -8.09 eV

HOMO(β) : -8.07 eV

SOMO(α) : -8.91 eV

EMPN

(b)

HOMO(α) : -8.05 eV

HOMO(β) : -8.03 eV

SOMO(α) : -8.91 eV
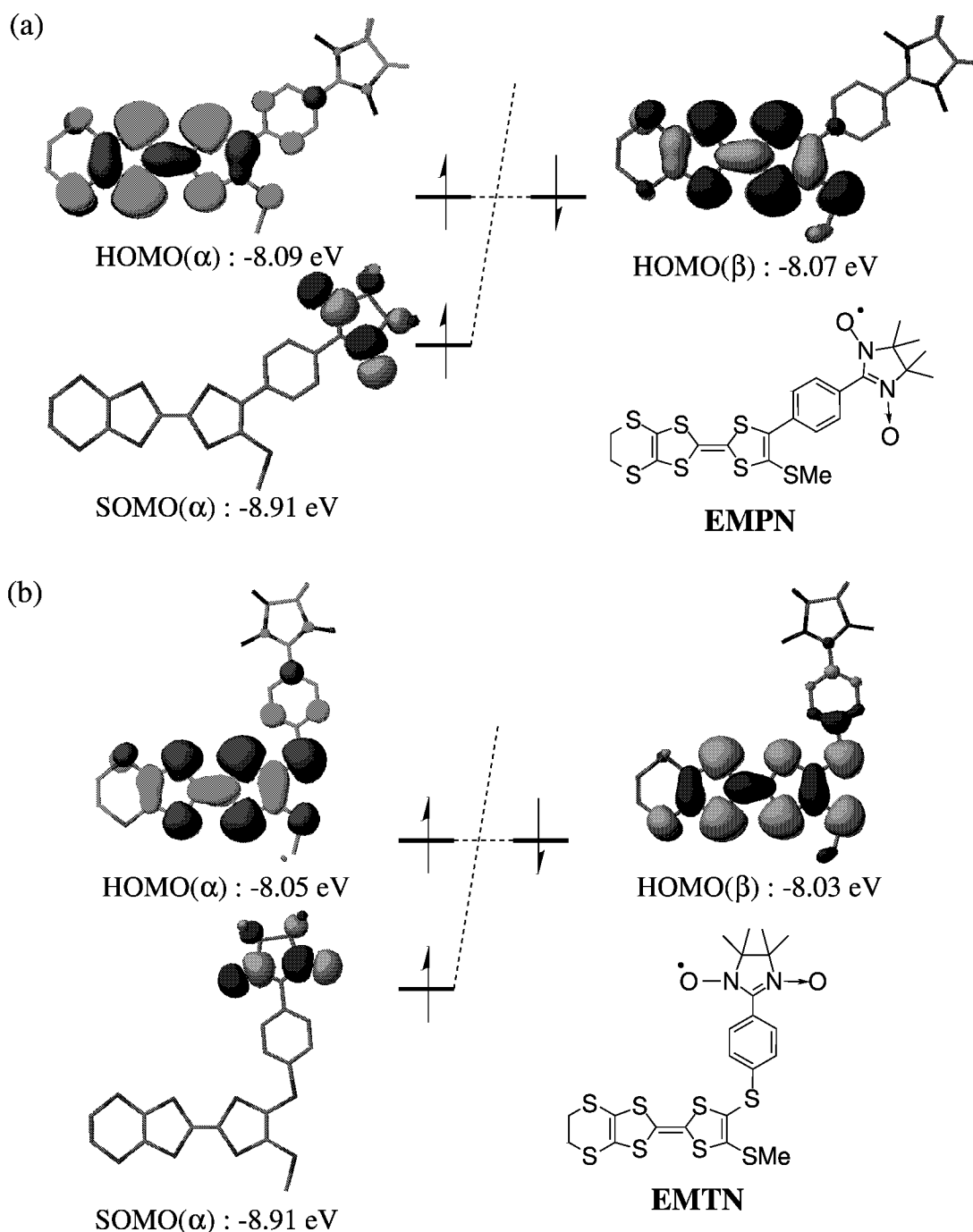
EMTN

Figure 3-15. Molecular orbitals of **EMPN** and **EMTN** calculated by MOPAC-PM3/UHF.

Molecular orbitals of **EMPN** and **EMTN** calculated by a PM3/UHF method are shown in Figure 3-15. Although the coefficients of HOMO on the NN site are very small for both compounds in the neutral state, the orbital energies of HOMO( ) is slightly higher than those of HOMO( ). One-electron oxidation of these compounds is expected to afford ground state triplet cation diradicals.

(a) EMPN⁺•

SOMO

SOMO'

(b) EMTN⁺•
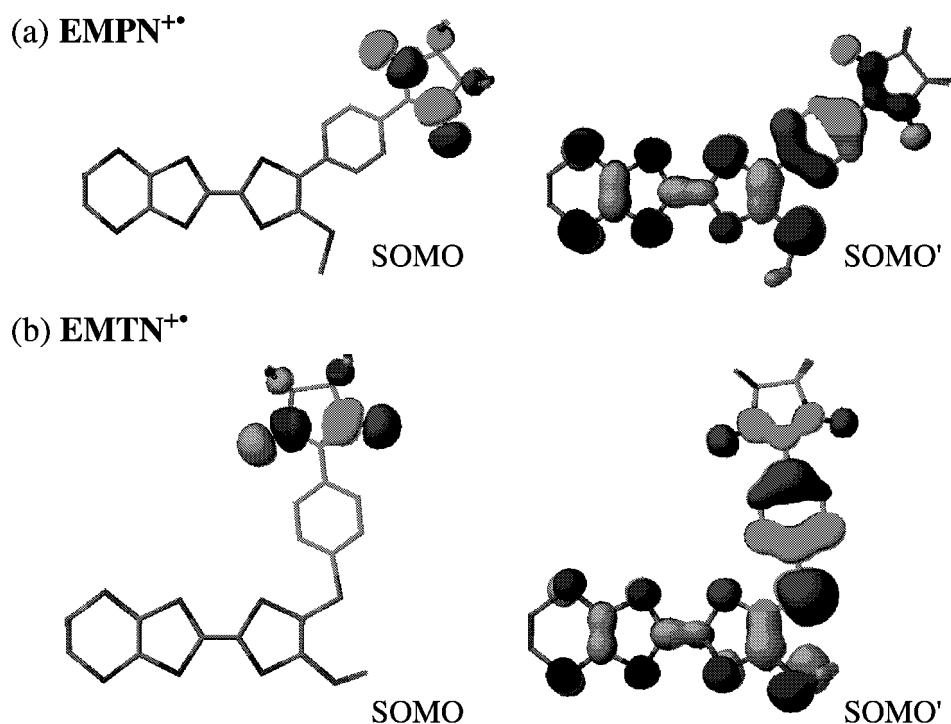
SOMO

SOMO'

Figure 3-16. Molecular orbitals of **EMPN⁺•** and **EMTN⁺•** in triplet configuration.

PM3/UHF calculation was also performed on **EMPN⁺•** and **EMTN⁺•** in triplet configuration, assuming a planar conformation (Figure 3-16). In both case, SOMO' spreads over entire molecule.

It is interesting to compare the efficiency of *p*-phenylene and *p*-thiophenylene groups as a transmitter of the spin-polarization caused at the radical site. The calculational data indicates that the coefficients on the NN site in SOMO' of **EMTN** is a little larger than those of **EMPN**. This tendency may lead to a larger ferromagnetic exchange interaction in **EMTN** which contains a *p*-thiophenylene group as a transmitter.

3-4-3. Electronic Features of TTF-Based Spin-Polarized Donors
--Comparison with Other Spin-Polarized Donors --

Amine-based or pyrrole-based spin-polarized donors showed significant change in oxidation potentials compared with their parent compounds. Such a change was rationalized based on a perturbational MO method to be a reflection of the large orbital interaction between *homo* of the donor site and *nhomo* of the radical site. The HOMOs of those spin-polarized donors are higher in energy than *homo* of the donor site or *somo* of the radical site (Figure 3-17(a)).

48

On the other hand, oxidation potentials of TTF-based spin-polarized donors are higher than those of TTF or BEDT-TTF. This is because the energy level of *homo* of the donor site is much higher than *somo* of the radical site. Since the energy level of *nhomo* of the radical site is even lower than *somo*, the perturbation between *homo* of the donor site and *nhomo* of the radical site is negligibly small (Figure 3-17(b)). Therefore, HOMO of the entire molecule is not raised by the orbital interaction. Furthermore, the energy level of HOMO may be lowered by the induction effect of NN group.[8]
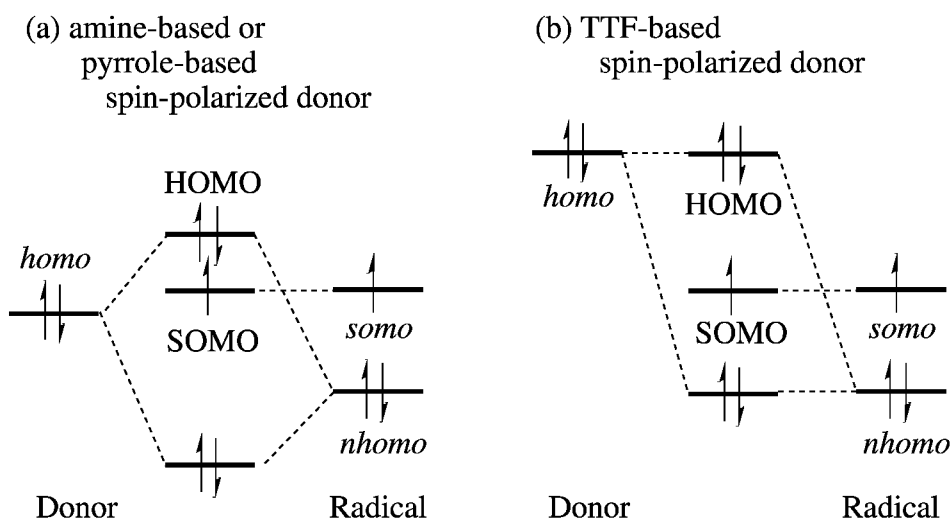
Figure 3-17. Comparison of PMO descriptions of spin-polarized donors.

Another feature of TTF-based spin-polarized donors is smaller distribution of the coefficients of HOMO or SOMO' on the NN site compared with amine-based spin-polarized donors. The fact implies that the exchange interactions in the cation diradicals of these donors are smaller. In spite of such a situation, Curie plots of triplet ESR signals of TTF-based spin-polarized donors are linear up to *ca.* 120 K, indicating that ferromagnetic coupling in cation diradicals is considerably larger than the thermal energy of that temperature.

§3-5. Solid State Properties of TTF-Based Spin-Polarized Donors

3-5-1. Crystal Structure and Magnetic Property of Neutral Donors

In spite of much efforts, structural features of TTF-based spin-polarized donors had not been revealed by X-ray crystallography. **TTF-NN** and **TTF-PN** are chemically unstable, and are difficult to be isolated. **EMPN** is stable enough to be isolated, but it gave only amorphous solids. Although **EMTN** also tends to solidify amorphous, careful crystallization from dichloromethane solution afforded block crystals of **EMTN**. The sample for X-ray crystallography was crystallized from dichloromethane-pyridine solution by slow evaporation.

The crystal of **EMTN** turned out to belong to a monoclinic space group $P2_1/c$. The crystallographic parameters are summarized in Table 3-3, and the detailed data are listed in Appendix. The **EMTN** molecule in the crystal is in a bent conformation, as shown in Fugure 3-18. These molecules are aligned in the *bc* plane as shown in Figure 3-19(a). Each TTF or phenylNN moiety forms a *face-to-face* dimer separately, and these dimers are arranged along the *b*-axis. These molecules form a slipped stack along the *a*-axis as shown in Figure 3-19 (b).
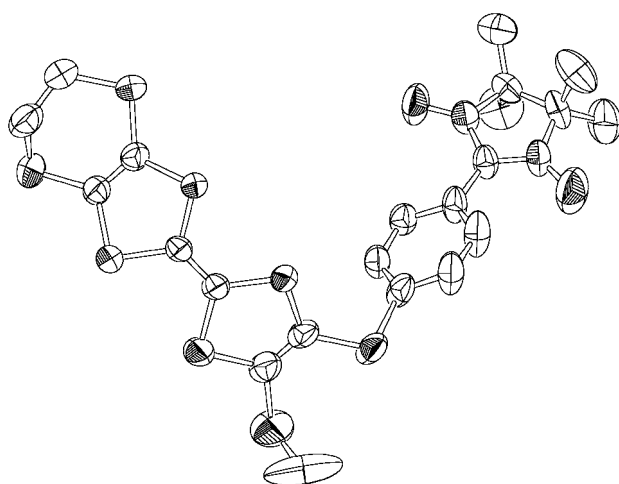
Figure 3-18. ORTEP drawing (50% probability) of molecular structure of **EMTN**.

Table 3-3.
Crystallographic Parameters of EMTN neutral crystal.

Space Group	$P2_1/c$ (#14)
a / Å	6.9919(6)
b / Å	16.817(2)
c / Å	23.037(2)
β /deg	96.674(6)
V /Å^3	2690.3401
Z	4
Observations	3181
Variables	308
Refl/Para Ratio	10.33
R	0.072
R_w	0.094
Goodness of Fit	2.26
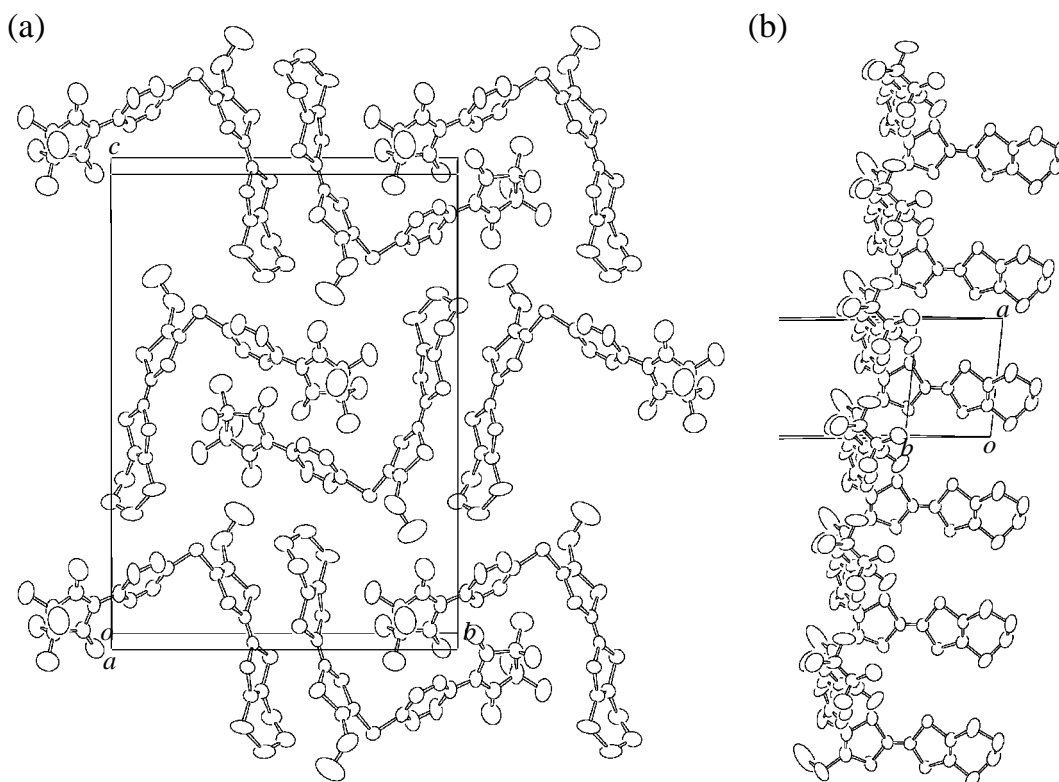
Figure 3-19. ORTEP drawings (50% probability) of crystal structure of **EMTN**.

Temperature dependence of magnetic susceptibility of the **EMTN** crystals measured by a SQUID magnetometer is shown in Figure 3-20. As shown in Figure 3-20(a), the plots of the raw data can be devided into singlet-triplet (S-T) model part (92%) and Curie-Weiss part (4%). When magnetic susceptibilities of amorphous samples of **EMTN** were measured, the plots were reproduced only by
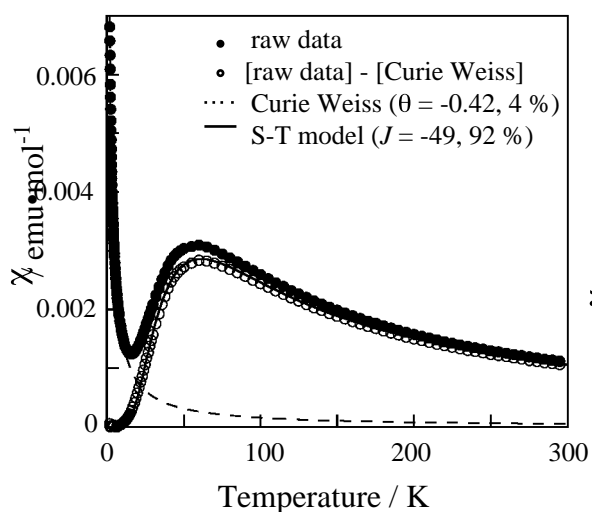
(a) χ vs. T plot   (b) χT vs. T plot
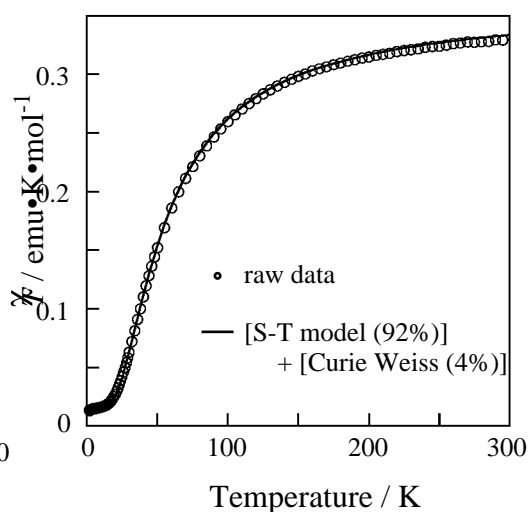
Figure 3-20. Temperature dependence of magnetic susceptibility of **EMTN**.

51

Curie-Weiss law with Weiss temperature $\theta \sim$ -0.45 K. The Curie-Weiss part in Figure 3-20(a) is considered to correspond to such amorphous phase. The residue was reproduced by a S-T model expressed below with J = -49 K.

$$\chi = \chi_{\text{S-T}} + \chi_{\text{Curie-Weiss}}$$
$$= 0.375 \times 0.92 \times 4 / [T\{3 + \exp(-2 \cdot J/T)\}] + 0.375 \times 0.04 / (T - \theta)$$

Figure 3-20(b) is the χT vs. T plot of the **EMTN** crystal. The behavior is fitted with the summation of a S-T model part and a Curie-Weiss part.

The magnetic interaction in the **EMTN** crystal is rationalized as follows. Since a stack of the dimers of phenylNN moieties is surrounded by TTF moieties, the stack is considered to be magnetically independent from outside. Within the stack, a pair of N-O moieties are located very close, making an effective overlap, whereas other N-O moieties are relatively remoted. Therefore, effective magnetic interaction is considered to be limited to the pair. The magnetic behavior of such
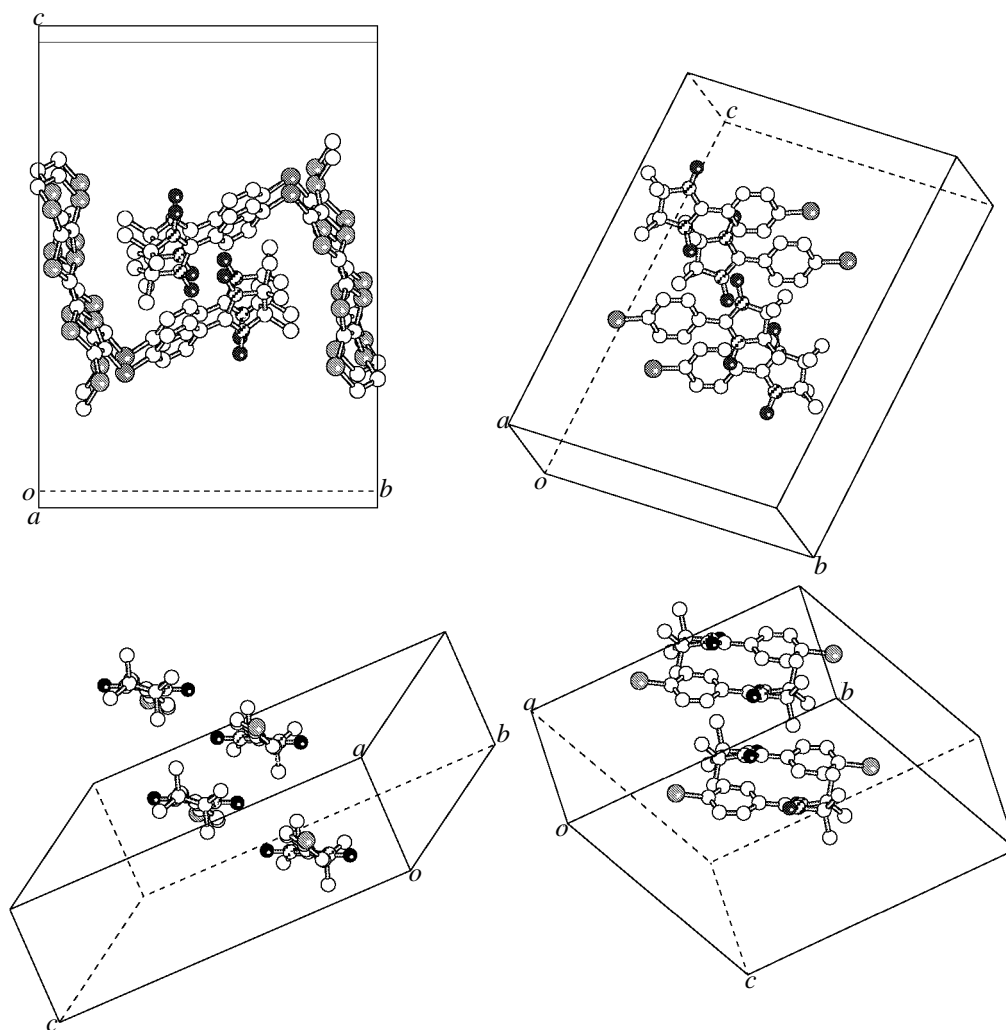
Figure 3-21. Plausible magnetic dimer.

pairs is expressed by the S-T model as described above. Such a large antiferromagnetic interaction is rarely observed for NN derivatives.

3-5-2. Preparation of Charge-Transfer Complexes

In order to obtain a conductive material, preparation of a charge-transfer complex of **EMTN** with an organic acceptor was attempted. The acceptors used here are 2,3,5,6-tetrafluoro-7,7,8,8-tetracyanoquinodimethane (F_4TCNQ), 2,3-dichloro-5,6-dicyano-1,4-benzoquinone (DDQ), 7,7,8,8-tetracyanoquinoquino-dimethane (TCNQ), and chloranil (CA).

At first, the donors and the acceptors were mixed in a solution. When a green solution of **EMTN** in CH_2Cl_2 was added to a yellow solution of an acceptor, the color of the solution turned immediately to dark blown in all cases. The ESR spectrum of a CH_2Cl_2 solution of **EMTN** and F_4TCNQ showed two signals: one is derived from an iminonitroxide radical, which is resulted from the NN radical, and the other is a sharp singlet line, which may be derived from an aggregated species. All these mixtures gave oily amorphous solids after the solvent evaporation.

When a green solution of **EMTN** in benzene was added to a yellow solution of an acceptor, the color of the solution was yellow-green, which gradually changed dark with solvent evaporation. Although these mixtures gave oily solids and crystals, the latter contained acceptors only.

Finally, a charge-transfer complex of **EMTN** with F_4TCNQ was prepared by grinding them with 1:1 ratio in a solid state.[9] IR spectrum of the complex showed some peaks different from that of the neutral donor and acceptor (Figure 3-22). The C-N stretching absorption (ν_{CN}) of the complex was observed at 2194 cm^{-1}, which is lower than that of neutral F_4TCNQ (2227 cm^{-1}).
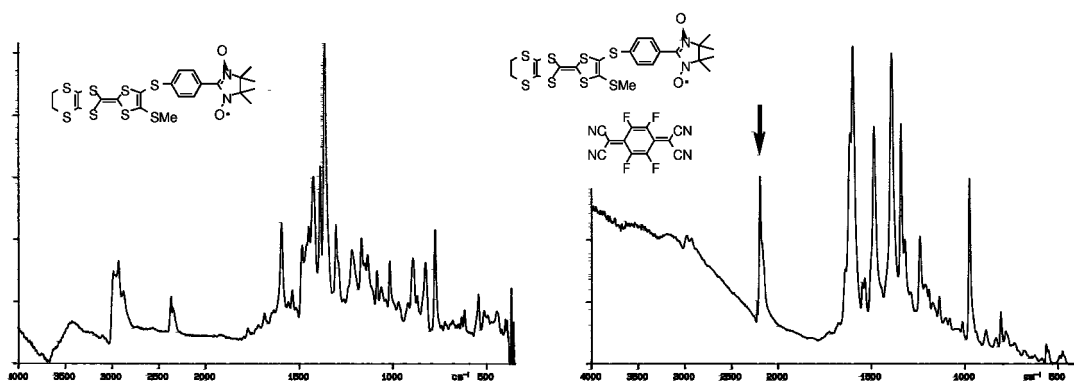
Figure 3-22. IR spectra of (a) neutral **EMTN**, (b) **EMTN** - F_4TCNQ.

Magnetic susceptibility of the complex was measured with a SQUID magnetometer. The magnetic property of the complex turned out to be paramagnetic, although decrease of χT value was observed at lower temperatures (Figure 3-23). The χT value at higher temperatures is *ca.* 0.3, which is slightly smaller than the theoretical value of $S = 1/2$ species (0.375). Therefore, a part of the sample is considered to be decomposed.
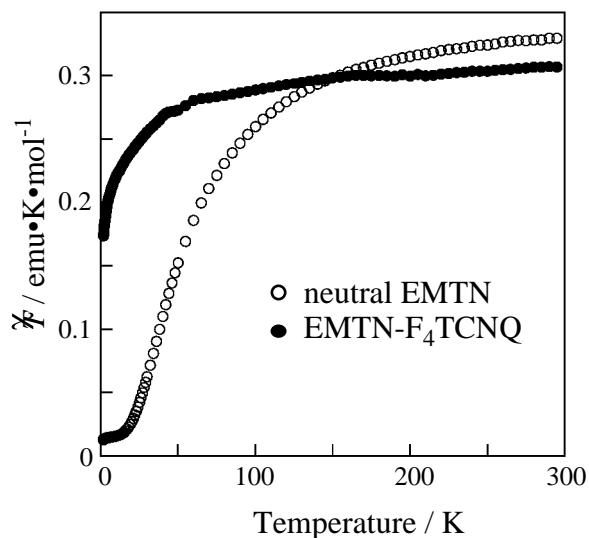
Figure 3-23. Temperature dependence of magnetic susceptibility of the CT-complex, **EMTN**-F_4TCNQ.

The plots could not be reproduced by a simple model. Since the mixing was performed in the solid sate, the sample may be heterolytic.

3-5-3. Discussion

In the case of **EMPN**, no single crystal was obtained, whereas **EMTN** afforded a single crystal. The difference may be derived from the shape of donor moiety, especially the presence of sulfur atoms. If the TTF moieties of two **EMPN** molecules are assembled, the phenylene moiety would disturb the interaction. On the other hand, the TTF moieties of **EMTN** form a *face-to-face* dimer in its crystal. An inserted sulfur atom of **EMTN** may also release the steric repulsion. Such a better crystallinity of **EMTN** is advangtageous to construct a conductive magnet.

As discussed in 3-4-1, twisting between the donor and the radical moieties may lead to a breakdown of the electronic framework of a spin-polarized donor. Although the determined molecular structure of **EMTN** in the neutral state is far from a planar conformation, the point is whether the conformation becomes planar in the oxidized state or not.

At present stage, the crystallinity of **EMTN** is not enough to afford single crystals of charge-transfer complexes or ion-radical salts.[10] Since the oxidation potential of **EMTN** is 0.60 V and the reduction potential of F_4TCNQ is 0.63 V, the charge-transfer complex between them is considered to be in an ionic state.

If **EMTN** affords an isolable ion-radical salt, triplet state of **EMTN**$^{+\bullet}$ may be detected from the magnetization curve at a low temperature. However, the existence of relatively large intermolecular antiferromagnetic interaction makes the detection difficult. Although the sample was prepared in the open-air, the loss of spin concentration is relatively small, indicating a reasonable kinetic stability of the complex.

§3-6. Summary

In order to realize a TTF-based spin-polarized donor which affords a ground state triplet cation diradical upon one-electron oxidation, *p*-phenylene inserted derivatives, **TTF-PN**, **EMPN**, and **EMTN**, were prepared. Although the oxidation potentials of these derivatives were higher than those of TTF or BEDT-TTF, these spin-polarized donors showed triplet ESR signals as a ground state. The *p*-phenylene group of these derivatives play a role to diminish a twisting of the NN group from the TTF plane by releasing a steric repulsion between these two groups.

The ionic CT complex of **EMTN** with F_4TCNQ showed resonable stability. Since isolation of cation diradical of a spin-polarized donor has been requested to confirm its ground state spin multiplicity by magnetic measurements,[11] a TTF-based spin-polarized donor is expected to be appropriate for this purpose.

A *p*-phenylene group is considered to be too frexible for a TTF-based spin-polarized donor to form a crystalline material. Development of another spacer group is discussed in the next chapter.

§3-7. Experimentals

General Procedures

NMR Spectroscopy. ^{1}H-NMR spectra were recorded on a JEOL JNM-GSX270 spectrometer. The chemical shift references were reported in δ relative to tetramethylsilane (0.00 ppm, for chloroform-*d* solution) or dimethylsulfoxide-d_5 (2.50 ppm, for dimethyl-sulfoxide-d_6 solution) as an internal standard.

IR Spectroscopy. Infrared spectra were recorded on a Perkin-Elmer 1640 infrared spectrometer using a KBr pellet.

ESR Spectroscopy (in solution). ESR spectra were recorded on a JEOL JES-TE300 (X-band) spectrometer. The resonance magnetic field value was measured with the aid of a JEOL ES-FC5 NMR field meter. The microwave frequency values are those displayed on the spectrometer.

Elemental Analysis. Elemental analyses were performed at the Organic Elemental Analysis Center of the Department of Chemistry, Faculty of Science, the University of Tokyo.

Materials

Most of the chemicals were purchased from Wako Pure Chemicals Industries Ltd. (WAKO), Tokyo Kasei Kogyo Co. Ltd. (TCI) and Kanto Chemical Co. Ltd. (Cica). 2,3-Bis(hydroxylamino)-2,3-dimethyl-butane was prepared by grinding its sulfate with pottasium hydrogen carbonate, followed by extraction with dichloromethane, and was recrystallized from benzene. There, the sulfate was prepared according literature,[12] while the sulfate used as a catalyst was purchased from Eastman Fine Chemicals (Kodak). Some of the products (**14** and **TTF-PN**) was prepared by Dr. Matsushita.[13] Tetrahydrofuran (WAKO) was distilled from sodium benzophenone ketyl under nitrogen. All the other reagents were used as purchased without further purification. Solvents were also purchased from Godo Yozai Co., Ltd. Silica gel is Cica-MERCK silica gel 60 (70-230 mesh ASTM).

Preparation

2-(1',3'-Dithiol-2'-ylidene)-4-(4''-formylphenyl)-1,3-dithiole (13)

To a solution of 1.4 mL (11 mmol) of diisopropylamine (TCI) in 10 mL of tetrahydrofuran, 3.8 mL (6 mmol) of *n*-butyllithium (1.6 M in hexane / WAKO) was added dropwise at -70 °C under nitrogen, and the mixture was warmed up to room temperature arbitrary with stirring. The mixture was added dropwise to a solution of 1.0 g (5 mmol) of tetrathiafulvalene (TCI) in 20 mL of tetrahydrofuran at -90 °C under nitrogen, and the reaction mixture was stirred at -50 °C for 1 hour. To this solution, 1.2 g (6 mmol) of trimethyltin chloride (WAKO-Aldlich) in 10 mL of tetrahydrofuran was added dropwise, and the mixture was stirred overnight. After solvents were removed under reduced pressure, the residue was extracted with diethylether and water. The organic layer was separated and concentrated in vacuo. The resulted light brownish oil

was dissolved in 20 mL of toluene. To this solution, 4-bromobenzaldehyde (950 mg, 5 mmol / TCI) and tetrakis(triphenylphosphine)palladium(0) (290 mg, 0.25 mmol / WAKO-Aldrich) were added, and the mixture was heated under reflux for 4 hours. After the mixture was cooled down to ambient temperature, the solution was passed through a silica gel short plug eluted with dichloromethane, and concentrated in vacuo. The resulted dark blown solid was purified by column chromatography on silica gel eluted with dichloromethane-hexane (1:1 to 7:3) to afford 830 mg (53 %) of blownish purple solid.

^{1}H-NMR(CDCl$_3$): δ = 10.00 (s, 1H), 7.87 (d, J = 8.5 Hz, 2H), 7.55 (d, J = 8.5 Hz, 2H), 6.75 (s, 1H), 6.35 (s, 2H).

1,3-Dihydroxy-2-[4'-{2''-(1''',3'''-dithiol-2'''-ylidene)-1'',3''-dithiol-4''-yl}phenyl]-4,4,5,5-tetramethylimidazolidine (14)

^{1}H-NMR(DMSO-d_6) δ 7.51 (d, J = 8.4 Hz, 2H), 7.42 (d, J = 8.4 Hz, 2H), 7.21 (s, 1H), 6.76 (s, 2H), 4.51 (s, 1H), 1.07 (s, 6H), 1.04 (s, 6H);

2-[4'-{2''-(1''',3'''-dithiol-2'''-ylidene)-1'',3''-dithiol-4''-yl}phenyl]-4,4,5,5-tetramethylimidazoline 3-oxide 1-oxyl (TTF-PN)

ESR(benzene) g = 2.0062, a_N = 0.74 mT (2N).

4-(Methylthio)-1,3-dithiol-2-thione (17) / Route A

To a solution of 19.0 mL (145 mmol) of diisopropylamine (TCI) in 25 mL of tetrahydrofuran, 55.0 mL (88 mmol) of n-butyllithium (1.6 M in hexane / WAKO) was added dropwise at -70 °C under nitrogen, and the mixture was warmed up to room temperature with stirring. The mixture was added dropwise to a solution of 10.2 g (76 mmol) of 1,3-dithiol-2-thione (TCI) in 50 mL of tetrahydrofuran at -90 °C under nitrogen, and the reaction mixture was stirred at -40 °C for 1.5 hours. The reaction mixture was cooled down to -90 °C again, and 10.3 g (320 mmol) of powdered sulfur (WAKO) was added in one portion. The mixture was stirred at -40 °C for 2 hours, and cooled down again. To this suspension, 20.0 mL (320 mmol) of methyl iodide (WAKO) was added dropwise, and the mixture was stirred for 8 hours with arbitrary increasing temperature. After the solvents were removed in vacuo, the residue was twice purified by column chromatography on silica gel eluted with dichloromethane-hexane (1:1) to afford 6.45 g (47 %) of light brown solid.

^{1}H-NMR(CDCl$_3$): δ = 6.90 (s, 1H), 2.51 (s, 3H).

4-(Methylthio)-1,3-dithiol-2-thione (17) / Route B

4-(methylthio)-5-(methoxycarbonyl)-1,3-dithiol-2-thione[14] (7.4 g, 31 mmol) was dissolved in 80 mL of pyridine, and stirred for 1 hour. To the solution, 60 g (570 mmol) of lithium bromide monohydrate (Cica) was added and the mixture was heated under gentle reflux for 5 hours. The reaction mixture was poured into a beaker filled with *ca.* 600 mL of crushed ice. Solids remaining the flask were washed with water and poured into the above beaker. The resulted 800 mL of aqueous mixture was filtrated, and the precipitates were air dried, and recrystallized from methanol-water. The resulted light yellow-green solid was dried in vacuo, and purified by column chromatography on silica gel eluted with hexane to afford 4.1 g (73 %) of yellow powder. ^{1}H-NMR (CDCl$_3$) spectral data were in accord with those of Route A.

2-[4'-(Methylthio)-1',3'-dithiol-2'-ylidene]-5,6-dihydro-1,3-dithiolo[4,5-b][1,4]dithiin (18)

A stirred mixture of 4-(methylthio)-1,3-dithiol-2-thione (**17**, 6.2 g, 34 mmol), 4,5-(ethylenedithio)-1,3-dithiol-2-one (**15**, 8.7 g, 42 mmol), and triethylphosphite (90 mL, 525 mmol / TCI) was heated to 110 ˚C for 4 hours. After triethylphosphite was removed under reduced pressure, the residue was suspended in 300 mL of chloroform and filtrated. The solution was concentrated and purified by column chromatography on silica gel eluted with chloroform-hexane (1:1) to afford 6.1 g (52 %) of reddish orange solid.

^{1}H-NMR(CDCl$_3$): δ = 6.29 (s, 1H), 3.29 (s, 4H), 2.39 (s, 3H).

2-(5',6'-dihydro-1',3'-dithiolo[4,5-b][1,4]dithiin-2'-ylidene)-4-(4''-formylphenyl)-5-(methylthio)-1,3-dithiole (20)

To a solution of 2.6 mL (20 mmol) of diisopropylamine (TCI) in 30 mL of tetrahydrofuran, 11.2 mL (18 mmol) of *n*-butyllithium (1.6 M in hexane / WAKO) was added dropwise at -70 ˚C under nitrogen, and the mixture was warmed up to room temperature with stirring. The mixture was added dropwise to a solution of 6.0 g (18 mmol) of **18** in 50 mL of tetrahydrofuran at -90 ˚C under nitrogen, and the reaction mixture was stirred at -50 ˚C for 3 hours. The mixture was cooled to -90 ˚C again, and 3.8 g (19 mmol) of trimethyltin chloride in 25 mL of tetrahydrofuran was added dropwise to the suspension. The mixture was stirred overnight with arbitrary increasing temperature. After the solvents were removed under reduced pressure, the residue was extracted with diethylether and water, and the separated organic layer was dried over sodium sulfate, filtrated, and concentrated in vacuo. The resulted brown oil was dissolved in 120 mL of toluene. To the solution, 4.2 g (18 mmol) of 4-iodobenzaldehyde (**16**), 120 mL of 1 M aqueous sodium carbonate, and 2.0 g (1.7 mmol) of tetrakis(triphenylphosphine)-palladium(0) were added, and the mixture was heated under reflux for 20 hours. The organic layer was separated and the aqueous layer was extracted with chloroform. The organic layers were conbined, dried over sodium sulfate, filtrated, and concentrated in vacuo. The residue was purified by column chromatography on silica gel eluted with chloroform and by gel permiation liquid chromatography to afford 4.1 g (52 %) of reddish oil. The oil solidified upon standing.

^{1}H-NMR(CDCl$_3$): δ = 10.03 (s, 1H), 7.90 (d, *J* = 8.1 Hz, 2H), 7.66 (d, *J* = 8.1 Hz, 2H), 3.31 (s, 4H), 2.38 (s, 3H).

1,3-Dihydroxy-2-[4'-{2''-(5''',6'''-dihydro-1''',3'''-dithiolo[4,5-b][1,4]dithiin-2'''-ylidene)-5''-(methylthio)-1'',3''-dithiol-4''-yl}phenyl]-4,4,5,5-tetramethylimidazolidine (21)

To a solution of 2.9 g (6.6 mmol) of aldehyde **20** in 100 mL of dichloromethane-hexane (1:1), 2.0 g (14 mmol) of 2,3-dimethyl-2,3-bis(hydroxylamino)butane and 43 mg (0.2 mmol) of its sulfate were added, and the mixture was heated under reflux for 2 days. During the heating, small amount of molecular sieves were placed between flask and condenser. After the solvents were removed under reduced pressure, the residue was suspended in chloroform and filtrated. The precipitates were washed with chloroform and dried to affod 2.2 g (60 %) of orange powder.

^{1}H-NMR(DMSO-d_6): δ = 7.56 (d, J = 8.4 Hz, 2H), 7.47 (d, J = 8.4 Hz, 2H), 4.80 (s, 1H), 3.30 (s, 4H), 2.33 (s, 3H), 1.19 (s, 6H), 1.15 (s, 6H).

2-[4'-{2''-(5''',6'''-dihydro-1''',3'''-dithiolo[4,5-b][1,4]dithiin-2'''-ylidene)-5''-(methylthio)-1'',3''-dithiol-4''-yl}phenyl]-4,4,5,5-tetramethylimidazoline 3-oxide 1-oxyl   (EMPN)

To a stirred suspension of 2.3 g (4.0 mmol) of hydroxylamine **21** and 200 mL of tetrahydrofuran, 20.0 g (145 mmol) of potassium carbonate was added, and the mixture was stirred for 1 hour. To the suspension, 10.0 g (42 mmol) of lead dioxide was added and stirred for 40 minutes. The reaction mixture was filtrated, concentrated, and purified by column chromatography on silica gel eluted with tetrahydrofuran-diethylether (1:1) to afford 1.2 g (52 %) of dark greenish brown solid.

ESR(benzene): g = 2.0056, a_N = 0.73 mT (2N).

Anal.: calc. C 46.20, H 4.05, N 4.90, S 39.25 %, found C 46.65, H 4.15, N 4.76, S 38.06 %.

4-[4'-(1'',3''-Dioxolan-2''-yl)phenylthio]-5-(methylthio)-1,3-dithiol-2-thione (24)

To a solution of 2.6 g (15 mmol) of thione **17** in 50 mL of diethylether, 8.6 mL (17 mmol) of lithiumdiisopropylamide (2.0 M in heptane-tetrahydrofuran-ethylbenzene / Aldrich) was added dropwise at -90 ˚C under nitrogen, and the mixture was stirred at -40˚C for 2 hours. To this suspension, 6.5 g (18 mmol) of disulfide **23** dissolved in 70 mL of benzene-diethylether (5:2) was added dropwise at -70 ˚C, and the mixture was stirred overnight at room temperature. After the solvents were removed and dried in vacuo, the residue was extracted with dichloromethane and water. The separated organic layer was dried over sodium sulfate, filtrated, concentrated, and purified by column chromatography on silica gel eluted with dichloromethane to afford 2.9 g (57 %) of blownish solid.

^{1}H-NMR(CDCl$_3$): δ = 7.40-7.50 (m, 4H), 5.81 (s, 1H), 4.00-4.12 (m, 4H), 2.51 (s, 3H).

2-(5',6'-Dihydro-1',3'-dithiolo[4,5-b][1,4]dithiin-2'-ylidene)-4-[4''-(1''',3'''-dioxolan-2'''-yl)phenylthio]-5-(methylthio)-1,3-dithiole (25)

A stirred mixture of thion-acetal **24** (4.0 g, 11 mmol), ketone **15** (4.8 g, 23 mmol), and triethylphosphite (45 mL, 250 mmol / TCI) was heated to 120 ˚C for 8 hours. After triethylphosphite was removed under reduced pressure, the residue was suspended in 100 mL of chloroform and filtrated. The solution was concentrated and purified by column chromatography on silica gel eluted with chloroform to afford 3.5 g (59 %) of red oil, which solidified upon standing.

^{1}H-NMR(CDCl$_3$): δ = 7.33-7.45 (m, 4H), 5.80 (s, 1H), 4.00-4.13 (m, 4H), 3.28 (s, 4H), 2.45 (s, 3H).

2-(5',6'-Dihydro-1',3'-dithiolo[4,5-b][1,4]dithiin-2'-ylidene)-4-(4''-formylphenylthio)-5-(methylthio)-1,3-dithiole (26)

To a solution of 550 mg (1.0 mmol) of acetal **25** in 10 mL of chloroform, 3 mL of acetone, a spoon of *p*-toluenesulfonic acid monohydrate, and a few drop of water were added, and the mixture was stirred overnight at room temperature. The reaction mixture was washed with saturated aqueous sodium hydrogen carbonate, and extracted with chloroform. The organic layer was concentrated under reduced pressure and purified by

gel permiation liquid chromatography to afford 460 mg (90 %) of orange solid.

^{1}H-NMR(CDCl$_3$): δ = 9.96 (s, 1H), 7.81 (d, J = 8.4 Hz, 2H), 7.39 (d, J = 8.4 Hz, 2H), 3.30 (s, 4H), 2.48 (s, 3H).

2-[4'-{2''-(5''',6'''-Dihydro-1''',3'''-dithiolo[4,5-b][1,4]dithiin-2'''-ylidene)-5''-(methylthio)-1'',3''-dithiol-4''-ylthio}phenyl]-1,3-dihydroxy-4,4,5,5-tetramethylimidazolidine (27)

To a solution of 1.18 g (2.5 mmol) of aldehyde **26** in 60 mL of benzene-methanol (5:1), 1.04 g (7.0 mmol) of 2,3-dimethyl-2,3-bis(hydroxylamino)butane and 304 mg (1.2 mmol) of its sulfate were added, and the mixture was heated under reflux for 36 hours. During the heating, small amount of molecular sieves were placed between flask and condenser. The precipitates were filtrated, washed with methanol and dried in vacuo to affod 1.09 g (73 %) of orange powder.

^{1}H-NMR(DMSO-d_6): δ = 7.79 (s, 2H), 7.51 (d, J = 8.2 Hz, 2H), 7.35 (d, J = 8.2 Hz, 2H), 4.50 (s, 1H), 3.32 (s, 4H), 2.50 (s, 3H), 1.07 (s, 6H), 1.04 (s, 6H).

2-[4'-{2''-(5''',6'''-Dihydro-1''',3'''-dithiolo[4,5-b][1,4]dithiin-2'''-ylidene)-5''-(methylthio)-1'',3''-dithiol-4''-ylthio}phenyl]-4,4,5,5-tetramethylimidazoline   3-oxide 1-oxyl   (EMTN)

To a stirred suspension of 1.09 g (1.8 mmol) of hydroxylamine **27** and 100 mL of tetrahydrofuran, 5.00 g (36 mmol) of potassium carbonate was added, and the mixture was stirred for 1 hour. To the suspension, 5.55 g (23 mmol) of lead dixide was added and stirred for 40 minutes. The reaction mixture was filtrated, concentrated, and purified by column chromatography on silica gel eluted with tetrahydrofuran-diethylether (1:1) to afford 960 mg (85 %) of green solid.

ESR(benzene): g = 2.0072, a_N = 0.75 mT (2N).

FAB-MS calcd. for C$_{22}$H$_{23}$N$_2$O$_2$S$_8$ (M$^+$) 602.95, found 602.8.

Measurements and Calculations

Cyclic Voltammetry. Cyclic voltammograms were recorded in benzonitrile solution in the presence of 0.1 M tetra-n-butylammonium perchlorate (Nacalai Tesque Inc.) as an supporting electrolyte with a platinum working electrode using a Hokuto Denko HAB 151 potentiostat/galvanostat at room temperature. An Ag/AgCl electrode (BAS Co.) was used for a reference electrode. Scanning rate was 200 mV/s.

Optical Measurement. UV absorption spectra were observed on a JASCO V-570 spectrometer using $ca.$ 10^{-5} M dichloromethane (Dojin Spectrozol) solution of samples.

ESR Measurement. ESR spectra were measured on a JEOL TE300 spectrometer equipped with an RMC liquid helium transfer system and a Scientific Instruments 9650 digital temperature indicator/controller. The resonance magnetic field value was measured with the aid of a JEOL ES-FC5 NMR field meter.

Zero-field parameters were determined by computational simulation as is reported by Kumai.[15]

Molecular Orbital Calculation. PM3/UHF molecular orbital calculation was carried out using a CAChe MOPAC program provided from SONY Techtronics. The molecular structure was optimized using a planar conformation as an initial structure.

Magnetic Measurement. Magnetic susceptibilities of polycrystalline EMTN and powdered EMTN-F_4TCNQ complex were measured with a Quantum Design MPMS-XL SQUID magnetometer by a reciprocating sample option (RSO) method. The diamagnetic susceptibility of neutral EMTN was estimated from the plot of the high temperature data, and that of CT complex was calculated as a summation of those of neutral EMTN and F_4TCNQ, the latter was experimentally measured independently.

X-ray Crystallographic Analysis of EMTN

A darkgreen needle crystal of **EMTN** having approximate dimensions of $1.00 \times 0.03 \times 0.01$ mm was mounted on a glass fiber. All measurements were made on a Rigaku RAXIS-IV imaging plate area detector with graphite monochromated Mo-Kα radiation.

Indexing was performed from 3 oscillations which were exposed for 55.0 minutes. The crystal-to-detector distance was 105.00 mm with the detector at the zero swing position. Readout was performed in the 0.100 mm pixel mode.

Cell constants and an orientation matrix for data collection corresponded to a primitive monoclinic cell with dimensions: $a = 6.9919(6)$ Å, $b = 16.817(2)$ Å, $c = 23.037(2)$ Å, $\beta = 96.674(6)°$, $V = 2690.3401$ Å^3. For $Z = 4$ and F.W. = 603.92, the calculated density is 1.49 g/cm^3. The systematic absences of: $h0l$ (l $2n$), $0k0$ (k $2n$), uniquely determine the space group to be $P2_1/c$ (#14).

The data were collected at room temperature to a maximum 2θ value of 55.3°. A total of thirtyfive 3.00° oscillation images were collected, each being exposed for 55.0 minutes. The crystal-to-detector distance was 105.00 mm with the detector at the zero swing position.Readout was performed in the 0.100 mm pixel mode.

A total of 4678 reflections was collected.

The linear absorption coefficient, μ, for Mo-Kα radiation is 30.4 cm^{-1}. The data were corrected for Lorentz and polarization effects. A correction for secondary extinction was applied (coefficient = 1.20134e-06).

The structure was solved by a direct method (SHELXS86)[16] and expanded using Fourier techniques (DIRDIF94).[17] The non-hydrogen atoms were refined anisotropically. Hydrogen atoms were included but not refined. The final cycle of full-matrix least-squares refinement[18] was based on 3181 observed reflections (I > 3.00σ(I)) and 308 variable parameters and converged (largest parameter shift was 0.00 times its esd) with unweighted and weighted agreement factors of: $R =$ $||Fo| - |Fc|| /$ $|Fo| = 0.072$, $Rw = [$ $w(|Fo| - |Fc|)^2 /$ $wFo^2]^{1/2} = 0.094$.

The standard deviation of an observation of unit weight [$w(|Fo|-|Fc|)^2/(No-Nv)]^{1/2}$ (No : number of observations; Nv : number of variables) was 2.26. The weighting scheme was based on counting statistics and included a factor (p = 0.050) to downweight the intense reflections. Plots of $w(|Fo| - |Fc|)^2$ versus $|Fo|$, reflection order in data collection, $\sin \theta/\lambda$ and various classes of indices showed no unusual trends. The maximum and minimum peaks on the final difference Fourier map corresponded to 0.33 and -0.34 e^-/Å^3, respectively.

All calculations were performed using the teXsan[19] crystallographic software package of Molecular Structure Corporation.

§3-8. References and Notes

1. Kumai R, Matsushita MM, Izuoka A, Sugawara T, "Intramolecular exchange interaction in a novel cross-conjugated spin system composed of -ion radical and nitronyl nitroxide", *J. Am. Chem. Soc.* **1994**, *116*, 4523-4524.
2. Ullman EF, Osiecki JH, Boocock DGB, Darcy R, "Studies of stable free radicals. X. Nitronyl nitroxide monoradicals and biradicals as possible small molecule spin labels", *J. Am. Chem. Soc.* **1972**, *94*, 7049-7059.
3. Stille JK, "The palladium-catalyzed cross-coupling reactions of organotin reagents with organic electrophiles", *Angew. Chem. Int. Ed. Engl.* **1986**, *25*, 508-524.
4.   , "   TTF   ",   **1994**.
5. van Haare JAEH, Groenendaal L, Peerlings HWI, Havinga EE, Vekemans JAJM, Janssen RAJ, Meijer EW, "Unusual redox behavior of -oligoheteroaromatic compounds: An increasing first oxidation potential with increasing conjugation length", *Chem. Mater.* **1995**, *7*, 1984-1989.
6.   , "   (   )",   , **1982**, 173.
7. While the doubly occupied HOMO is almost localized on TTF site, the singly occupied SOMO' spreads over the entire molecule. Such a mechanism may be rationalized on the basis of a perturbational MO method. In general, an orbital interaction between two doubly occupied orbitals affords no net gain in energy, whereas an orbital interaction between a singly occupied orbital and a doubly occupied one causes a stabilization effect, as seen in a two-centered three-electron bond. Since energy difference between *homo* of the TTF site and *nhomo* of the PhNN site is large, there is negligibly small orbital interaction, and these orbitals would exist separately in the neutral state. If the orbital interaction is considered between *somo'* of the TTF$^{+\bullet}$ site and *nhomo* of the PhNN site, the perturbational interaction becomes significantly larger, and these orbitals should be hybridized. As a result, SOMO' of TTF-PN$^{+\bullet}$ are extended to the both sites.
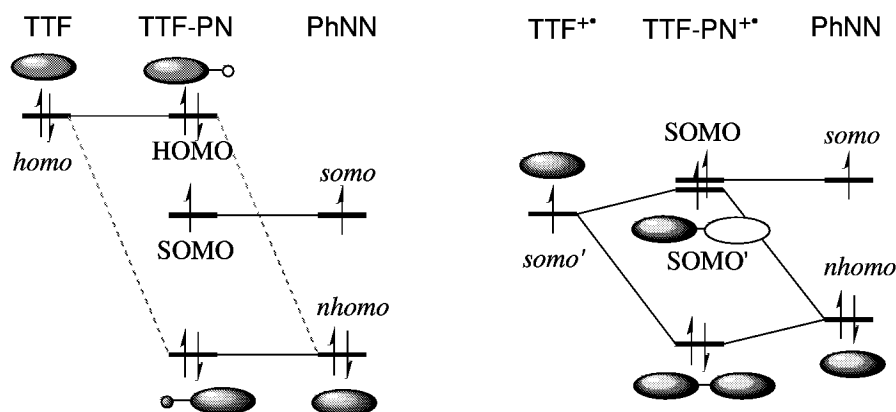
8. Contribution of *lumo* of the radical site is also plausible as shown below.
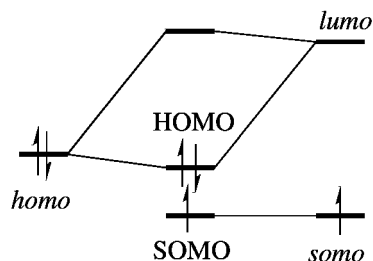
9.a) Sakurai H, Izuoka A, Sugawara T, "Preparation and property of ionic CT complex of dimethylamino nitronyl nitroxide with DDQ", *Mol. Cryst. Liq. Cryst.* **1997**, *306*, 415-421.
  b) Sakurai H, "High-spin cation diradical derived from open-shell donors", *Ph.D thesis, The Univ. of Tokyo, Japan,* **1996**.

10. Several attempts of electrocrystallization of EMTN have been made, but no ion-radical salt was obtained.

11. The linear Curie plot of the signal intensity of the triplet ESR spectrum also indicates the existence of nearly degenerated singlet and triplet states. In order to exclude such a possibility and to confirm the triplet ground state, magnetic measurements of isolated oxidized species should be carried out.

12. Lamchen M, Mttag TW, "Nitrones. part IV. Synthesis and properties of a monocyclic -dinitrone", *J. Chem. Soc. C* **1966**, 2300-2303.

13. Matsushita MM, private communication.

14. Sudmale IV, Tormos GV, Khodorkovsky VY, Edzina AS, Neillands OJ, Cava MP, "Synthesis and properties of new bridged tetrathiafulvalenes", *J. Org. Chem.* **1993**, *58*, 1355-1358.

15. Kumai R, "Preparation of open-shell donors and intramolecular exchange interaction of their one-electron oxidation states", *Thesis, The University of Tokyo*, **1994**, p85.

16. SHELXS86: Sheldrick GM, In: Sheldrick GM, C. Kruger C, Goddard R, eds. *"Crystallographic Computing 3"*, Oxford Univ. Press **1985**, 175-189.

17. DIRDIF94: Beurskens PT, Admiraal G, Beurskens G, Bosman WP, de Gelder R, Israel R, Smits JMM, "The DIRDIF-94 program system", *Technical Report of the Crystallography Laboratory, Univ. of Nijmegen, The Netherlands,* **1994**.

18. Least-Squares: Function minimized: $w(|Fo|-|Fc|)^2$.

19. teXsan: Crystal Structure Analysis Package, Molecular Structure Corporation (1985 & 1992).

Chapter 4

Preparation and Properties of Annulated TTF-Based Spin-Polarized Donors

§4-1. Introduction

As a promising constituting unit of an organic conducting magnet, several TTF-based spin-polarized donors, in which a TTF skeleton is connected with a nitronyl nitroxide (NN) group in a cross-conjugating manner, have been reported. Those TTF-based spin-polarized donors proved to exhibit a ferromagnetic intramolecular coupling upon one-electron oxidation between a -delocalizing spin generated on the donor site and a localized spin on the radical site. The kinetic stability of the singly oxidized species derived from these spin-polarized donors, however, is not high enough to yield isolable ion-radical salts.

Organic crystalline environment is known to be effective to stabilize very reactive species.[1] If the singly oxidized species of the spin-polarized donors are packed in a crystalline environment, they are expected to live longer. In order to produce a crystalline environment, the crystallinity of the constituent donors should be improved further. From this viewpoint, increasement of coplanarity of the donor or idealization of molecular symmetry was intended by the use of annulated ring systems.

The donor radicals discussed in this chapter are listed in Figure 4-1. Annulation of the benzene ring of **EMPN** to the TTF skeleton affords a benzo-annulated derivative, **ETBN**. The connectivity between the NN site and the donor site is similar to that of a sulfur-containing spin-polarized donor, thianthrene-NN, which affords ground state triplet cation diradical upon one-electron oxidation. **ETBN**

can be regarded as a combination of BEDT-TTF and thianthrene-NN. If the benzene ring is replaced by a thiophene ring, the radical site is expected to be located along the molecular long axis. Crystallinity of the thieno-annulated derivative, **ETTN**, is expected to be good. Annulation of 4-(1'-pyrrolyl)phenylNN (**N-PN**) to the TTF-skeleton affords a phenylpyrrolo-annulated derivative, **EPPN**, of which molecular symmetry along the molecular long axis is very high.
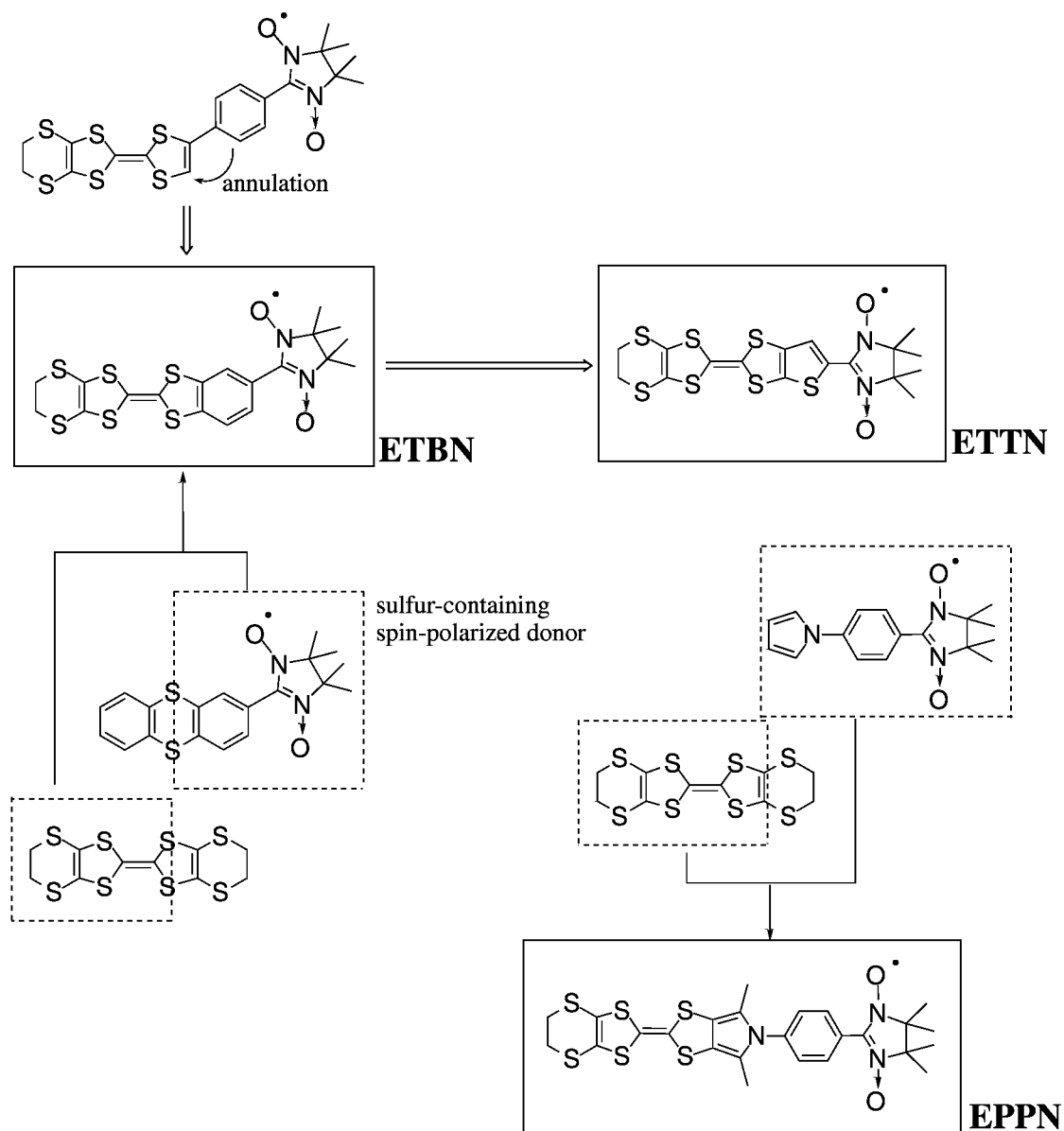
Figure 4-1. Design of ring-annulated donor radicals.

Preparation and structural features of these annulated TTF-based donor radicals are described in Section 2, and their electronic features as spin-polarized donors are examined in Section 3.

Among these donor radicals, the benzo-annulated derivative turned out to afford an isolable ion radical salt for the first time as a spin-polarized donor. The preparation of ion radical salts are documented in Section 4, and the physical behavior of the ion radical salts are discussed in Section 5.

§4-2. Preparation of Annulated TTF-Based Donor Radicals

4-2-1. Synthesis of Annulated TTF-Based Donor Radicals

The aldehyde precursors of these donor radicals were prepared by Kawada, *et al.*[2] These precursors were converted to nitronyl nitroxide derivatives by the ordinal method[3] (Figure 4-2). Among these donor radicals, **ETBN** and **EPPN** turned out to be chemically stable, while **ETTN** easily decomposes to diamagnetic species.
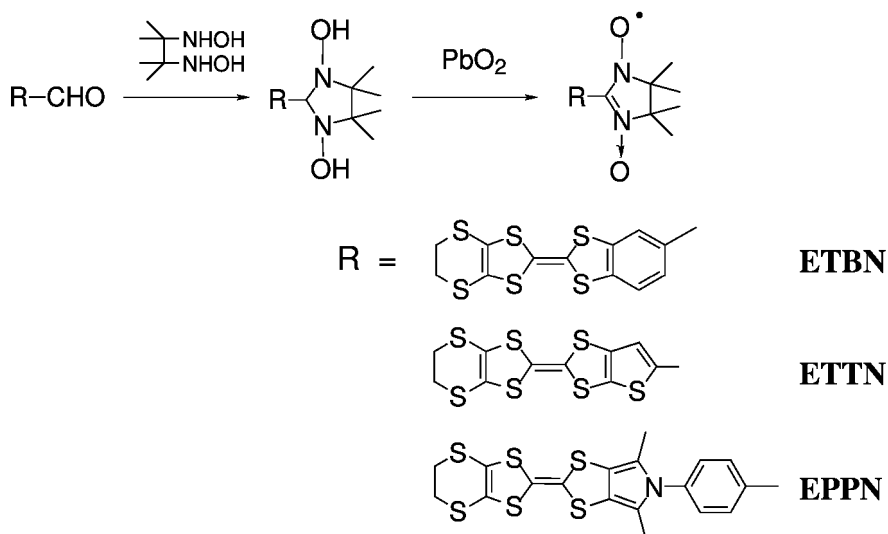
Figure 4-2. Preparation of ring-annulated donor radicals.

4-2-2. Molecular Structures of Annulated TTF-Based Donor Radicals

These annulated TTF-based donor radicals have good crystallinity, and are able to be examined by X-ray crystallography. The molecular structures of these donor radicals determined by X-ray crystallography are shown in Figure 4-3. The crystallographic parameters are summarized in Table 4-1, and the detailed data are listed in Appendix.

The donor moieties of these donor radicals are slightly bent as often seen in neutral TTF derivatives. In the case of **ETBN**, the bending occurred on the 1,3-dithiole ring at the remote side from NN, while **ETTN** is bent at the near side. Both 1,3-dithiole rings are bent in **EPPN**.

The NN moiety of **ETTN** is located along the molecular long axis. Although there is a disorder in reference to the thiophene ring of **ETTN**, the disorder does not affect the location of the NN moiety. On the other hand, the molecular long axis of **EPPN** is curved when it is viewed vertical to the donor plane.

The dihedral angles between the donor and radical parts are also shown in Figure 4-3. **ETTN** is the most flat among them, **ETBN** is the second, and **EPPN** is twisted as much as 60˚. The *p*-phenylene moiety of **EPPN** is more twisted from pyrrole ring than in the case of *N*-**PN** (4-(pyrrol-1'-yl)phenyl NN) due to a steric effect of the methyl groups on -positions of the pyrrole ring.

Table 4-1. Crystallographic parameters of donor radicals

	ETBN	ETTN	EPPN
Space Group	$R\bar{3}$ (#148)	$P\bar{1}$ (#2)	$C2/c$ (#15)
a / Å	43.24(7)	12.080(3)	19.252(7)
b / Å	a	12.694(2)	8.660(6)
c / Å	6.381(4)	9.725(2)	32.715(6)
α / deg	90	110.15(2)	90
β / deg	90	108.04(2)	93.43(3)
γ / deg	120	93.48(2)	90
V / Å^3	10327(25)	1307.5(5)	5444(4)
Z	18	2	8
Observations	2694	3730	2806
Variables	262	325	334
Refl/Para Ratio	10.28	11.48	8.40
R	0.108	0.078	0.059
R_w	0.173	0.207	0.046
R_1	0.063	0.063	0.059
Goodness of Fit	2.15	2.24	2.83

(a) **ETBN**
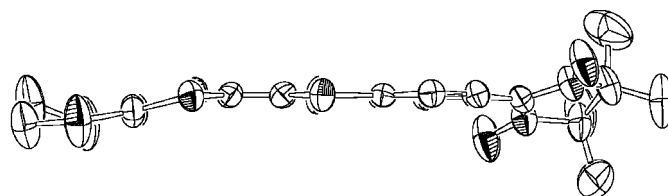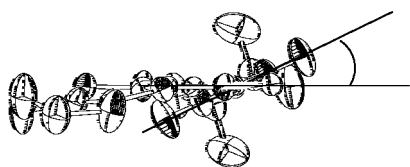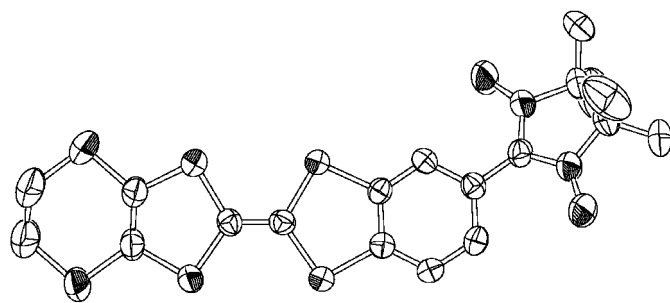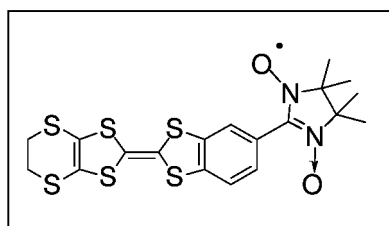
(b) **ETTN**
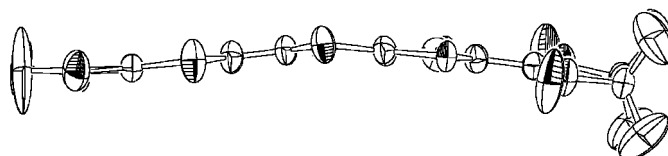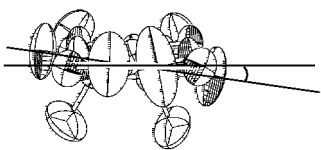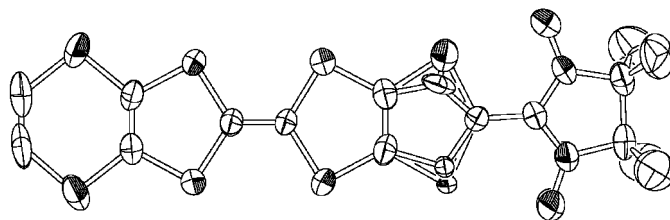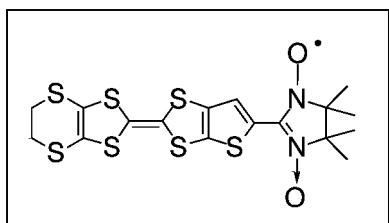
(c) **EPPN**
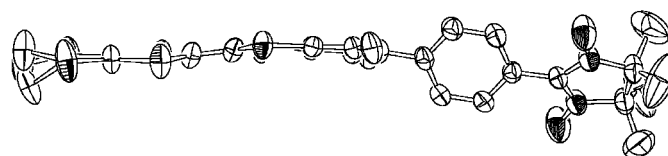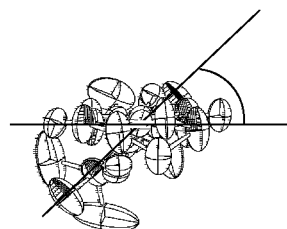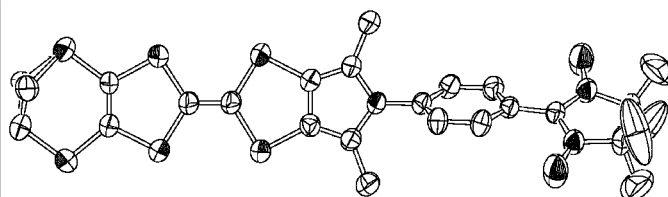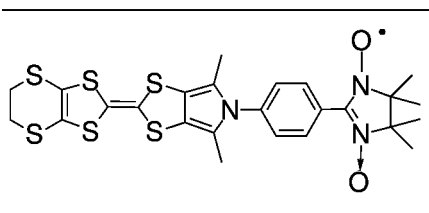
Figure 4-3. ORTEP drawings (50% probability) of molecular structures of donor radicals.

4-2-3. Crystal Structures of Annulated TTF-Based Donor Radicals

Crystal packing of these donor radicals are shown in Figures 4-4 to 4-6. The crystal of **ETBN** turned out to belong to a trigonal space group $R\bar{3}$. The trigonal hexagonal unit cell contains 18 crystallographic equivalent molecules (Figure 4-4(a),(c)). When the unit cell is viewed along the *c*-axis, each **ETBN** molecule forms a *face-to-face* dimer with an inversion symmetry. Each of these dimers is correlated by a 3-fold rotatory-inversion axis, forming a propeller-like six-membered ring structure. The **ETBN** molecules are arranged *side-by-side* along the *c*-axis by translation (Figure 4-4(b)). Along the 3-fold screw axes at (1/3, 0), (2/3, 0), (0, 1/3), (0, 2/3), (1/3, 1/3), (2/3, 2/3) positions in the *ab* plane, triangular prismatic structures are constructed.

(a) *ab* plane
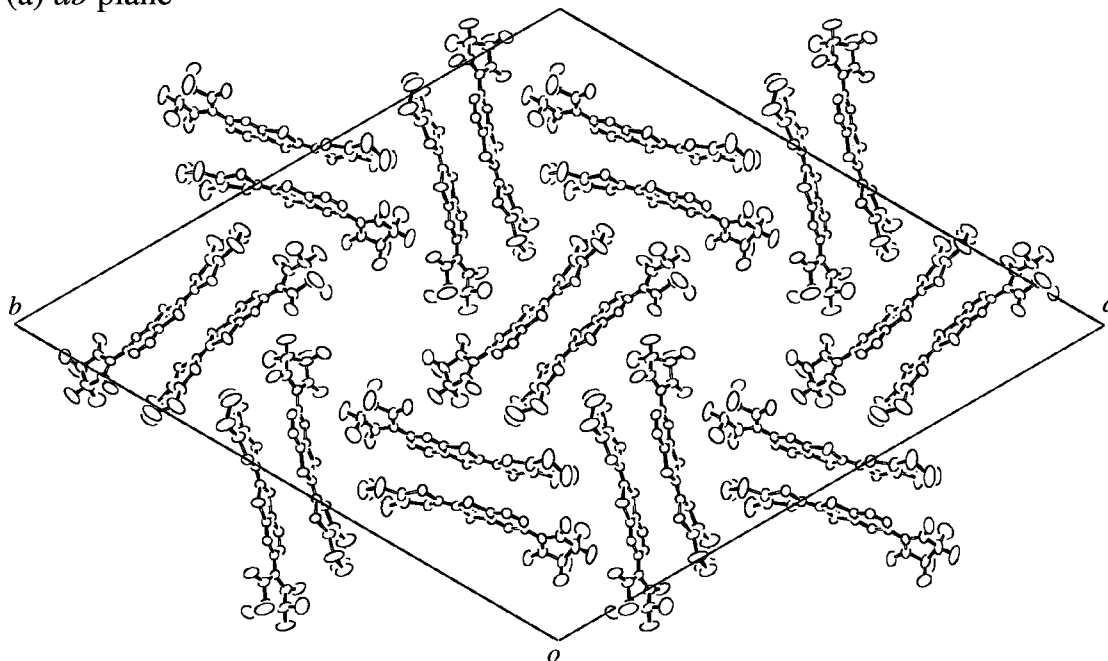
(b) *c*-axis
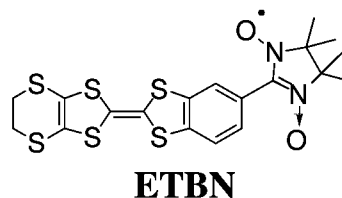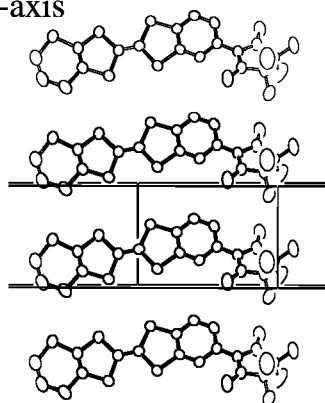
ETBN

Figure 4-4. Crystal structure of **ETBN** determined by X-ray crystallography.

(c) symmetry operations

(iv) -x, -y+1, -z

(ii) -y+1, x-y+1, z   (v) y, -x+y, -z
(iii) -x+y, -x+1, z   (vi) x-y+1, x+1, -z

(vii) x+2/3, y+1/3, z+1/3
(viii) -y+2/3, x-y+4/3, z+1/3
(ix) -x+y-1/3, -x+1/3 z+1/3
(x) -x+2/3, -y+4/3, -z+1/3
(xi) y-1/3, -x+y+1/3, -z+1/3
(xii) x-y+2/3, x+1/3, -z+1/3

(xiii) x+1/3, y-1/3, z+2/3
(xiv) -y+4/3, x-y+2/3, z+2/3
(xv) -x+y+1/3, -x+2/3, z+2/3
(xvi) -x+1/3, -y+2/3, -z+2/3
(xvii) y+1/3, -x+y-1/3, -z+2/3
(xviii) x-y+4/3, x+2/3, -z+2/3
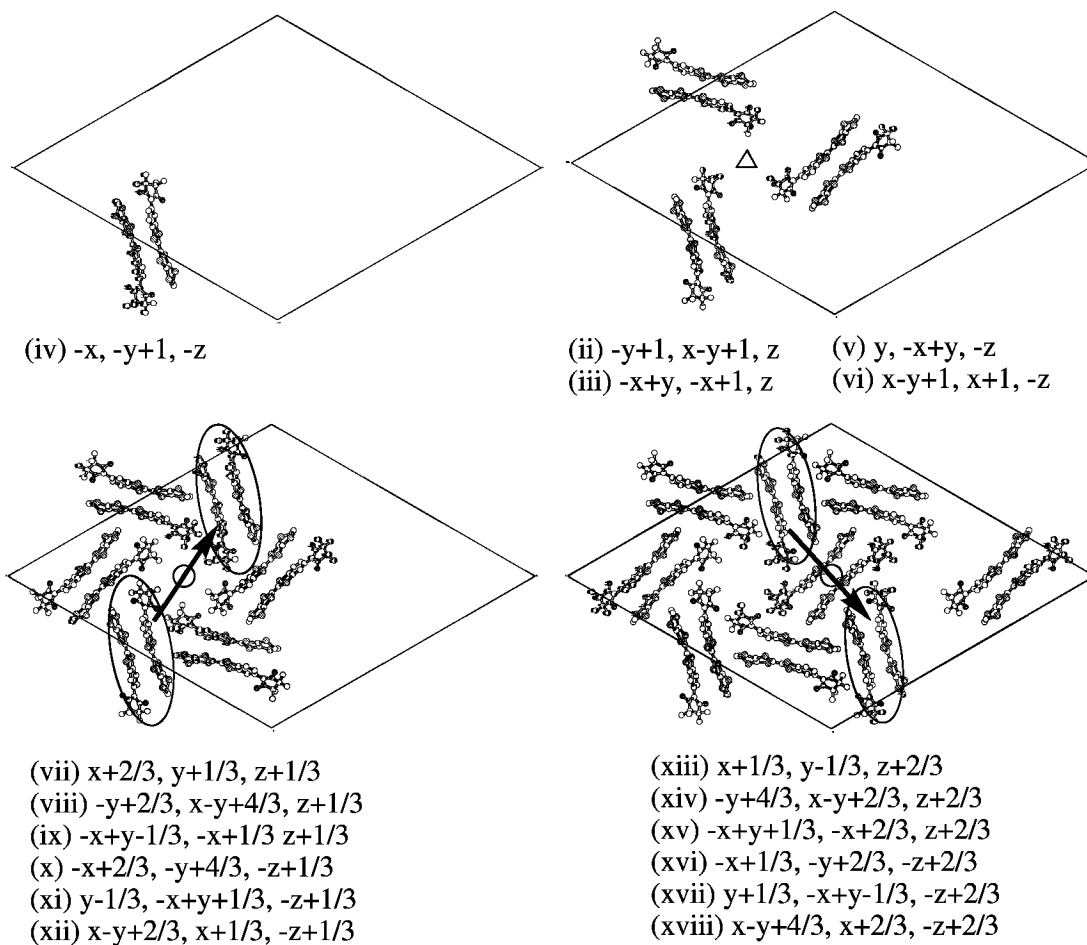
Figure 4-4. (Continued).

As seen in Figure 4-4(a), there is a vacant space around the rotetory-inversion axis, which is surrounded by the NN groups of six **ETBN** molecules. The space is considered to be really vacant because (i) the final difference Fourier map showed only weak peaks, (ii) the result of elemental analysis is in agree with **ETBN** only, and (iii) the crystal tend to be pyrolyted along its long axis, which is attributed to the crystallographic c-axis. The needle crystal of **ETBN** can be characterized as a "straw-like" structure by the existence of cavities along its long axis.[4] The cavity structure may be constructed by the aid of dichloromethane, which is considered to be lost on drying procedure. Such a structure reminds the honey-comb structured inclusion complex of urea.

70

The crystal of **ETTN** belongs to a triclinic space group $P\bar{1}$. Solvent molecules (pyridine) are incorporated in the crystal. Since the position of the nitrogen atom was not determined, all the six atoms were processed as carbon atoms.

The **ETTN** molecules are forming a sheet structure. Within the sheet, the **ETTN** molecules are aligned *side-by-side* in an antiparallel manner (Figure 4-5(b)). The ribbons are aligned by translation, sandwiching pyridine molecules. Therefore, the sheet is featured by the stripe structure composed of TTF ribbons and NN-pyridine ribbons.

(a) viewed along *c*-axis
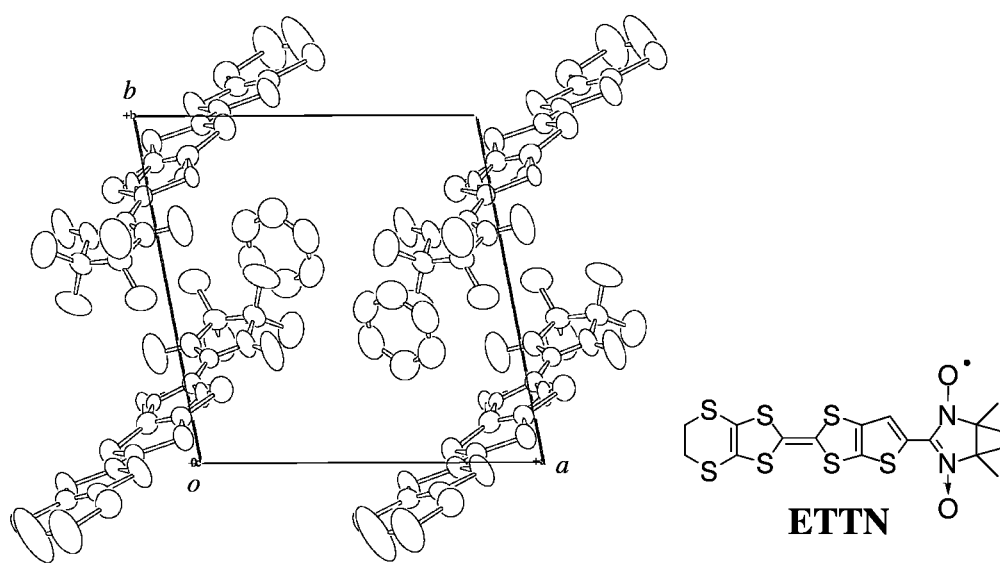
ETTN

(b) alignment in molecular plane   (c) stacking mode
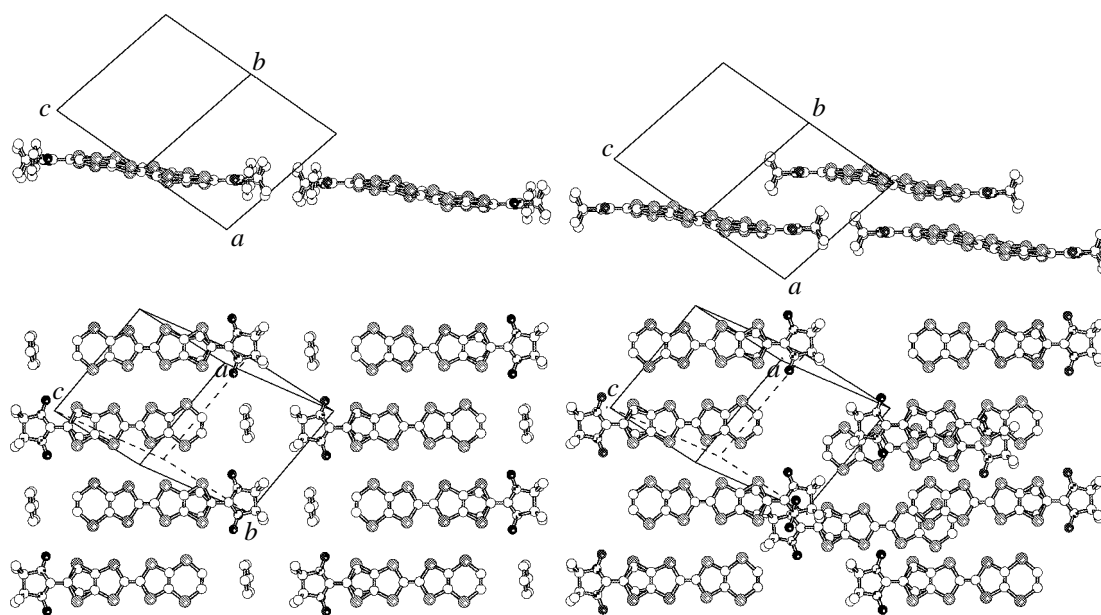
Figure 4-5. Crystal structure of **ETTN** determined by X-ray crystallography.

The crystal of **EPPN** belongs to a monoclinic space group *C2/c*. Within the *bc* plane, the **EPPN** molecules are aligned in a *zig-zag* manner, forming a slipped stack of TTF moieties along the *b*-axis (Figure 4-6(b)). The phenylNN moieties are stacked along the *a*-axis by a "cross" manner (Figure 4-6(c)).

(a) *ac* plane
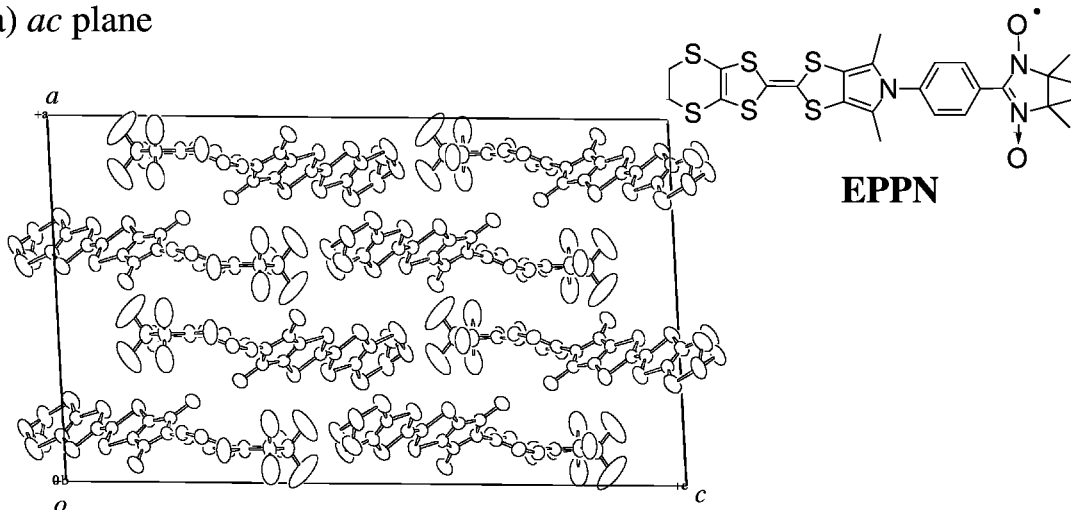
EPPN

(b) *bc* plane
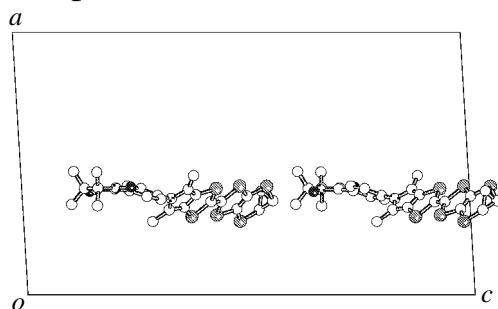
(c) stacking mode
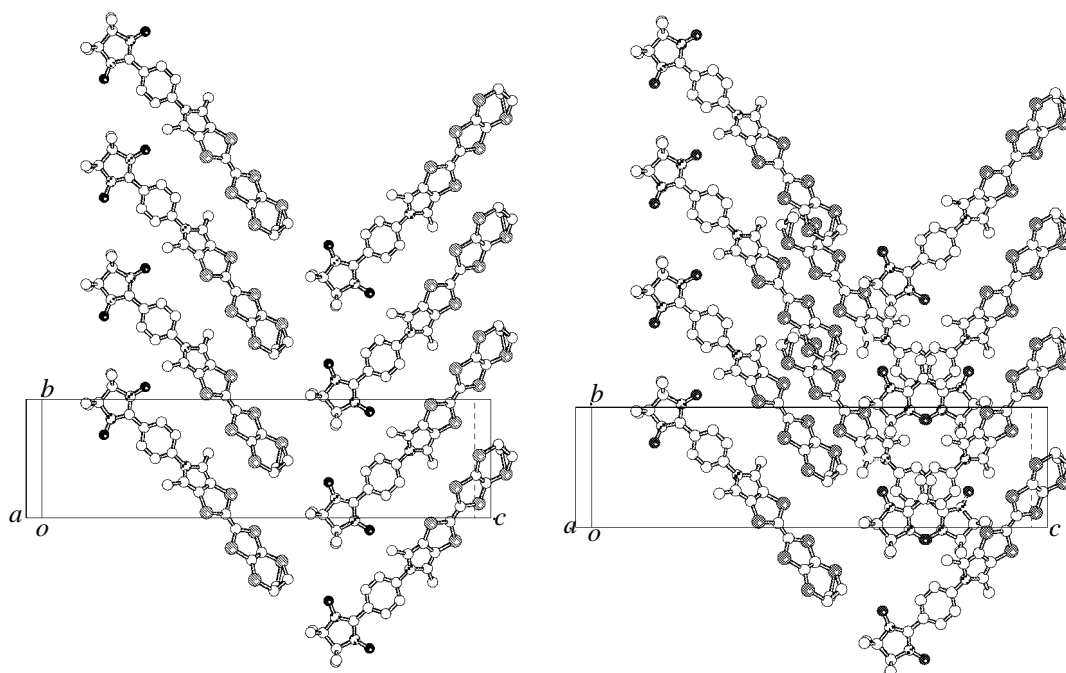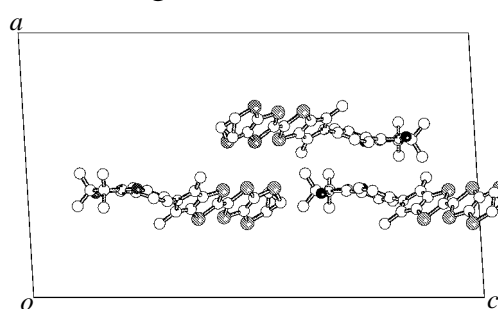
Figure 4-6. Crystal structure of **EPPN** determined by X-ray crystallography.

4-2-4. Magnetic Property of ETBN in Neutral Crystal

Magnetic propery of the **ETBN** crystal was measured with a SQUID magnetometer. Temperature dependence of the magnetic susceptibility showed a presence of ferromagnetic interaction. The plots are well reproduced by Curie-Weiss law with positive Weiss temperature of 0.48 K. Although the χT value is increasing toward lower temperatures, the increasing rate is slightly suppressed around the lowest temperature. Therefore, an antiferromagnetic interaction may appear at much lower temperatures.
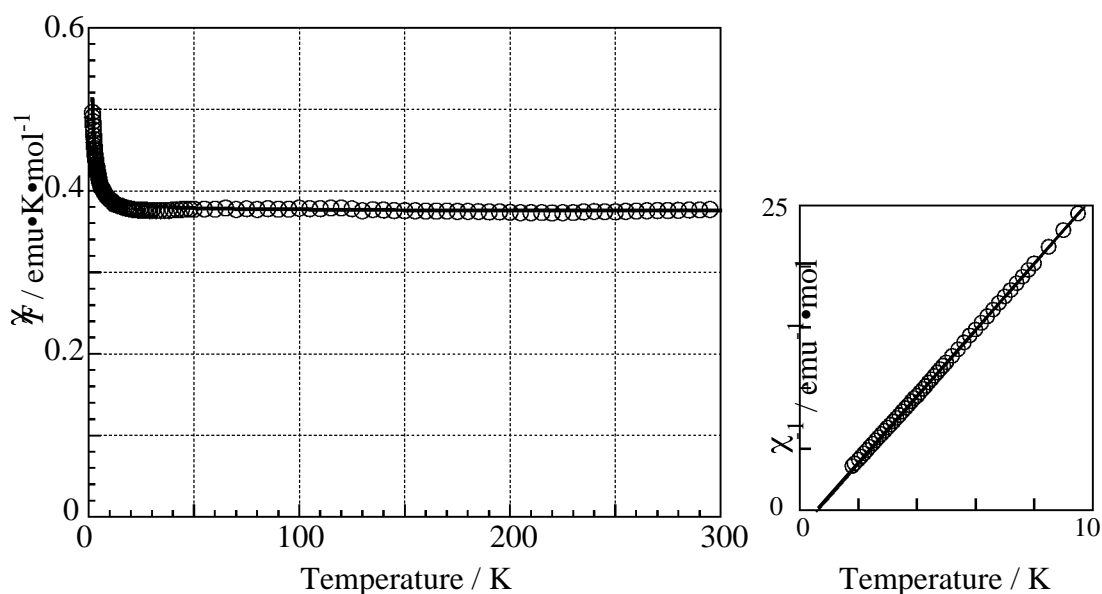
Figure 4-7. Temperature dependence of magnetic susceptibility of **ETBN** in neutral crystals.

4-2-5. Discussion

These annulated TTF-based donor radicals showed good crystallinity as expected. The fact is advantageous on constructing a conductive magnet.

As described in 3-4-1, a twisting between donor and radical parts may cause a breakdown of the electronic structure of spin-polarized donor. Obtained molecular structures of donor radicals indicate that -conjugation between donor and radical parts is maintained even in the neutral state, especially in **ETTN** and **ETBN**. It is to be noted that the coplanarity of a donor radical is expected to be improved when it is singly oxidized.

In order to construct a conductive material, S•••S contacts between donor parts must be enabled. Since the NN group is bulky, it may disturb the contacts.[5] Judging from the crystal structure of **ETBN**, *face-to-face* dimer can be easily

formed. A *side-by-side* contact is also guaranteed as seen in the donor alignment along the *c*-axis. At least, such conduction paths are possible.

Magnetic susceptibility measurements of **ETBN** showed a presence of ferromagnetic interaction. Judging from the crystal structure, the ferromagnetic interaction is considered to be based on CH•••ON type contacts[6] between neighboring nitronyl nitroxide moieties of translated molecules along the *c*-axis (C-O : 3.60(1) Å) or the rotatory-inverted ones within the *ab* plane (C-O : 3.38(1), 3.52(1) Å).
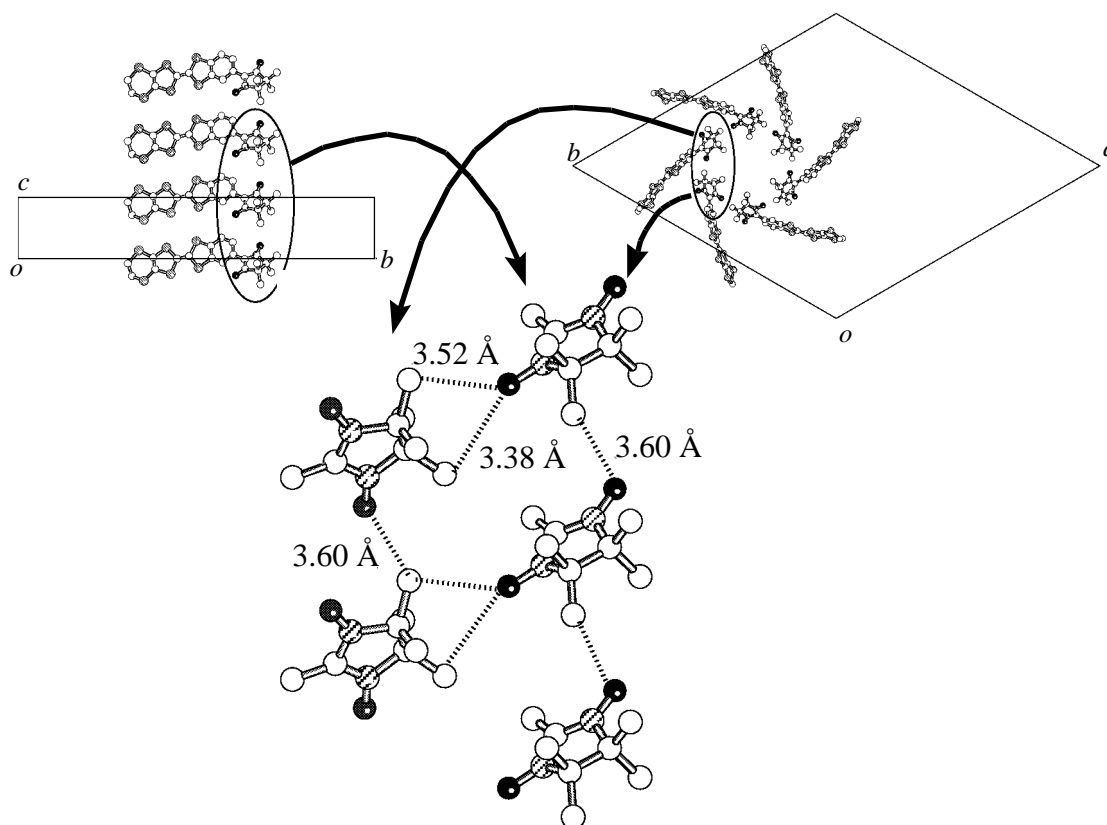
Figure 4-8. CH•••ON type contacts in **ETBN** crystal.

4-2-6. Summary

Three kinds of annulated TTF-based donor radicals, **ETBN**, **ETTN**, and **EPPN** were prepared. These donor radicals turned out to have good crystallinity, and their structures were analyzed by X-ray crystallography. The molecular structures of these donor radicals indicated an existence of effective -interaction between the donor site and the radical site. In the crystal of **ETBN**, a characteristic cavity structure was found. The crystal of **ETBN** also showed an existence of ferromagnetic intermolecular interaction (θ = +0.48 K).

§4-3. Properties of Annulated TTF-Based Donor Radicals

4-3-1. Cyclic Voltammmetry of Annulated TTF-Based Donor Radicals

Oxidation potentials of these annulated TTF-based donor radicals determined by cyclic voltammetry are shown in Table 4-2. The benzo-annulated donor radical, **ETBN**, turned out to show three reversible redox waves at $E_{1/2} = 0.62$, 0.89, and 1.04 V (Figure 4-9). Compared to parent molecules, benzo(ethylenedithio)TTF ($E_{1/2} = 0.60$, 0.93 V) and phenyl NN ($E_{1/2} = 0.80$ V), the first oxidation potential of **ETBN** is similar to the first oxidation of the parent donor. Since the second oxidation potential of **ETBN** is nearer to the oxidation potential of phenyl NN than the second oxidation potential of benzo(ethylenedithio)TTF, oxidation of NN radical of **ETBN** is considered to occur at the second potential. This assignment is also supported by the fact that the bis(NN) derivative shows a two-electron process at the second potential. The third oxidation potential of **ETBN** should correspond to the second oxidation potential of the parent donor. One-electron oxidation of **ETBN** is, therefore, expected to give rise to a reasonably stable cation diradical species.

The thieno-annulated donor radical, **ETTN**, showed three reversible redox waves at $E_{1/2} = 0.58$, 0.89, and 1.10 V. The phenylpyrrolo-annulated donor radical, **EPPN**, showed two reversible waves, the second wave of which corresponds a two-electron process. Determined three oxidation potentials of these donor radicals showed similar tendency with those of **ETBN**, indicating
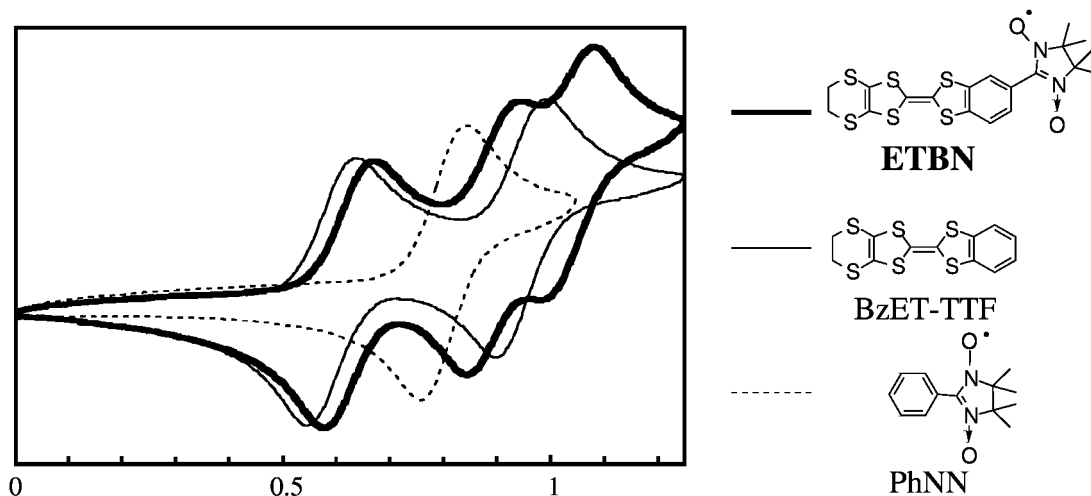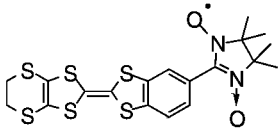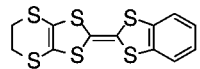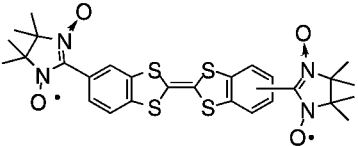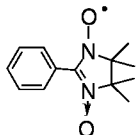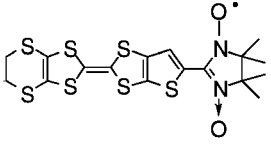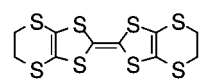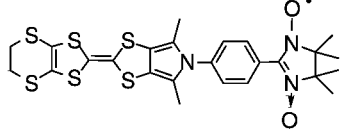
Figure 4-9. Cyclic voltammograms of **ETBN** and related compounds measured in 0.1 M n-Bu$_4$N·ClO$_4$ - PhCN solution by 200 mV·s^{-1}.

75

Table 4-2. Oxidation potentials of donor radicals and related compounds.

Donor radical	$E_{1/2}$ / V	Donor or Radical	$E_{1/2}$ / V
ETBN	0.62 0.89 1.04		0.60 0.95
	0.75 0.90 (2e) 1.20		0.80
ETTN	0.58 0.89 1.10		0.56 0.86
EPPN	0.52 0.87 0.90		

(measured in 0.1 M n-Bu$_4$N·ClO$_4$ - PhCN solution)

that these donor radicals should also afford cation diradical species upon one-electron oxidation. It is to be noted that the first oxidation potentials of these donor radicals are lower than that of **ETBN**. The first oxidation potential of **EPPN** (0.52 V) is lower than that of BEDT-TTF (0.56 V).

4-3-2. Electronic Spectrum of ETBN

UV absorption spectum of **ETBN** in dichloromethane solution is shown in Figure 4-10 together with those of related compounds. The spectrum of **ETBN** showed absorption maxima at 298, 331, and 369 nm. The absorptions of **ETBN** at 298 and 331 nm correspond to those of benzo(ethylenedithio)TTF, and that at 369 nm can be assigned to NN. The absorption of **ETBN** is extended to a longer wavelength region, reflecting the extention of a conjugation length.

The spectra of three donor radicals, **EMPN**, **EMTN**, and **ETBN**, are shown in Figure 4-11. A weak absorption which corresponds to n-π* transition appeared in longer wavelength region. The peak position of the absorption of **ETBN** is the longest in wave length among those of the donor radicals. On the other hand, the absorptions around 300 and 370 nm have maxima at the shortest wavelength

positions for **ETBN**. The latter fact corresponds the highest oxidation potential of **ETBN** among these three donor radicals.
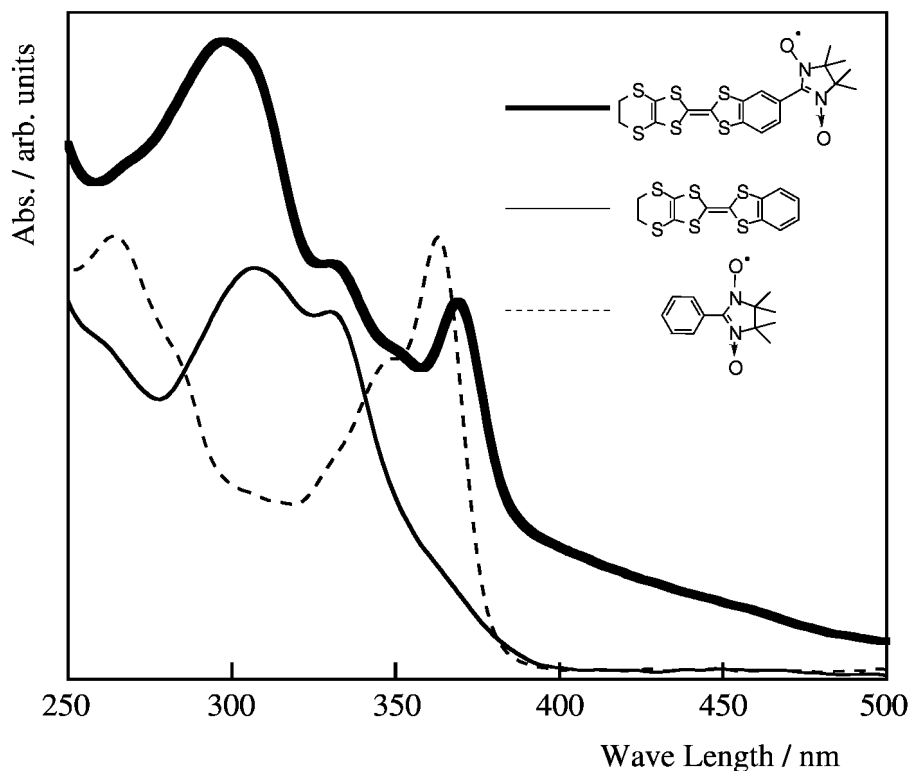
Figure 4-10. Absorption spectra of **ETBN** and parent molecules in CH_2Cl_2.
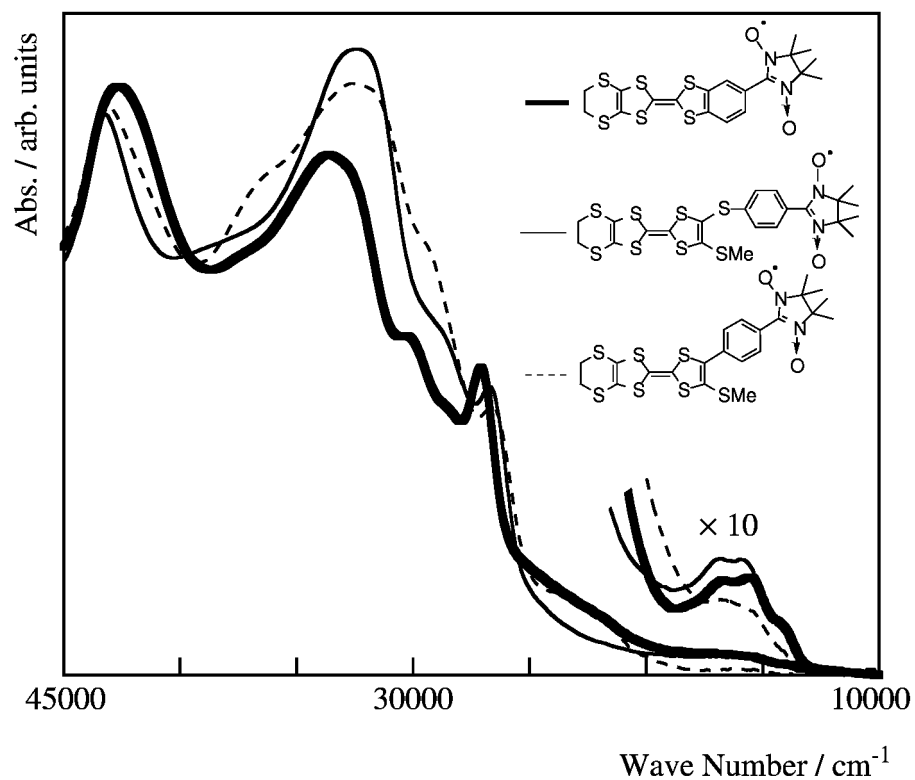
Figure 4-11. Absorption spectra of donor radicals in CH_2Cl_2.

4-3-3. ESR Spectra of Oxidized Species of Annulated TTF-Based Donor Radicals

The annulated TTF-based donor radicals were oxidized by the treatment with iodine in tetrahydrofuran solution at room temperature. When the oxidation of **ETBN** was performed in a higher concentration (*ca.* 10^{-4} M), which was adopted for **EMPN**, *etc.*, no triplet signal was detected. On the other hand, diluted samples (*ca.* 10^{-5} - 10^{-6} M) of **ETBN** afforded a fine structured ESR signal derived from a triplet species ($| D | = 0.0255$ cm^{-1}, $| E | = 0.0021$ cm^{-1}) upon the oxidation by the iodine treatment. A plot of the signal intensity *versus* inverse temperature is linear, indicating that the triplet state is the ground state of **ETBN$^{+\bullet}$**. Because of the weak signal intensity, the plot is limited up to 10 K. Increase in the concentration of the sample may cause an aggregation of cation diradicals themselves or that of a cation diradial and a neutral radical.
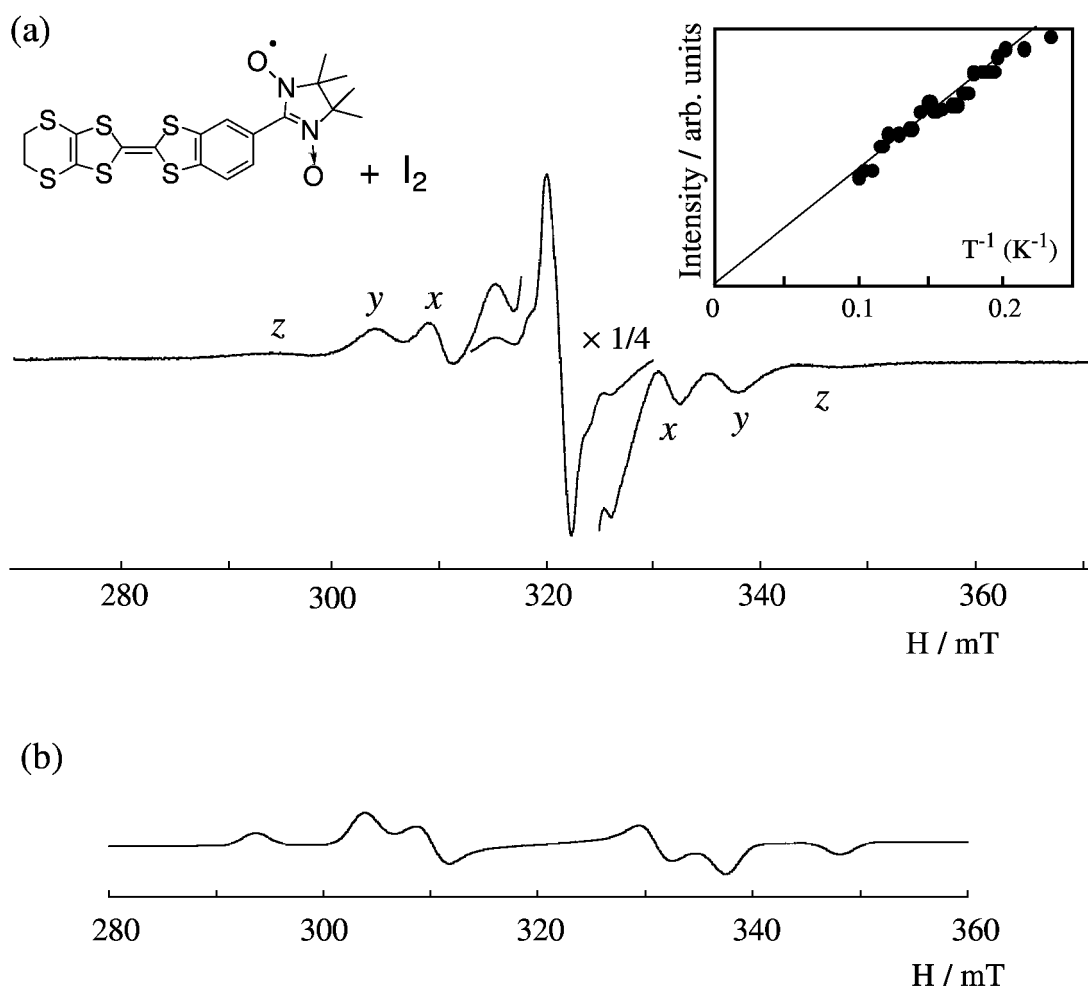
Figure 4-12. ESR spectrum of **ETBN$^{+\bullet}$**. (a) observed spectrum in THF glass at 5 K and temperature dependence of signal intensity, (b) simulated spectrum.
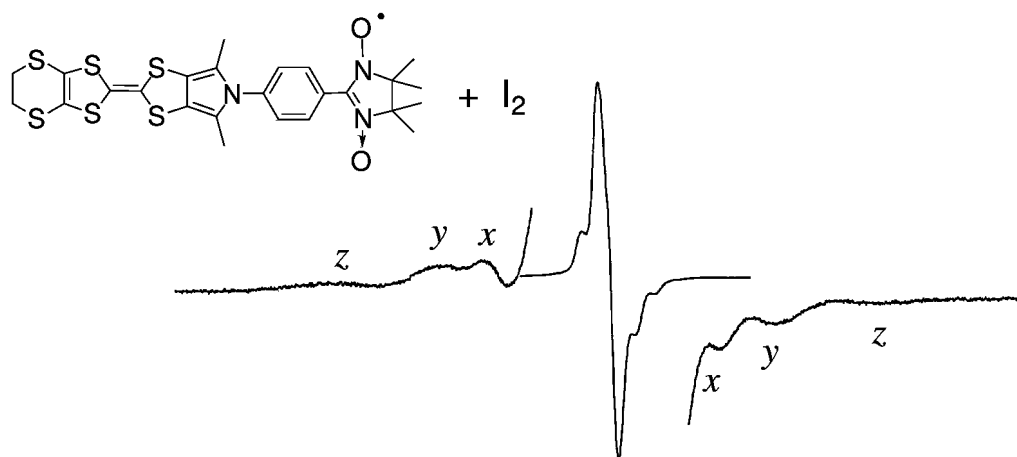
Figure 4-13. ESR spectrum of **EPPN**$^{+\bullet}$ observed in THF glass at 5 K.

A triplet ESR signal has not been observed for **ETTN**$^{+\bullet}$ provably because of aggregation (under high concentration) or weak intensity (under low concentration). On the other hand, **EPPN**$^{+\bullet}$ showed a weak triplet signal, and the signal intensity is almost linear to the inverse temperature. The aggregating tendency of these donor radicals is considered to be suitable for constructing self-assembled materials.

4-3-4. UHF MO Calculation on Annulated TTF-Based Donor Radicals

Molecular orbitals of **ETBN** calculated by a PM3/UHF method are shown in Figure 4-14. The orbital energy of SOMO ( ) is lower than those of HOMO( ) and HOMO( ) because coefficients of SOMO are restricted only on the electronegative N-O groups. Moreover, HOMO( ) is further destabilized by spin-dependent Coulombic repulsion caused by the -spin in SOMO. Such an

HOMO(α) : -8.04 eV   HOMO(β) : -8.02 eV

SOMO(α) : -9.05 eV
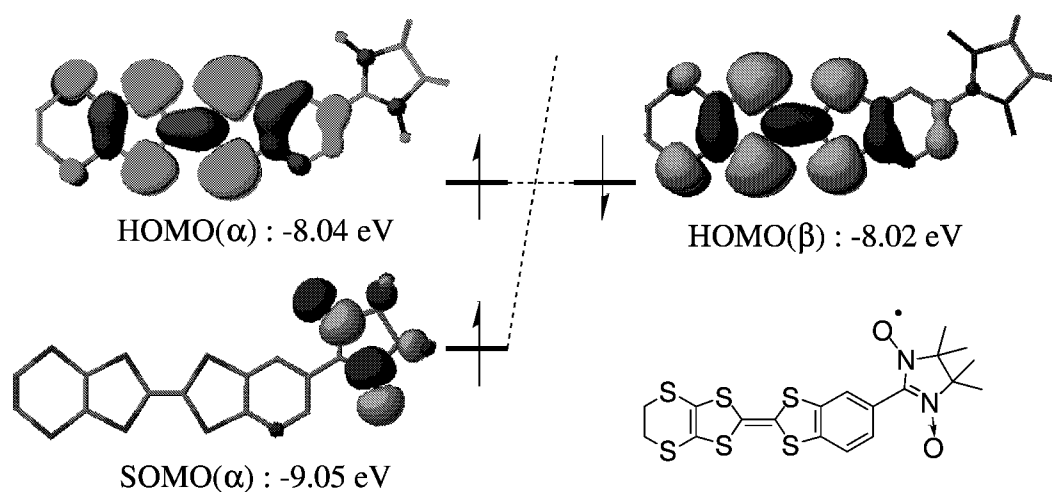
Figure 4-14. Molecular orbitals of **ETBN** calculated by MOPAC/PM3/UHF.

electronic structure is in agree with the generation of triplet species upon one-electron oxidation.

In order to confirm the ground state of the singly oxidized species of **ETBN**, UHF calculation was also performed on **ETBN**$^{+\bullet}$. Since a self-consistent field (SCF) solution was not obtained for the singlet configuration, the comparison of the heat of formation between the triplet configuration and the singlet one was not performed. As shown in Figure 4-15, the coefficients of SOMO' are distributed on the NN site although most of them are distributed on the donor site. Under such a situation, a moderate exchange interaction operates between SOMO and SOMO'. The smaller coefficients on the NN site of **ETBN**$^{+\bullet}$ is in contrast with those of **EMPN**$^{+\bullet}$ or **EMTN**$^{+\bullet}$ (See Figure 3-16).

SOMO   SOMO'
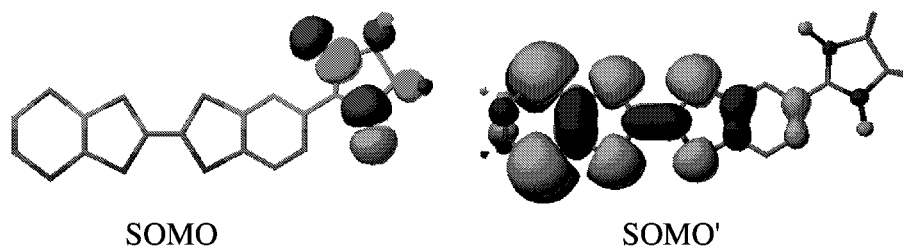
Figure 4-15. Molecular orbitals of **ETBN**$^{+\bullet}$ in triplet configuration.

Molecular orbitals of **ETTN** and **EPPN** calculated by PM3/UHF method are shown in Figure 4-16 and 4-17. In these cases, the orbital energy of HOMO( ) is lower than that of HOMO( ). However, triplet species was observed on the ESR measurements of **EPPN**$^{+\bullet}$. The fact indicates that the spin-correlation in cation diradical species is important, although the present calculational level is not enough to consider such an information.

HOMO(α) : -8.10 eV   HOMO(β) : -8.11 eV

SOMO(α) : -9.02 eV
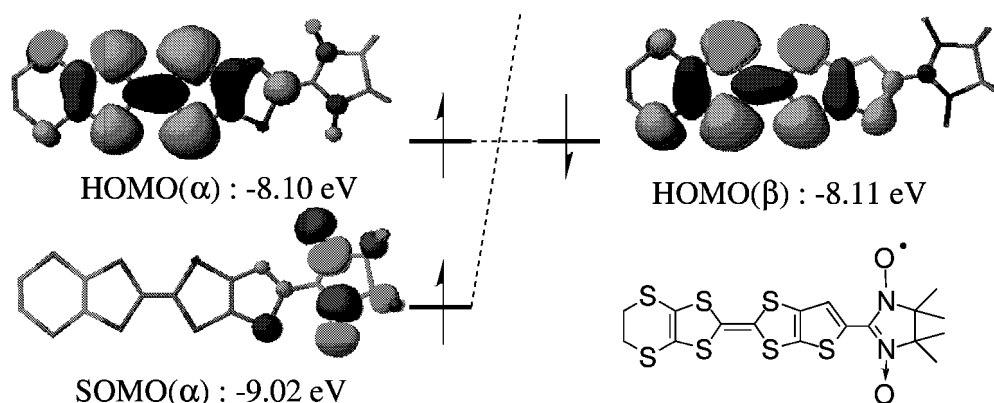
Figure 4-16. Molecular orbitals of **ETTN**.

HOMO(α) : -7.71 eV   HOMO(β) : -7.78 eV

SOMO(α) : -8.96 eV
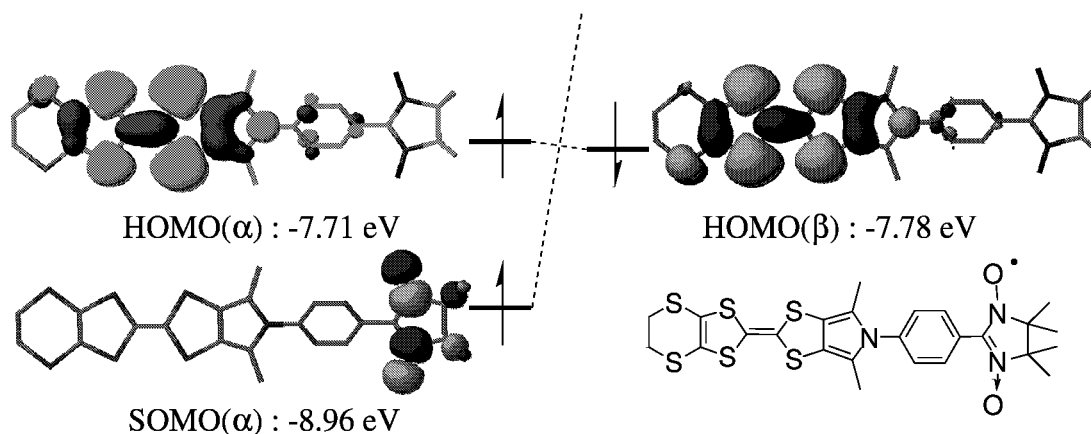
Figure 4-17. Molecular orbitals of **EPPN**.

Molecular orbitals of **ETTN**$^{+\bullet}$ in triplet configuration are shown in Figure 4-18. The localizing tendency of SOMO' to the donor site is obribious. The ground state of **ETTN**$^{+\bullet}$ can not be ensured as triplet.

SOMO   SOMO'
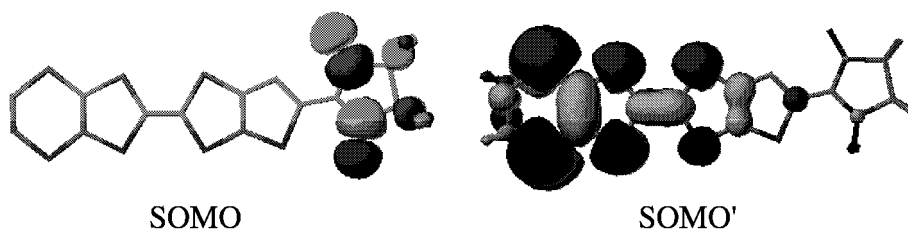
Figure 4-18. Molecular orbitals of **ETTN**$^{+\bullet}$ in triplet configuration.

4-3-5. Summary

The electronic structures of three annulated TTF-based donor radicals were examined. Among these donor radicals, the benzo-annulated one **ETBN** afforded a ground state triplet cation diradical upon one-electron oxidation, and **ETBN** can be designated as a spin-polarized donor based on its spin-polarized electronic structure. The electronic structures of the others are found to need more careful processing.

§4-4. Preparation of Ion-Radical Salts of ETBN

Since the solubility of ETBN to organic solvents is very high compared to ordinary donors, electrocrystallization of ETBN was performed in a relatively non-polar solvent, 1,1,1-trichloroethane (TCE). When electro-crystallization was performed in a 1.8 mM TCE solution of ETBN using 5 mM n-Bu$_4$N• ClO$_4$ as a supporting electrolyte, very thin black plate-like crystals were obtained for the first time. The composition of the salt was estimated by elemental analysis to be [ETBN]$_2$ClO$_4$[TCE]$_{0.5}$. When galvanostatic electrocrystallization was performed in a 1 mM TCE - tetrahydrofuran (9:1 v/v) solution of ETBN using 5 mM n-Bu$_4$N•ClO$_4$ with a constant current of 0.7 µA for a period of a week, the best crystals were obtained, although

Figure 4-19.

the quality of the crystals is not high enough for an X-ray crystallographic analysis.[7] It is to be noted that the salt is stable even at room tempeature at least for a month despite of a rather limited kinetic stability of ETBN$^{+•}$ in solution.

Attempts using other solvents were unsuccessful. Among attempts using other electrolytes, similar crystals were obtained when n-Bu$_4$N•BF$_4$ was used. Utilization of n-Bu$_4$N•PF$_6$, n-Bu$_4$N•Br, or n-Bu$_4$N•Cl resulted beads-like solids. The composition of the PF$_6^-$-salt was estimated by elemental analysis to be ETBN:PF$_6$ = 9:4

Table 4-3. Elemental analysis result of [ETBN]$_2$ClO$_4$[TCE]$_{0.5}$.

	C	H	N	S	Cl
Calcd.	40.19	3.42	4.81	33.01	7.60 %
Found.	39.60	3.64	5.04	32.71	7.63 %

§4-5. Physical Properties of Ion-Radical Salts of ETBN

4-5-1. UV-VIS-NIR and IR Spectra of Ion-Radical Salt of ETBN

The UV-VIS-NIR spectrum of the ClO_4^--salt showed absorption maxima at 456, 876 nm, and a broad absorption band due to an interband transition was extended from 1300 nm to an IR region. The IR spectrum of the salt showed a sharp peak at 1350 cm^{-1} which can be assigned to the ν_{N-O} absorption. Since the corresponding absorption was observed at 1348 cm^{-1} in neutral ETBN, the presence of the NO stretching at a regular position suggests that the nitronyl nitroxide group is intacted in the ion radical salt even after the electrocrystallization.
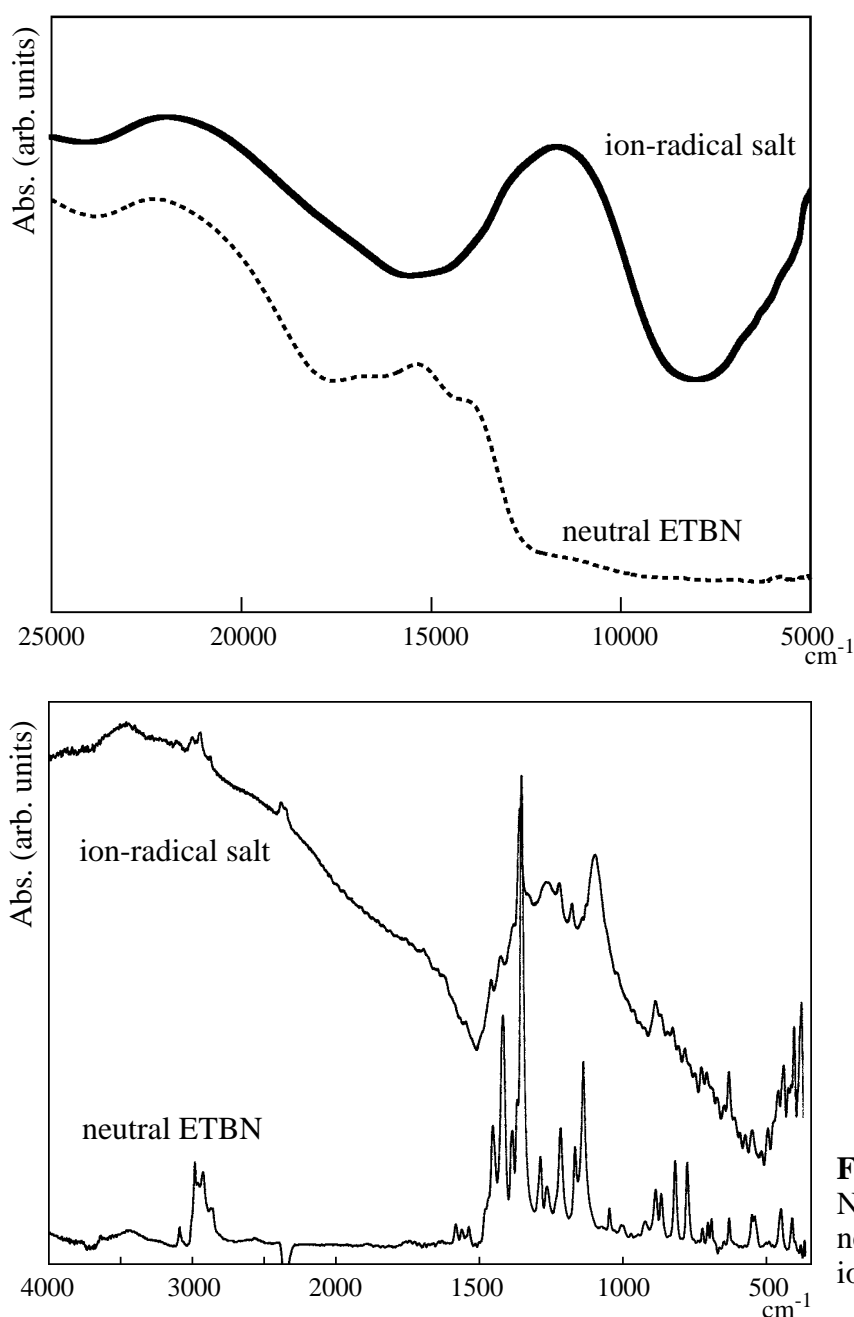
Figure 4-20. UV-VIS-NIR and IR spectra of neutral ETBN and the ion-radical salt.

4-5-2. Conduction Behavior of Ion-Radical Salt of ETBN

Conduction behavior of the ClO_4^--salt measured by a two-probe method turned out to be semiconducting. The conductivity of the salt at room temperature σ_{rt} was 1×10^{-2} S•cm^{-1}. An Arrhenius plot of the resistivity of the salt was linear down to 150 K, and the activation energy E_a was evaluated to be 0.16 eV.
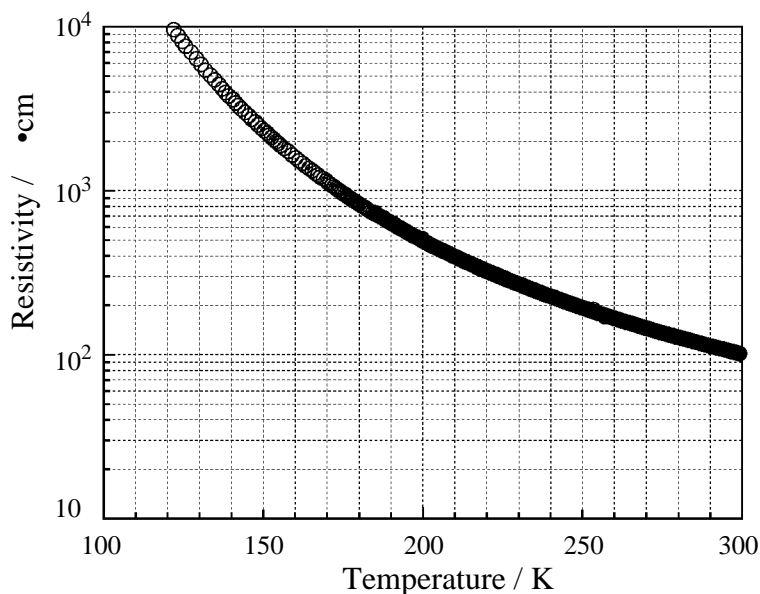
Figure 4-21. Temperature dependence of resistivity of $[ETBN]_2ClO_4[TCE]_{0.5}$.

4-5-3. Magnetic Property of Ion-Radical Salts of ETBN

Temperature dependence of the paramagnetic susceptibility of the ClO_4^--salt measured by a SQUID magnetometer was almost reproduced by Curie-Weiss law with a Weiss temperature of $\theta = -5.2$ K. Curie constant is *ca.* 0.75, which corresponds to two independent $S = 1/2$ spins per chemical formula, suggesting that each donor radical carries one paramagnetic spin.
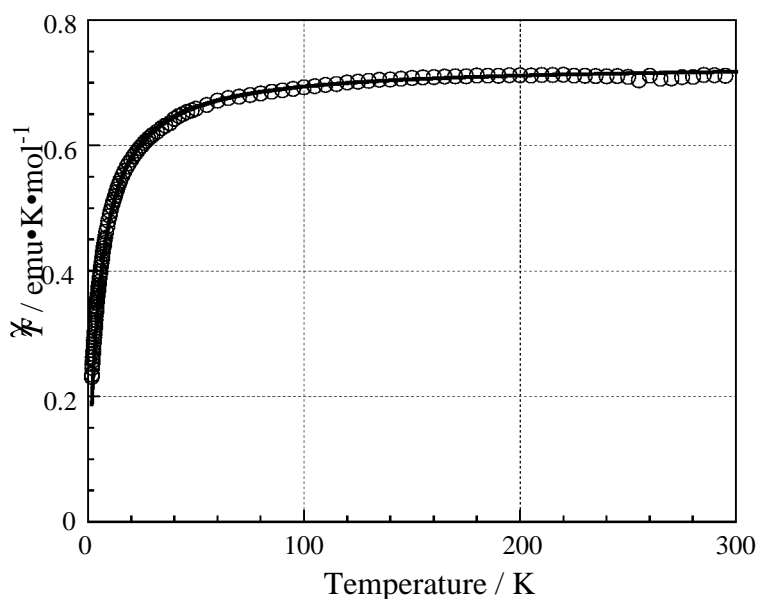
Figure 4-22. Temperature dependence of magnetic susceptibility of the salt, $[ETBN]_2ClO_4[TCE]_{0.5}$.

84

Temperature dependence of the paramagnetic susceptibility of the PF_6^--salt was also reproduced by Curie-Weiss law with a Weiss temperature of $\theta = -4.8$ K although the data are affected by oxygen. If $[ETBN]_2[PF_6]_{8/9}$ (and solvents) is adopted as a chemical formula, Curie constant is *ca.* 1.08, which corresponds to two and 8/9 independent $S = 1/2$ spins.
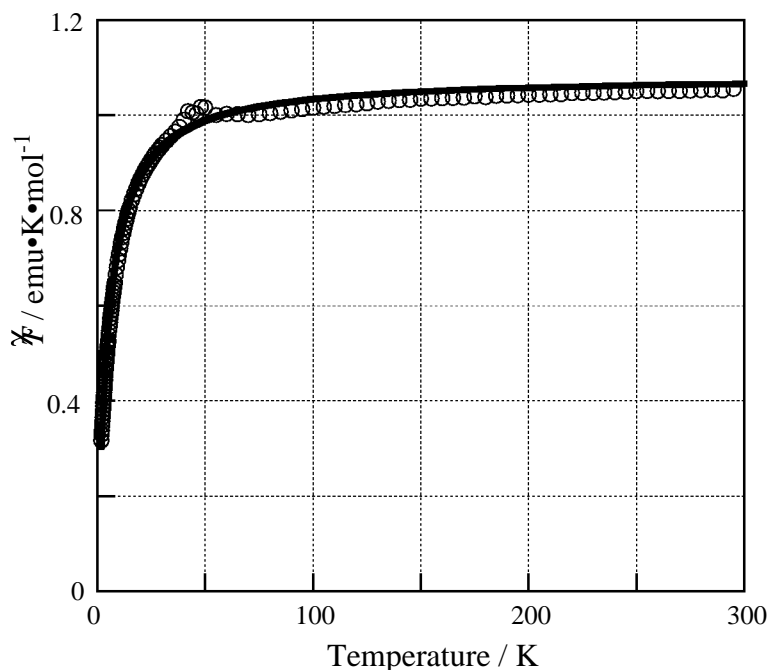
Figure 4-23. Temperature dependence of magnetic susceptibility of PF_6^--salt.

4-5-4. ESR Spectra of Ion-Radical Salt of ETBN

The ESR spectrum of the polycrystalline sample of the ClO_4^--salt showed a narrow peak at $g = 2.0068$ with a peak-to-peak line width of 0.8 mT at room temperature. The ESR signals of powdered neutral ETBN and phenyl NN were observed at $g = 2.0070$ and 2.0068, respectively, whereas that of bis(ethylene-dithio)TTF (ET) in its ion-radical salt is known to show a relatively large anisotropy (*cf.* $(ET)_2ClO_4(TCE)_{0.5}$: $g = 2.0125, 2.0022$).[8] Accordingly, the ESR signal of the salt may be derived mainly from the NN unit.
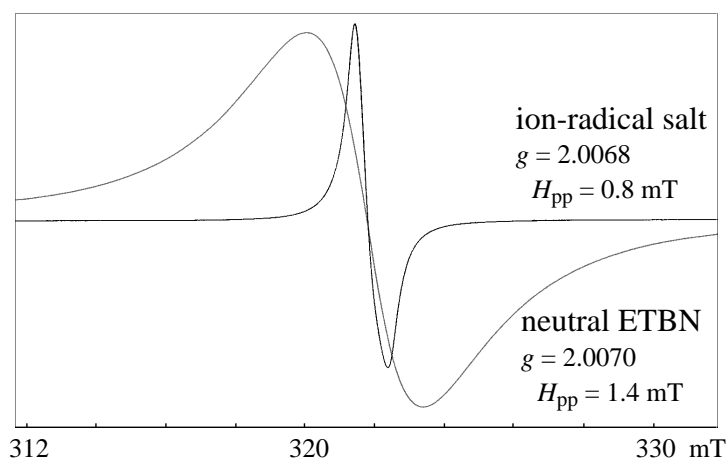
Figure 4-24. ESR spectra of neutral ETBN and the salt, $[ETBN]_2ClO_4[TCE]_{0.5}$.

Temperature dependence of the ESR signal intensity also obeyed Curie-Weiss law and no thermal excitation was recognized. Decrease of signal intensity at the lowest temperature may be due to saturation of the microwave power.
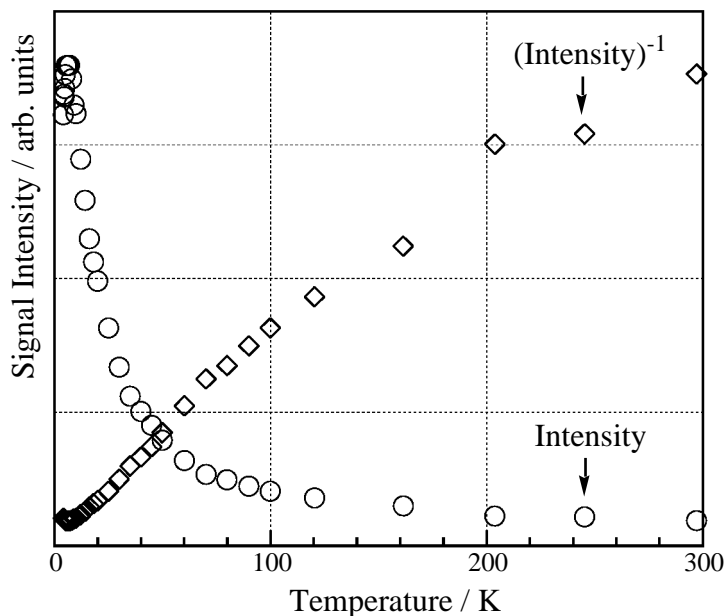
Figure 4-25. Temperature dependence of ESR signal intensity of the salt, $[ETBN]_2ClO_4[TCE]_{0.5}$.

Angular dependence of the g value of the ESR signal was measured using a single crystal of the ClO_4^--salt. When the long axis of the crystal was oriented along the external field, the smallest g value was observed, although the anisotoropy is small as seen in polycrystalline samples. Since the principal axis which shows the smallest g value is, in general, aligned along the p_z orbital of a radical molecule, the spin-carrying sites of this salt are considered to be stacked along the long axis of the crystal.
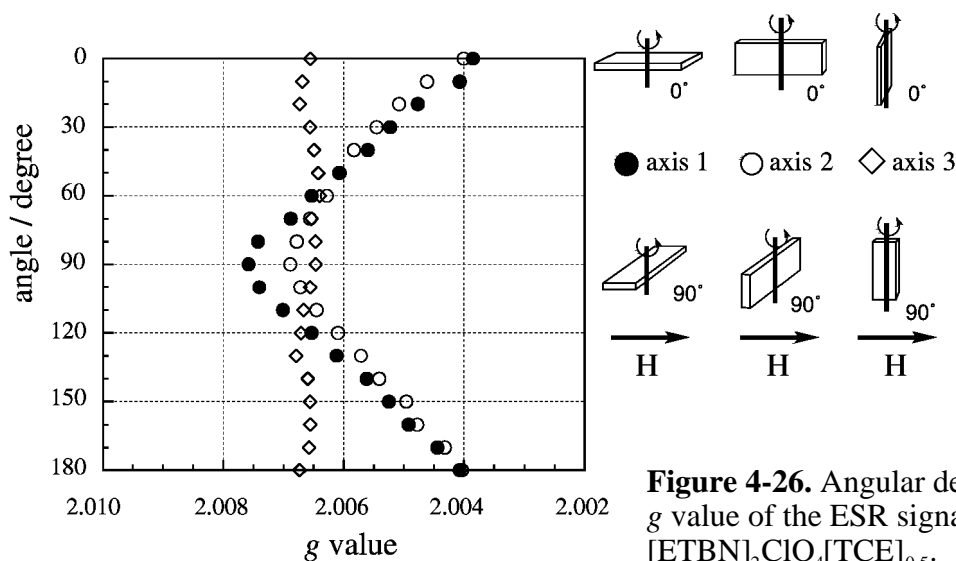
Figure 4-26. Angular dependence of g value of the ESR signal of the salt, $[ETBN]_2ClO_4[TCE]_{0.5}$.

4-5-5. Discussion

According to the magnetic data of the ClO_4^--salt, each ETBN molecule has only one paramagnetic spin in spite of the 2:1 ratio of donor and counter ion. The result suggests that the generated π-delocalizing spin on the donor site does not contribute to the magnetic susceptibility of the ClO_4^--salt. The result of ESR measurements also supports such a consideration. Since the conductivity data of the ClO_4^--salt indicate the existence of relatively large band gap, the salt is considered to be a band insulator.[9] Although π-spins on the donor sites are conductive, they are considered to be coupled strongly in an antiferromagnetic manner.
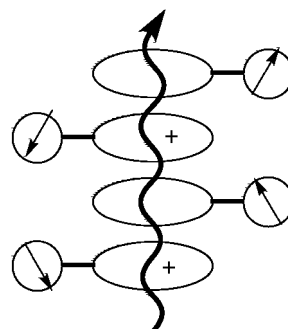
Figure 4-27. Schematic drawing of the ion-radical salt.

Two explanations are possible to rationalize such a strong antiferromagnetic coupling. If one π-spin is located over two molecules, an antiferromagnetic coupling between two dimers leads to four-molecular periodicity (Figure 4-28(a)). On the other hand, a regular arrangement of donors may also afford a large band gap, if the transfer integral is very small. In the latter case, the valence band should be filled with same number of α-spin electrons and β-spin ones (Figure 4-28(b)).

(a) four-molecular periodicity   (b) band picture
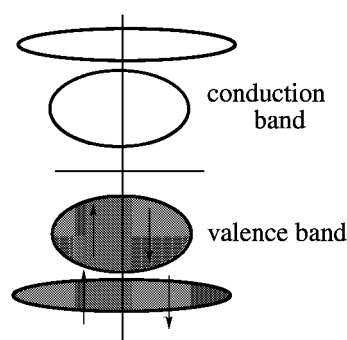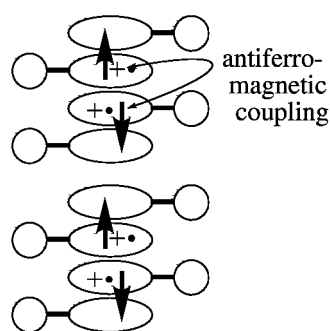
Figure 4-28. Two explanations for antiferromagnetic coupling between π-spins.

In either case, the density of the effective charge carrier is very low in this salt. The spin polarization of the π-spin caused by the local spin on the radical site, therefore, can not be transmitted to the local spin on the adjacent donor radical.

Since the PF_6^--salt is amorphous, the -spin on the donor site may tend to be localized, and the spin polarization of the -spin also can not be transmitted to the local spin on the adjacent donor radical.

§4-6. Summary

An isolable ion-radical salt of the 2:1 donor to a counter ion ratio was prepared, using the annulated TTF-based spin-polarized donor, ETBN, which gives rise to a ground state triplet cation diradical upon one-electron oxidation. The donor ETBN was also found to afford a single crystal in the neutral state with ferromagnetic interaction ($\theta = +0.48$ K). Although the local spins on the radical sites in the ion-radical salt behave paramagnetically at the present stage, magnetic ordering of the local spins may be observed if the effective carrier concentration in the ion-radical salt becomes reasonably high. The stability of the ion-radical salt would encourage further studies on organic conductive magnets.

§4-7. Experimentals

General Procedures

NMR Spectroscopy. ^{1}H-NMR spectra were recorded on a JEOL JNM-GSX270 spectrometer. The chemical shift references were reported in δ relative to tetramethylsilane (0.00 ppm, for chloroform-*d* solution) or dimethylsulfoxide-d_5 (2.50 ppm, for dimethyl-sulfoxide-d_6 solution) as an internal standard.

IR Spectroscopy. Infrared spectra were recorded on a Perkin-Elmer 1640 infrared spectrometer using a KBr pellet.

ESR Spectroscopy (in solution). ESR spectra were recorded on a JEOL JES-TE300 (X-band) spectrometer. The resonance magnetic field value was measured with the aid of a JEOL ES-FC5 NMR field meter. The microwave frequency values are those displayed on the spectrometer.

Elemental Analysis. Elemental analyses were performed at the Organic Elemental Analysis Center of the Department of Chemistry, Faculty of Science, the University of Tokyo.

Materials

2,3-Bis(hydroxylamino)-2,3-dimethyl-butane was prepared by grinding its sulfate with pottasium hydrogen carbonate, followed by extraction with dichloromethane, and was recrystallized from benzene. There, the sulfate was prepared according literature,[10] while the sulfate used as a catalyst was purchased from Eastman Fine Chemicals (Kodak). Tetrahydrofuran (WAKO) was distilled from sodium benzophenone ketyl under nitrogen. Solvents were purchased from Godo Yozai Co., Ltd. Silica gel is Cica-MERCK silica gel 60 (70-230 mesh ASTM), and alumina is WAKO activated alumina (200 mesh).

X-ray Crystal Structure Analysis

All measurements were made on a Rigaku AFC7R diffractometer with graphite monochromated Mo-Kα radiation and a rotating anode generator. The data were collected at room temperature using the ω-2θ scan technique to a maximum 2θ value of 55.0˚. The weak reflections (I < 10.0σ(I)) were rescanned (maximum of 5 scans) and the counts were accumulated to ensure good counting statistics. Stationary background counts were recorded on each side of the reflection. The ratio of peak counting time to background counting time was 2:1. The diameter of the incident beam collimator was 1.0 mm and the crystal to detector distance was 235 mm. The intensities of three representative reflection were measured after every 150 reflections. No decay correction was applied. Neutral atom scattering factors were taken from Cromer and Waber.[11] Anomalous dispersion effects were included in Fcalc[12]; the values for f' and f" were those of Creagh and McAuley.[13] The values for the mass attenuation coefficients are those of Creagh and Hubbel.[14] All calculations were performed using the teXsan[15] crystallographic software package of Molecular Structure Corporation.

ETBN

A darkgreen needle crystal of ETBN having approximate dimensions of $0.40 \times 0.05 \times 0.05$ mm was mounted on a glass fiber. Cell constants and an orientation matrix for data collection, obtained from a least-squares refinement using the setting angles of 24 carefully centered reflections in the range $28.29 < 2\theta < 31.98°$ corresponded to a trigonal hexagonal cell (laue class: $\bar{3}$) with dimensions: $a = 43.24(7)$ Å, $c = 6.381(4)$ Å, $V = 10327(25)$ Å^3. For $Z = 18$ and F.W. = 499.73, the calculated density is 1.45 g/cm^3. Based on the systematic absences of $hkil$ ($-h+k+l \neq 3n$), packing considerations, a statistical analysis of intensity distribution, and the successful solution and refinement of the structure, the space group was determined to be $R\bar{3}$ (#148).

The computer-controlled slits were set to 3.0 mm (horizontal) and 3.0 mm (vertical). Scans of $(1.37 + 0.30\ tan\ \theta)°$ were made at a speed of 16.0°/min (in omega). Of the 5909 reflections which were collected, 2682 were unique ($R_{int} = 0.089$). The linear absorption coefficient, μ, for Mo-Kα radiation is 28.5 cm^{-1}. An empirical absorption correction based on azimuthal scans of several reflections was applied which resulted in transmission factors ranging from 0.51 to 1.00. The data were corrected for Lorentz and polarization effects.

The structure was solved by a direct method (SHELX86)[16] and expanded using Fourier techniques (DIRDIF94).[18] The non-hydrogen atoms were refined anisotropically. Hydrogen atoms were included but not refined. The final cycle of full-matrix least-squares refinement* was based on 2694 observed reflections (I > 3.00σ(I)) and 262 variable parameters and converged (largest parameter shift was 0.00 times its esd) with unweighted and weighted agreement factors of: $R = \sum (Fo^2 - Fc^2) / \sum Fo^2 = 0.108$, $R_w = [\sum w(Fo^2 - Fc^2)^2 / \sum w(Fo^2)^2]^{1/2} = 0.173$. ($R_1 = 0.063$). The standard deviation of an observation of unit weight: $[\sum w(|Fo| - |Fc|)^2 / (No - Nv)]^{1/2}$ was 2.15 (No:number of observations; Nv:number of variables). The weighting scheme was based on counting statistics and included a factor (p = 0.050) to downweight the intense reflections. Plots of $\sum w(Fo^2 - Fc^2)^2$ versus Fo^2, reflection order in data collection, $sin\ \theta/\lambda$ and various classes of indices showed no unusual trends. The maximum and minimum peaks on the final difference Fourier map corresponded to 0.77 and -0.52 $e^-/$Å^3, respectively.

(*) Least-Squares: Function minimized: $\sum w(Fo^2-Fc^2)^2$, where $w = [\sigma^2(Fo^2)]^{-1} = [\sigma_c^2(Fo^2) + (p(Max(Fo^2,0)+2Fc^2)/3)^2]^{-1}$; $\sigma_c(Fo^2)$ = e.s.d. based on counting statistics; p = p-factor.

ETTN

A darkbrown prismatic crystal of ETTN having approximate dimensions of $0.40 \times 0.30 \times 0.20$ mm was mounted on a glass fiber. Cell constants and an orientation matrix for data collection, obtained from a least-squares refinement using the setting angles of 25 carefully centered reflections in the range $29.80 < 2\theta < 29.98°$ corresponded to a primitive triclinic cell with dimensions: $a = 12.080(3)$ Å, $b = 12.694(2)$ Å, $c = 9.725(2)$ Å, $\alpha = 110.15(2)°$, $\beta = 108.04(2)°$, $\gamma = 93.48(2)°$, $V = 1307.5(5)$ Å^3. For $Z = 2$ and F.W. = 584.85 (ETTN+pyridine), the calculated density is 1.49 g/cm^3. Based on a statistical analysis of intensity distribution, and the successful solution and refinement of the structure, the space group was determined to be $P\bar{1}$ (#2).

The computer-controlled slits were set to 3.0 mm (horizontal) and 3.5 mm (vertical). Scans of (1.84 + 0.30 $tan\ \theta$)° were made at a speed of 16.0°/min (in omega). Of the 6356 reflections which were collected, 3740 were unique (R_{int} = 0.012). The linear absorption coefficient, μ, for Mo-Kα radiation is 29.2 cm^{-1}. An empirical absorption correction based on azimuthal scans of several reflections was applied which resulted in transmission factors ranging from 0.97 to 1.00. The data were corrected for Lorentz and polarization effects.

The structure was solved by a direct method (SIR88)[17] and expanded using Fourier techniques (DIRDIF94).[18] The non-hydrogen atoms were refined anisotropically. Hydrogen atoms were included but not refined. The final cycle of full-matrix least-squares refinement* was based on 3730 observed reflections (I > 3.00σ(I)) and 325 variable parameters and converged (largest parameter shift was 0.03 times its esd) with unweighted and weighted agreement factors of: R = $(Fo^2 - Fc^2)$ / Fo^2 = 0.078, R_w = [$w(Fo^2 - Fc^2)^2$ / $w(Fo^2)^2$]$^{1/2}$ = 0.207. (R_1 = 0.063). The standard deviation of an observation of unit weight: [$w(|Fo| - |Fc|)^2$ / $(No - Nv)$]$^{1/2}$ was 2.24 (No:number of observations; Nv:number of variables). The weighting scheme was based on counting statistics and included a factor (p = 0.068) to downweight the intense reflections. Plots of $w(Fo^2 - Fc^2)^2$ versus Fo^2, reflection order in data collection, $sin\ \theta/\lambda$ and various classes of indices showed no unusual trends. The maximum and minimum peaks on the final difference Fourier map corresponded to 0.46 and -0.37 $e^-/Å^3$, respectively.

(*) Least-Squares: Function minimized: $w(Fo^2-Fc^2)^2$, where $w = [\sigma^2(Fo^2)]^{-1} = [\sigma_c^2(Fo^2)$ + $(p(Max(Fo^2,0)+2Fc^2)/3)^2]^{-1}$; $\sigma_c(Fo^2)$ = e.s.d. based on counting statistics; p = p-factor.

EPPN

A darkgreen plate crystal of EPPN having approximate dimensions of 0.20 × 0.20 × 0.03 mm was mounted on a glass fiber. Cell constants and an orientation matrix for data collection, obtained from a least-squares refinement using the setting angles of 14 carefully centered reflections in the range 25.12 < 2θ < 30.04° corresponded to a C-centered monoclinic cell with dimensions: a = 19.252(7) Å, b = 8.660(6) Å, c = 32.715(6) Å, β = 93.43(3)°, V = 5444(4) Å^3. For Z = 8 and F.W. = 592.86, the calculated density is 1.45 g/cm^3. Based on the systematic absences of hkl ($h+k$ 2n), $h0l$ (l 2n), packing considerations, a statistical analysis of intensity distribution, and the successful solution and refinement of the structure, the space group was determined to be $C2/c$ (#15).

The computer-controlled slits were set to 3.0 mm (horizontal) and 3.0 mm (vertical). Scans of (1.60 + 0.35 $tan\ \theta$)° were made at a speed of 16.0°/min (in omega). Of the 6858 reflections which were collected, 2820 were unique (R_{int} = 0.031). The linear absorption coefficient, μ, for Mo-Kα radiation is 5.3 cm^{-1}. An empirical absorption correction based on azimuthal scans of several reflections was applied which resulted in transmission factors ranging from 0.96 to 1.00. The data were corrected for Lorentz and polarization effects.

The structure was solved by a direct method (SHELXS86)[16] and expanded using Fourier techniques (DIRDIF94).[18] The non-hydrogen atoms were refined anisotropically.

Hydrogen atoms were included but not refined. The final cycle of full-matrix least-squares refinement* was based on 2806 observed reflections (I > 3.00σ(I)) and 334 variable parameters and converged (largest parameter shift was 0.07 times its esd) with unweighted and weighted agreement factors of: $R = \sum ||Fo| - |Fc|| / \sum |Fo| = 0.059$, $Rw = [\sum w(|Fo| - |Fc|)^2 / \sum wFo^2]^{1/2} = 0.046$. The standard deviation of an observation of unit weight: $[\sum w(|Fo| - |Fc|)^2 / (No - Nv)]^{1/2}$ was 2.83 (*No*:number of observations; *Nv*:number of variables). The weighting scheme was based on counting statistics and included a factor (p = 0.006) to downweight the intense reflections. Plots of $\sum w(|Fo| - |Fc|)^2$ versus $|Fo|$, reflection order in data collection, $sin\,\theta/\lambda$ and various classes of indices showed no unusual trends. The maximum and minimum peaks on the final difference Fourier map corresponded to 0.40 and -0.34 $e^{-}/Å^3$, respectively.

(*) Least-Squares: Function minimized: $\sum w(|Fo|-|Fc|)^2$, where $w = [\sigma^2(Fo)]^{-1} = [\sigma_c^2(Fo) + p^2 Fo^2/4]^{-1}$; $\sigma_c(Fo)$ = e.s.d. based on counting statistics; p = p-factor.

Measurements and Calculations

Cyclic Voltammetry. Cyclic voltammograms were recorded in 0.1 M n-Bu_4N•ClO_4 – PhCN solution with an Ag/AgCl reference electrode (BAS Co.) and a platinum working electrode, using a Hokuto Denko HAB 151 potentiostat/galvanostat with a scanning rate of 200 mV/s.

Optical Measurements. UV absorption spectra were observed on a JASCO V-570 spectrometer using a *ca.* 10^{-5} M dichloromethane (Dojin Spectrozole) solution, or a KBr pellet. IR spectra were observed on a Perkin-Elmer 1400 series spectrometer using a KBr pellet.

ESR Measurements. ESR spectra were measured on a JEOL TE300 spectrometer equipped with an RMC liquid helium transfer system and a Scientific Instruments 9650 digital temperature indicator/controller. The resonance magnetic field value was measured with the aid of a JEOL ES-FC5 NMR field meter. Single crystal samples were mounted on a Tefron tube with silicone grease, and were put into a quartz tube. Zero-field parameters of triplet spectra were determined by computational simulation.

Electric Conductivity Measurements. Electric conductivity was measured along the longer axis of a plate-like crystal of the ion-radical salt by a two-probe method. Gold wires (15 μm) were attached to the sample with gold past.

Magnetic Measurements. Magnetic susceptibilities of ETBN and its salts were measured with a Quantum Design MPMS-XL SQUID magnetometer by a reciprocating sample option (RSO) method under a static field of 0.5 T.

Molecular Orbital Calculation. PM3/UHF molecular orbital calculation was carried out using a CAChe MOPAC program provided from SONY Techtronics. The molecular structure was optimized using a planar conformation as an initial structure.

§4-8. References and Notes

1. Sasaki A, Mahé L, Izuoka A, Sugawara T, "Chemical consequences of arylnitrenes in the crystalline environment", *Bull. Chem. Soc. Jpn.* **1998**, *71*, 1259-1275.
2. Ishikawa Y, Miyamoto T, Yoshida A, Kawada Y, Nakazaki J, Izuoka A, Sugawara T, "New synthesis of 2-[1,3-dithiol-2-ylidene]-4,5-dihydro-1,3-dithiolo[4,5-b][1,4]dithiins with formyl group on fused-benzene, [1,4]dithiin, or thiophene ring", *Tetrahedron Lett.* **1999**, *40*, 8819-8822.
3. Ullman EF, Osiecki JH, Boocock DGB, Darcy R, "Studies of stable free radicals. X. Nitronyl nitroxide monoradicals and biradicals as possible small molecule spin labels", *J. Am. Chem. Soc.* **1972**, *94*, 7049-7059.
4.a) Aoyama Y, Endo K, Anzai T, Yamaguchi Y, Sawaki T, Kobayashi K, Kanehisa N, Hashimoto H, Kai Y, Masuda H, "Crystal engineering of stacked aromatic columns. Three-dimensional control of the alignment of orthogonal aromatic triads and guest quinones via self-assembly of hydrogen-bonded networks", *J. Am. Chem. Soc.* **1996**, *118*, 5562-5571.
   b) Hayashi N, Kuruma K, Mazaki Y, Imakubo T, Kobayashi K, "Guest-incorporation in ternary clathrate formation is random but shows site-selectivity", *J. Am. Chem. Soc.* **1998**, *120*, 3799-3800.
   c)   , "   ",   , **1997**.
5. Some metallic materials composed of TTF derivatives with a very bulky substituent have been reported. See: Yamada J, Nishikawa H, Kikuchi K, "Newly modified TTF and DSDTF donors for developing molecular-based organic metals", *J. Mater. Chem.* **1999**, *9*, 617-628.
6.a) Matsushita MM, Izuoka A, Sugawara T, Kobayashi T, Wada N, Takeda N, Ishikawa M, "Hydrogen-bonded organic ferromagnet", *J. Am. Chem. Soc.* **1997**, *119*, 4369-4379.
   b) Nogami T, Ishida T, Yasui M, Iwasaki F, Takeda N, Ishikawa M, Kawakami T, Yamaguchi K, "Proposed mechanism of ferromagnetic interaction of organic ferromagnets: 4-(Arylmethyleneamino)-2,2,6,6-tetramethylpiperidin-1-oxyls and related compounds", *Bull. Chem. Soc. Jpn.* **1996**, *69*, 1841-1848.
7. The salt is not an amorphous material, but tends to be an associated crystal. The oscillation photographs observed by imaging plate detector are shown here.
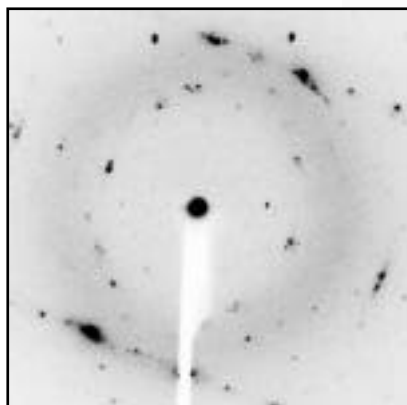
8. Enoki T, Imaeda K, Kobayashi M, Inokuchi H, Saito G, *Phys. Rev. B* **1986**, *33*, 1553.
9.a) Enoki T, Yamaura J, Miyazaki A, "Molecular magnets based on organic charge transfer complexes", *Bull. Chem. Soc. Jpn.* **1997**, *70*, 2005-2023.
   b) Yoneyama N, Miyazaki A, Enoki T, Saito G, "Magnetic properties of TTF-type charge transfer salts in the Mott insulator regime", *Bull. Chem. Soc. Jpn.* **1999**, *72*, 639-651.

10. Lamchen M, Mttag TW, "Nitrones. part IV. Synthesis and properties of a monocyclic -dinitrone", *J. Chem. Soc. C* **1966**, 2300-2303.

11. Cromer DT, Waber JT, In: *"International Tables for X-ray Crystallography Vol. IV"*, The Kynoch Press, Birmingham, England, **1974**, Table 2.2 A.

12. Ibers JA, Hamilton WC, *Acta Cryst.* **1964**, *17*, 781.

13. Creagh DC, McAuley WJ, In: Wilson AJC ed, *"International Tables for Crystallography Vol C"*, Kluwer Academic Publishers, Boston, **1992**, 219-222, Table 4.2.6.8.

14. Creagh DC, Hubbell JH, In: Wilson AJC ed, *"International Tables for Crystallography Vol C"*, Kluwer Academic Publishers, Boston, **1992**, 200-206, Table 4.2.4.3.

15. teXsan: Crystal Structure Analysis Package, Molecular Structure Corporation (1985 & 1992).

16. SHELXS86: Sheldrick GM, In: Sheldrick GM, Kruger C, Goddard R, eds, *"Crystallographic Computing 3"*, Oxford University Press **1985**, 175-189.

17. SIR88: Burla MC, Camalli M, Cascarano G, Giacovazzo C, Polidori G, Spagna R, ViterboD, *J. Appl. Cryst.* **1989**, *22*, 389-303.

18. DIRDIF94: Beurskens PT, Admiraal G, Beurskens G, Bosman WP, de Gelder R, Israel R, Smits JMM, "The DIRDIF-94 program system", *Tech. Report of Crystallography Lab., Univ. of Nijmegen, The Netherlands*, **1994**.

Chapter 5

Concluding Remarks

As building blocks for organic conductive magnets, several pyrrole-based or TTF-based spin-polarized donors have been designed and examined.

In Chapter 2, spin correlation in cation diradicals derived from pyrroles carrying nitronyl nitroxide (NN) was discussed. Since *homo* of pyrrole has a node at the *N*-position, **N**-**NN** did not afford a triplet species upon one-electron oxidation, while β-**NN** afforded a ground state triplet cation diradical. A ground state triplet cation diradical was also detected for **N**-**PN**, and the difference between **N**-**NN** and **N**-**PN** was rationalized based on a perturbational MO method. The *p*-phenylene group turned out to play an important role in the spin correlation in **N**-**PN**$^{+\bullet}$.

In Chapter 3, TTF-based spin-polarized donors, where a TTF skeleton is connected with a NN group through a *p*-phenylene moiety, were prepared, and their singly oxidized species proved to have a triplet ground state. The *p*-phenylene group of such a TTF-based spin-polarized donor also plays an important role to diminish a twisting of the NN group from the TTF plane by releasing a steric repulsion between them.

Based on the above results, annulated TTF-based spin-polarized donors were prepared in Chapter 4. The annulated donors have good crystallinity, and their structures were analized by X-ray crystallography. Among these donors, a benzo-annulated derivative, **ETBN**, afforded an isolable ion-radical salt of the 2:1 donor to a counter ion ratio. Although the local spins on the radical sites in the ion-radical salt behave paramagnetically at the present stage, magnetic ordering of the local spins may be observed if the effective carrier concentration in the ion-radical salt becomes resonably high.

In order to obtain a metallic ion-radical salt, tetrathiapentalene (TTP) derivatives are considered to be useful. A *p*-thiophenylene- or benzo-derivative of TTP-based spin-polarized donor is expected to afford an organic metallic magnet.
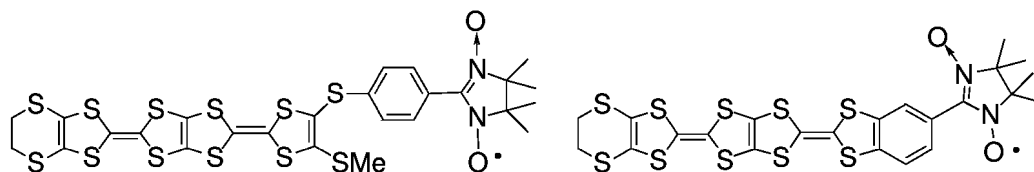
An advantage of organic spin system is that one can prepare a certain system with uni-molecular scale. Recently, preparation of structured molecules, such as dendrimers, hyper-branched polymers, *etc.*, has been developed, and studies on "hyper-structured molecules" or "uni-molecular scale electronics" have launched. The basic knowledges obtained here will be utilized in such a field as "organic quantum spin device".

Appendix / X-ray Diffraction Data Collections

	N-NN	β-NN	*N*-PN
A. Crystal Data			
Empirical Formula	$C_{11}H_{16}N_3O_2$	$C_{11}H_{16}N_3O_2$	$C_{17}H_{20}N_3O_2$
Formula Weight	222.27	222.27	298.36
Crystal Color, Habit	blue, block	blue, block	blue, prism
Crystal Dimensions	$0.44 \times 0.40 \times 0.32$ mm	$0.56 \times 0.48 \times 0.30$ mm	$0.40 \times 0.28 \times 0.10$ mm
Crystal System	monoclinic	orthorhombic	monoclinic
Lattice Type	Primitive	Primitive	Primitive
No. of Reflections Used for Unit Cell Determination = 25 (2θ range= 20.0 - 25.0˚)			
Lattice Parameters	$a =$ 9.845(2) Å	$a =$ 13.065(1) Å	$a =$ 12.284(4) Å
	$b =$ 16.530(3) Å	$b =$ 14.417(2) Å	$b =$ 12.657(5) Å
	$c =$ 7.2587(9) Å	$c =$ 12.874(2) Å	$c =$ 10.953(4) Å
	$\beta =$ 96.53(1)˚		$\beta =$ 111.72(2)˚
	$V = 1173.7(3)$ Å^3	$V = 2425.0(4)$ Å^3	$V = 1582.2(10)$ Å^3
Space Group	$P2_1/n$ (#14)	$Pbca$ (#61)	$P2_1/a$ (#14)
Z value	4	8	4
D_{calc}	1.258 g/cm^3	1.217 g/cm^3	1.252 g/cm^3
F_{000}	4662.00	952.00	636.00
μ(MoKα)	0.89	0.89	0.84
B. Intensity Measurements			
Diffractometer	Rigaku AFC5S	Rigaku AFC5S	Rigaku AFC5S
Radiation	MoKα (λ = 0.71069 Å) graphite monochromated		
Attenuator	Zr foil	Zr foil	Zr foil
Detector Aperture	3/4 horizontal	3/4 horizontal	3/4 horizontal
	3/4 vertical	3/4 vertical	3/4 vertical
Temperature	room temperature	room temperature	room temperature
Scan Type	ω	ω	ω
Scan Rate	8.0˚/min (up to 3 scans)	8.0˚/min (up to 3 scans)	8.0˚/min (up to 3 scans)
2 max	55.0˚	55.0˚	55.0˚
No. of Reflections	Total: 2977	Total: 3123	Total: 3933
Measured	Unique: 2768		Unique: 3743
	(R_{int} = 0.019)		(R_{int} = 0.059)
Corrections	Lorentz-polarization	Lorentz-polarization	Lorentz-polarization
	Secondary Extinction	Secondary Extinction	Secondary Extinction
	(coefficient: 1.55017e^{-06})	(coefficient: 1.11822e^{-06})	(coefficient: 1.16090e^{-07})
C. Structure Solution and Refinement			
Structure Solution	SAPI91	SAPI91	SAPI91
Refinement	Full-matrix least-squares	Full-matrix least-squares	Full-matrix least-squares
Function Minimized	$w(|Fo| - |Fc|)^2$	$w(|Fo| - |Fc|)^2$	$w(|Fo| - |Fc|)^2$
Least Squares Weights	$w = [\sigma^2(Fo^2)]^{-1}$	$w = [\sigma^2(Fo^2)]^{-1}$	$w = [\sigma^2(Fo^2)]^{-1}$
Anomalous Dispersion	All non-hydrogen atoms	All non-hydrogen atoms	All non-hydrogen atoms
No. Observations(I>3.00σ(I))	1631	1836	1314
No. Variables	162	162	232
Reflection/Parameter Ratio	10.07	11.33	5.66
Residuals: R; Rw	0.045 ; 0.030	0.043 ; 0.032	0.046 ; 0.043
Goodness of Fit Indicator	2.79	3.08	0.32
Max Shift/Error in Final Cycle	0.00	0.00	0.01
Max.peak in Final Diff. Map	0.14 e^-/Å^3	0.17 e^-/Å^3	0.20 e^-/Å^3
Min.peak in Final Diff. Map	-0.11 e^-/Å^3	-0.13 e^-/Å^3	-0.18 e^-/Å^3

	ETBN	**ETTN**·pyridine
A. Crystal Data		
Empirical Formula	$C_{19}H_{19}N_2O_2S_6$	$C_{22}H_{22}N_3O_2S_7$
Formula Weight	499.73	584.85
Crystal Color, Habit	green, needle	darkbrown, prismatic
Crystal Dimensions	$0.40 \times 0.05 \times 0.05$ mm	$0.40 \times 0.30 \times 0.20$ mm
Crystal System	trigonal	triclinic
Lattice Type	R-centered	Primitive
No. of Reflections Used for Unit Cell Determination (2θ range)	24 (28.3 - 32.0˚)	25 (29.8 - 30.0˚)
Omega Scan Peak Width at Half-height	0.35˚	0.36˚
Lattice Parameters	$a = 43.24(7)$ Å	$a = 12.080(3)$ Å
	$b = a$	$b = 12.694(2)$ Å
	$c = 6.381(4)$ Å	$c = 9.725(2)$ Å
	$\alpha = 90$˚	$\alpha = 110.15(2)$˚
	$\beta = 90$˚	$\beta = 108.04(2)$˚
	$\gamma = 120$˚	$\gamma = 93.48(2)$˚
	$V = 10327(25)$ Å^3	$V = 1307.5(5)$ Å^3
Space Group	$R\overline{3}$ (#148)	$P\overline{1}$ (#2)
Z value	18	2
D_{calc}	1.446 g/cm^3	1.485 g/cm^3
F_{000}	4662.00	606.00
μ(MoKα)	28.45 cm^{-1}	29.19 cm^{-1}
B. Intensity Measurements		
Diffractometer	Rigaku AFC7R (rotating anode)	Rigaku AFC7R (rotating anode)
Radiation	MoKα ($\lambda = 0.71069$ Å) graphite monochromated	MoKα ($\lambda = 0.71069$ Å) graphite monochromated
Attenuator	Zr foil (factor = 8.15)	Zr foil (factor = 8.15)
Take-off Angle	6.0˚	6.0˚
Detector Aperture	3.0 mm horizontal 3.0 mm vertical	3.0 mm horizontal 3.5 mm vertical
Crystal to Detector Distance	235 mm	235 mm
Temperature	room temperature	room temperature
Scan Type	ω-2θ	ω-2θ
Scan Rate	16.0˚/min (in ω) (up to 5 scans)	16.0˚/min (in ω) (up to 5 scans)
Scan Width	$(1.37 + 0.30\ tan\ \theta)$˚	$(1.84 + 0.30\ tan\ \theta)$˚
2 max	55.3˚	55.0˚
No. of Reflections Measured	Total: 5909 Unique: 2682 ($R_{int} = 0.089$)	Total: 6356 Unique: 3740 ($R_{int} = 0.012$)
Corrections	Lorentz-polarization Absorption (trans. factors: 0.5141 - 0.9956)	Lorentz-polarization Absorption (trans. factors: 0.9687 - 0.9994)

	ETBN (continued)	**ETTN·pyridine** (continued)
C. Structure Solution and Refinement		
Structure Solution	Direct Methods (SHELXS-86)	Direct Methods (SIR88)
Refinement	Full-matrix least-squares	Full-matrix least-squares
Function Minimized	$w(Fo^2 - Fc^2)^2$	$w(Fo^2 - Fc^2)^2$
Least Squares Weights	$1/\sigma^2(Fo^2)$	$1/\sigma^2(Fo^2)$
p-factor	0.0500	0.0680
Anomalous Dispersion	All non-hydrogen atoms	All non-hydrogen atoms
No. Observations (I>3.00σ(I))	2694	3730
No. Variables	262	325
Reflection/Parameter Ratio	10.28	11.48
Residuals: R; Rw	0.108 ; 0.173	0.078 ; 0.207
Residuals: R_1	0.063	0.063
No. of Reflections to calc R_1	2694	3730
Goodness of Fit Indicator	2.15	2.24
Max Shift/Error in Final Cycle	0.00	0.03
Max. peak in Final Diff. Map	$0.77\ e^-/\text{Å}^3$	$0.46\ e^-/\text{Å}^3$
Min. peak in Final Diff. Map	$-0.52\ e^-/\text{Å}^3$	$-0.37\ e^-/\text{Å}^3$

	EPPN	**EMTN**
A. Crystal Data		
Empirical Formula	$C_{25}H_{26}N_3O_2S_6$	$C_{22}H_{23}N_2O_2S_8$
Formula Weight	592.86	603.92
Crystal Color, Habit	darkgreen, plate	darkgreen, needle
Crystal Dimensions	$0.20 \times 0.20 \times 0.03$ mm	$1.00 \times 0.03 \times 0.01$ mm
Crystal System	monoclinic	monoclinic
Lattice Type	C-centered	Primitive
No. of Reflections Used for Unit Cell Determination (2θ range)	14 (25.1 - 30.0˚)	
Omega Scan Peak Width at Half-height	0.35˚	
Indexing Images		3 oscillations @ 10.0 minutes
Detector Position		105.00 mm
Detector Swing Angle		0.00˚
Pixel Size		0.100 mm
Lattice Parameters	$a = 19.252(7)$ Å	$a = 6.9919(6)$ Å
	$b = 8.660(6)$ Å	$b = 16.817(2)$ Å
	$c = 32.715(6)$ Å	$c = 23.037(2)$ Å
	$\alpha = 90˚$	$\alpha = 90˚$
	$\beta = 93.43(3)˚$	$\beta = 96.674(6)˚$
	$\gamma = 90˚$	$\gamma = 90˚$
	$V = 5444(4)$ Å^3	$V = 2690.3401$ Å^3
Space Group	$C2/c$ (#15)	$P2_1/c$ (#14)
Z value	8	4
D_{calc}	1.446 g/cm^3	1.491 g/cm^3
F_{000}	2472.00	1252.00
μ(MoKα)	26.59 cm^{-1}	30.42 cm^{-1}

	EPPN (continued)	EMTN (continued)
B. Intensity Measurements		
Diffractometer	Rigaku AFC7R (rotating anode)	Rigaku RAXIS-IV
Radiation	MoKα (λ = 0.71069 Å)	MoKα (λ = 0.71069 Å)
	graphite monochromated	graphite monochromated
Attenuator	Zr foil (factor = 8.15)	
Take-off Angle	6.0˚	
Detector Aperture	3.0 mm horizontal	300 mm × 300 mm
	3.0 mm vertical	
Crystal to Detector Distance	235 mm	
Temperature	room temperature	room temperature
Scan Type	ω	
Scan Rate	16.0˚/min (in ω) (up to 5 scans)	
Scan Width	$(1.60 + 0.35\ tan\ \theta)$˚	
Data Images		35 exposures @ 55.0 minutes
Oscillation Range		3.0˚
Detector Position		105.00 mm
Detector Swing Angle		0.00˚
Pixel Size		0.100 mm
2 max	55.0˚	55.3˚
No. of Reflections Measured	Total: 6858	Total: 4678
	Unique: 2820 (R_{int} = 0.031)	
Corrections	Lorentz-polarization	Lorentz-polarization
	Absorption	Secondary Extinction
	(trans. factors: 0.9606 - 0.9993)	(coefficient: $1.20134e^{-06}$)

C. Structure Solution and Refinement

	EPPN	EMTN
Structure Solution	Direct Methods (SHELXS-86)	Direct Methods (SHELXS86)
Refinement	Full-matrix least-squares	Full-matrix least-squares
Function Minimized	$w(|Fo| - |Fc|)^2$	$w(|Fo| - |Fc|)^2$
Least Squares Weights	$1/\sigma^2(Fo^2) = 4Fo^2/\sigma^2(Fo^2)$	$1/\sigma^2(Fo^2)$
p-factor	0.0060	0.0500
Anomalous Dispersion	All non-hydrogen atoms	All non-hydrogen atoms
No. Observations (I>3.00σ(I))	2806	3181
No. Variables	334	308
Reflection/Parameter Ratio	8.40	10.33
Residuals: R; Rw	0.059 ; 0.046	0.072 ; 0.094
Residuals: R_1	0.059	
No. of Reflections to calc R_1	2806	
Goodness of Fit Indicator	2.83	2.26
Max Shift/Error in Final Cycle	0.07	0.00
Max. peak in Final Diff. Map	0.40 e^-/Å^3	0.33 e^-/Å^3
Min. peak in Final Diff. Map	-0.34 e^-/Å^3	-0.34 e^-/Å^3

N-NN
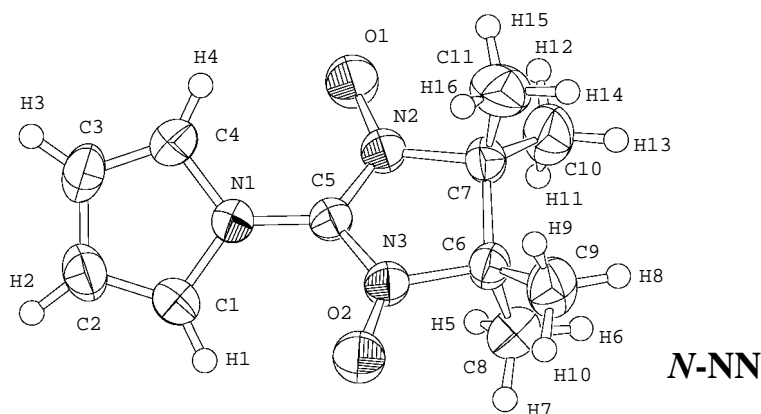
Atomic coordinates and Biso/Beq

atom	x	y	z	Beq	atom	x	y	z	Beq
O(1)	0.5917(2)	0.01980(9)	0.7736(2)	5.96(5)	H(1)	0.843(2)	-0.055(1)	1.326(3)	5.6(6)
O(2)	0.8112(2)	-0.18011(8)	1.1385(2)	5.48(4)	H(2)	0.977(2)	0.073(1)	1.406(3)	5.6(6)
N(1)	0.8061(2)	-0.00782(10)	1.0695(2)	3.51(4)	H(3)	0.974(2)	0.149(1)	1.109(3)	4.9(6)
N(2)	0.6271(2)	-0.05008(10)	0.8367(2)	3.85(5)	H(4)	0.826(2)	0.071(1)	0.872(3)	5.1(6)
N(3)	0.7292(2)	-0.14506(10)	1.0138(2)	3.65(4)	H(5)	0.4702	-0.1504	1.0750	5.8409
C(1)	0.8599(2)	-0.0100(2)	1.2544(3)	4.39(6)	H(6)	0.4237	-0.2301	0.9743	5.8409
C(2)	0.9350(3)	0.0576(2)	1.2888(4)	4.88(7)	H(7)	0.5364	-0.2319	1.1420	5.8409
C(3)	0.9297(2)	0.1024(2)	1.1243(4)	4.81(7)	H(8)	0.5887	-0.2995	0.7681	6.3198
C(4)	0.8506(3)	0.0625(1)	0.9921(4)	4.34(6)	H(9)	0.7318	-0.2614	0.7590	6.3198
C(5)	0.7240(2)	-0.0658(1)	0.9775(3)	3.30(5)	H(10)	0.6977	-0.3029	0.9399	6.3198
C(6)	0.6127(2)	-0.1886(1)	0.9036(3)	3.43(5)	H(11)	0.3728	-0.1098	0.7915	6.6557
C(7)	0.5739(2)	-0.1270(1)	0.7460(3)	3.46(5)	H(12)	0.4017	-0.0759	0.6005	6.6557
C(8)	0.5046(3)	-0.2006(1)	1.0319(3)	5.25(7)	H(13)	0.3846	-0.1684	0.6272	6.6557
C(9)	0.6599(2)	-0.2702(1)	0.8412(3)	5.28(7)	H(14)	0.6199	-0.1874	0.5073	7.7336
C(10)	0.4228(2)	-0.1190(1)	0.6873(3)	5.75(7)	H(15)	0.6358	-0.0944	0.4907	7.7336
C(11)	0.6495(3)	-0.1375(1)	0.5771(3)	6.10(8)	H(16)	0.7463	-0.1443	0.6108	7.7336

Anisotropic Displacement Parameters

atom	U11	U22	U33	U12	U13	U23
O(1)	0.101(1)	0.0383(9)	0.078(1)	0.0036(10)	-0.031(1)	0.0121(9)
O(2)	0.076(1)	0.0474(10)	0.076(1)	0.0027(9)	-0.0298(9)	0.0162(9)
N(1)	0.050(1)	0.039(1)	0.042(1)	-0.0059(9)	-0.0025(9)	0.0026(9)
N(2)	0.059(1)	0.034(1)	0.050(1)	0.0005(9)	-0.0092(10)	0.0054(10)
N(3)	0.049(1)	0.036(1)	0.050(1)	0.0012(9)	-0.0072(9)	0.0062(9)
C(1)	0.059(2)	0.058(2)	0.047(2)	-0.007(1)	-0.009(1)	0.005(1)
C(2)	0.061(2)	0.060(2)	0.059(2)	-0.008(1)	-0.012(1)	-0.009(2)
C(3)	0.058(2)	0.045(2)	0.078(2)	-0.014(1)	0.000(1)	-0.004(1)
C(4)	0.069(2)	0.042(1)	0.053(2)	-0.009(1)	0.004(1)	0.004(1)
C(5)	0.047(1)	0.035(1)	0.042(1)	0.000(1)	-0.001(1)	0.003(1)
C(6)	0.044(1)	0.036(1)	0.049(1)	-0.003(1)	-0.001(1)	-0.001(1)
C(7)	0.050(1)	0.037(1)	0.043(1)	-0.003(1)	-0.003(1)	-0.004(1)
C(8)	0.074(2)	0.059(2)	0.067(2)	-0.015(1)	0.008(1)	0.008(1)
C(9)	0.075(2)	0.038(1)	0.083(2)	0.009(1)	-0.012(1)	-0.006(1)
C(10)	0.060(2)	0.058(2)	0.093(2)	-0.001(1)	-0.026(1)	0.008(2)
C(11)	0.109(2)	0.073(2)	0.051(2)	-0.003(2)	0.014(2)	-0.002(1)

Bond Lengths(Å)

atom - atom	distance	atom - atom	distance	atom - atom	distance
O(1) - N(2)	1.277(2)	O(2) - N(3)	1.281(2)	N(1) - C(1)	1.386(3)
N(1) - C(4)	1.384(3)	N(1) - C(5)	1.377(2)	N(2) - C(5)	1.342(2)
N(2) - C(7)	1.498(2)	N(3) - C(5)	1.336(2)	N(3) - C(6)	1.505(2)
C(1) - C(2)	1.347(3)	C(2) - C(3)	1.402(3)	C(3) - C(4)	1.339(3)
C(6) - C(7)	1.547(3)	C(6) - C(8)	1.505(3)	C(6) - C(9)	1.513(3)
C(7) - C(10)	1.505(3)	C(7) - C(11)	1.515(3)		

Bond Angles(°)

atom - atom - atom	angle	atom - atom - atom	angle
C(1) - N(1) - C(4)	108.1(2)	C(1) - N(1) - C(5)	126.2(2)
C(4) - N(1) - C(5)	125.7(2)	O(1) - N(2) - C(5)	126.2(2)
O(1) - N(2) - C(7)	122.8(2)	C(5) - N(2) - C(7)	110.7(2)
O(2) - N(3) - C(5)	126.1(2)	O(2) - N(3) - C(6)	122.7(2)
C(5) - N(3) - C(6)	110.7(2)	N(1) - C(1) - C(2)	107.4(2)
C(1) - C(2) - C(3)	108.3(2)	C(2) - C(3) - C(4)	108.2(2)
N(1) - C(4) - C(3)	107.9(2)	N(1) - C(5) - N(2)	124.2(2)
N(1) - C(5) - N(3)	125.4(2)	N(2) - C(5) - N(3)	110.4(2)
N(3) - C(6) - C(7)	100.8(2)	N(3) - C(6) - C(8)	106.5(2)
N(3) - C(6) - C(9)	110.1(2)	C(7) - C(6) - C(8)	114.3(2)
C(7) - C(6) - C(9)	115.1(2)	C(8) - C(6) - C(9)	109.3(2)
N(2) - C(7) - C(6)	100.9(1)	N(2) - C(7) - C(10)	109.6(2)
N(2) - C(7) - C(11)	105.9(2)	C(6) - C(7) - C(10)	114.8(2)
C(6) - C(7) - C(11)	114.8(2)	C(10) - C(7) - C(11)	110.0(2)

β-NN
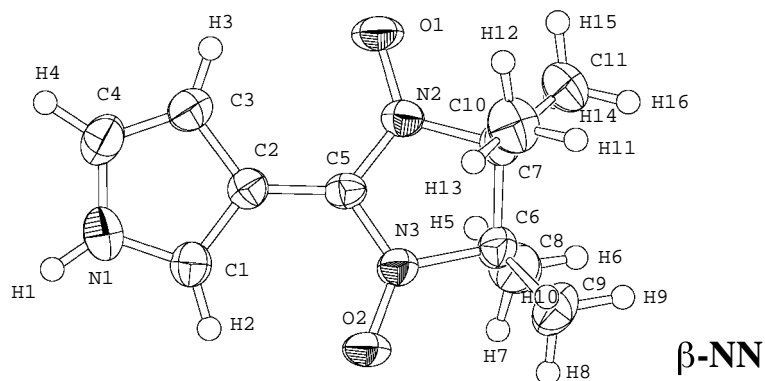
Atomic coordinates and Biso/Beq

atom	x	y	z	Beq	atom	x	y	z	Beq
O(1)	0.9199(1)	0.01170(9)	0.7293(1)	3.97(4)	H(1)	0.655(2)	-0.003(2)	1.098(2)	6.7(7)
O(2)	0.9015(1)	-0.21969(9)	0.9771(1)	4.50(4)	H(2)	0.771(1)	-0.129(1)	1.046(1)	3.8(5)
N(1)	0.6985(1)	-0.0008(1)	1.0423(1)	3.82(4)	H(3)	0.803(1)	0.092(1)	0.850(1)	4.0(5)
N(2)	0.9373(1)	-0.0642(1)	0.7798(1)	2.85(4)	H(4)	0.668(2)	0.132(1)	0.985(2)	6.1(6)
N(3)	0.9285(1)	-0.1736(1)	0.8965(1)	3.09(4)	H(5)	0.8685	-0.2442	0.7184	5.4532
C(1)	0.7637(2)	-0.0688(2)	1.0125(2)	3.19(5)	H(6)	0.9591	-0.3102	0.6937	5.4532
C(2)	0.8154(2)	-0.0384(1)	0.9252(2)	2.83(5)	H(7)	0.8926	-0.3267	0.7918	5.4532
C(3)	0.7788(2)	0.0529(2)	0.9038(2)	3.90(6)	H(8)	1.0619	-0.3186	0.9051	5.8729
C(4)	0.7079(2)	0.0736(2)	0.9766(2)	4.21(6)	H(9)	1.1278	-0.2969	0.8078	5.8729
C(5)	0.8907(2)	-0.0897(1)	0.8690(1)	2.58(5)	H(10)	1.1275	-0.2290	0.9013	5.8729
C(6)	0.9951(2)	-0.2146(1)	0.8133(2)	3.19(5)	H(11)	1.1824	-0.1120	0.7871	5.2528
C(7)	1.0263(2)	-0.1254(1)	0.7544(2)	3.01(5)	H(12)	1.1300	-0.0165	0.7718	5.2528
C(8)	0.9273(2)	-0.2791(1)	0.7504(2)	4.84(6)	H(13)	1.1137	-0.0713	0.8741	5.2528
C(9)	1.0817(2)	-0.2682(2)	0.8626(2)	5.21(7)	H(14)	0.9784	-0.1639	0.6084	4.8449
C(10)	1.1194(2)	-0.0773(2)	0.8003(2)	4.67(6)	H(15)	1.0482	-0.0769	0.6045	4.8449
C(11)	1.0383(2)	-0.1360(2)	0.6383(2)	4.34(6)	H(16)	1.0960	-0.1744	0.6202	4.8449

Anisotropic Displacement Parameters

atom	U11	U22	U33	U12	U13	U23
O(1)	0.073(1)	0.0384(9)	0.0397(9)	0.0012(8)	-0.0003(9)	0.0134(7)
O(2)	0.088(1)	0.0406(9)	0.0421(9)	0.0102(9)	0.0162(9)	0.0152(8)
N(1)	0.042(1)	0.059(1)	0.044(1)	0.002(1)	0.004(1)	-0.012(1)
N(2)	0.043(1)	0.0334(10)	0.0316(10)	-0.0028(9)	-0.0012(9)	0.0029(8)
N(3)	0.051(1)	0.0343(10)	0.0325(10)	0.0050(9)	0.0018(9)	0.0028(8)
C(1)	0.041(1)	0.040(1)	0.040(1)	0.000(1)	-0.001(1)	-0.006(1)
C(2)	0.039(1)	0.035(1)	0.034(1)	0.001(1)	-0.002(1)	-0.0023(10)
C(3)	0.059(2)	0.042(1)	0.047(1)	0.009(1)	0.002(1)	0.004(1)
C(4)	0.059(2)	0.047(2)	0.054(2)	0.016(1)	-0.002(1)	-0.006(1)
C(5)	0.038(1)	0.030(1)	0.029(1)	-0.002(1)	-0.0042(10)	0.0017(9)
C(6)	0.049(1)	0.037(1)	0.035(1)	0.007(1)	0.002(1)	-0.002(1)
C(7)	0.038(1)	0.042(1)	0.034(1)	0.000(1)	0.000(1)	-0.003(1)
C(8)	0.083(2)	0.044(1)	0.057(2)	-0.013(1)	0.008(2)	-0.012(1)
C(9)	0.074(2)	0.060(2)	0.064(2)	0.031(1)	0.001(2)	0.004(1)
C(10)	0.046(1)	0.067(2)	0.064(2)	-0.009(1)	-0.002(1)	-0.006(1)
C(11)	0.063(2)	0.064(2)	0.038(1)	0.002(1)	0.009(1)	-0.002(1)

Bond Lengths(Å)

atom - atom	distance	atom - atom	distance	atom - atom	distance
O(1)- N(2)	1.293(2)	O(2)- N(3)	1.281(2)	N(1)- C(1)	1.355(3)
N(1)- C(4)	1.371(3)	N(2)- C(5)	1.351(2)	N(2)- C(7)	1.496(2)
N(3)- C(5)	1.354(2)	N(3)- C(6)	1.502(2)	C(1)- C(2)	1.382(3)
C(2)- C(3)	1.427(3)	C(2)- C(5)	1.428(3)	C(3)- C(4)	1.350(3)
C(6)- C(7)	1.547(3)	C(6)- C(8)	1.518(3)	C(6)- C(9)	1.510(3)
C(7)- C(10)	1.520(3)	C(7)- C(11)	1.511(3)		

Bond Angles(°)

atom - atom - atom	angle	atom - atom - atom	angle
C(1)- N(1)- C(4)	109.6(2)	O(1)- N(2)- C(5)	125.4(2)
O(1)- N(2)- C(7)	121.7(2)	C(5)- N(2)- C(7)	112.0(2)
O(2)- N(3)- C(5)	125.1(2)	O(2)- N(3)- C(6)	122.2(2)
C(5)- N(3)- C(6)	112.1(2)	N(1)- C(1)- C(2)	107.9(2)
C(1)- C(2)- C(3)	106.6(2)	C(1)- C(2)- C(5)	125.7(2)
C(3)- C(2)- C(5)	127.7(2)	C(2)- C(3)- C(4)	107.5(2)
N(1)- C(4)- C(3)	108.4(2)	N(2)- C(5)- N(3)	107.5(2)
N(2)- C(5)- C(2)	126.9(2)	N(3)- C(5)- C(2)	125.6(2)
N(3)- C(6)- C(7)	100.1(2)	N(3)- C(6)- C(8)	106.4(2)
N(3)- C(6)- C(9)	109.6(2)	C(7)- C(6)- C(8)	113.7(2)
C(7)- C(6)- C(9)	115.7(2)	C(8)- C(6)- C(9)	110.4(2)
N(2)- C(7)- C(6)	100.3(2)	N(2)- C(7)- C(10)	105.5(2)
N(2)- C(7)- C(11)	110.9(2)	C(6)- C(7)- C(10)	113.5(2)
C(6)- C(7)- C(11)	115.4(2)	C(10)- C(7)- C(11)	110.4(2)

N-PN
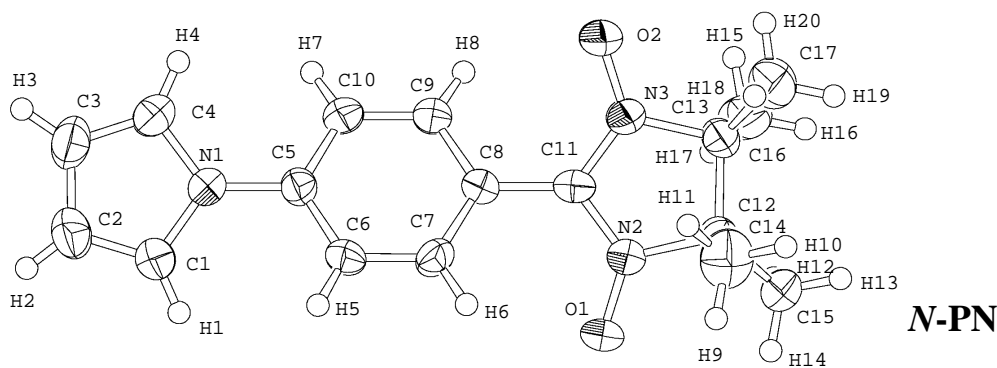
Atomic coordinates and Biso/Beq

atom	x	y	z	Beq	atom	x	y	z	Beq
O(1)	0.4032(3)	0.5927(2)	0.3726(3)	4.66(9)	H(1)	0.101(4)	0.573(4)	0.753(4)	4.8(2)
O(2)	0.2967(3)	0.2433(2)	0.2738(3)	4.76(9)	H(2)	-0.011(4)	0.521(3)	0.888(4)	4.4(2)
N(1)	0.0942(3)	0.4210(3)	0.7029(3)	3.22(8)	H(3)	-0.055(4)	0.331(3)	0.853(4)	4.5(2)
N(2)	0.3847(3)	0.5020(3)	0.3169(3)	3.09(8)	H(4)	0.045(4)	0.271(3)	0.702(4)	3.9(2)
N(3)	0.3374(3)	0.3362(3)	0.2729(3)	3.23(9)	H(5)	0.133(3)	0.574(3)	0.565(4)	4.0(2)
C(1)	0.0722(4)	0.5089(4)	0.7635(5)	3.9(1)	H(6)	0.232(3)	0.572(3)	0.424(4)	3.4(2)
C(2)	0.0073(5)	0.4796(4)	0.8342(5)	4.6(1)	H(7)	0.208(4)	0.269(4)	0.645(4)	5.4(1)
C(3)	-0.0134(5)	0.3708(5)	0.8157(5)	4.9(1)	H(8)	0.300(3)	0.269(3)	0.493(4)	2.6(2)
C(4)	0.0402(4)	0.3364(4)	0.7355(5)	4.2(1)	H(9)	0.2996	0.6059	0.0945	6.0288
C(5)	0.1558(3)	0.4199(3)	0.6163(4)	2.86(9)	H(10)	0.3137	0.5219	-0.0018	6.0288
C(6)	0.1661(4)	0.5114(3)	0.5523(4)	3.2(1)	H(11)	0.2326	0.4995	0.0753	6.0288
C(7)	0.2259(4)	0.5108(3)	0.4684(4)	3.2(1)	H(12)	0.5871	0.5061	0.2764	5.4666
C(8)	0.2757(4)	0.4180(3)	0.4436(4)	2.90(9)	H(13)	0.5389	0.5243	0.1256	5.4666
C(9)	0.2640(4)	0.3269(4)	0.5085(5)	3.4(1)	H(14)	0.5205	0.6095	0.2180	5.4666
C(10)	0.2063(4)	0.3269(3)	0.5942(4)	3.5(1)	H(15)	0.5256	0.2394	0.2810	5.8169
C(11)	0.3319(3)	0.4181(3)	0.3487(4)	2.89(9)	H(16)	0.5829	0.3252	0.2231	5.8169
C(12)	0.4080(4)	0.4826(3)	0.1934(4)	3.09(10)	H(17)	0.5643	0.3462	0.3536	5.8169
C(13)	0.4100(4)	0.3602(3)	0.1922(4)	3.5(1)	H(18)	0.2762	0.3378	0.0118	6.7172
C(14)	0.3051(5)	0.5317(4)	0.0830(5)	5.7(1)	H(19)	0.3984	0.3235	0.0028	6.7172
C(15)	0.5216(4)	0.5352(4)	0.2023(5)	4.2(1)	H(20)	0.3468	0.2348	0.0630	6.7172
C(16)	0.5301(4)	0.3139(4)	0.2678(6)	5.4(1)					
C(17)	0.3563(5)	0.3087(5)	0.0594(5)	6.2(2)					

Anisotropic Displacement Parameters

atom	U11	U22	U33	U12	U13	U23
O(1)	0.090(3)	0.029(2)	0.077(2)	-0.013(2)	0.053(2)	-0.015(2)
O(2)	0.078(2)	0.038(2)	0.083(2)	-0.018(2)	0.051(2)	-0.017(2)
N(1)	0.046(2)	0.036(2)	0.045(2)	-0.004(2)	0.023(2)	0.001(2)
N(2)	0.045(2)	0.032(2)	0.044(2)	0.000(2)	0.021(2)	-0.002(2)
N(3)	0.041(2)	0.036(2)	0.050(2)	-0.008(2)	0.022(2)	-0.006(2)
C(1)	0.062(3)	0.045(3)	0.046(3)	-0.003(2)	0.027(3)	-0.004(2)
C(2)	0.070(4)	0.067(4)	0.046(3)	0.001(3)	0.031(3)	-0.005(3)
C(3)	0.071(4)	0.067(4)	0.064(4)	0.004(3)	0.044(3)	0.013(3)
C(4)	0.062(3)	0.043(3)	0.067(4)	-0.004(3)	0.037(3)	0.004(3)
C(5)	0.037(2)	0.038(2)	0.035(2)	-0.003(2)	0.016(2)	-0.004(2)
C(6)	0.048(3)	0.030(2)	0.048(3)	0.007(2)	0.022(2)	0.001(2)
C(7)	0.048(3)	0.034(3)	0.046(3)	0.003(2)	0.024(2)	0.011(2)
C(8)	0.041(2)	0.032(2)	0.040(2)	-0.002(2)	0.018(2)	-0.004(2)
C(9)	0.057(3)	0.030(2)	0.053(3)	0.004(2)	0.031(3)	0.002(2)
C(10)	0.061(3)	0.031(2)	0.047(3)	0.000(2)	0.027(3)	0.005(2)
C(11)	0.038(2)	0.028(2)	0.042(3)	0.000(2)	0.012(2)	-0.002(2)
C(12)	0.038(2)	0.040(3)	0.041(3)	-0.003(2)	0.016(2)	-0.004(2)
C(13)	0.045(3)	0.043(3)	0.051(3)	-0.006(2)	0.026(2)	-0.012(2)
C(14)	0.067(4)	0.083(4)	0.061(3)	0.017(3)	0.019(3)	0.019(3)
C(15)	0.060(3)	0.048(3)	0.062(3)	-0.012(2)	0.034(3)	-0.005(2)
C(16)	0.059(3)	0.046(3)	0.113(5)	0.007(3)	0.045(3)	0.003(3)
C(17)	0.107(5)	0.078(4)	0.064(3)	-0.031(4)	0.046(3)	-0.027(3)

Bond Lengths(Å)

atom – atom	distance	atom – atom	distance
O(1)– N(2)	1.281(4)	O(2)– N(3)	1.280(4)
N(1)– C(1)	1.373(5)	N(1)– C(4)	1.375(5)
N(1)– C(5)	1.416(5)	N(2)– C(11)	1.355(5)
N(2)– C(12)	1.503(5)	N(3)– C(11)	1.346(5)
N(3)– C(13)	1.501(5)	C(1)– C(2)	1.353(6)
C(2)– C(3)	1.401(7)	C(3)– C(4)	1.349(6)
C(5)– C(6)	1.384(6)	C(5)– C(10)	1.393(6)
C(6)– C(7)	1.373(6)	C(7)– C(8)	1.396(6)
C(8)– C(9)	1.390(6)	C(8)– C(11)	1.445(5)
C(9)– C(10)	1.370(6)	C(12)– C(13)	1.550(6)
C(12)– C(14)	1.522(6)	C(12)– C(15)	1.516(6)
C(13)– C(16)	1.516(7)	C(13)– C(17)	1.505(6)

Bond Angles(˚)

atom – atom – atom	angle	atom – atom – atom	angle
C(1)– N(1)– C(4)	107.8(4)	C(1)– N(1)– C(5)	125.5(4)
C(4)– N(1)– C(5)	126.6(4)	O(1)– N(2)– C(11)	126.7(3)
O(1)– N(2)– C(12)	121.0(3)	C(11)– N(2)– C(12)	111.9(3)
O(2)– N(3)– C(11)	126.5(3)	O(2)– N(3)– C(13)	120.7(3)
C(11)– N(3)– C(13)	112.6(3)	N(1)– C(1)– C(2)	108.5(4)
C(1)– C(2)– C(3)	107.5(5)	C(2)– C(3)– C(4)	107.8(5)
N(1)– C(4)– C(3)	108.5(5)	N(1)– C(5)– C(6)	120.2(4)
N(1)– C(5)– C(10)	120.5(4)	C(6)– C(5)– C(10)	119.3(4)
C(5)– C(6)– C(7)	120.4(4)	C(6)– C(7)– C(8)	121.1(4)
C(7)– C(8)– C(9)	117.6(4)	C(7)– C(8)– C(11)	120.0(4)
C(9)– C(8)– C(11)	122.4(4)	C(8)– C(9)– C(10)	121.9(4)
C(5)– C(10)– C(9)	119.7(4)	N(2)– C(11)– N(3)	107.9(3)
N(2)– C(11)– C(8)	125.9(4)	N(3)– C(11)– C(8)	126.1(4)
N(2)– C(12)– C(13)	100.3(3)	N(2)– C(12)– C(14)	105.6(3)
N(2)– C(12)– C(15)	110.4(3)	C(13)– C(12)– C(14)	114.4(4)
C(13)– C(12)– C(15)	115.0(4)	C(14)– C(12)– C(15)	110.3(4)
N(3)– C(13)– C(12)	100.5(3)	N(3)– C(13)– C(16)	105.7(4)
N(3)– C(13)– C(17)	109.7(4)	C(12)– C(13)– C(16)	113.4(4)
C(12)– C(13)– C(17)	116.0(4)	C(16)– C(13)– C(17)	110.5(4)
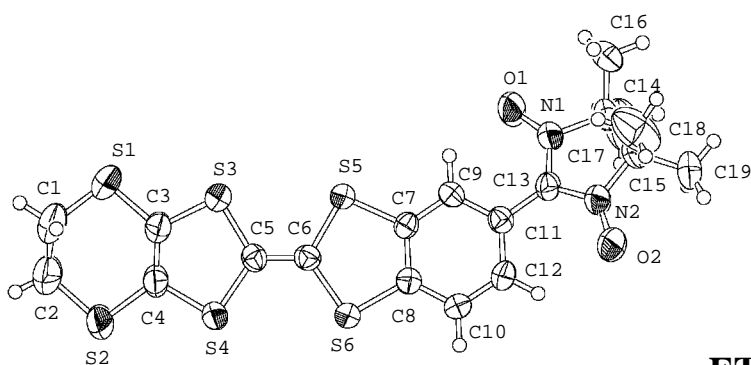
ETBN

Atomic coordinates and Biso/Beq

atom	x	y	z	Beq	atom	x	y	z	Beq
S(1)	-0.03609(9)	0.35283(7)	-0.3636(3)	8.89(7)	H(1)	-0.0879	0.2999	-0.3808	12.8395
S(2)	-0.07300(8)	0.33857(6)	0.1350(3)	8.32(6)	H(2)	-0.0954	0.3298	-0.3068	12.8395
S(3)	-0.00084(5)	0.42827(5)	-0.2509(2)	4.44(4)	H(3)	-0.1084	0.2888	-0.0543	10.8334
S(4)	-0.02944(5)	0.41656(4)	0.1780(2)	4.20(4)	H(4)	-0.0692	0.2967	-0.0581	10.8334
S(5)	0.05745(5)	0.50664(5)	-0.1498(2)	4.70(4)	H(5)	0.1177	0.5764	-0.2048	4.1293
S(6)	0.03147(5)	0.50048(4)	0.2862(2)	4.17(4)	H(6)	0.0749	0.5695	0.4832	4.4779
O(1)	0.1750(2)	0.6112(1)	-0.2729(9)	7.3(2)	H(7)	0.1238	0.6229	0.3621	4.7443
O(2)	0.1567(2)	0.6794(1)	0.2100(9)	7.5(2)	H(8)	0.2404	0.7039	-0.4358	10.6111
N(1)	0.1777(2)	0.6375(1)	-0.1681(8)	4.7(1)	H(9)	0.2005	0.6803	-0.4967	10.6111
N(2)	0.1694(2)	0.6698(1)	0.0610(9)	5.0(1)	H(10)	0.2247	0.6634	-0.4765	10.6111
C(1)	-0.0793(3)	0.3197(3)	-0.284(2)	10.0(3)	H(11)	0.2623	0.6927	-0.0754	11.2249
C(2)	-0.0845(3)	0.3081(2)	-0.075(1)	8.2(3)	H(12)	0.2337	0.6651	0.0757	11.2249
C(3)	-0.0281(2)	0.3844(2)	-0.172(1)	5.2(2)	H(13)	0.2438	0.6522	-0.1263	11.2249
C(4)	-0.0419(2)	0.3789(2)	0.0204(10)	4.8(2)	H(14)	0.1677	0.7198	-0.1527	11.7748
C(5)	0.0021(2)	0.4460(2)	-0.0010(9)	3.6(1)	H(15)	0.1958	0.7265	-0.3243	11.7748
C(6)	0.0267(2)	0.4798(2)	0.0426(8)	3.6(1)	H(16)	0.1613	0.6895	-0.3078	11.7748
C(7)	0.0806(2)	0.5444(2)	0.0093(8)	3.3(1)	H(17)	0.2455	0.7433	-0.0320	10.4872
C(8)	0.0681(2)	0.5418(2)	0.2119(8)	3.3(1)	H(18)	0.2171	0.7377	0.1353	10.4872
C(9)	0.1092(2)	0.5750(2)	-0.0634(8)	3.4(1)	H(19)	0.2371	0.7163	0.1493	10.4872
C(10)	0.0839(2)	0.5711(2)	0.3428(9)	3.7(1)					
C(11)	0.1255(2)	0.6044(2)	0.0684(9)	3.4(1)					
C(12)	0.1127(2)	0.6023(2)	0.2702(9)	3.9(1)					
C(13)	0.1565(2)	0.6362(2)	-0.0111(9)	3.8(1)					
C(14)	0.2101(2)	0.6735(2)	-0.194(1)	5.5(2)					
C(15)	0.1989(2)	0.6967(2)	-0.077(1)	5.7(2)					
C(16)	0.2200(3)	0.6808(2)	-0.418(1)	9.1(3)					
C(17)	0.2396(3)	0.6712(3)	-0.076(2)	9.8(3)					
C(18)	0.1807(3)	0.7104(3)	-0.225(2)	10.6(4)					
C(19)	0.2264(3)	0.7262(2)	0.052(1)	8.8(3)					

Anisotropic Displacement Parameters

atom	U11	U22	U33	U12	U13	U23
S(1)	0.148(3)	0.067(1)	0.074(1)	0.017(2)	0.010(1)	-0.027(1)
S(2)	0.135(2)	0.051(1)	0.065(1)	-0.002(1)	0.000(1)	0.0041(9)
S(3)	0.058(1)	0.0507(10)	0.0487(9)	0.0185(8)	-0.0010(7)	-0.0055(7)
S(4)	0.053(1)	0.0425(9)	0.0568(9)	0.0188(8)	0.0077(7)	0.0002(7)
S(5)	0.056(1)	0.051(1)	0.0450(8)	0.0066(8)	0.0072(7)	-0.0080(7)
S(6)	0.053(1)	0.0470(9)	0.0445(8)	0.0145(8)	0.0060(7)	-0.0024(6)
O(1)	0.089(4)	0.049(3)	0.117(4)	0.016(3)	0.045(3)	-0.018(3)
O(2)	0.116(5)	0.048(3)	0.102(4)	0.027(3)	0.035(4)	-0.018(3)
N(1)	0.061(4)	0.043(3)	0.063(3)	0.016(3)	0.014(3)	-0.002(3)
N(2)	0.071(4)	0.040(3)	0.070(4)	0.021(3)	0.015(3)	-0.003(3)
C(1)	0.17(1)	0.059(6)	0.097(7)	0.018(7)	0.002(7)	-0.026(5)
C(2)	0.132(9)	0.055(5)	0.094(7)	0.022(6)	-0.003(6)	-0.012(4)
C(3)	0.072(5)	0.050(4)	0.055(4)	0.016(4)	-0.007(3)	-0.005(3)
C(4)	0.068(5)	0.041(4)	0.058(4)	0.015(3)	-0.012(3)	0.001(3)
C(5)	0.039(3)	0.044(4)	0.049(3)	0.017(3)	-0.003(3)	0.002(3)
C(6)	0.041(3)	0.050(4)	0.043(3)	0.021(3)	0.002(2)	0.001(3)
C(7)	0.039(3)	0.043(3)	0.042(3)	0.020(3)	-0.006(2)	-0.005(2)
C(8)	0.044(3)	0.041(3)	0.043(3)	0.023(3)	-0.003(2)	0.002(2)
C(9)	0.039(3)	0.044(3)	0.045(3)	0.020(3)	0.003(2)	0.004(3)
C(10)	0.051(4)	0.050(4)	0.042(3)	0.026(3)	0.002(3)	-0.003(3)
C(11)	0.045(4)	0.038(3)	0.049(3)	0.023(3)	0.002(3)	0.003(2)
C(12)	0.054(4)	0.040(4)	0.055(3)	0.023(3)	-0.004(3)	-0.009(3)
C(13)	0.055(4)	0.037(3)	0.053(3)	0.023(3)	0.000(3)	-0.002(3)
C(14)	0.061(5)	0.042(4)	0.079(5)	0.006(4)	0.015(4)	-0.007(3)
C(15)	0.092(6)	0.036(4)	0.071(5)	0.018(4)	0.017(4)	0.009(3)
C(16)	0.128(9)	0.065(6)	0.094(6)	0.005(6)	0.056(6)	0.005(5)
C(17)	0.062(6)	0.097(8)	0.20(1)	0.030(6)	-0.001(7)	-0.007(7)
C(18)	0.14(1)	0.113(9)	0.17(1)	0.079(8)	0.052(8)	0.072(8)
C(19)	0.106(8)	0.052(5)	0.113(7)	-0.009(5)	0.025(6)	-0.022(5)

Bond Lengths(Å)

atom - atom	distance	atom - atom	distance	atom - atom	distance
S(1)- C(1)	1.77(1)	S(1)- C(3)	1.735(7)	S(2)- C(2)	1.766(9)
S(2)- C(4)	1.743(7)	S(3)- C(3)	1.731(7)	S(3)- C(5)	1.747(6)
S(4)- C(4)	1.753(7)	S(4)- C(5)	1.746(6)	S(5)- C(6)	1.755(6)
S(5)- C(7)	1.749(6)	S(6)- C(6)	1.753(6)	S(6)- C(8)	1.759(6)
O(1)- N(1)	1.273(7)	O(2)- N(2)	1.270(7)	N(1)- C(13)	1.338(8)
N(1)- C(14)	1.493(8)	N(2)- C(13)	1.348(8)	N(2)- C(15)	1.506(9)
C(1)- C(2)	1.41(1)	C(3)- C(4)	1.332(9)	C(5)- C(6)	1.336(8)
C(7)- C(8)	1.383(7)	C(7)- C(9)	1.364(8)	C(8)- C(10)	1.378(8)
C(9)- C(11)	1.386(8)	C(10)- C(12)	1.380(9)	C(11)- C(12)	1.387(8)
C(11)- C(13)	1.451(8)	C(14)- C(15)	1.51(1)	C(14)- C(16)	1.48(1)
C(14)- C(17)	1.53(1)	C(15)- C(18)	1.52(1)	C(15)- C(19)	1.48(1)

Bond Angles(°)

atom - atom - atom	angle	atom - atom - atom	angle	atom - atom - atom	angle
C(1)- S(1)- C(3)	98.6(4)	C(2)- S(2)- C(4)	102.5(4)	C(3)- S(3)- C(5)	94.3(3)
C(4)- S(4)- C(5)	93.9(3)	C(6)- S(5)- C(7)	95.8(3)	C(6)- S(6)- C(8)	95.5(3)
O(1)- N(1)- C(13)	126.9(5)	O(1)- N(1)- C(14)	119.3(5)	C(13)- N(1)- C(14)	113.2(5)
O(2)- N(2)- C(13)	126.5(6)	O(2)- N(2)- C(15)	121.5(6)	C(13)- N(2)- C(15)	111.5(5)
S(1)- C(1)- C(2)	118.5(9)	S(2)- C(2)- C(1)	121.3(7)	S(1)- C(3)- S(3)	114.5(4)
S(1)- C(3)- C(4)	127.8(5)	S(3)- C(3)- C(4)	117.6(5)	S(2)- C(4)- S(4)	114.4(4)
S(2)- C(4)- C(3)	128.2(5)	S(4)- C(4)- C(3)	117.3(5)	S(3)- C(5)- S(4)	114.7(3)
S(3)- C(5)- C(6)	120.9(5)	S(4)- C(5)- C(6)	124.4(5)	S(5)- C(6)- S(6)	115.2(3)
S(5)- C(6)- C(5)	120.2(4)	S(6)- C(6)- C(5)	124.6(5)	S(5)- C(7)- C(8)	116.8(4)
S(5)- C(7)- C(9)	121.7(4)	S(6)- C(8)- C(7)	116.7(4)	C(7)- C(8)- C(10)	119.9(5)
S(6)- C(8)- C(10)	123.3(4)	C(7)- C(9)- C(11)	118.8(5)	C(8)- C(10)- C(12)	119.0(5)
C(9)- C(11)- C(12)	120.0(5)	C(9)- C(11)- C(13)	117.6(5)	C(12)- C(11)- C(13)	122.4(5)
C(10)- C(12)- C(11)	120.7(5)	N(1)- C(13)- N(2)	107.7(5)	N(1)- C(13)- C(11)	126.1(5)
N(2)- C(13)- C(11)	126.2(6)	N(1)- C(14)- C(15)	100.9(6)	N(1)- C(14)- C(16)	110.5(6)
N(1)- C(14)- C(17)	105.1(7)	C(15)- C(14)- C(16)	119.1(7)	C(15)- C(14)- C(17)	110.8(7)
C(16)- C(14)- C(17)	109.3(8)	N(2)- C(15)- C(14)	101.7(5)	N(2)- C(15)- C(18)	105.1(7)
N(2)- C(15)- C(19)	110.2(6)	C(14)- C(15)- C(18)	110.6(7)	C(14)- C(15)- C(19)	117.2(8)
C(18)- C(15)- C(19)	110.9(9)				

ETTN • pyridine
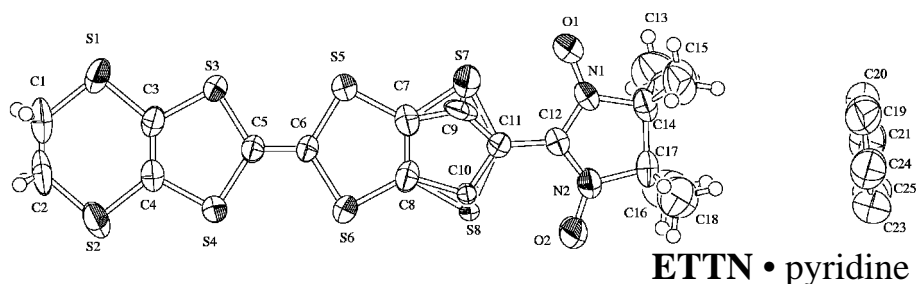
Atomic coordinates and Biso/Beq

atom	x	y	z	Beq	occ
S(1)	0.7092(2)	−0.1150(2)	1.0931(2)	5.74(4)	
S(2)	0.4444(1)	−0.1680(2)	0.7755(2)	6.24(4)	
S(3)	0.8170(1)	−0.0237(2)	0.9173(2)	5.99(4)	
S(4)	0.5946(1)	−0.0661(1)	0.6521(2)	5.39(3)	
S(5)	0.9636(1)	0.0739(1)	0.7503(2)	4.54(3)	
S(6)	0.7412(1)	0.0323(1)	0.4810(1)	4.57(3)	
S(7)	1.1017(4)	0.2130(3)	0.6404(5)	5.39(9)	0.5
S(8)	0.8646(4)	0.1753(6)	0.3545(6)	2.83(8)	0.5
O(1)	1.2706(4)	0.3225(6)	0.5974(7)	9.1(2)	
O(2)	0.9264(4)	0.3159(6)	0.2288(7)	10.1(2)	
N(1)	1.1988(4)	0.3436(4)	0.4876(6)	5.2(1)	
N(2)	1.0355(4)	0.3406(4)	0.3121(6)	4.9(1)	
C(1)	0.5690(9)	−0.194(1)	1.051(1)	12.4(4)	
C(2)	0.473(1)	−0.206(1)	0.940(1)	16.9(5)	
C(3)	0.6862(5)	−0.0832(4)	0.9247(5)	3.8(1)	
C(4)	0.5869(4)	−0.1032(4)	0.8055(6)	3.9(1)	
C(5)	0.7481(4)	−0.0150(4)	0.7359(5)	3.9(1)	
C(6)	0.8099(4)	0.0262(4)	0.6651(5)	3.42(10)	
C(7)	0.9683(4)	0.1339(4)	0.6158(6)	4.0(1)	
C(8)	0.8654(5)	0.1160(4)	0.4930(6)	4.1(1)	
C(9)	1.0424(9)	0.197(1)	0.584(1)	4.5(3)	0.5
C(10)	0.895(1)	0.175(2)	0.394(2)	2.4(3)	0.5
C(11)	1.0177(4)	0.2308(4)	0.4703(5)	3.40(10)	
C(12)	1.0825(4)	0.3027(4)	0.4230(5)	3.54(10)	
C(13)	1.2830(9)	0.5381(7)	0.554(1)	10.5(3)	
C(14)	1.2384(5)	0.4234(5)	0.4227(6)	4.6(1)	
C(15)	1.3381(7)	0.3825(9)	0.367(1)	9.0(3)	
C(16)	1.0809(8)	0.5237(7)	0.297(1)	10.4(3)	
C(17)	1.1214(5)	0.4138(4)	0.2883(7)	4.6(1)	
C(18)	1.1213(8)	0.3519(10)	0.1249(9)	10.2(3)	
C(19)	0.7363(8)	0.3198(9)	−0.087(1)	8.5(3)	
C(20)	0.7394(7)	0.4207(8)	0.0242(10)	7.5(2)	
C(21)	0.6539(8)	0.4835(7)	−0.012(1)	7.9(2)	
C(23)	0.5662(7)	0.3475(9)	−0.256(1)	8.5(2)	
C(24)	0.6504(8)	0.2805(7)	−0.231(1)	7.8(2)	
C(25)	0.5705(7)	0.4486(8)	−0.147(1)	7.4(2)	
H(1)	0.5803	−0.2704	1.0324	14.8648	
H(2)	0.5509	−0.1638	1.1430	14.8648	
H(3)	0.4246	−0.1635	0.9937	20.0460	
H(4)	0.4396	−0.2839	0.8969	20.0460	
H(5)	1.3463	0.5337	0.6369	12.3952	
H(6)	1.3085	0.5921	0.5177	12.3952	
H(7)	1.2199	0.5614	0.5906	12.3952	
H(8)	1.3092	0.3078	0.2877	10.7694	
H(9)	1.3625	0.4328	0.3238	10.7694	
H(10)	1.4017	0.3819	0.4514	10.7694	
H(11)	1.0807	0.5640	0.3986	12.5302	
H(12)	1.1343	0.5686	0.2745	12.5302	
H(13)	1.0041	0.5085	0.2219	12.5302	
H(14)	1.0443	0.3416	0.0508	12.1442	
H(15)	1.1768	0.3957	0.1047	12.1442	
H(16)	1.1424	0.2794	0.1146	12.1442	

Anisotropic Displacement Parameters

atom	U11	U22	U33	U12	U13	U23
S(1)	0.082(1)	0.099(1)	0.0643(9)	0.0168(9)	0.0375(8)	0.0525(9)
S(2)	0.0532(8)	0.090(1)	0.105(1)	−0.0027(8)	0.0331(8)	0.050(1)
S(3)	0.0547(8)	0.118(1)	0.0556(8)	−0.0201(8)	0.0020(6)	0.0557(9)
S(4)	0.0478(7)	0.101(1)	0.0541(8)	−0.0138(7)	0.0067(6)	0.0429(8)
S(5)	0.0442(7)	0.0757(9)	0.0570(7)	0.0005(6)	0.0137(6)	0.0364(7)
S(6)	0.0529(7)	0.0832(10)	0.0467(7)	0.0038(6)	0.0172(6)	0.0374(7)
S(7)	0.062(2)	0.082(2)	0.077(2)	0.012(2)	0.028(2)	0.049(2)
S(8)	0.022(2)	0.051(2)	0.038(2)	0.001(2)	0.003(1)	0.030(2)
O(1)	0.048(2)	0.188(6)	0.124(4)	−0.016(3)	0.000(3)	0.111(4)
O(2)	0.060(3)	0.196(6)	0.168(5)	−0.007(3)	0.006(3)	0.156(5)
N(1)	0.038(2)	0.087(3)	0.077(3)	−0.006(2)	0.015(2)	0.046(3)
N(2)	0.048(2)	0.074(3)	0.079(3)	0.003(2)	0.020(2)	0.049(3)
C(1)	0.107(7)	0.23(1)	0.18(1)	−0.035(8)	0.042(7)	0.16(1)

atom	U11	U22	U33	U12	U13	U23
C(2)	0.131(9)	0.36(2)	0.154(10)	-0.12(1)	0.010(7)	0.17(1)
C(3)	0.063(3)	0.045(3)	0.043(2)	0.004(2)	0.024(2)	0.021(2)
C(4)	0.054(3)	0.045(3)	0.054(3)	0.004(2)	0.028(2)	0.020(2)
C(5)	0.052(3)	0.057(3)	0.040(2)	-0.004(2)	0.014(2)	0.022(2)
C(6)	0.046(2)	0.051(3)	0.039(2)	0.004(2)	0.017(2)	0.023(2)
C(7)	0.049(3)	0.051(3)	0.062(3)	0.007(2)	0.027(2)	0.025(2)
C(8)	0.060(3)	0.058(3)	0.054(3)	0.016(2)	0.031(2)	0.033(2)
C(9)	0.022(5)	0.074(8)	0.057(7)	0.003(5)	-0.002(5)	0.020(6)
C(10)	0.022(9)	0.038(6)	0.04(1)	0.010(7)	0.012(7)	0.027(8)
C(11)	0.041(2)	0.051(3)	0.044(2)	0.009(2)	0.015(2)	0.025(2)
C(12)	0.041(2)	0.044(3)	0.051(3)	0.003(2)	0.019(2)	0.019(2)
C(13)	0.146(9)	0.071(5)	0.120(7)	-0.029(5)	0.010(6)	0.006(5)
C(14)	0.056(3)	0.056(3)	0.067(3)	-0.004(2)	0.029(3)	0.023(3)
C(15)	0.088(5)	0.161(8)	0.147(8)	0.043(5)	0.077(6)	0.087(7)
C(16)	0.117(7)	0.074(5)	0.179(10)	0.014(5)	-0.003(6)	0.071(6)
C(17)	0.070(3)	0.050(3)	0.074(3)	0.005(2)	0.039(3)	0.032(3)
C(18)	0.108(7)	0.20(1)	0.070(5)	0.000(7)	0.041(5)	0.034(6)
C(19)	0.089(6)	0.131(8)	0.137(8)	0.034(5)	0.040(6)	0.090(7)
C(20)	0.082(5)	0.118(6)	0.092(5)	0.003(5)	0.023(4)	0.057(5)
C(21)	0.113(7)	0.098(6)	0.095(6)	0.017(5)	0.046(5)	0.038(5)
C(23)	0.073(5)	0.144(8)	0.099(6)	0.002(5)	0.013(4)	0.059(6)
C(24)	0.102(6)	0.108(6)	0.100(6)	0.021(5)	0.042(5)	0.051(5)
C(25)	0.078(5)	0.121(7)	0.097(6)	0.037(5)	0.031(4)	0.054(5)

Bond Lengths(Å)

atom - atom	distance	atom - atom	distance	atom - atom	distance
S(1)-C(1)	1.766(9)	S(1)-C(3)	1.763(4)	S(2)-C(2)	1.763(10)
S(2)-C(4)	1.755(5)	S(3)-C(3)	1.742(5)	S(3)-C(5)	1.747(5)
S(4)-C(4)	1.737(5)	S(4)-C(5)	1.755(5)	S(5)-C(6)	1.750(5)
S(5)-C(7)	1.738(5)	S(6)-C(6)	1.755(4)	S(6)-C(8)	1.734(5)
S(7)-C(7)	1.750(6)	S(7)-C(9)	0.721(9)	S(7)-C(11)	1.750(5)
S(8)-C(8)	1.752(7)	S(8)-C(10)	0.44(1)	S(8)-C(11)	1.786(6)
O(1)-N(1)	1.271(6)	O(2)-N(2)	1.267(6)	N(1)-C(12)	1.334(6)
N(1)-C(14)	1.490(6)	N(2)-C(12)	1.314(6)	N(2)-C(17)	1.474(6)
C(1)-C(2)	1.28(1)	C(3)-C(4)	1.321(7)	C(5)-C(6)	1.351(6)
C(7)-C(8)	1.372(7)	C(7)-C(9)	1.35(1)	C(8)-C(10)	1.52(2)
C(9)-C(11)	1.27(1)	C(10)-C(11)	1.44(2)	C(11)-C(12)	1.444(6)
C(13)-C(14)	1.497(9)	C(14)-C(15)	1.515(9)	C(14)-C(17)	1.564(8)
C(16)-C(17)	1.491(9)	C(17)-C(18)	1.509(9)	C(19)-C(20)	1.35(1)
C(19)-C(24)	1.36(1)	C(20)-C(21)	1.38(1)	C(21)-C(25)	1.29(1)
C(23)-C(24)	1.38(1)	C(23)-C(25)	1.34(1)		

Bond Angles(°)

atom - atom - atom	angle	atom - atom - atom	angle	atom - atom - atom	angle
C(1)-S(1)-C(3)	101.9(4)	C(2)-S(2)-C(4)	101.1(4)	C(3)-S(3)-C(5)	94.3(2)
C(4)-S(4)-C(5)	94.5(2)	C(6)-S(5)-C(7)	93.5(2)	C(6)-S(6)-C(8)	93.5(2)
C(7)-S(7)-C(9)	45(1)	C(7)-S(7)-C(11)	84.2(3)	C(9)-S(7)-C(11)	38(1)
C(8)-S(8)-C(10)	51(3)	C(8)-S(8)-C(11)	84.9(3)	C(10)-S(8)-C(11)	33(3)
O(1)-N(1)-C(12)	125.4(4)	O(1)-N(1)-C(14)	121.7(4)	C(12)-N(1)-C(14)	112.9(4)
O(2)-N(2)-C(12)	124.1(4)	O(2)-N(2)-C(17)	121.5(4)	C(12)-N(2)-C(17)	114.4(4)
S(1)-C(1)-C(2)	127.4(6)	S(2)-C(2)-C(1)	131.3(6)	S(1)-C(3)-S(3)	112.7(3)
S(1)-C(3)-C(4)	129.0(4)	S(3)-C(3)-C(4)	118.2(3)	S(2)-C(4)-S(4)	113.6(3)
S(2)-C(4)-C(3)	128.6(4)	S(4)-C(4)-C(3)	117.8(4)	S(3)-C(5)-S(4)	115.1(3)
S(3)-C(5)-C(6)	121.9(4)	S(4)-C(5)-C(6)	123.0(4)	S(5)-C(6)-S(6)	116.3(2)
S(5)-C(6)-C(5)	121.7(4)	S(6)-C(6)-C(5)	121.9(4)	S(5)-C(7)-S(7)	119.6(3)
S(5)-C(7)-C(8)	117.6(4)	S(5)-C(7)-C(9)	142.1(6)	S(7)-C(7)-C(8)	122.8(4)
S(7)-C(7)-C(9)	22.5(5)	C(8)-C(7)-C(9)	100.3(6)	S(6)-C(8)-S(8)	122.9(3)
S(6)-C(8)-C(7)	117.5(3)	S(6)-C(8)-C(10)	136.1(7)	S(8)-C(8)-C(7)	119.6(4)
S(8)-C(8)-C(10)	13.3(6)	C(7)-C(8)-C(10)	106.4(7)	S(7)-C(9)-C(8)	112(1)
S(7)-C(9)-C(11)	120(1)	C(7)-C(9)-C(11)	127.4(9)	S(8)-C(10)-C(8)	114(3)
S(8)-C(10)-C(11)	136(4)	C(8)-C(10)-C(11)	107.8(9)	S(7)-C(11)-S(8)	128.6(3)
S(7)-C(11)-C(9)	20.8(5)	S(8)-C(11)-C(9)	107.7(6)	S(8)-C(11)-C(10)	9.9(8)
S(8)-C(11)-C(12)	117.3(4)	C(9)-C(11)-C(12)	98.0(9)	C(9)-C(11)-C(10)	134.9(6)
C(10)-C(11)-C(12)	127.1(8)	N(1)-C(12)-N(2)	109.3(4)	N(1)-C(12)-C(11)	125.3(4)
N(2)-C(12)-C(11)	125.3(4)	N(1)-C(14)-C(13)	106.6(6)	N(1)-C(14)-C(15)	108.7(5)
N(1)-C(14)-C(17)	101.5(4)	C(13)-C(14)-C(15)	109.9(7)	C(13)-C(14)-C(17)	115.1(6)
C(15)-C(14)-C(17)	114.3(5)	N(2)-C(17)-C(14)	101.5(4)	N(2)-C(17)-C(16)	109.4(6)
N(2)-C(17)-C(18)	106.8(6)	C(14)-C(17)-C(16)	115.4(5)	C(14)-C(17)-C(18)	114.8(6)
C(16)-C(17)-C(18)	108.3(7)	C(20)-C(19)-C(24)	120.9(8)	C(19)-C(20)-C(21)	118.6(8)
C(20)-C(21)-C(25)	122.2(8)	C(24)-C(23)-C(25)	122.2(8)	C(19)-C(24)-C(23)	116.9(8)
C(21)-C(25)-C(23)	119.2(8)				

EPPN
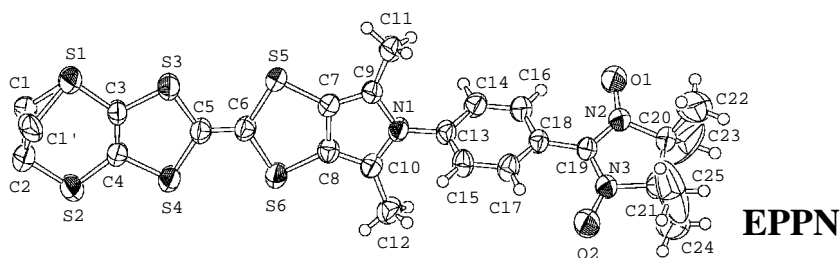
Atomic coordinates and Biso/Beq

atom	x	y	z	Beq	occ
S(1)	0.4122(1)	-0.3693(2)	0.54847(6)	8.18(7)	
S(2)	0.2804(1)	-0.5255(2)	0.48442(6)	6.77(6)	
S(3)	0.41281(10)	-0.1191(2)	0.48819(6)	5.94(5)	
S(4)	0.30270(10)	-0.2566(2)	0.43334(5)	6.29(5)	
S(5)	0.40378(9)	0.1957(2)	0.43476(5)	4.81(4)	
S(6)	0.29760(9)	0.0444(2)	0.37679(5)	5.49(5)	
O(1)	0.4111(3)	1.1029(5)	0.2445(1)	8.2(2)	
O(2)	0.3930(3)	0.7009(6)	0.1522(1)	9.0(2)	
N(1)	0.3661(2)	0.4349(6)	0.3331(1)	3.9(1)	
N(2)	0.4069(3)	1.0249(6)	0.2111(2)	4.8(1)	
N(3)	0.4000(3)	0.8361(6)	0.1682(2)	4.8(1)	
C(1)	0.358(1)	-0.518(2)	0.5603(5)	6.0(6)	0.4
C(1')	0.3958(7)	-0.578(1)	0.5364(4)	6.3(4)	0.6
C(2)	0.3244(4)	-0.6168(8)	0.5284(2)	7.2(2)	
C(3)	0.3765(3)	-0.2932(7)	0.5027(2)	4.4(2)	
C(4)	0.3265(3)	-0.3572(7)	0.4782(2)	4.1(2)	
C(5)	0.3554(3)	-0.0951(7)	0.4443(2)	4.3(2)	
C(6)	0.3539(3)	0.0320(7)	0.4218(2)	4.2(2)	
C(7)	0.3804(3)	0.2918(7)	0.3888(2)	3.6(1)	
C(8)	0.3331(3)	0.2175(7)	0.3615(2)	3.7(1)	
C(9)	0.4014(3)	0.4267(7)	0.3722(2)	3.7(2)	
C(10)	0.3244(3)	0.3046(7)	0.3271(2)	4.0(2)	
C(11)	0.4532(3)	0.5444(7)	0.3867(2)	5.5(2)	
C(12)	0.2780(3)	0.2785(8)	0.2895(2)	5.6(2)	
C(13)	0.3783(3)	0.5472(7)	0.3030(2)	3.7(2)	
C(14)	0.3643(3)	0.6998(7)	0.3097(2)	4.4(2)	
C(15)	0.4035(3)	0.5017(7)	0.2665(2)	4.3(2)	
C(16)	0.3744(3)	0.8084(7)	0.2793(2)	4.4(2)	
C(17)	0.4130(3)	0.6081(7)	0.2361(2)	4.4(2)	
C(18)	0.3975(3)	0.7611(7)	0.2417(2)	3.4(1)	
C(19)	0.4026(3)	0.8714(7)	0.2083(2)	3.6(2)	
C(20)	0.4061(4)	1.1071(8)	0.1704(2)	5.2(2)	
C(21)	0.4047(4)	0.9724(8)	0.1404(2)	5.5(2)	
C(22)	0.4655(6)	1.215(1)	0.1706(2)	14.1(4)	
C(23)	0.3392(6)	1.201(1)	0.1678(2)	15.0(4)	
C(24)	0.3440(7)	0.9675(10)	0.1106(3)	16.0(4)	
C(25)	0.4687(7)	0.954(1)	0.1191(4)	18.1(5)	
H(1)	0.4293	0.6418	0.3880	6.6522	
H(2)	0.4691	0.5168	0.4140	6.6522	
H(3)	0.4889	0.5493	0.3696	6.6522	
H(4)	0.2454	0.3611	0.2866	6.3688	
H(5)	0.3060	0.2789	0.2662	6.3688	
H(6)	0.2553	0.1841	0.2915	6.3688	
H(7)	0.3472	0.7325	0.3350	5.2529	
H(8)	0.4142	0.3961	0.2618	5.2349	
H(9)	0.3653	0.9139	0.2841	5.3425	
H(10)	0.4296	0.5736	0.2104	5.1864	
H(11)	0.5058	1.1642	0.1755	16.7023	
H(12)	0.4575	1.2895	0.1923	16.7023	
H(13)	0.4620	1.2693	0.1454	16.7023	
H(14)	0.3399	1.2716	0.1901	15.7415	
H(15)	0.3003	1.1336	0.1694	15.7415	
H(16)	0.3356	1.2555	0.1428	15.7415	
H(17)	0.3437	0.8748	0.0956	16.6890	
H(18)	0.3017	0.9749	0.1247	16.6890	
H(19)	0.3457	1.0534	0.0924	16.6890	
H(20)	0.4708	1.0387	0.0999	19.8970	
H(21)	0.5066	0.9485	0.1364	19.8970	
H(22)	0.4629	0.8608	0.1024	19.8970	

Anisotropic Displacement Parameters

atom	U11	U22	U33	U12	U13	U23
S(1)	0.144(2)	0.073(1)	0.086(1)	-0.023(1)	-0.058(1)	0.031(1)
S(2)	0.101(2)	0.064(1)	0.088(1)	-0.030(1)	-0.028(1)	0.021(1)
S(3)	0.079(1)	0.071(1)	0.073(1)	-0.025(1)	-0.024(1)	0.026(1)
S(4)	0.092(2)	0.079(1)	0.065(1)	-0.029(1)	-0.026(1)	0.028(1)
S(5)	0.080(1)	0.057(1)	0.0445(10)	-0.007(1)	-0.0082(9)	0.0111(9)
S(6)	0.079(1)	0.072(1)	0.055(1)	-0.024(1)	-0.0109(9)	0.019(1)
O(1)	0.185(6)	0.061(3)	0.062(3)	-0.009(4)	-0.005(4)	-0.001(3)

108

atom	U11	U22	U33	U12	U13	U23
O(2)	0.214(7)	0.060(4)	0.067(4)	-0.004(4)	0.008(4)	-0.003(3)
N(1)	0.051(3)	0.052(3)	0.046(3)	-0.004(3)	-0.005(3)	0.011(3)
N(2)	0.088(4)	0.046(4)	0.049(3)	-0.002(3)	-0.004(3)	-0.002(3)
N(3)	0.093(5)	0.036(3)	0.052(4)	0.003(3)	0.002(3)	0.000(3)
C(1)	0.12(2)	0.06(1)	0.05(1)	-0.05(1)	-0.02(1)	0.018(10)
C(1')	0.09(1)	0.035(8)	0.10(1)	-0.001(7)	-0.038(9)	0.018(7)
C(2)	0.125(7)	0.083(6)	0.062(5)	-0.025(5)	-0.032(5)	0.032(4)
C(3)	0.064(5)	0.048(4)	0.055(4)	-0.010(4)	-0.008(3)	0.018(3)
C(4)	0.056(4)	0.051(4)	0.047(4)	-0.004(3)	0.000(3)	0.009(3)
C(5)	0.052(4)	0.061(4)	0.050(4)	-0.008(4)	-0.001(3)	0.015(3)
C(6)	0.053(4)	0.060(4)	0.045(4)	-0.005(4)	0.005(3)	0.014(4)
C(7)	0.052(4)	0.048(4)	0.038(3)	0.003(3)	0.004(3)	0.005(3)
C(8)	0.042(4)	0.051(4)	0.047(4)	-0.003(3)	0.004(3)	0.006(3)
C(9)	0.051(4)	0.044(4)	0.046(4)	0.005(3)	-0.002(3)	0.004(3)
C(10)	0.046(4)	0.060(4)	0.045(4)	-0.003(4)	-0.001(3)	0.007(3)
C(11)	0.080(5)	0.060(5)	0.067(4)	-0.007(4)	-0.025(4)	0.015(4)
C(12)	0.058(4)	0.090(6)	0.063(4)	-0.009(4)	-0.009(3)	0.017(4)
C(13)	0.046(4)	0.046(4)	0.046(4)	0.006(3)	-0.005(3)	0.013(3)
C(14)	0.068(5)	0.052(4)	0.045(4)	0.006(4)	0.000(3)	0.005(3)
C(15)	0.060(4)	0.041(4)	0.061(4)	0.012(3)	0.004(3)	0.009(3)
C(16)	0.063(5)	0.046(4)	0.055(4)	0.008(4)	-0.005(3)	0.004(3)
C(17)	0.063(5)	0.049(4)	0.054(4)	0.016(4)	0.007(3)	0.008(3)
C(18)	0.041(4)	0.044(4)	0.046(4)	0.000(3)	-0.001(3)	0.011(3)
C(19)	0.048(4)	0.042(4)	0.047(4)	0.004(3)	-0.003(3)	0.000(3)
C(20)	0.094(6)	0.056(5)	0.045(4)	-0.003(4)	-0.005(4)	0.014(4)
C(21)	0.105(6)	0.046(4)	0.057(4)	0.008(4)	0.007(4)	0.015(4)
C(22)	0.25(1)	0.20(1)	0.090(7)	-0.17(1)	0.014(7)	0.003(7)
C(23)	0.28(1)	0.20(1)	0.090(7)	0.18(1)	-0.019(8)	0.016(7)
C(24)	0.34(2)	0.080(7)	0.164(9)	-0.004(9)	-0.17(1)	0.019(7)
C(25)	0.32(2)	0.092(8)	0.30(1)	0.054(9)	0.27(1)	0.062(9)

Bond Lengths(Å)

atom - atom	distance	atom - atom	distance	atom - atom	distance
S(1) - C(1)	1.72(2)	S(1) - C(1')	1.87(1)	S(1) - C(3)	1.740(6)
S(2) - C(2)	1.808(6)	S(2) - C(4)	1.725(6)	S(3) - C(3)	1.740(6)
S(3) - C(5)	1.772(6)	S(4) - C(4)	1.745(6)	S(4) - C(5)	1.753(6)
S(5) - C(6)	1.750(6)	S(5) - C(7)	1.752(5)	S(6) - C(6)	1.779(6)
S(6) - C(8)	1.734(6)	O(1) - N(2)	1.284(6)	O(2) - N(3)	1.286(6)
N(1) - C(9)	1.412(6)	N(1) - C(10)	1.393(7)	N(1) - C(13)	1.415(6)
N(2) - C(19)	1.334(7)	N(2) - C(20)	1.509(7)	N(3) - C(19)	1.346(7)
N(3) - C(21)	1.496(7)	C(2) - C(1)	1.47(2)	C(1') - C(2)	1.42(1)
C(3) - C(4)	1.335(7)	C(5) - C(6)	1.323(7)	C(7) - C(8)	1.394(7)
C(7) - C(9)	1.361(7)	C(8) - C(10)	1.358(7)	C(9) - C(11)	1.484(8)
C(10) - C(12)	1.492(7)	C(13) - C(14)	1.369(7)	C(13) - C(15)	1.372(7)
C(14) - C(16)	1.391(7)	C(15) - C(17)	1.376(7)	C(16) - C(18)	1.393(7)
C(17) - C(18)	1.373(7)	C(18) - C(19)	1.460(7)	C(20) - C(21)	1.523(8)
C(20) - C(22)	1.479(9)	C(20) - C(23)	1.523(10)	C(21) - C(24)	1.477(10)
C(21) - C(25)	1.46(1)				

Bond Angles(°)

atom - atom - atom	angle	atom - atom - atom	angle	atom - atom - atom	angle
C(1) - S(1) - C(3)	105.3(6)	C(1') - S(1) - C(3)	97.6(4)	C(2) - S(2) - C(4)	104.1(3)
C(3) - S(3) - C(5)	94.7(3)	C(4) - S(4) - C(5)	96.2(3)	C(6) - S(5) - C(7)	93.9(3)
C(6) - S(6) - C(8)	93.4(3)	C(9) - N(1) - C(10)	109.3(5)	C(9) - N(1) - C(13)	125.1(5)
C(10) - N(1) - C(13)	125.1(5)	O(1) - N(2) - C(19)	125.6(6)	O(1) - N(2) - C(20)	120.0(5)
C(19) - N(2) - C(20)	114.4(5)	O(2) - N(3) - C(19)	126.9(5)	O(2) - N(3) - C(21)	118.7(5)
C(19) - N(3) - C(21)	114.4(5)	S(1) - C(1) - C(2)	121(1)	S(1) - C(1') - C(2)	114.5(9)
S(2) - C(2) - C(1)	118.4(9)	S(2) - C(2) - C(1')	116.5(7)	S(1) - C(3) - S(3)	114.7(3)
S(1) - C(3) - C(4)	126.4(5)	S(3) - C(3) - C(4)	118.9(4)	S(2) - C(4) - S(4)	114.2(3)
S(2) - C(4) - C(3)	129.6(5)	S(4) - C(4) - C(3)	116.2(5)	S(3) - C(5) - S(4)	113.4(3)
S(3) - C(5) - C(6)	122.7(5)	S(4) - C(5) - C(6)	123.9(5)	S(5) - C(6) - S(6)	116.7(3)
S(5) - C(6) - C(5)	123.1(5)	S(6) - C(6) - C(5)	120.1(5)	S(5) - C(7) - C(8)	117.1(5)
S(5) - C(7) - C(9)	133.1(5)	C(8) - C(7) - C(9)	109.7(5)	S(6) - C(8) - C(7)	117.9(4)
S(6) - C(8) - C(10)	133.5(5)	C(7) - C(8) - C(10)	108.6(5)	N(1) - C(9) - C(7)	105.5(5)
N(1) - C(9) - C(11)	122.2(5)	C(7) - C(9) - C(11)	132.2(6)	N(1) - C(10) - C(8)	106.9(5)
N(1) - C(10) - C(12)	123.5(5)	C(8) - C(10) - C(12)	129.6(6)	N(1) - C(13) - C(14)	120.6(6)
N(1) - C(13) - C(15)	119.4(6)	C(14) - C(13) - C(15)	120.0(6)	C(13) - C(14) - C(16)	120.0(6)
C(13) - C(15) - C(17)	120.3(6)	C(14) - C(16) - C(18)	119.9(6)	C(15) - C(17) - C(18)	120.7(6)
C(16) - C(18) - C(17)	119.0(6)	C(16) - C(18) - C(19)	120.6(6)	C(17) - C(18) - C(19)	120.4(6)
N(2) - C(19) - N(3)	107.0(5)	N(2) - C(19) - C(18)	127.4(6)	N(3) - C(19) - C(18)	125.6(6)
N(2) - C(20) - C(21)	101.9(5)	N(2) - C(20) - C(22)	109.3(6)	N(2) - C(20) - C(23)	105.4(6)
C(21) - C(20) - C(22)	118.2(7)	C(21) - C(20) - C(23)	113.0(7)	C(22) - C(20) - C(23)	108.2(8)
N(3) - C(21) - C(20)	102.2(5)	N(3) - C(21) - C(24)	107.6(7)	N(3) - C(21) - C(25)	106.7(7)
C(20) - C(21) - C(24)	115.4(7)	C(20) - C(21) - C(25)	114.2(8)	C(24) - C(21) - C(25)	109.8(9)

EMTN
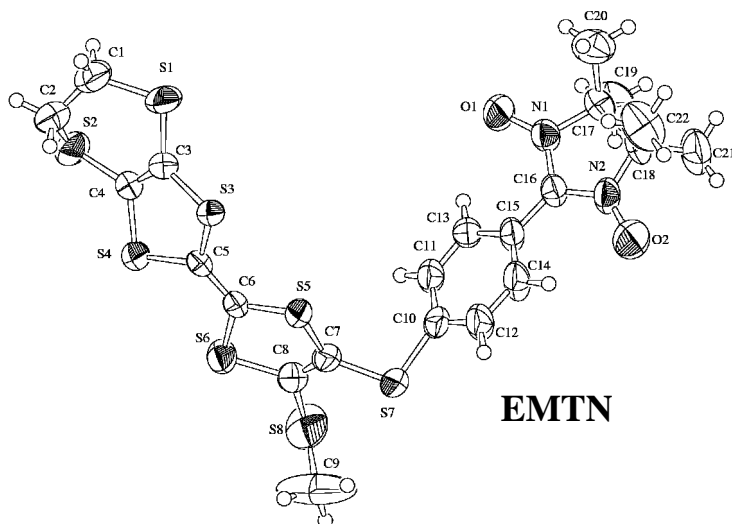
Atomic coordinates and Biso/Beq

atom	x	y	z	Beq
S(1)	0.5267(3)	0.8764(1)	0.32091(5)	8.13(5)
S(2)	0.0975(2)	0.9611(1)	0.32762(6)	6.41(4)
S(3)	0.5841(2)	0.89176(7)	0.44890(4)	4.25(3)
S(4)	0.1994(2)	0.95728(7)	0.45722(5)	4.46(3)
S(5)	0.6138(2)	0.83647(7)	0.58517(5)	4.63(3)
S(6)	0.2327(2)	0.90537(8)	0.59291(5)	5.57(3)
S(7)	0.6102(2)	0.74485(8)	0.69699(5)	6.31(4)
S(8)	0.1663(3)	0.8186(1)	0.70070(8)	8.89(5)
O(1)	0.7587(6)	0.4520(2)	0.4944(2)	7.6(1)
O(2)	1.0922(8)	0.4042(3)	0.6729(2)	10.1(1)
N(1)	0.8602(5)	0.4185(2)	0.5372(2)	4.83(8)
N(2)	1.0195(6)	0.3979(2)	0.6212(2)	5.17(9)
C(1)	0.4092(9)	0.9407(4)	0.2661(2)	7.4(2)
C(2)	0.2816(9)	1.0018(4)	0.2861(2)	6.6(1)
C(3)	0.4314(7)	0.9018(3)	0.3839(2)	4.51(9)
C(4)	0.2580(7)	0.9325(3)	0.3876(2)	4.55(9)
C(5)	0.4035(6)	0.9079(2)	0.4929(2)	3.70(8)
C(6)	0.4149(7)	0.8850(2)	0.5485(2)	4.16(8)
C(7)	0.4876(8)	0.8030(3)	0.6421(2)	4.79(10)
C(8)	0.3184(8)	0.8340(3)	0.6459(2)	5.5(1)
C(9)	0.297(2)	0.8673(7)	0.7621(4)	16.2(4)
C(10)	0.6915(8)	0.6612(3)	0.6604(2)	5.2(1)
C(11)	0.5775(7)	0.6199(3)	0.6157(2)	4.9(1)
C(12)	0.8801(10)	0.6330(3)	0.6787(2)	7.1(1)
C(13)	0.6450(7)	0.5532(3)	0.5921(2)	4.56(10)
C(14)	0.9378(9)	0.5649(3)	0.6579(2)	6.7(1)
C(15)	0.8286(7)	0.5231(3)	0.6133(2)	4.85(10)
C(16)	0.9015(6)	0.4489(3)	0.5919(2)	4.34(9)
C(17)	0.9250(7)	0.3343(3)	0.5344(2)	5.06(9)
C(18)	1.0746(6)	0.3313(3)	0.5878(2)	5.4(1)
C(19)	0.7459(9)	0.2841(4)	0.5412(3)	8.0(2)
C(20)	0.9908(9)	0.3174(5)	0.4760(3)	8.1(2)
C(21)	1.075(1)	0.2545(3)	0.6231(3)	8.0(2)
C(22)	1.2785(8)	0.3488(5)	0.5705(4)	8.8(2)
H(1)	0.5023	0.9643	0.2450	8.6807
H(2)	0.3272	0.9070	0.2386	8.6807
H(3)	0.2248	1.0317	0.2535	8.0754
H(4)	0.3642	1.0380	0.3108	8.0754
H(5)	0.4230	0.8435	0.7720	18.2717
H(6)	0.3163	0.9225	0.7548	18.2717
H(7)	0.2309	0.8631	0.7965	18.2717
H(8)	0.4500	0.6398	0.6018	5.7749
H(9)	0.9642	0.6613	0.7078	7.9640
H(10)	0.5663	0.5249	0.5619	5.4517
H(11)	1.0600	0.5432	0.6743	7.7369
H(12)	0.6996	0.2961	0.5783	9.6016
H(13)	0.6425	0.2977	0.5112	9.6016
H(14)	0.7720	0.2299	0.5394	9.6016
H(15)	1.0298	0.2629	0.4743	9.4490
H(16)	0.8869	0.3258	0.4453	9.4490
H(17)	1.0951	0.3505	0.4690	9.4490
H(18)	0.9435	0.2446	0.6336	9.4465
H(19)	1.1077	0.2103	0.6012	9.4465
H(20)	1.1567	0.2578	0.6588	9.4465
H(21)	1.3696	0.3533	0.6061	10.2640
H(22)	1.3214	0.3041	0.5494	10.2640
H(23)	1.2819	0.3949	0.5491	10.2640

Anisotropic Displacement Parameters

atom	U11	U22	U33	U12	U13	U23
S(1)	0.130(1)	0.135(1)	0.0433(7)	0.071(1)	0.0095(7)	-0.0088(8)
S(2)	0.0766(9)	0.103(1)	0.0586(7)	0.0199(8)	-0.0131(6)	-0.0001(7)
S(3)	0.0638(7)	0.0564(7)	0.0412(5)	0.0145(6)	0.0054(5)	-0.0016(5)
S(4)	0.0613(7)	0.0576(7)	0.0508(6)	0.0131(6)	0.0078(5)	0.0019(5)
S(5)	0.0751(8)	0.0562(7)	0.0458(6)	0.0159(6)	0.0122(5)	0.0082(5)
S(6)	0.0825(9)	0.0674(8)	0.0670(8)	0.0197(7)	0.0302(6)	0.0175(6)
S(7)	0.141(1)	0.0546(8)	0.0439(6)	0.0201(8)	0.0080(7)	0.0076(5)
S(8)	0.127(1)	0.118(1)	0.104(1)	0.000(1)	0.061(1)	0.038(1)
O(1)	0.119(3)	0.082(3)	0.075(2)	0.029(2)	-0.043(2)	-0.010(2)
O(2)	0.165(5)	0.109(4)	0.092(3)	0.042(3)	-0.053(3)	-0.018(3)
N(1)	0.061(2)	0.052(2)	0.067(2)	0.005(2)	-0.008(2)	-0.004(2)
N(2)	0.063(2)	0.055(2)	0.073(2)	0.011(2)	-0.014(2)	0.008(2)
C(1)	0.111(5)	0.118(5)	0.052(3)	0.033(3)	0.015(3)	0.006(2)
C(2)	0.112(4)	0.084(4)	0.052(3)	0.004(3)	-0.003(2)	-0.001(3)
C(3)	0.071(2)	0.053(3)	0.045(2)	0.006(2)	-0.001(1)	-0.006(2)
C(4)	0.074(2)	0.048(3)	0.050(2)	0.011(2)	0.002(2)	-0.002(2)
C(5)	0.060(2)	0.033(2)	0.048(2)	0.005(2)	0.008(1)	-0.005(2)
C(6)	0.077(2)	0.035(2)	0.047(2)	0.009(2)	0.012(1)	0.000(2)
C(7)	0.092(3)	0.047(3)	0.044(2)	0.000(2)	0.013(2)	0.005(2)
C(8)	0.101(3)	0.052(3)	0.055(2)	0.006(2)	0.012(2)	0.002(2)
C(9)	0.26(1)	0.25(1)	0.122(6)	-0.117(10)	0.111(6)	-0.104(7)
C(10)	0.102(3)	0.043(2)	0.050(2)	0.003(2)	-0.004(2)	0.011(2)
C(11)	0.065(3)	0.054(3)	0.064(3)	0.011(2)	-0.006(2)	0.007(2)
C(12)	0.115(4)	0.056(3)	0.084(4)	0.024(3)	-0.045(3)	-0.011(3)
C(13)	0.066(2)	0.049(2)	0.055(2)	0.002(2)	-0.007(2)	-0.003(2)
C(14)	0.103(4)	0.040(3)	0.096(4)	0.003(2)	-0.053(3)	-0.007(2)
C(15)	0.071(2)	0.037(2)	0.070(3)	0.005(2)	-0.018(2)	0.003(2)
C(16)	0.053(2)	0.041(2)	0.067(2)	0.002(2)	-0.012(2)	-0.002(2)
C(17)	0.063(2)	0.054(2)	0.077(2)	0.012(2)	0.014(2)	-0.005(2)
C(18)	0.052(2)	0.049(2)	0.101(3)	-0.006(2)	0.017(2)	0.004(2)
C(19)	0.103(4)	0.073(4)	0.126(5)	-0.044(3)	0.011(4)	-0.010(4)
C(20)	0.099(4)	0.129(6)	0.083(3)	0.028(4)	0.024(3)	-0.015(4)
C(21)	0.121(5)	0.057(3)	0.124(5)	0.011(4)	0.003(4)	0.020(3)
C(22)	0.054(3)	0.109(5)	0.176(7)	0.011(3)	0.027(3)	-0.009(5)

Bond Lengths(Å)

atom - atom	distance	atom - atom	distance	atom - atom	distance
S(1)- C(1)	1.787(9)	S(1)- C(3)	1.719(7)	S(2)- C(2)	1.824(9)
S(2)- C(4)	1.744(7)	S(3)- C(3)	1.744(7)	S(3)- C(5)	1.731(6)
S(4)- C(4)	1.750(7)	S(4)- C(5)	1.769(6)	S(5)- C(6)	1.744(7)
S(5)- C(7)	1.757(7)	S(6)- C(6)	1.758(6)	S(6)- C(8)	1.766(7)
S(7)- C(7)	1.742(7)	S(7)- C(10)	1.768(8)	S(8)- C(8)	1.762(8)
S(8)- C(9)	1.79(1)	O(1)- N(1)	1.277(7)	O(2)- N(2)	1.243(7)
N(1)- C(16)	1.361(8)	N(1)- C(17)	1.490(9)	N(2)- C(16)	1.320(8)
N(2)- C(18)	1.436(9)	C(1)- C(2)	1.47(1)	C(3)- C(4)	1.329(10)
C(5)- C(6)	1.330(8)	C(7)- C(8)	1.30(1)	C(10)- C(11)	1.410(10)
C(10)- C(12)	1.42(1)	C(11)- C(13)	1.355(10)	C(12)- C(14)	1.32(1)
C(13)- C(15)	1.413(9)	C(14)- C(15)	1.395(9)	C(15)- C(16)	1.456(9)
C(17)- C(18)	1.52(1)	C(17)- C(19)	1.53(1)	C(17)- C(20)	1.50(1)
C(18)- C(21)	1.53(1)	C(18)- C(22)	1.55(1)		

Bond Angles(˚)

atom - atom - atom	angle	atom - atom - atom	angle	atom - atom - atom	angle
C(1)- S(1)- C(3)	104.7(4)	C(2)- S(2)- C(4)	95.2(4)	C(3)- S(3)- C(5)	94.1(3)
C(4)- S(4)- C(5)	93.0(3)	C(6)- S(5)- C(7)	94.0(3)	C(6)- S(6)- C(8)	93.4(3)
C(7)- S(7)- C(10)	105.0(3)	C(8)- S(8)- C(9)	101.7(5)	O(1)- N(1)- C(16)	126.1(6)
O(1)- N(1)- C(17)	122.0(6)	C(16)- N(1)- C(17)	111.3(5)	O(2)- N(2)- C(16)	126.5(7)
O(2)- N(2)- C(18)	118.3(6)	C(16)- N(2)- C(18)	115.1(6)	S(1)- C(1)- C(2)	116.6(6)
S(2)- C(2)- C(1)	113.2(7)	S(1)- C(3)- S(3)	116.2(4)	S(1)- C(3)- C(4)	126.7(5)
S(3)- C(3)- C(4)	117.0(5)	S(2)- C(4)- S(4)	117.6(4)	S(2)- C(4)- C(3)	124.2(5)
S(4)- C(4)- C(3)	117.7(5)	S(3)- C(5)- S(4)	113.9(3)	S(3)- C(5)- C(6)	123.5(5)
S(4)- C(5)- C(6)	122.6(5)	S(5)- C(6)- S(6)	113.6(3)	S(5)- C(6)- C(5)	123.9(5)
S(6)- C(6)- C(5)	122.5(5)	S(5)- C(7)- S(7)	118.3(4)	S(5)- C(7)- C(8)	117.4(6)
S(7)- C(7)- C(8)	123.3(5)	S(6)- C(8)- S(8)	114.2(5)	S(6)- C(8)- C(7)	117.6(6)
S(8)- C(8)- C(7)	128.1(6)	S(7)- C(10)- C(11)	123.7(6)	S(7)- C(10)- C(12)	117.6(6)
C(11)- C(10)- C(12)	118.7(7)	C(10)- C(11)- C(13)	120.5(7)	C(10)- C(12)- C(14)	119.5(7)
C(11)- C(13)- C(15)	120.1(6)	C(12)- C(14)- C(15)	122.7(7)	C(13)- C(15)- C(14)	118.1(6)
C(13)- C(15)- C(16)	121.9(6)	C(14)- C(15)- C(16)	119.9(6)	N(1)- C(16)- N(2)	106.4(6)
N(1)- C(16)- C(15)	126.2(6)	N(2)- C(16)- C(15)	127.4(6)	N(1)- C(17)- C(18)	100.4(6)
N(1)- C(17)- C(19)	105.2(6)	N(1)- C(17)- C(20)	110.2(7)	C(18)- C(17)- C(19)	113.2(7)
C(18)- C(17)- C(20)	117.8(7)	C(19)- C(17)- C(20)	109.0(7)	N(2)- C(18)- C(17)	101.9(5)
N(2)- C(18)- C(21)	111.0(7)	N(2)- C(18)- C(22)	107.6(7)	C(17)- C(18)- C(21)	114.6(7)
C(17)- C(18)- C(22)	110.6(8)	C(21)- C(18)- C(22)	110.7(7)		

List of Publication

Parts of this thesis were published in the following journals:

[1]   "Ground State Spin Multiplicity of Cation Diradicals Derived from Pyrroles
       Carrying Nitronyl Nitroxide"
       Jotaro Nakazaki, Michio M. Matsushita, Akira Izuoka, Tadashi Sugawara,
       Mol. Cryst. Liq. Cryst. **1997**, *306*, 81-88.

[2]   "Novel Spin-Polarized TTF Donors Affording Ground State Triplet Cation
       Diradicals"
       Jotaro Nakazaki, Michio M. Matsushita, Akira Izuoka, Tadashi Sugawara,
       Tetrahedron Lett. **1999**, *40*, 5027-5030.

[3]   "Preparation of Isolable Ion-Radical Salt Derived from TTF-Based Spin-
       Polarized Donor"
       Jotaro Nakazaki, Yoshihiro Ishikawa, Akira Izuoka, Tadashi Sugawara, Yuzo
       Kawada, *Chem. Phys. Lett.* **2000**, *319,* 385-390.

The following publications were not included in this thesis:

[1]   "New Synthesis of 2-[1,3-Dithiol-2-ylidene]-5,6-dihydro-1,3-dithiolo[4,5-
       b][1,4]dithiins with Formyl Group on Fused-Benzene, [1,4]Dithiin, or
       Thiophene Ring"
       Yoshihiro Ishikawa, Tomoko Miyamoto, Asami Yoshida, Yuzo Kawada,
       Jotaro Nakazaki, Akira Izuoka, Tadashi Sugawara, *Tetrahedron Lett.* **1999**,
       40, 8819-8822.

[2]   "Organic Paramagnetic Building Blocks for Ferromagnetic Materials"
       Tadashi Sugawara, Michio M. Matsushita, Jotaro Nakazaki, In: Paul M.
       Lahti, ed., *'Magnetic Properties of Organic Materials'*, Marcel Dekker, **1999**,
       535-552.

[3]   "Self-Assembling Organic Ferromagnet: Frontier Orbital Control of Spin-
       Polarized Organic Radicals"
       Tadashi Sugawara, Jotaro Nakazaki, Michio M. Matsushita, In: Hiroyuki
       Sasabe, ed., *'Hyper-Structured Molecules III'*, Gordon&Breach, in press.

Acknowledgments

Mats O. Sandberg

SQUID   ESR   UV   IR

SQUID